HALL LIBRARY

BULLETIN

OF THE

CHEMICAL SOCIETY OF JAPAN

Vol. 33 No. 11 November 1960

JAN 4 1961

CONTENTS

General and Physical

T. MORITA: Self-consistent Field Molecular Orbital Treatment of Benzenium Ion for a Simplified Model of Hyperconjugation 1486

M. SENŌ and T. YAMABE: The Ion-Exchange Behavior of Some Neutral Amino Acids 1532

S. OTANI: Crystal Habit Modification of Strontium Sulfate. I. Habit-Modifying Action of Foreign Substances 1543

S. OTANI: Crystal Habit Modification of Strontium Sulfate. II. Characteristic Effect of Sodium Triphosphate on Crystallization and Mechanism of Spherulite Formation 1549

S. SHIBA: Flow Properties of Aluminum Soaps-Hydrocarbon Systems 1563

K. ARAKAWA: Stress Relaxation of Thermo-reversible Gels. Molecular Weight Dependence of Relaxation Spectrum. Polyvinyl Alcohol-Congo Red-Water System 1568

T. KOIDE, Y. KATO and T. ODA: Physical Properties and Crystal Structure of 2-Bromo-2,3,3-trimethylbutane 1572

K. ITO, H. WATANABE and M. KUBO: Proton Magnetic Resonance of Borazole 1588

K. FUKUI, A. IMAMURA, T. YONEZAWA and C. NAGATA: A Quantum-mechanical Approach to the Theory of Aromaticity 1591

K. NUKADA: NMR Spectra of Aliphatic Compounds Containing Oxygen Atoms and the Related Compounds. 1606

Analytical and Inorganic

M. MORI, R. TSUCHIYA and H. FUKUDA: Thermodynamic Studies on Cobalt Complexes. VI. Solubility of Nitropentamminecobalt(III), *cis*- and *trans*-Dinitrotetramminecobalt(III) and Trinitrotriamminecobalt(III) Complexes 1503

M. MORI, R. TSUCHIYA, E. KYUNO and T. NISHIDE: Thermodynamic Studies on Cobalt Complexes. VII. Solubility of Erdmann's Salt and Related Complexes 1510

K. KIGOSHI and Y. TOMIKURA: Variation of Radiocarbon Concentration in Modern Wood. . .1576

H. ONISHI and N. ISHIWATARI: Spectrophotometric Determination of Bismuth with Xylenol Orange 1581

Organic and Biological

S. INOKAWA: Studies on the Mucilage of the Root of "*Tororo-aoi*" (*Abelmoschus manihot*, MEDIC). I. On the Characteristic Colloidal Nature of the Mucilage. 1473

S. INOKAWA: Studies on the Mucilage of the Root of "*Tororo-aoi*" (*Abelmoschus manihot*, MEDIC). II. Effect of Heating on the Colloidal Characteristics of the Mucilage. 1476

H. YASUI: Studies on Constituents of Coal Carbonization Light Oil. I. On Saturated Hydrocarbons Contained in High-Temperature Coal Carbonization Light Oil. 1493

H. YASUI: Studies on Constituents of Coal Carbonization Light Oil. II. On Saturated Hydrocarbons Contained in Low-temperature Coal Carbonization Light Oil 1498

K. MARUYAMA: Oxidizing Action of Hydroperoxides. IV. On the Oxidation of Aryl Alkyl Ketones 1516

(*Continued on inside cover*)

Published by the Chemical Society of Japan

THE CHEMICAL SOCIETY OF JAPAN
(NIPPON KAGAKUKAI)

Founded in 1948

Successor to the former Chemical Society of Japan founded in 1878 and to the Society of Chemical Industry, Japan founded in 1898.

BULLETIN OF THE CHEMICAL SOCIETY OF JAPAN

Editor: Yoshiyuki URUSHIBARA, The University of Tokyo, Tokyo
Assistant Editor: Saburo NAGAKURA, The University of Tokyo, Tokyo
Editorial Board:

Toshio ANDO	Ichiro MIYAGAWA	Tadashi SUEHIRO
Yoshié BANSHO	Masazumi NAKAGAWA	Kenzi TAMARU
Hidehiro GOTŌ	Koji NAKANISHI	Takeo WATASE
Yoshimasa HIRATA	Shigeo OKUMURA	Iwao YASUMORI
Kenichi HONDA	Kazuo SAITO	Tsuneo YOSHINO
Sunao IMANISHI	Naoyasu SATA	Koshiro YOSHIOKA

(*Continued from outside cover*)

K. TOI, K. MORI and Y. IZUMI: Synthesis of α,α'-Diaminodicarboxylic Acids 1529

S. SAKAKIBARA and Y. NAGAI: Syntheses of Peptides Containing Proline. I. Syntheses of Glycyl-L-prolyl-L-leucyl-glycyl-L-proline and its Related Compounds. 1537

S. NAWA: The Structure of the Yellow Pigment from Drosophila 1555

M. YAMAGUCHI: Total Syntheses of Renieratene and Renierapurpurin 1560

A. SUGIMORI: Intermediate Compounds in the Catalytic Reduction of Aromatic Nitro Compounds with Raney Nickel Catalyst 1599

M. ŌKI and H. IWAMURA: Intramolecular Intraction between Hydroxyl Group and π-Electrons. X. Tertiary Alcohols Related to Phenethyl Alcohol and 3-Buten-1-ol 1600

Applied

Y. SANADA, N. MOCHIDA and H. HONDA: Glass Transition of Coal. 1479

S. KIKUCHI et H. UEDA: Préparation de l'Emulsion à Grand Contraste pour l'Usage Lithographique 1520

S. OKAMURA and T. MANABE: Graft Polymerization by Pre-heating Method Applied to Polyethylene Containing Benzoyl Peroxide 1526

N. OGATA: Studies on Polymerization and Depolymerization of ε-Caprolactam Polymer. VIII. The Solution Viscosity of Poly-ε-capramide of Super-high Degree of Polymerization 1584

Short Communications

S. FUJIWARA and M. NAKAJIMA: Proton Magnetic Resonance in Cocoon 1615

N. OI: Separation of Uranium from Fission Products Using Cellulose 1617

Y. NAMBA, T. ODA, H. ITO and T. WATANABE: The Crystal Structure of Pyridine *N*-Oxide Hydrochloride and Hydrobromide 1618

M. KOIZUMI, R. KIRIYAMA and W. MURAYAMA: The Crystallization of "Allophane" under Hydrothermal Conditions 1620

N. SAITO, T. TOMINAGA and H. SANO: Hot-atom Chemistry of Radiocobalt in Nitroammine Cobalt Complex Salts. 1621

H. INOKUCHI, K. IKEDA and H. AKAMATU: The Electron Spin Resonance Absorption of Molecular Addition Compounds 1622

I. MATSUBARA: Detection of End-groups in Polyacrylonitrile by Differential Infrared Spectroscopy. 1624

T. SAITO: Proton Magnetic Resonance Studies on the Thermally Dehydrated Products of Alumina Trihydrate 1626

H. INOKUCHI and M. KINOSHITA: The Oxygen Effect on Electronic Properties of α,α'-Diphenyl-β-picrylhydrazyl 1627

J. OKAMOTO: The Distribution of Recoil Tritium in Benzoic Acid 1629

M. OHASHI, S. YAMAMURA, A. TERAHARA and K. NAKANISHI: Monascoflavin 1630

M. ŌKI and H. IWAMURA: Intramolecular Interaction between Hydroxyl Group and π-Electrons. XI. High Resolution Proton Magnetic Resonance Spectra of Tertiary Alcohols Having π-Electrons 1632

N. NAKAGAWA and S. FUJIWARA: Association Shifts of NMR Spectra of Phenylacetylene . . .1634

Studies on the Mucilage of the Root of "Tororo-aoi" (Abelmoschus manihot, MEDIC). I. On the Characteristic Colloidal Nature of the Mucilage

By Saburo INOKAWA

(Received January 22, 1960)

Japanese hand-made paper, as is well known, is very elegant and refined, strong and tenacious, and is considered as a piece of work of Japanese characteristic arts. It is said that its elegance and strength mainly depend upon the properties of "*Neri*" which is indispensable for making Japanese hand-made paper.

"*Neri*" is a plant mucilage, and the mucilage obtained from the root of "*Tororo-aoi*" (*Abelmoschus manihot*, MEDIC) is most widely used. The chemical constituent of this plant mucilage was first investigated by Ozawa[1], and later Oguri[2] studied its distribution in cellular tissue. Oguri et al.[3,4], Machida et al.[5], and Oshibuchi et al.[6] reported that this plant mucilage was mainly made of polyrhamnogalacturonide, which contained rhamnose and galacturonic acid in the ratio of 1 : 1 or 1 : 2, and was accompanied by small quantities of araban, xylan, galactosan, and glucosan. However, concerning the colloidal behavior of this plant mucilage, little work has been done[7,8]. Taking an interest in this mucilage, we have been studying it for several years[9-13]. In this paper, such a purification method in which colloidal characteristics are kept well, was studied and then some colloidal characteristics of the purified mucilage were observed.

Experimental

Material. — Roots of "*Tororo-aoi*" were stored in 0.5% formalin.

Crude Mucilage.—The roots were washed with water, ground with a hammer, extracted with distillated water at 0°C for 24 hrs. and the extracted mucilage was filtered through a piece of cotton cloth.

Viscosity.—Viscosity determinations were carried out at 20°C by an Ostwald viscometer.

Intrinsic Viscosity. — Intrinsic viscosity determinations were carried out at 20°C in 1% sodium chloride solution.

Spinnability.—Spinnability was expressed by the maximum length (cm.) of the mucilage threads spun by a rod (7 mm. diameter) raised out of the mucilage. The determinations were carried out at 20°C and the velocity of the ascending of a testing rod was controlled at 4 cm./sec.

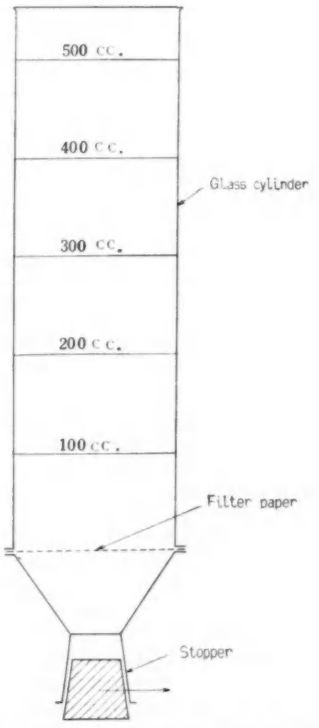

Fig. 1. Apparatus for the measurement of filterability.

1) T. Ozawa, *J. Chem. Soc. Japan, Ind. Chem. Sec.* (*Kogyo Kagaku Zasshi*), **24**, 389 (1922).
2) S. Oguri and H. Kawasaki, ibid., **45**, 307 (1942).
3) S. Oguri and K. Tomamezi, ibid., **46**, 146 (1943).
4) S. Oguri and K. Tomamezi, ibid., **47**, 432 (1944).
5) S. Machida and N. Uchino, *J. Chem. Soc. Japan, Pure Chem. Sec.* (*Nippon Kagaku Zasshi*), **74**, 615 (1954).
6) T. Oshibuchi and H. Kusunose, *J. Agr. Chem. Soc. Japan* (*Nippon Nogei-kagaku Kaishi*), **31**, 481 (1957).
7) S. Machida and N. Uchino, *J. Chem. Soc. Japan, Pure Chem. Sec.* (*Nippon Kagaku Zasshi*), **74**, 183 (1953).
8) I. Shinohara, T. Ono and S. Oguri, *J. Chem. Soc. Japan, Ind. Chem. Sec.* (*Kogyo Kagaku Zasshi*), **61**, 877 (1958).
9) S. Inokawa and R. Goto, *Wood Research* (*Japan*), **No. 14**, 50 (1955).
10) S. Inokawa and R. Goto, ibid., **No. 17**, 50 (1956).
11) S. Inokaxa, R. Goto and A. Takatsuki, ibid., **No. 21**, 26 (1959).
12) S. Inokawa and R. Goto, *J. Chem. Soc. Japan, Pure Chem. Sec.* (*Nippon Kagaku Zasshi*), **79**, 409 (1958).
13) S. Inokawa, R. Goto and I. Morimoto, ibid., **81**, 783 (1960).

Filterability.—Filterability means the rate of clogging up a filter paper. The determinations were carried out at 20°C as follows. A filter paper was fitted at the end of a glass cylinder (500 cc.) as in Fig. 1. a) Five hundred cc. of distilled water were poured into the cylinder and the times to filter 100 cc., 200 cc., 300 cc. and 400 cc. of water were measured (respectively, t_1, t_2, t_3 and t_4 sec.). b) Five hundred cc. of mucilage were poured into the cylinder, 400 cc. of the mucilage were filtered, and the residual mucilage (100 cc.) was discarded. c) Again, 500 cc. of distillated water were poured into the cylinder, and the times to filter 100 cc., 200 cc., 300 cc. and 400 cc. of water were measured (respectively, T_1, T_2, T_3 and T_4 sec.). Mean values of T_1/t_1, T_2/t_2, T_3/t_3 and T_4/t_4 are indicated as values for filterability.

Elasticity.—Elasticity determinations were carried out at 30°C by Schwedoff's method[14].

Results and Discussion

Effect of Heat Treatment on Spinnability, Filterability, Elasticity, and Viscosity, of the Mucilage.—Although spinnability, filterability, elasticity, and viscosity, of the crude mucilage were considerably large, spinnability, filterability, and elasticity decrease very rapidly by heating at 80°C, as shown in Fig. 2. These are the characteristic properties of the mucilage.

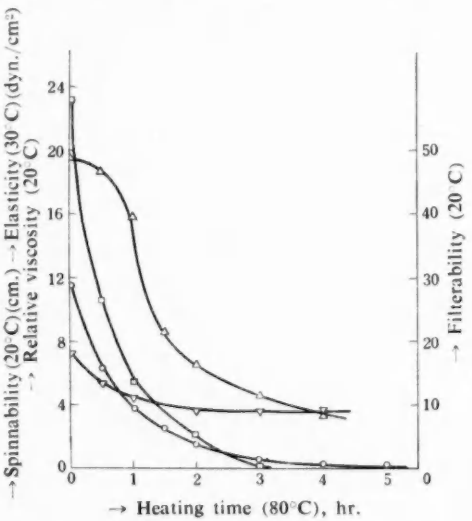

Fig. 2. Effect of heat treatment on the crude mucilage. Concentration of mucilage: 0.20%; 3.2×10^{-5}% (filterability).
○, Spinnability △, Filterability
□, Elasticity ▽, Relative viscosity

Effect of Mixer Treatment on Spinnability, Filterability, Elasticity, and Viscosity, of the Mucilage.—The crude mucilage in the original state was difficult to filter through a filter paper, but by homogenizing with a mixer, it was made easily filterable. Starch and other impurities contained in the crude mucilage could be removed by the filtration. The change of colloidal properties by mixer treatment is shown in Fig. 3. The spinnability and filterability almost disappeared by mixer treatment but the high elasticity remained. However, the high elasticity decreased considerably by heating or by longer standing in the similar way to that of the crude mucilage. The viscosity decreased rapidly also in the first 1 hr. of heating, the initial rapid fall being followed by a further slow reduction. The white precipitates obtained by the addition of alcohol-ether (8:2) mixture to the mucilage, were composed mainly of rhamnose and galacturonic acid and the mucilage prepared by redissolving the precipitates in water, had nearly equal elasticity to the original mucilage treated by a mixer. The mucilage thus obtained was used in subsequent studies as purified mucilage.

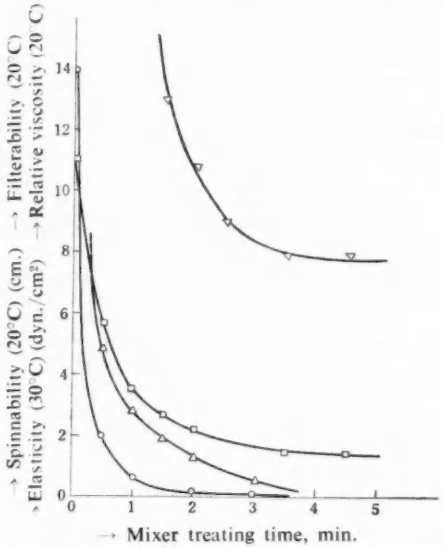

Fig. 3. Effect of mixer treatment on the crude mucilage. Concentration of mucilage: 0.16%; 1.1×10^{-5}% (filterability).
○, Spinnability △, Filterability
□, Elasticity ▽, Relative viscosity

Effect of Heat Treatment on Elasticity and Intrinsic Viscosity of the Purified Mucilage.—By heating at 80°C for varying periods of time, the elasticity of the purified mucilage fell down very rapidly to nearly zero. The intrinsic viscosity decreased rapidly in the first 30 min. of heating, the initial rapid fall being followed

14) Th. Schwedoff, *J. de Phys.*, [2] **8**, 341 (1889).

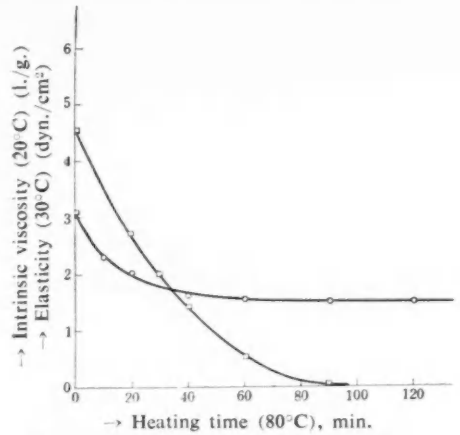

Fig. 4. Effect of heat treatment on the purified mucilage. Concentration of mucilage: 0.37%.
○, Intrinsic viscosity (in 1% NaCl solution)
□, Elasticity

by a slow reduction over a period of some hours as shown in Fig. 4. It seems that the fall of the elasticity does not always depend upon degradation of molecules of the mucin.

Effect of Electrolytic Groups in the Mucin on Elasticity of the Purified Mucilage. — 1) Effect of sodium chloride, calcium chloride, disodium ethylenediaminetetraacetate, and sodium oxalate on the elasticity of the purified mucilage was observed (Fig. 5). The elasticity

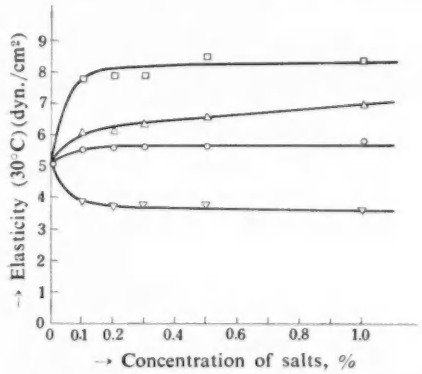

Fig. 5. Effect of addition of salts on the elasticity of the purified mucilage. Concentration of mucilage: 0.37%
○, Sodium chloride
△, Disodium ethylenediaminetetraacetate
□, Sodium oxalate ▽, Calcium chloride

was hardly influenced at all by the addition of sodium chloride, but increased by the addition of disodium ethylenediaminetetraacetate and sodium oxalate which are able to interchange calcium (about 40%) contained in ash of the mucilage, with sodium, and decreased by the addition of calcium chloride. 2) Electrodialysis experiments were carried out. By electrodialysis of the purified mucilage, pH of the mucilage changed from 6.1 to 2.9 and the value for the elasticity of 0.35% mucilage changed from 4.3 (dyn./cm²) to 10 (dyn./cm²). The change of the elasticity of the electrodialyzed mucilage is plotted against the change of pH with the addition of sodium carbonate in Fig. 6. The addition of calcium oxide to

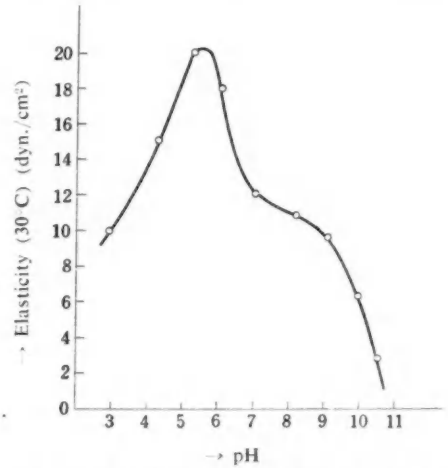

Fig. 6. Effect of pH on the elasticity of the electrodialyzed mucilage. Concentration of mucilage: 0.35%

the electrodialyzed mucilage always decreased the elasticity and at pH 4.2, the value for the elasticity fell to 4.2 (dyn./cm²). From results of above two experiments, it is considered that electrolytic groups in the mucin have effect on the elasticity but are not a major cause for the elasticity.

Summary

1) The crude mucilage could be filtered after homogenizing by a mixer. By the addition of alcohol-ether mixture to the filtrate, the precipitates were obtained, which gave purified mucilage on redissolving in water.

2) The purified mucilage had noticeable elasticity and could be used for the research work instead of crude mucilage.

3) Some colloidal behavior of the purified mucilage was observed.

The author wishes to express his hearty thanks to Professor R. Goto, Kyoto University,

for his invaluable advice and encouragement throughout this work and to Koshin Kogyo Co. for the generous supply of roots of "*Tororo-aoi*".

Department of Chemistry
Faculty of Science
Kyoto University
Sakyo-ku, Kyoto

Studies on the Mucilage of the Root of "Tororo-aoi" (Abelmoschus manihot, MEDIC). II. Effect of Heating on the Colloidal Characteristics of the Mucilage

By Saburo INOKAWA

(Received February 16, 1960)

In the previous paper[1] it has been shown that the elasticity, spinnability, and filterability of the crude mucilage and the elasticity of the purified mucilage decreased remarkably by heating at 80°C for 1~3 hr. Taking an interest in this characteristic of the mucilage, the present investigation was undertaken in order to observe the effect of heating on the mucilage by electron micrography, sedimentation in an ultracentrifuge, and electrophoresis.

Experimental

Material.—Roots of "*Tororo-aoi*" were stored in 0.5% formalin.

Crude Mucilage and Purified Mucilage.—These preparations were similar to those described in the previous paper[1].

Electron Microscope.—The sample mucilage was mounted on a specimen holder for electron microscopy with a formvar supporting-film and dried. After chromium-shadowing the specimen was observed by an electron microscope of the type Shimadzu SM-T4.

Ultracentrifuge.—Sedimentation diagrams of an approximately 0.4% solution of mucilage in the presence of a 0.7% sodium chloride were taken by an ultracentrifuge of the type Spinco E under the centrifugal force of 259700 ***g*** at speed of 59780 r. p. m..

Electrophoresis.—Electrophoresis patterns of an approximately 0.3% solution of mucilage in a phosphate and sodium chloride buffer of ionic strength 0.02 and 0.18 respectively, were taken by a Tiselius electrophoresis apparatus of the type Hitachi HT-B.

Elasticity and Intrinsic Viscosity.—These determinations were the same as those described in the previous paper[1].

Results and Discussion

Observations from Electron Micrographs.—The microscopic observation of network structure, which appears by the addition of methylene blue solution to the crude mucilage, is reported[2]; but the structure has been presumed[3] not to exist originally in the mucilage

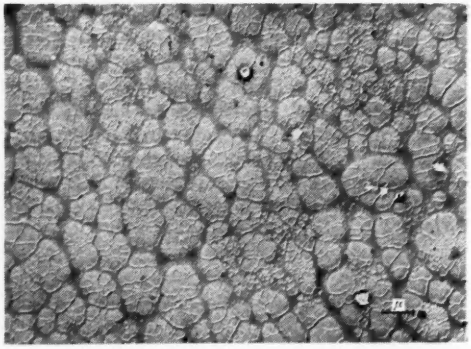

Fig. 1. Electron micrograph of the crude mucilage.
(0.2% aqueous solution) (Cr-shadowing)

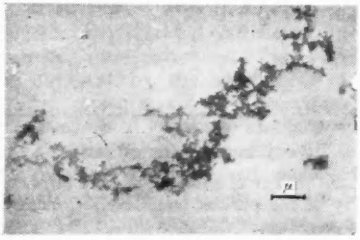

Fig. 2. Electron micrograph of the mucilage heated at 80°C for 3 hr.
(0.2% aqueous solution) (Cr-shadowing)

1) S. Inokawa, This Bulletin, **33**, 1473 (1960).
2) S. Oguri and K. Tomamezi, *J. Soc. Chem. Indust. Japan*, (*Kogyo Kagaku Zassi*), **46**, 146 (1943).
3) S. Oguri, I. Shinohara, and T. Ono, *J. Chem. Soc. Japan, Ind. Chem. Sec.* (*Kogyo Kagaku Zassi*), **58**, 227 (1955).

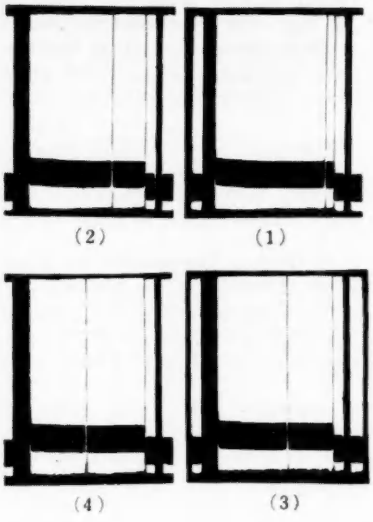

Fig. 3. Sedimentation diagram of the purified fresh mucilage in 0.7% NaCl solution. Speed 59700 r. p. m.; approximate concentration 0.4%; times for each measurement, 16 (1), 90 (2), 112 (3) and 144 (4) min. after reaching full speed.

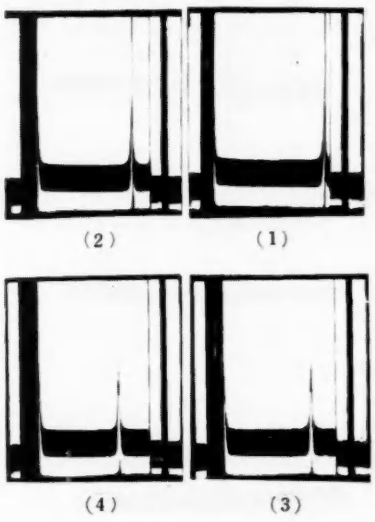

Fig. 4. Sedimentation diagram of the mucilage heated at 80°C for 2 hr. in 0.7% NaCl solution. Speed 59700 r.p.m.; Approximate concentration 0.4%; times for each measurement, 16 (1), 56 (2), 80 (3) and 104 (4) min. after reaching full speed.

but to be formed by an aggregation of composing substances by the addition of the reagent. The present writer has observed that the electron micrograph of the crude mucilage showed a typical network structure as shown in Fig. 1, which by heating at 80°C for 2 hr., was broken to a granular structure as shown in Fig. 2.

Observation from Sedimentation Diagrams in an Ultracentrifuge.—Sedimentation diagrams of the purified fresh mucilage and the mucilage heated at 80°C for 2 hr. are shown in Fig. 3 and in Fig. 4 respectively. The shape of the initial strikingly sharp boundary, as a line, of the fresh mucilage, remained perfectly unchanged through sedimentation. The sedimentation boundary of the heated mucilage was also very sharp, but a little spreading of the boundary occurred with the elapse of time. From Figs. 3 and 4 it may be considered that in the fresh mucilage, a network built by a very strong interaction between the mucin molecular chains moves as a whole under the influence of the centrifugal field, and the considerable weakening of the intermolecular force between chains occurs by heat treatment[4].

Observation from Electrophoresis Patterns.—Electrophoresis patterns of the purified fresh mucilage and the mucilage heated at 80°C for 2 hr. are shown in Fig. 5 and in Fig. 6, respectively. The initial strikingly sharp ascending pattern[5] of the fresh mucilage remained unchanged through electrophoresis similar to the

TABLE I. RELATIONS BETWEEN pH AND MOBILITY AT 0°C IN PHOSPHATE AND NaCl BUFFER OF IONIC STRENGTH 0.02 AND 0.18

	pH	2.1	5.3	6.9	9.6
Mobility	Purified fresh mucilage	1.1×10^{-5}	1.2×10^{-4}	1.3×10^{-4}	2.2×10^{-5}
(cm^2/sec. V.)	Heated mucilage	3.0×10^{-5}	2.6×10^{-4}	2.4×10^{-4}	5.0×10^{-5}

4) In the heated mucilage it was observed that there was something which sedimented rapidly in the initial few minits.

5) The pronounced boundary disturbance in the descending boundary was caused by the adhering of the mucilage on the electrophoresis cell-wall.

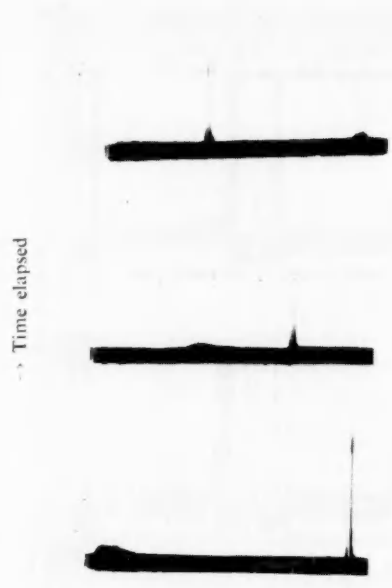

Fig. 5. Electrophoresis pattern of the purified mucilage. Approximate concentration 0.3%; phosphate-NaCl buffer; pH 6.5.

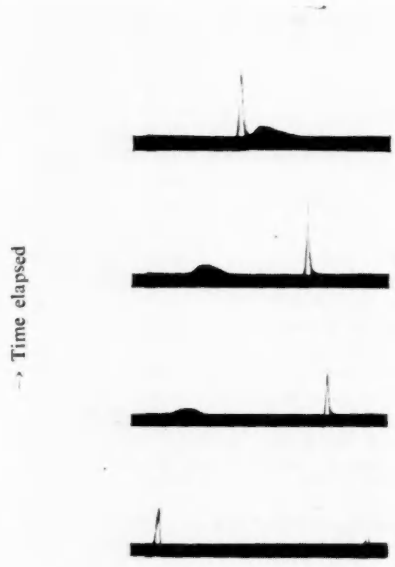

Fig. 6. Electrophoresis pattern of the mucilage heated at 80°C for 2 hr. Approximate concentration 0.3%; phosphate-NaCl buffer; pH 6.5.

centrifugal boundary (Fig. 4). The ascending pattern of the heated mucilage became somewhat broader as time went by. From Figs. 5 and 6 it may also be considered that there exists a very strong interaction between the mucin molecular chains in the fresh mucilage, and that the interaction decreases considerably by heating.

Measurements of the electrophoresis patterns over pH 2.1~9.6 were carried out without observing any change of the shape, and the relations between pH and mobility are tabulated in Table I.

Effect of Heating Temperature on Elasticity and Intrinsic Viscosity of the Mucilage.—Relations between heating temperature and decrease of elasticity and intrinsic viscosity of the purified mucilage were observed at heating time of 30, 60 and 90 min. as shown in Fig. 7. The decrease of the elasticity was gradual up to approximately 50°C and then sharp at the higher temperature, but that of intrinsic viscosity was nearly constant. The results seem to indicate that the decrease of elasticity by heating is not caused simply by degradation of mucin molecules. This is also supported by the previous experimental results[6] that

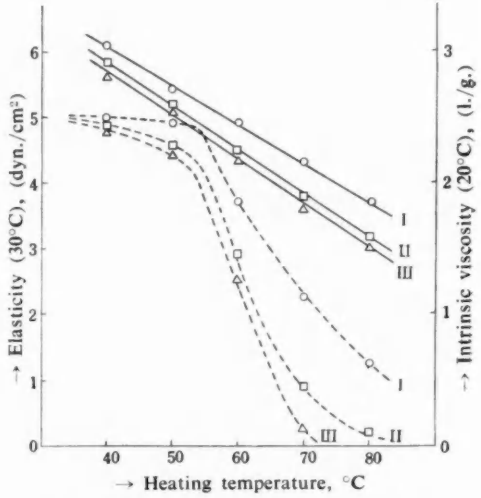

Fig. 7. Relations between heating temperature and decrease of elasticity and intrinsic viscosity.
Mucilage concentration 0.37%
—— Intrinsic viscosity
---- Elasticity
Curve I Heating time 30 min.
Curve II Heating time 60 min.
Curve III Heating time 90 min.

6) S. Inokawa, R. Goto and I. Morimoto, *J. Chem. Soc. Japan, Pure Chem. Sec.* (*Nippon Kagaku Zasshi*), **81**, 783 (1960).

there was no considerable difference in molecular weight between the fresh and the heated mucilage.

Summary

1) From electron micrographs it was observed that in the crude mucilage there exists a network structure, but its structure is broken by heating.

2) From sedimentation diagrams and electrophoresis patterns it seems reasonable to assume that in the purified fresh mucilage there exist very strong intermolecular forces like those in gel and these forces decrease markedly by heating.

3) It is conceivable that the degradation of the mucin macromolecule does not play an important role in the marked decrease of the elasticity of the purified fresh mucilage by heating.

Finally the writer wishes to express his hearty thanks to Professor R. Goto, Kyoto University, for his invaluable advice and encouragement throughout this work. He is also indebted to Professor E. Suito and Dr. K. Takiyama of Kyoto University for their help in taking the electron micrographs, to Dr. K. Fukai of Osaka University for taking the sedimentation photographs, to Professor S. Tanaka of Kyoto University for his help in taking electrophoresis photographs. It is also a pleasure to thank Koshin Kogyo Co. for their generous supply of the root of "*Tororo-aoi*".

Department of Chemistry
Faculty of Science
Kyoto University
Sakyo-ku, Kyoto

Glass Transition of Coal

By Yuzō Sanada, Naoyuki Mochida and Hidemasa Honda

(Received September 29, 1959)

The study of mechanical or thermal properties of coal on heating is of great importance in structural investigation and industrial problems. It is well known that coals, especially caking or coking coals, have a polymeric character, and show plastic deformation at room temperature[1] and softening or flow phenomena on heating.[2] It appears, however, that very few detailed investigations on the change of mechanical or thermal properties of coals heated over the range from room temperature to the softening point have yet been made. D. H. Bangham and R. E. Franklin[3] measured the thermal expansion coefficient of three bright coals. They showed that coals have a gradual increase in the thermal expansion coefficient over the range from room temperature to about 300°C. The present authors have measured the change of hardness and volume for several vitrains of every rank over the range from room temperature to about 160°C by using two distinct hardness methods and one dilatometric method, and have found that coals have a few characteristic points over this temperature range.

Experimental Procedure

Indentation Hardness Method.—Coal specimens about 1 cm. wide and 5 cm. long, and about of 2 cm. thick parallel plane were cut perpendicular to the bedding planes, using a motor-driven diamond cutter. One plane of surface perpendicular to the bedding planes of the specimen was highly polished by using glass plates with carborundum and alumina, and woollen cloth with alumina. The specimens were air-dried at room temperature and ordinary humidity.

Fig. 1 shows the experimental apparatus which modified the Akashi micro-hardness tester having a diamond Knoop indenter.[4] The coal specimen, of which the base and two long sides are covered with three electric heating plates settled in a vise, is placed on a steel table with a copper block cooled by water. The position of the vitrain layer can be adjusted by means of screws. The temperature of the vitrain layer is measured by a thermistor surface thermometer located very closely to the indenter and controlled by a suitable variable resistor. The coal specimen is heated at the heating rate of 1°C/min. over the range from room temperature to 160°C. The load of indenter is 100 g. and

1) D. W. van Krevelen and J. Schuyer, "Coal Science, Aspects of Coal Constitution", Elsevier, Amsterdam (1957), p. 275.
2) D. W. van Krevelen and J. Schuyer, loc. cit. p. 286.
3) D. H. Bangham and R. E. Franklin, *Trans. Faraday Soc.*, **42B**, 289 (1946).
4) H. Honda and Y. Sanada, *Fuel*, **36**, 403 (1957).

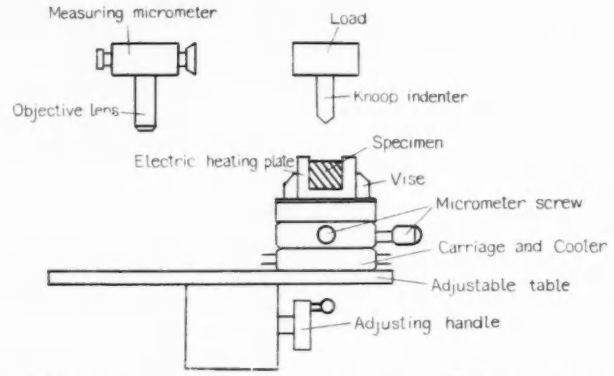

Fig. 1. Apparatus for the determination of the indentation hardness.

the time taken in the duration of the load is 30 sec. The hot impression under the elevated temperature is made every five minutes, i.e. every 5°C. After an impression has been made, the specimen is moved to a new position along the vitrain layer by means of the screw for the distance of 15/100 mm. After all impression have been completed, the furnace is cooled to room temperature and then Knoop hardness numbers are determined from the length of the long diagonal of indentation.

Pendulum Hardness Method. — The preparation of coal specimens, the heating method, the heating rate, and the measurements of temperature are the same as those in the case of indentation hardness test.

The apparatus of the pendulum hardness tester of Walker Steele type is given in Fig. 2. It consists of the wedge-type agate fulcrum, two brass arms with weights and a small mirror. The length between the weights at the ends of the arms of the pendulum is 20 cm. The weight of the pendulum is 78 g. The damping of the pendulum hardness tester on the vitrain layer of the specimens is determined by the lamp-and-scale method. The apparatus is held in an air-thermostat. The logarithmic decrement λ of the pendulum is given by the following equation, provided that the periodic time is a constant :[5]

$$\lambda = (2.303 \log \theta/\theta')/2n$$

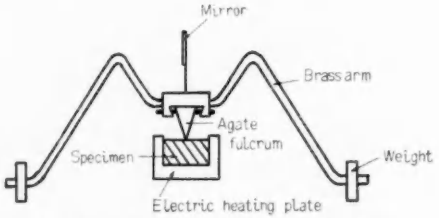

Fig. 2. Apparatus for the determination of the logarithmic decrement.

where θ and θ' are the angle from the position of rest, n is the frequency of the pendulum between θ and θ'. In this experiment, the chosen values of θ and θ' were 4° and 3°26′ respectively.

Dilatometric Method.—The coal specimen was pulverized to pass through a 30 and stand on a 60 Tyler mesh sieve. The vitrain, of specific gravity less than 1.30, was isolated by the float-or-sink method using mixtures of benzene and carbon tetrachloride. The volume change of vitrain with temperature was measured using a Pyrex glass

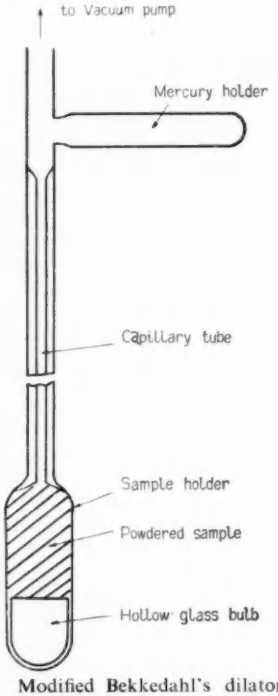

Fig. 3. Modified Bekkedahl's dilatometer.

5) Y. Inoue, K. Kanai and K. Hiroi, *J. Chem. Soc. Japan, Ind. Chem. Sec.* (*Kogyo Kagaku Zasshi*) **59**, 231 (1956).

6) N. Bekkedahl, *J. Research NBS*, **42**, 145 (1949).

TABLE I. ANALYSIS OF VARIOUS VITRAINS

Source		Proximate analysis, %				Ultimate analysis (d. a. f.) %		
		Moisture	Ash	V. M.	Fixed Carbon	C	H	O+N+S
Brown coal	Tempoku-Menashi	12.41	1.40	42.91	43.28	69.82	4.91	25.26
	Nakagō	13.32	3.96	38.03	44.69	74.33	5.26	20.41
Bituminous coal	Takamatsu	4.67	2.29	41.10	51.94	78.95	5.01	16.04
	Bibai	2.78	3.10	41.81	52.31	80.90	5.87	13.23
	Ashibetsu	2.98	4.05	42.93	50.04	81.11	5.49	13.40
	Akabira	3.01	3.21	42.50	51.28	82.29	5.92	11.79
	Futago	1.54	2.31	46.86	49.29	83.16	6.31	10.53
	Miike	1.21	3.36	43.95	51.48	84.53	6.11	9.36
	Ōyūbari	1.35	2.76	40.34	55.55	84.79	6.23	8.93
	Yūbari	2.28	2.70	42.08	52.94	84.85	5.96	11.16
	Hashima	1.24	2.09	35.91	60.76	86.59	5.56	7.85
	Donegan No. 1 (U.S.A)	1.75	1.16	31.29	65.80	87.16	5.26	7.22
	American (U.S.A.)	1.55	1.17	26.26	71.02	87.68	4.80	7.52
	Yatake	1.26	3.04	20.54	75.16	88.71	4.35	6.94
	Shikamachi	1.16	2.52	21.16	75.16	88.76	4.70	6.54
	Amonate and Bishop (U.S.A.)	1.06	1.40	23.53	74.01	89.16	5.19	5.20
Anthracite	Uonuki	1.68	1.80	10.80	85.72	91.16	3.97	4.87
	Hongei (Indo-China)	2.08	0.98	6.14	90.80	93.02	3.26	3.72

dilatometer following the modified Bekkedahl's method[6]. The dilatometer employed in the test is shown in Fig. 3. The dilatometer consists of the capillary tube, the sample holder and the mercury holder. The inner diameter and the length of the capillary tube are 1.5 mm. and about 70 cm. respectively. The inner diameter and the length of the sample holder are 15 mm. and about 13 cm. respectively. One end of the sample holder is left open at first. About 15 g. of the air-dried sample is weighed into the sample holder. A hollow glass bulb, of which the outer diameter is a little smaller than 15 mm. and of which the height is about 3 cm., is settled in the sample holder, and then the end of the sample holder is sealed up. This method makes it possible to avoid any heating of the sample during the sealing operation. Mercury is put in the mercury holder. The coal sample in the dilatometer is evacuated to 10^{-3} mmHg for 6 to 8 hr. at room temperature in order to remove gas and then the desired volume of mercury is filled through the capillary. The dilatometer is settled in a stirring liquid paraffin bath, whose temperature is controlled under the heating rate of 1°C/min. The measurements of the height of mercury in the capillary tube were made visually, usually once every minute, from room temperature to 160°C.

The accuracy of determination of the Knoop hardness number itself has already been described in detail.[4] The scatter of the results in this indentation hardness method depends upon the inhomogeneity of the vitrain layer and the temperature control. Though the pendulum hardness is used as a conventional method in the measurements of the glass transition point of high polymers, the scatter of the results in this method may also depend upon the inhomogeneity of vitrain, the temperature control, and the error in the reading of n. The dilatometric method is the most conventional and its experimental accuracy is most high in the measurements of the glass transition point of high polymers. The surface temperature of vitrain is easily measured and precisely detected within 1°C by the thermistor having a very small thermo-sensitive element.[7] When the load is applied to the indenter, the surface temperature of vitrain decreases instantaneously. The maximum instantaneous decrease of temperature was about 2°C over the range of 50 to 100°C and about 5°C over the range of 100 to 160°C. In general, the glass transition temperature obtained by the pendulum method is considerably higher than that obtained by the dilatometric method. But this discrepancy becomes smaller by using a wedge instead of two balls as the fulcrum of the pendulum.[8]

The characteristics of various vitrains used are listed in Table I.

Results and Discussion

The relation between the Knoop hardness number, H_K, of air-dried coals and temperature is shown in Fig. 4. For brown coal, H_K

7) B. M. Zeffert and S. Hormas, *Anal. Chem.*, **21**, 1420 (1949).
8) K. Sato and Y. Inoue, *Chem. High Polymers, Japan (Kobunshi Kagaku)*, **15**, 421 (1958).

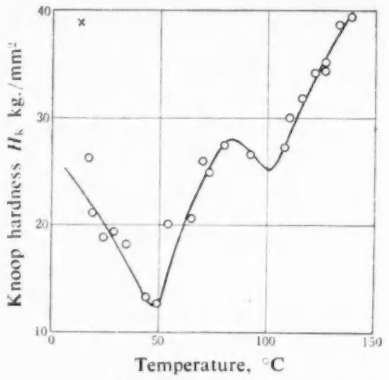

Fig. 4a. Variation of Knoop hardness with temperature for Nakagō brown coal (d. a. f. C=74.33%).

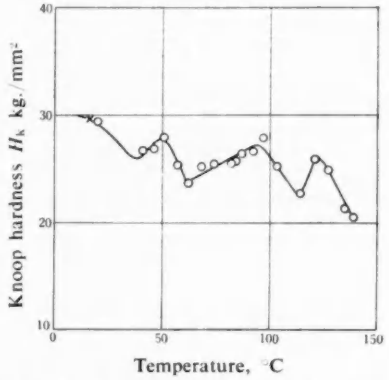

Fig. 4b. Variation of Knoop hardness with temperature for Yūbari coking coal (d. a. f. C=84.85%).

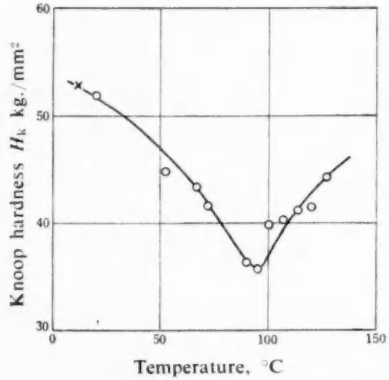

Fig. 4c. Variation of Knoop hardness with temperature for Hongei anthracite (d. a. f. C=93.02%).

decreases with temperature increase to a minimum at about 50°C, increases with temperature to a maximum, decreases again with temperature increase to a second minimum at about 100°C, and then increases with temperature. For bituminous coal H_k shows three minimum values over the range from room temperature to 160°C. For anthracite H_k decreases with temperature increase to a minimum at about 100°C, and then increases with temperature. The temperatures showing the minimum values of H_k of various air-dried vitrains are listed in the first column of Table II. Namely, over this temperature range, air-dried brown coal, bituminous coal and anthracite have two, three and one characteristic points respectively.

After the specimens heated to about 160°C were allowed to cool in an ordinary atmosphere, the Knoop hardness of the specimens was again measured at room temperature. These values of H_k at room temperature are shown by cross marks in Fig. 4. The values of H_k of the cooled bituminous coal and anthracite coincide almost exactly with those of the non-heated original coals respectively. This shows that these coals do not change their chemical constitutions if heated over the range from room temperature to about 160°C. However the value of H_k of the cooled brown coal is much higher than that of the non-heated original brown coal and the cooled brown coal has many tiny cracks on the surface. These phenomena may be attributed to the fact that some chemical reactions such as dehydration occur in the specimen of brown coal by heating over the range from room temperature to about 160°C, as if in the curing of thermosetting plastics, e. g. phenol-formaldehyde resin.

The relations between the logarithmic

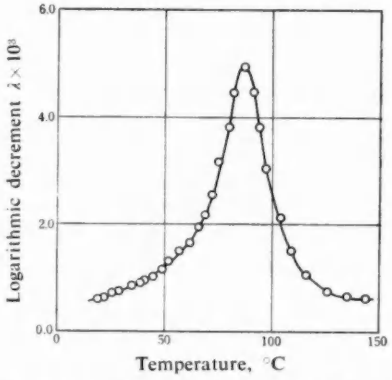

Fig. 5. Variation of logarithmic decrement with temperature for maleic acid-glycol-styrene resin.

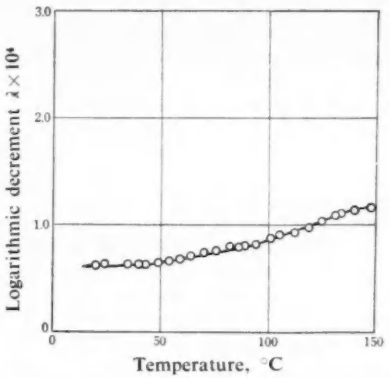

Fig. 6. Variation of logarithmic decrement with temperature for phenol-formaldehyde resin.

decrement, λ, of the pendulum on maleic acid-glycol-styrene resin, loosely cross-linked linear polymer, and phenol-formaldehyde resin (moulded C state), three-dimensional network polymer, and temperature are shown in Fig. 5 and Fig. 6 respectively. The value of λ of maleic acid-glycol-styrene resin increases suddenly with temperature to a maximum at 87°C. Thereafter the value of λ decreases suddenly with temperature increase and becomes almost the same at about 150°C as that of room temperature. This change of λ with temperature shows a typical glass transition phenomenon of loosely cross-linked linear polymer. Further, the glass transition point of maleic acid-glycol-styrene resin is 87°C. On the other hand, the value of λ of phenol-formaldehyde resin increases slowly with the temperature over the range from room temperature to 150°C and does not show a maximum. This change of λ with temperature shows a character of three-dimensional network polymer.

The relation between the logarithmic decrement, λ, of the pendulum on air-dried coals and temperature is shown in Fig. 7. For brown coal λ increases with temperature to a maximum at about 50°C, decreases with temperature increase to a minimum, increases again with temperature to a second maximum at about

Table II. Glass transition points of various vitrains

Source		Carbon (d. a. f.) %	Glass transition temperature, °C: by indentation hardness method, Air-dried coal T_{g_1}	T_{g_2}	T_{g_3}	by pendulum hardness method, Air-dried coal T_{g_1}	T_{g_2}	T_{g_3}	by dilatometric method, Air-dried coal T_{g_1}	T_{g_2}	T_{g_3}	Strongly dried coal T_{g_1}	T_{g_2}	T_{g_3}
Brown coal	Tempoku-Menashi	69.82		50	100		50	100		50	106		52	—
	Nakagō	74.33		50	100		65	110		50	117			
Bituminous coal	Takamatsu	78.95	43	70	120	30	57	120	—	51	129			
	Bibai	80.90	45	80	160									
	Ashibetsu	81.11	60	80	120	60	80	145						
	Akabira	82.29	30	80	140	35	90	116						
	Futago	83.16	48	70	105									
	Miike	84.53	40	65	95		92	125						
	Ōyūbari	84.79	50	72	96	40	70	140						
	Yūbari	84.85	38	62	113	40	67	135	29	75	145	38	61	133
	Hashima	86.59	25	50	85									
	Donegan No. 1 (U.S.A.)	87.16	35	80	93	30		105						
	American (U.S.A.)	87.68	33	70	120		80	110						
	Yatake	88.71							34	68	149	20	65	100
	Shikamachi	88.76	35	60	105	40	77	120						
	Amonate and Bishop (U.S.A.)	89.16	35	75	105		70	120						
Anthracite	Uonuki	91.16	25		90	25		105						
	Hongei (Indo-China)	93.02			95			130			122			—

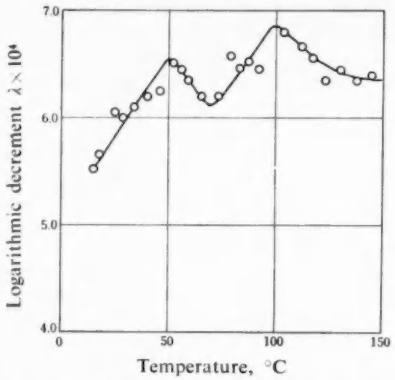

Fig. 7a. Variation of logarithmic decrement with temperature for Tempoku-Menashi brown coal (d. a. f. C=69.82%).

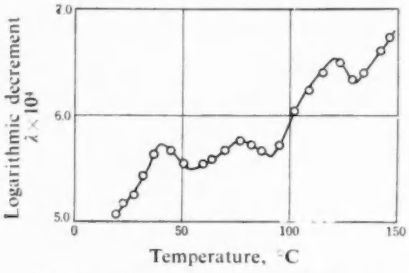

Fig. 7b. Variation of logarithmic decrement with temperature for Shikamachi coking coal (d. a. f. C=88.76%).

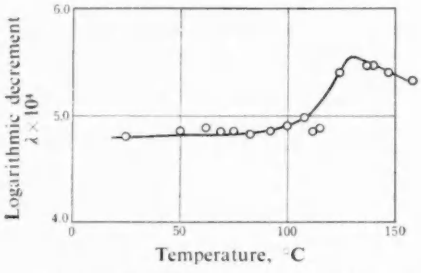

Fig. 7c. Variation of logarithmic decrement with temperature for Hongei anthracite (d. a. f. C=93.02%).

100°C, and then decreases with temperature increase. For bituminous coal λ shows three maximum values over the range from room temperature to 160°C. For anthracite λ increases with temperature to a maximum at about 130°C and then decreases with temperature increase. The temperature showing the maximum values of λ of various air-dried vitrains are listed in the second column of Table II. Over this temperature range, air-dried brown coal, bituminous coal and anthracite have two, three and one characteristic points respectively.

The relation between the reading of mercury height, V, in the glass capillary tube of dilatometer containing powdered maleic acid-glycol-styrene resin and temperature is shown in Fig. 8. The value of V increases with temperature and shows a break at 77°C. This change of V with temperature shows a typical glass transition phenomena of loosely cross-linked linear polymer. That is to say, the glass transition point of maleic acid-glycol-styrene resin obtained by the dilatometric method is 77°C and this value is slightly lower than that obtained by the pendulum method.

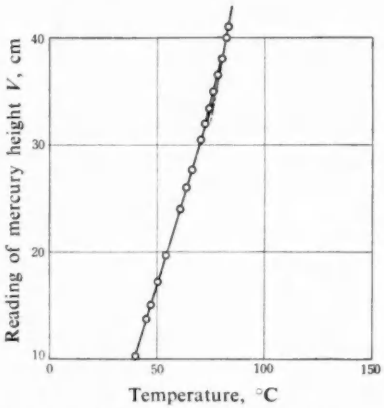

Fig. 8. Variation of reading of mercury height with temperature for maleic acid-glycol-styrene resin.

The relation between the reading of the mercury height, V, in the glass capillary tube of dilatometer containing air-dried powdered coals and heating temperature is shown in Fig. 9. As to brown coal V increases suddenly at about 50°C and again at about 100°C. For bituminous coal the sudden increase of V appears three times over the range from room temperature to 160°C, As for anthracite V increases suddenly at about 120°C. The temperatures showing the breaks of V-temperature curve of various air-dried vitrains are listed in the third column in Table II. In this case too, the characteristic points of air-dried brown coal, bituminous coal and anthracite are two, three and one respectively.

In order to ensure whether the characteristic points, especially the one at about 100°C, are affected by moisture or combined water of coals or not, the V-temperature relations of the samples dried strongly at 130 to 140°C

in vacuo of 10^{-3} mmHg for 6 to 8 hr. have been measured using the dilatometer over the range from room temperature to 160°C. The characteristic points in this case are shown in the last column of Table II. For brown coal the break of V-temperature curve at about 50°C does not vanish but the one at about 100°C disappears. For bituminous coal the three breaks coincide almost exactly with those of the air-dried sample, though the third break of the strongly dried sample somewhat diminishes. For anthracite the break at about 100°C disappears. Therefore, the V-temperature curve of bituminous coal dried at room temperature in vacuo does not show the thermal hysterisis, though those of brown coal and anthracite dried at room temperature in vacuo have the thermal hysteresis as shown in Fig. 9, if heated coals are cooled under the cooling rate of 1°C/min.

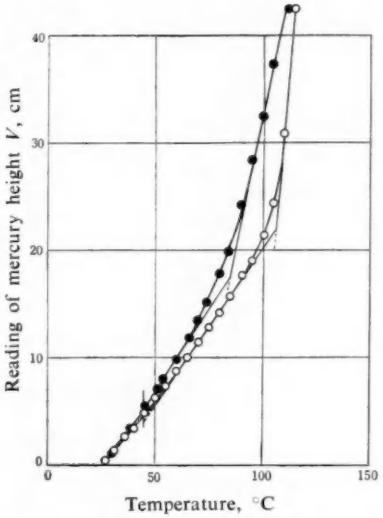

Fig. 9a. Variation of reading of mercury height with temperature for Tempoku-Menashi brown coal (d. a. f. C=69.82%).
○ heating, ● cooling

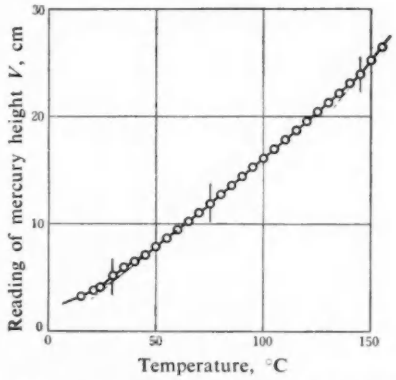

Fig. 9b. Variation of reading of mercury height with temperature for Yūbari coking coal (d. a. f. C=84.85%).

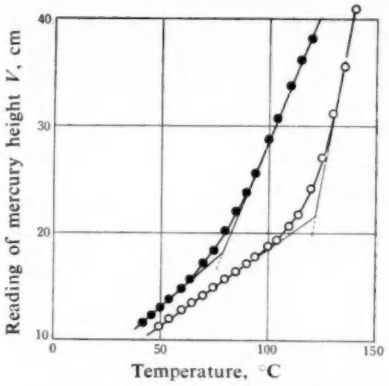

Fig. 9c. Variation of reading of mercury height with temperature for Hongei anthracite (d. a. f. C=93.02%).
○ heating, ● cooling

The influence of moisture on the characteristic points is great in brown coal and anthracite, though it is almost negligible in bituminous coal. This may be attributed to the relation between internal surface area and the rank of coal.[9] On the other hand, the glass transition point of completely dried poly(vinylalcohol), one of the hydrophilic polymers, is 73°C. When the moisture content of the sample increases, this glass transition point shifts to a lower temperature and another transition point appears at a higher temperature.[10] Consequently it may be supposed that the effects of moisture on the characteristic points of brown coal are similar to those on the transition points of poly(vinylalcohol). The disappearance of the characteristic point at about 100°C in strongly dried anthracite may be attributed to the cross-linkages among the base units which anthracite has by nature.[11]

When amorphous polymers are heated, in general, they show a minimum of indentation hardness,[12] a maximum of logarithmic decrement of the pendulum[5], and a change of slope of volume-temperature curve[13] at the glass transition point or zone. Table II shows that

9) Y. Kawana, *J. Chem. Soc. Japan, Ind. Chem. Sec.* (*Kogyo Kagaku Zasshi*), **61**, 1275 (1958).
10) Y. Sone and I. Sakurada, *Chem. High Polymers, Japan* (*Kobunshi Kagaku*), **14**, 574 (1957).
11) H. Honda and Y. Hirose, *Fuel*, **37**, 323 (1958).
12) K. Ito, *J. Japanese Soc. Mech. Eng.*, **58**, 263 (1955).
13) T. Alfrey, Jr., "Mechanical Behavior of High Polymer," Interscience, New York (1948), p. 121.

the temperatures showing minimum values of Knoop hardness, the temperatures showing maximum values of logarithmic decrement and the temperatures showing breaks of V-temperature curve of the air-dried vitrain roughly coincide with one another, though the hardness methods and the dilatometric method are independent respectively. Moreover, in the dilatometric method, the temperatures showing breaks of V-temperature curve of the strongly dried bituminous coal coincide almost exactly with those of the same air-dried sample and the temperature showing a break of V-temperature curve of the strongly dried brown coal also coincides with that of lower temperature of the same air-dried sample. Therefore it seems that these characteristic points, which are not constant but change with experimental time scale etc., are the glass transition points of coals (although D. H. Bangham and R. E. Franklin[13] did not detect them) over the range from room temperature to 160°C, though the influence of adsorbed water films can not be neglected at all.

In an investigation of microplasticity, D. H. Bangham and N. Berkowitz[14] measured the critical deformation force, F_c, at which the coal particles flowed to form a translucent film. They found that F_c does not vary uniformly with temperature, but F_c shows its maxima at 120, 200 and 300°C. Also they concluded that the undulating character of the curves representing the variation of F_c with increasing temperature is associated with monolayer films adsorbed on the internal surface of the coal which are evaporated at specific temperatures; the maximum at 120°C, they relate to the loss of water vapor from the coal structure. Results similar to those of D. H. Bangham et al. were reported by C. Ellis[15] following an investigation by a similar method.

On the other hand, J. C. Macrae and A. R. Mitchell[16] studied the shapes of the curves relating failure stress to temperature for two bituminous coals and found that the maxima at 120 and 200°C are closely similar to those reported by both D. H. Bangham et al. and C. Ellis for the F_c, at which microplasticity is observable in particles of less than 30 μ in size. They, however, emphasized that it seems probable that heating to 120°C results in an increase of the failure stress by a mechanism in the nature of a strain relief in which an increased thermal vibration modifies the effect of weakness in the coal structure upon the failure stress and influence of adsorbed water films can not be considered to be wholly acceptable.

The authors' experimental results of bituminous coals may rather give support to the opinion of J. C. Macrae et al. than those of D. H. Bangham et al. and C. Ellis.

Shigengijutsu-Shikenjo
Resources Research Institute
Kawaguchi-Saitama, Japan

14) D. H. Bangham and N. Berkowitz, *Coal Res.*, Dec., 139 (1945).

15) C. Ellis, *Publ. Instn. Gas Engrs.*, No. 436, 7 (1953).
16) J. C. Macrae and A. R. Mitchell, *Fuel*, **36**, 423 (1957).

Self-consistent Field Molecular Orbital Treatment of Benzenium Ion for a Simplified Model of Hyperconjugation

By Toshifumi MORITA

(Received December 16, 1959)

Electronic spectra of a number of aromatic carbonium ions were studied theoretically by several investigators[1]. In their explorating work which was greatly suggestive, Muller, Pickett and Mulliken[2] treated the benzenium ion by the simple LCAO MO method including self-consistent technique taking into account the variations of resonance integrals with interatomic distances and of Coulomb integrals with charge distributions. These authors as well as Morita[3,4], who tried to explain spectral shifts of the protonated methyl benzenes by

1) As to a general survey, see, T. Morita, *Progress Reports on Electronic Processes in Chemistry* (Published by the Japanese Research Group on the Electronic States), No. 1, 60 (1959) (in Japanese).

2) N. Muller, L. W. Pickett and R. S. Mulliken, *J. Chem. Phys.*, **21**, 1400 (1953); *J. Am. Chem. Soc.*, **76**, 4770 (1954).
3) T. Morita, *J. Chem. Phys.*, **25**, 1290 (1956).
4) T. Morita, This Bulletin, **31**, 322 (1958).

the methyl substituents, ignored the inter-electronic interaction. In explaining electronic spectra, the self-consistent field molecular orbital (SCF MO) treatment seems to be most satisfactory. Works going along this are those of Mackor et al.[5,6] However, hyperconjugation of the H_2–C bond of protonated aromatics was shut out of their computations. When hyperconjugation of the H_2 quasi-atom is taken into account, aromatic carbonium ions have odd numbered centers and belong to the so-called "strongly hyperconjugated" system, or system of "isovalent hyperconjugation"[2,7,8]. Morita[9] also indicated that basic properties of isomeric xylenes were interpreted considerably well in terms of hyperconjugation of the H_2–C bond in their protonated compounds. Owing to reasons mentioned above, it seems to be of great significance to carry out the SCF MO calculations, taking the hyperconjugative effect into consideration. However, even in the benzenium ion, the simplest of the aromatic carbonium ions, the SCF MO calculation is rather cumbersome and simplification of the model for computation of hyperconjugation may be desired. This paper contains simplification of the model for hyperconjugation in the semiempirical SCF LCAO MO method and discussion of importance of hyperconjugation deduced from the calculated results for the hyperconjugation model compared with those for the bond localization model of the benzenium ion, a prototype of the aromatic carbonium ions.

A Model for Hyperconjugation in the Semi-empirical SCF MO Method

From the proton magnetic resonance absorption measurement of aromatic carbonium ions, MacLean, van der Waals and Mackor[10] showed that, when a bond was formed between a proton and a carbon atom in an aromatic hydrocarbon ring, valence state of the carbon atom attacked by a proton was altered from sp^2- to sp^3-hybridization. Accordingly, the configuration of the methylene group constructed at the position of proton attack should be tetrahedral. In a technique for the theory of hyperconjugation, however, it is customary, subject to Mulliken's original idea[11], to assume the sp^2-hybridized carbon atom and group orbitals of H_2, $\psi_1=2^{-1/2}(1+S)^{-1/2}(h_a+h_b)$ and $\psi_2=2^{-1/2}(1-S)^{-1/2}\times(h_a-h_b)$: ($h_a$, h_b: 1s orbital of hydrogen atoms a and b; S: overlap integral between H atoms). Of the two group orbitals ψ_1 and ψ_2, ψ_1 forms σ-bond and ψ_2 π-bond, the latter being in conjugation with the benzene ring. Aono[12], in his non-empirical SCF MO treatment of hyperconjugation in methylacetylene, replaced one of the H_3 group orbitals by the $2p\pi$ carbon orbital itself and assumed the distance between this orbital and the next carbon to be the same as the length of the C–H bond of the methyl group. We intend, however, in the following way, to treat the orbital ψ_2 in question as the quasi-$2p\pi$ orbital and to give a reasonable value of the distance between this quasi-$2p\pi$ and the next lying carbon $2p\pi$ orbitals.

In the SCF MO calculations, the quantities associated with the ψ_2 orbital, which embody its characteristics well, are its energy and the effective nuclear charge of H_2^+ core. The former determines the valence state ionization potential of the H_2 group and the latter contributes to the estimation of interelectronic Coulomb repulsion integrals. In consequence, the matter reduces to the estimation of these quantities. The energy of the ψ_2 orbital is calculated from

$$W(\psi_2)=\int \psi_2^* H \psi_2 d\tau \qquad (1)$$

using the Hartree-Fock type Hamiltonian,

$$H=T+U,\ U=-\frac{1}{r_a}-\frac{1}{r_b}+(\psi_1\psi_1\mid -\frac{1}{2}(\psi_1\mid\psi_1 \qquad (2)$$

where, $1/r_i$ is the operator showing the potential energy from the i'th hydrogen nucleus; $(\psi_1\psi_1\mid$ and $(\psi_1\mid\psi_1$ are respectively electronic Coulomb and exchange potential energy operators. $I(H_2)=-W(\psi_2)$ indicates the valence state ionization potential of the H_2 group. For the isoelectronic series of C, N^+ and O^{++}, the empirical relation between valence state ionization potentials (I_μ) and effective nuclear charges (Z_μ) determined using the Slater rule for $2p\pi$ orbitals is formulated by the use of energy values of appropriate valence state[13] and of the atomic spectroscopic data[14]. Knowledge of $I(H_2)$, hence, enables us to obtain the effective nuclear charge $Z(\psi_2)$ associated with the ψ_2 orbital. The $Z(\psi_2)$ value is also determined by the alternative method. Subject to Paoloni[15] an empirical relation exists between the nuclear effective charges obtained by the use of Slater rule and one center electronic Coulomb repulsion integrals, for the first row atoms, as follows:

$$(\mu\mu\mid\mu\mu)=3.29_4 Z_\mu \qquad (3)$$

The calculated value of one center Coulomb repulsion integral on the ψ_2 orbital, $(\psi_2\psi_2\mid\psi_2\psi_2)$, allows us to estimate the value of the effective nuclear charge associated with the ψ_2 orbital by the use of Eq. 3.

5) A. A. V. Stuart and E. L. Mackor, *J. Chem. Phys.*, **27**, 826 (1957).
6) G. Dallinga, E. L. Mackor and A. A. V. Stuart, *Mol. Phys.*, **1**, 123 (1958).
7) N. Muller and R. S. Mulliken, *J. Am. Chem. Soc.*, **80**, 3489 (1958).
8) R. S. Mulliken, *Tetrahedron*, **5**, 253 (1959).
9) T. Morita, This Bulletin, **32**, 893 (1959).
10) C. MacLean, J. H. van der Waals and E. L. Mackor, *Mol. Phys.*, **1**, 247 (1958).
11) R. S. Mulliken, C. A. Riecke and W. G. Brown, *J. Am. Chem. Soc.*, **63**, 41 (1941); see also, C. A. Coulson, "Valence", Oxford University Press, London (1952), p. 310.
12) S. Aono, *Busseiron Kenkyu*, No. 94, p. 24 (1956).
13) H. A. Skinner and H. O. Pritchard, *Trans. Faraday Soc.*, **49**, 1254 (1953); see also, R. S. Mulliken, *J. Chem. Phys.*, **2**, 782 (1934).
14) Landolt-Börnstein, "Zahlenwerte und Funktionen", I Band, 1 Teil Springer, Berlin (1950); C. E. Moore, "Atomic Energy Levels", Vol. I, N. B. S., Circular 467 (1949).
15) L. Paoloni, *Nuovo Cimento*, **4**, 410 (1956).

The distance between the quasi-$2p\pi$ and the next lying carbon $2p\pi$ orbitals may be estimated in the following way. The interelectronic Coulomb integral between ϕ_2 and the next lying carbon $2p\pi$ orbitals is evaluated legitimately by the equation[16] (cf. Fig. 1),

$$(\phi_2\phi_2 \mid 2p\pi C\ 2p\pi C) = [(aa \mid CC) - (ab \mid CC)]/(1-S) \quad (4)$$

The empirical formula indicating the same quantity may be formulated by the Pariser-Parr's method[17] using the value of the effective nuclear charge $Z(\phi_2)$ obtained by either $I_\mu \sim Z_\mu$ relation or Eq. 3, this being a functional relation of the distance $r(H_2\text{-}C)$ between ϕ_2 and carbon $2p\pi$ orbitals. By putting the value obtained by Eq. 4 into this empirical formula, the distance $r(H_2\text{-}C)$ in question may be evaluated.

Core integral $\beta_{H_2\text{-}C}$ between H_2 and C can be obtained by the assumption of the proportionality relation,

$$\beta_{H_2\text{-}C}/\beta = S_{H_2\text{-}C}/S \quad (5)$$

where, β is the core integral in benzene molecule; S the overlap integral between two carbon $2p\pi$ orbitals separated by 1.39Å; $S_{H_2\text{-}C}$ the overlap integral between carbon $2p\pi$ and next lying H_2 quasi-$2p\pi$ orbitals.

As above mentioned, the role of the methylene in the SCF MO method may be understood in the simplified manner.

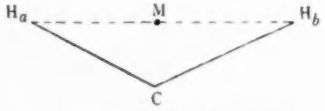

Fig. 1. Assumed geometrical structure of CH_2. $C\text{-}H_a = C\text{-}H_b = 1.071$ Å, $\angle H_aCH_b = 120°$.

In the actual calculation, geometrical structure of $C\text{-}H_2$ assumed is the same as that of ethylene by Gallaway and Barker[18] and is indicated in Fig. 1; $C\text{-}H_a = C\text{-}H_b = 1.071$ Å, $H_aCH_b = 120°$. (Assumption of $\angle H_aCH_b = 109°28'$ does not seriously affect the calculated results). Semi-empirically calculated values of the quantities determining the model for hyperconjugation are shown in Table I. Although the procedure of this paper goes along the approximation including zero differential overlap by Pariser-Parr[19], or Pople[20], it is desirable to obtain $W(\phi_2)$ with moderate exactness. Indeed, the value calculated with neglect of differential overlap is -11.834 eV., and unsuitable for our purpose, if we remember the valence state ionization potential of the $2p\pi$ carbon is 11.54 eV. The value calculated with inclusion of differential overlap is -11.176 eV. and this value also may not be said to be appropriate. The moderate value, -10.256 eV., is obtained omitting the interelectronic Coulomb integral, $(ab \mid ab)$[21].

Using the value, 2.83, of the effective nuclear charge $Z(\phi_2)$, estimated from Eq. 3, the empirical formula of the interelectronic Coulomb integral $(H_2H_2 \mid CC)$ is obtained as follows,

$$(H_2H_2 \mid CC) = 10.203 - 2.4607r + 0.1933r^2 \quad (r \leq 2.8\text{A}) \quad (6)$$

Substituting the value of $(\phi_2\phi_2 \mid 2p\pi C\ 2p\pi C)$ in the $C\text{-}H_2$ group calculated from Eq. 4 into Eq. 6, the distance $r(C\text{-}H_2)$ between quasi-$2p\pi$ and carbon $2p\pi$ orbitals in the $C\text{-}H_2$ group is estimated as 1.383 and 1.031 Å for the cases with and without differential overlap. (For the case with differential overlap, $r(H_2\text{-}C)$ is estimated to be 1.031 Å from somewhat different equation from Eq. 6 based on somewhat different value of $Z(\phi_2)$). It will be noticed here that when differential overlap is neglected Eq. 4 reduces to

$$(\phi_2\phi_2 \mid 2p\pi C\ 2p\pi C) = (aa \mid CC) \quad (7)$$

It is clear that this approximation 7 is too crude. It is desirable, therefore, to adopt for $r(H_2\text{-}C)$ the middle value between 1.031 and 1.383 Å.

We have performed calculations by the use of some assumed values of $r(H_2\text{-}C)$ between 1.031 and 1.383 Å, and, for $r(H_2\text{-}C) = 1.10$ Å, obtained satisfactory results in agreement with experimental observations. Hence, we describe below on the assumption of $r(H_2\text{-}C) = 1.10$Å. Table I indicates the semi-empirically fixed values of quantities determining the model of hyperconjugation for $C\text{-}H_2$ group (values on the last row of Table I are referred to in the next paragraph).

Somewhat larger value of the C-H distance than that usually accepted in aliphatic hydrocarbons is seen in some papers[22] published after our calculations have finished. Reasonable assumption of $r(H\text{-}C) = 1.11$Å based on these papers leads to $r(H_2\text{-}C) = 1.10$Å by the similar calculations with

16) T. Morita, *J. Chem. Phys.*, **27**, 1442 (1957).
17) R. Pariser and R. G. Parr, ibid., **21**, 767 (1953).
18) W. S. Gallaway and E. F. Barker, ibid., **10**, 88 (1942).
19) R. Pariser and R. G. Parr, ibid., **21**, 466 (1953).
20) J. A. Pople, *Trans. Faraday Soc.*, **49**, 1375 (1953); *J. Phys. Chem.*, **61**, 6 (1957).

21) In the semi-empirical calculation of $W(\phi_2)$, it is assumed that $\int \frac{h_a h_a}{r_b} d\tau = (aa \mid bb)$ and $\int \frac{h_a h_b}{r_b} d\tau = (ab \mid bb) = S\,(MM \mid bb)$, where M is the midpoint of $H_a\text{-}H_b$ (Fig. 1). We also obtained $W(\phi_2) = -9.602$ eV. by the non-empirical calculation. Of these four values $W(\phi_2) = -10.256$ eV. is the most appropriate. In our calculations was omitted the correction to be considered in evaluating one center Coulomb repulsion integral $(1s1s \mid 1s1s)$. See, R. D. Brown, *Mol. Phys.*, **1**, 304 (1958).

22) a) K. Kuchitsu, This Bulletin, **32**, 748 (1959); R. A. Bonham, L. S. Bartell and D. A. Kohl, *J. Am. Chem. Soc.*, **81**, 4765 (1959). These authors revealed by the sectormicrophotometer method of electron diffraction that the C-H distances in *n*-butane, *n*-pentane, *n*-hexane and *n*-heptane are 1.100 ± 0.003, 1.118 ± 0.0004, 1.118 ± 0.006 and 1.121 ± 0.007Å, respectively.

b) B. K. Vainshtein, *Kristallografiya*, **3**, 452 (1958); *Chem. Abstr.*, **52**, 19299 (1958). Vainshtein showed that the C-H distance in solid paraffins is 1.123 ± 0.015Å.

c) For ethylene also, recent measurements show somewhat larger value of the C-H distance; see, L. S. Bartell and R. A. Bonham, *J. Chem. Phys.*, **27**, 1414 (1957); H. C. Allen, Jr. and E. K. Plyler, *J. Am. Chem. Soc.*, **80**, 2673 (1958).

d) It ought to be noticed here that the problem of the C-H bond distance has been recently discussed in a wider scope. See, H. J. Bernstein, *J. Phys. Chem.*, **63**, 565 (1959); L. E. Sutton, *Tetrahedron*, **5**, 118 (1959); M. J. S. Dewar and H. N. Schmeising, ibid., **5**, 166 (1959); R. S. Mulliken, ibid., **6**, 68 (1959).

Table I. Semi-empirically fixed values of quantities determining the model of hyperconjugation for C-H_2 group

$W(\phi_2)$	$(\phi_2\phi_2 \mid \phi_2\phi_2)$	$Z(\phi_2)$	$(\phi_2\phi_2 \mid 2p\pi C 2p\pi C)$	$r(H_2\text{-}C)$
eV.	eV.		eV.	Å
−10.256	9.326	2.83	7.73	1.10
−10.373	9.214	2.80	7.73	1.10

zero differential overlap to those mentioned above. Values of quantities relating to hyperconjugation of C-H_2 group are listed on the last row of Table I, and these are almost identical with those mentioned in the preceding paragraph, hence leading to seriously unaffected results.

At any rate we assume for the orbital of H_2 group, which take part in hyperconjugation with the residual part of the molecule, the $2p\pi$ orbital, associated with the effective nuclear charge, 2.83, and standing at a distance, 1.10 Å, from the carbon $2p\pi$ orbital in the methylene group.

The SCF LCAO MO CI calculation for benzenium ion whose co-ordinate system and numbering are as indicated in Fig. 2, is carried out by means of Poples scheme[23] which is based on the theory of Roothaan[24] and combined with Pariser-Parr's approximation[17,19]. The technical procedure for computation is described elsewhere[23,25,26]. What should be stated here is that the core integral $H_{\mu\mu}$ is assumed as follows,

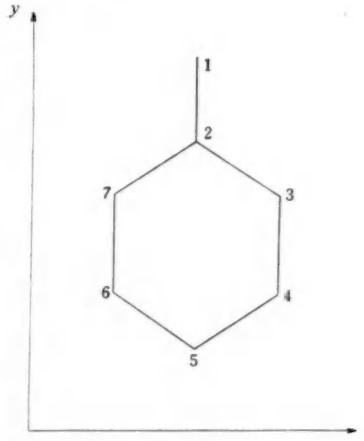

Fig. 2. Co-ordinate system and numbering of benzenium ion for computation.
$\overline{12}=1.10$ Å, $\overline{23}=\overline{34}=\cdots\cdots=\overline{72}=1.39$ Å

$$H_{\mu\mu}=U_{\mu\mu}-\sum_{\alpha(\neq\mu)}{}'(\mu \mid V_\alpha \mid \mu)$$
$$=U_{\mu\mu}-\sum_{\alpha(\neq\mu)}{}'Z_\alpha(\mu\mu \mid \alpha\alpha) \qquad (8)$$

where, Z_α is assumed to be unity.

The approximation of Eq. 8, which Sidman[27] also assumed, leads to that of Pariser and Parr[17,19].

The value of the core integral β is taken to be −2.39 eV. except for $\beta_{H_2\text{-}C}$ which is estimated to be −4.111 eV. from Eq. 5. Values of valence state ionization potentials are taken from the tables of Skinner and Pritchard[18]. Values of electronic Coulomb repulsion integrals are evaluated using Pariser-Parr's approximations[17].

Results and Discussion

(a) Self-consistent Field Molecular Orbitals. —SCF MO's calculated and expressed by the linear combination of atomic orbitals, χ_μ, for the models of hyperconjugation and bond localization are shown in Tables II (A) (hyperconjugation) and II (B) (bond localization), which include also the energies, ε, of MO's. The highest occupied molecular orbital is ϕ_3 in each case and $-\varepsilon_3$ correspond to the ionization potential.

Table II. Calculated self-consistent field molecular orbitals and energies

(A) For the hyperconjugation model

$\varepsilon_1=-21.379$ eV. $\phi_1(1b_2)=0.500\chi_1+0.715\chi_2+0.294(\chi_3+\chi_7)+0.151(\chi_4+\chi_6)+0.143\chi_5$

$\varepsilon_2=-18.381$ eV. $\phi_2(2b_2)=0.248\chi_1+0.239\chi_2-0.103(\chi_3+\chi_7)-0.462(\chi_4+\chi_6)-0.658\chi_5$

$\varepsilon_3=-16.592$ eV. $\phi_3(1a_2)=0.464(\chi_4-\chi_6)+0.534(\chi_3-\chi_7)$

$\varepsilon_4=-8.249$ eV. $\phi_4(3b_2)=0.561\chi_1-0.043\chi_2-0.503(\chi_3+\chi_7)-0.045(\chi_4+\chi_6)+0.416\chi_5$

$\varepsilon_5=-5.607$ eV. $\phi_5(2a_2)=0.534(\chi_4-\chi_6)-0.464(\chi_3-\chi_7)$

$\varepsilon_6=-4.083$ eV. $\phi_6(4b_2)=0.461\chi_1-0.396\chi_2+0.012(\chi_3+\chi_7)+0.408(\chi_4+\chi_6)-0.545\chi_5$

$\varepsilon_7=-2.122$ eV. $\phi_7(5b_2)=0.400\chi_1-0.523\chi_2+0.548(\chi_3+\chi_7)-0.437(\chi_4+\chi_6)-0.274\chi_5$

(B) For the bond localization model

$\varepsilon_1=-19.757$ eV. $\phi_1(1b_2)=0.644\chi_1+0.765\chi_2$

$\varepsilon_2=-19.198$ eV. $\phi_2(2b_2)=0.214(\chi_3+\chi_7)+0.484(\chi_4+\chi_6)+0.664\chi_5$

$\varepsilon_3=-17.056$ eV. $\phi_3(1a_2)=0.457(\chi_4-\chi_6)+0.540(\chi_3-\chi_7)$

$\varepsilon_4=-8.277$ eV. $\phi_4(3b_2)=0.602(\chi_3+\chi_7)+0.085(\chi_4+\chi_6)-0.512\chi_5$

$\varepsilon_5=-6.023$ eV. $\phi_5(2a_2)=0.540(\chi_4-\chi_6)-0.457(\chi_3-\chi_7)$

$\varepsilon_6=-3.684$ eV. $\phi_6(4b_2)=0.765\chi_1-0.644\chi_2$

$\varepsilon_7=-3.678$ eV. $\phi_7(5b_2)=0.304(\chi_3+\chi_7)-0.509(\chi_4+\chi_6)+0.545\chi_5$

23) J. A. Pople, *Proc. Phys. Soc.* (*London*), **A 68**, 81 (1955).
24) C. C. J. Roothaan, *Revs. Mod. Phys.*, **23**, 69 (1951).
25) N. Mataga and K. Nishimoto, *Z. physik. Chem., N. F.*, **13**, 140 (1957).
26) As to the expressions for the interconfigurational matrix elements, see, Ref. 23 and also, R. Pariser, *J. Chem. Phys.*, **24**, 250 (1956). As to the expression for the oscillator strength, see, R. Pariser, loc. cit.
27) J. W. Sidman, ibid., **27**, 429 (1957).

(b) **Electronic Spectra.**—In the calculations with configurational interactions (CI), the singlet configurations considered of excited states for $^1B_1$ symmetry are $V_{3\to4}$, $V_{3\to6}$ and $V_{2\to5}$; those for $^1A_1$ symmetry are $V_{2\to4}$, $V_{3\to5}$ and $V_{1\to4}$. Table III shows, for the hyperconjugation model, the wave functions of excited states with the values of matrix elements.

Electronic spectra theoretically calculated are denoted in Tables IV, V and Fig. 3. The calculated energy of the first transition is, for example, in the case with no configuration interactions, considerably larger for the bond localization model than for the hyperconjugation (Table IV). This suggests that the hyperconjugative effect would possibly be much larger in such a system of isovalent hyperconjugation as benzenium ion than is in the ordinary hyperconjugated molecules.

It is seen in Fig. 3, that the order of excited configurations differs considerably between bond localization and hyperconjugation models.

As the experimental absorption data for protonated compounds of benzene and methylbenzenes are referred those of Reid[28], of Kilpatrick and Hyman[29], as well as of Dallinga, Mackor and Stuart[6]. Among these, the data of Kilpatrick-Hyman and Dallinga-Mackor-Stuart coincide with each other for methylbenzenes. Methyl shifts of the spectra by these investigators are reasonably bathochromic, while are hypsochromic by Reid's measurements. We take up, therefore, the data by Dallinga, Mackor and Stuart, 3700, 2600 and 2000 Å absorptions for benzenium ion, although the experimental extinction curve has not been given explicitly. Theoretical data agree satisfactorily with those experimentally observed (Table V). The oscillator strengths calculated also coincide, in the tendency, with the experimental extinction coefficients by Dallinga, Mackor and Stuart[6] for the protonated compounds of some methylbenzenes. Among these, for example, the mesitylene carbonium ion has the following values of the molar extinction coefficients, 11100, 8800, >13000, respectively, for the first, second and third bands. Further the calculated oscillator strengths by Dallinga, Mackor and Stuart are cited in Table V. These also agree well with our values.

It is striking that the hyperconjugation shift of the first absorption band is, as is seen in Table IV, toward red, while it is, in the Hückel MO calculations, toward blue. Indeed, our Hückel MO calculations using $\alpha_1=\alpha-0.4\beta$ show for the first transition energy the values 1.0709 $(-\beta)$ and 1.0000 $(-\beta)$, of which the former refers to the hyperconjugation and the latter to the bond localization model[30]. By means of the semi-empirical ASMO method also the similar tendency is seen. In performing the semi-empirical ASMO calculations our

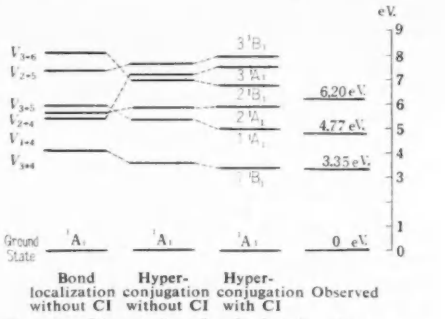

Fig. 3. Observed and calculated π-electron configurational energy levels.

TABLE III. WAVE FUNCTIONS OF EXCITED STATES WITH THE VALUES OF THE MATRIX ELEMENTS

$^1B_1$-Symmetry

$\Phi(1\,^1B_1)=0.985\,V_{3\to4}-0.017\,V_{3\to6}-0.174\,V_{2\to5}$
$\Phi(2\,^1B_1)=0.082\,V_{3\to4}+0.924\,V_{3\to6}+0.373\,V_{2\to5}$
$\Phi(3\,^1B_1)=0.155\,V_{3\to4}-0.381\,V_{3\to6}+0.911\,V_{2\to5}$
$\{V_{3\to4}\mid V_{3\to6}\}=-0.00988$ eV.
$\{V_{3\to4}\mid V_{2\to5}\}=0.73213$ eV.
$\{V_{3\to6}\mid V_{2\to5}\}=-0.39409$ eV.
$\{V_{3\to4}\mid V_{3\to4}\}=-204.03227$ eV.
$\{V_{3\to6}\mid V_{3\to6}\}=-200.64365$ eV.
$\{V_{2\to5}\mid V_{2\to5}\}=-199.98658$ eV.

$^1A_1$-Symmetry

$\Phi(1\,^1A_1)=0.884\,V_{2\to4}+0.445\,V_{3\to5}+0.143\,V_{1\to4}$
$\Phi(2\,^1A_1)=0.370\,V_{2\to4}-0.854\,V_{3\to5}+0.366\,V_{1\to4}$
$\Phi(3\,^1A_1)=0.285\,V_{2\to4}-0.271\,V_{3\to5}-0.919\,V_{1\to4}$
$\{V_{2\to4}\mid V_{3\to5}\}=-0.45738$ eV.
$\{V_{2\to4}\mid V_{1\to4}\}=-0.52381$ eV.
$\{V_{3\to5}\mid V_{1\to4}\}=0.34067$ eV.
$\{V_{2\to4}\mid V_{2\to4}\}=-202.22097$ eV.
$\{V_{3\to5}\mid V_{3\to5}\}=-201.73760$ eV.
$\{V_{1\to4}\mid V_{1\to4}\}=-200.36226$ eV.

TABLE IV. TRANSITION ENERGIES CALCULATED WITHOUT CONFIGURATION INTERACTIONS

Bond localization model (eV.)	Hyperconjugation model (eV).
0 (ground state)	0 (ground state)
4.116 ($V_{3\to4}$)	3.529 ($V_{3\to4}$)
5.358 ($V_{1\to4}$)	5.341 ($V_{3\to5}$)
5.621 ($V_{2\to4}$)	5.824 ($V_{2\to4}$)
5.864 ($V_{3\to5}$)	6.918 ($V_{3\to6}$)
7.344 ($V_{2\to5}$)	7.199 ($V_{1\to4}$)
7.959 ($V_{3\to6}$)	7.575 ($V_{2\to5}$)

28) C. Reid, *J. Am. Chem. Soc.*, **76**, 3264 (1954).
29) M. Kilpatrick and H. H. Hyman, ibid., **80**, 77 (1958).
30) The Hückel MO method for toluenium and mesitylenium ions also shows the hypsochromic shift for the hyperconjugative effect. See, Refs. 3 and 4.

TABLE V. CALCULATED ELECTRONIC SPECTRA FOR HYPERCONJUGATION MODEL COMPARED WITH EXPERIMENTS

Symmetry	Polarization	Transition energies for hyperconjugation with CI (eV.)	Transition energies observed (eV.)	Oscillator strengths calculated	
$1\ ^1B_1$	x	3.400	3.35	0.219[a]	(0.21)[b]
$1\ ^1A_1$	y	5.025	4.77	0.012[a]	(0.06)[b]
$2\ ^1A_1$	y	5.876	6.20	0.630[a]	(0.99)[b]
$2\ ^1B_1$	x	6.758		0.117[a]	
$3\ ^1A_1$	y	7.462		0.017[a]	
$3\ ^1B_1$	x	7.864		0.354[a]	

a) These values are calculated by the use of the wave functions in Table III.
b) Values in parentheses are those calculated by Dailinga, Mackor and Stuart; see, Ref. 6.

TABLE VI. ENERGIES OF THE FIRST TRANSITION CALCULATED BY THE HÜCKEL AND PARISER-PARR METHODS

	Hückel method	Pariser-Parr's method	Modified Hückel method	Modified Pariser-Parr's method
Hyperconjugation	1.0709 $(-\beta)$	3.798 eV.	1.0709 $(-\beta)$	3.798 eV.
Bond localization	1.0000 $(-\beta)$	3.575 eV.	1.0833 $(-\beta)$	3.864 eV.

procedure is almost the same as that for toluene by Morita[16]. The value of the core integral β_{H_2-C} used is -4.435 eV., which is somewhat different from that in the semi-empirical SCF MO method extended in the early part of this paper. Values of the atomic integrals also differ from those used in the SCF MO method. This does not prevent us, however, from judging the calculated results. The calculated energies for the first transition are 3.798 eV. for the hyperconjugation model and 3.575 eV. for the bond localization.

This discrepancy between the results of the SCF MO and ASMO methods might be taken off by introducing the laborious technique of configurational interaction. This seems to be in vain, however, if we take into account the same extent of configurations as in the SCF MO calculations. If any simple modification is tried, however, for the naive and the anti-symmetrized molecular orbital calculations, the identical tendency in all cases will be accomplished.

The modification is done as follows. In the bond localization model, as is seen in Fig. 4, the π-electron system is cut off into two parts, one being the system 1-2 (A), the other the system 3-4-5-6-7 (B). In the part B, terminal carbons (3 and 7) seem to be electropositive compared to the inner carbons[31]. Consequently, we should give negative value of δ for the Coulomb integral α_3 or $\alpha_7=\alpha+\delta\beta$. We have no thorough materials which suggest the exact way determining the value of δ in this case. It may not be said, however, that the

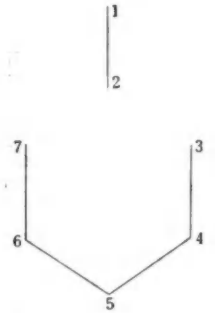

Fig. 4. The effective π-electron system of the benzenium ion for its bond localization model.

leectropositiveness of the carbon atom 3 or 7 is not satisfactory when it is equated to that of the H_2 group. Hence, we assume, for a moment, $\alpha_3=\alpha_7=\alpha-0.4\beta$. The corresponding modification in the ASMO method is to equalize I_3 (the valence state ionization potential of the carbon atom 3 or 7) to $I(H_2)$ (the valence state ionization potential of the H_2 group, namely $I(H_2)=-W(\phi_2)=-\int\phi_2^*H\phi_2 d\tau$) in the formula expressing the core integral α_3 or α_7 (Pariser-Parr's notation)

$$\alpha_3=\alpha_7=-I_3-\sum_{\nu\neq 3}{}' (33\mid\nu\nu) \qquad (9)$$

(Although the electronic Coulomb repulsion integrals, $(33\mid\nu\nu)$, have to take different values corresponding to the change in I_3, this correction may be omitted for the present purpose.) These modifications in the naive and antisymmetrized molecular orbital methods lead to the

31) R. G. Parr and R. S. Mulliken, *J. Chem. Phys.*, **18**, 1338 (1950).

same tendency as in the SCF MO method with regard to the absorption spectra. Calculated results are indicated in Table VI.

(c) Charge Densities and Bond Orders.—Fig. 5 shows π-electron densities and π-bond orders calculated for the hyperconjugation and bond localization models.

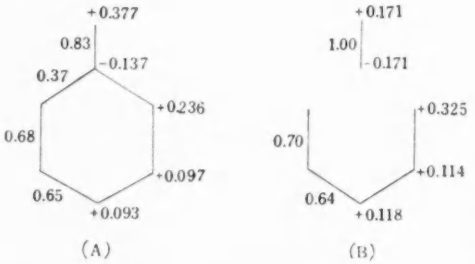

Fig. 5. Calculated formal charges (unit of $+e$) and π-bond orders of benzenium ion.
A: hyperconjugation, B: bond localization

The proton magnetic resonance spectra of pentamethylbenzene in $CF_3COOH+H_2O\cdot BF_3$ and in $HF+BF_3$ show for the methyl groups the following shifts compared to the benzene proton signal; 196, 199, 204 and 180, 187, 198 (in c/sec.) in each case[10]. The manner in which the assignment of the signals is undertaken is different, according as which model, hyperconjugation or bond localization, is adopted. Namely, the hyperconjugation model predict the signals 196, 199, 204 or 180, 187, 198 (in c/sec.) attributing, in order, to the methyl groups at the positions 3, 4, 5; in contrast, for the bond localization model, these signals should be assigned to the methyl groups at the positions 3, 5, 4 in order. This discrepancy will probably be due to the crudeness of approximations. It will be probably necessary, in the configurational interaction calculations, to take into account further more configurations including the ground state configuration, V_0, which is shut out of our computations.

(d) Hyperconjugation Energy.—The hyperconjugation energy is obtained by subtracting the energy of hyperconjugation model from that of bond localization one, taking further the compressional energy correction into consideration. The compression energy is evaluated on the assumption of harmonical distortion of a bond. Calculated energy of hyperconjugation is 19.7 kcal./mol., which is much larger than in the case of the ordinary hyperconjugation.

Summary

Semi-empirical SCF LCAO MO calculations of benzenium ion was undertaken for the model of localization as well as hyperconjugation of the H_2–C bond constructed at the position of proton attack. A simplified model of hyperconjugation in the semi-empirical SCF MO method was extended. Calculated results for the hyperconjugation model agreed satisfactorily with the experimental electronic spectra.

Superiority of the SCF MO method to the Hückel MO or ASMO method was indicated in connection with the ordinarily accepted spectral shift through hyperconjugation. Further, some modifications were tried, for the bond localization model, which would have to be taken in the Hückel MO as well as ASMO calculations.

The proton magnetic resonance signals due to methyl substituents in the carbonium ions of methylbenzenes were discussed from charge densities of benzenium ion.

The author wishes to thank Professor T. Titani, Tokyo Metropolitan University, for his interest and to Professors A. Kotera, Tokyo University of Education, and S. Nagakura, the University of Tokyo, and Mr. Y. Mori, Tokyo Institute of Technology, for their kind advices and helpful discussions. This work was financially supported by a grant-in-aid from the Ministry of Education.

Department of Chemistry
Tokyo Metropolitan University
Setagaya-ku, Tokyo

Studies on Constituents of Coal Carbonization Light Oil. I. On Saturated Hydrocarbons Contained in High-temperature Coal Carbonization Light Oil

By Hiroshi YASUI

(Received December 23, 1959)

Constituents and their contents of coal carbonization light oil, are influenced by their carbonization temperature. It has been reported, that components contained in high-temperature coal carbonization light oil differ from those in low-temperature coal carbonization light oil, qualitatively and quantitatively[1,2]. Apparently, such constituents of low-temperature coal carbonization light oil are mainly saturated hydrocarbons and less aromatic and unsaturated hydrocarbons. By contrast, those of high temperature coal carbonization light oil are mainly aromatic and less saturated and unsaturated hydrocarbons. In the studies on the constituents of high-temperature coal carbonization, nearly all the aromatic hydrocarbons contained in the light oil have been determined[3-5]. But the saturated hydrocarbons in the light oil are not present in any large quantity, but separation of these saturated hydrocarbons is difficult, resulting data of such separation being scanty. Saturated hydrocarbons contained in the light oil, previously reported, are *n*-heptane[6-8], octane[9], *n*-decane[10,11] as *n*-paraffin, and 2, 2, 4-trimethylpentane[6,7] and 3-ethyl-3-metylpentane[12] as isoparaffin, and cyclopentane[10], methylcyclopentane[6,10] cyclohexane[7,8,10], methylcyclohexane[10], 1, 2-, 1, 3- and 1, 4-dimethylcyclohexane[10], 1, 3, 5-[13] and 1, 2, 4-trimethylcyclohexane[14] and 1, 2, 4, 5-tetramethylcyclohexane[13] as cycloparaffin. While, the presence of *n*-decane, *n*-undecane and 1, 2, 3, 4-tetramethylcyclohexane in solvent naphtha produced from Yawata Iron & Steel Co., Ltd. in 1949, has been already ascertained by S. Kimura and the author[15]. In this research, the author has ascertained and identified the saturated hydrocarbons contained in benzene[16,17], toluene[17,18] and solvent naphtha fractions[19,20] separated from high-temperature coal carbonization light oil (carbonization temperature, 1250°C) of Yawata Iron & Steel Co., Ltd. in 1952.

Experimental

Materials. — Crude Saturated Hydrocarbon Oil Obtained from Benzene Fraction.—A residual oil after chlorination of benzene fractiton (b. p. 79.5~81°C) at Nihon Kayaku Co., Ltd., which is colorless oil and has $d_4^{20}=0.7755$ and $n_D^{20}=1.444$, was used as material.

Toluene Fraction.—Toluene fraction purified by treatment with conc. sulfuric acid, manufactured by Yawata Iron & Steel Co., Ltd. in January, 1952, a colorless oil of b. p. 110.3~111.2°C, $d_4^{20}=0.8633$ and $n_D^{20}=1.493$, was used as material.

Solvent naphtha.—Solvent naphtha prepared at Yawata Iron & Steel Co., Ltd. in January, 1952, consisting of 17.8% of 10°-xylene (136~142°C fraction), 40.5% of solvent naphtha I (125~172°C fraction) and 41.7% of solvent naphtha II (149~203°C fraction) in proportion to each rate of production, a pale yellow oil of $d_4^{20}=0.8698$ and $n_D^{20}=1.496$, was used as material.

Separation of Saturated Hydrocarbon Oil in the Materials.—Saturated Hydrocarbons Contained in Benzene Fraction.—As benzene was expected to be contained in the material from its physical constants, 500 ml. of it was shaken vigorously with the mixture of 50 ml. of conc. nitric acid ($d_4^{20}=1.42$) and 100 ml. of conc. sulfuric acid ($d_4^{20}=1.84$); and aromatic hydrocarbons were removed. The residual oil was washed by water, neutralized with 10% sodium hydroxide solution, rewashed similarly and dried with calcium chloride to obtain 433 ml. of

1) M. Vahrman, *J. Appl. Chem.*, **2**, 532 (1952).
2) C. H. Lander and R. F. Mackay, "Low Temperature Carbonization", Ernest Benn, Ltd., London, (1924) p. 164.
3) S. Kimura, H. Suzumura and H. Yasui, *J. Japan Tar Ind. Association*, **4**, 35 (1952).
4) H. Steinbrecher and H. Kuhn, *Angew. Chem.*, **50**, 233 (1937).
5) O. Kruber, *Erdöl und Kohle.*, **8**, 637 (1955).
6) J. A. Anderson, C. J. E. Engelder, *Ind. Eng. Chem.*, **37**, 541 (1945).
7) J. Griswold, R. H. Bowden, ibid., **38**, 509 (1946).
8) R. F. Marschner and W. P. Cropper, ibid., **38**, 262 (1946).
9) F. B. Ahrens, *Ber.*, **40**, 848 (1907).
10) H. H. Lowry, "Chemistry of Coal Utilization", Vol. II, John Wiley & Sons, Inc., New York (1947), p. 1357.
11) O. Jacobsen, *Ann.*, **184**, 179 (1877).
12) H. Stinzendorfer, *Oel und Kohle*, **38**, 193 (1942).
13) A. Pictet and M. Bouvier, *Ber.*, **56**, 162 (1923).
14) F. B. Ahrens and L. V. Modzenski, *Z. Angew. Chem.*, **21**, 1411 (1908).
15) S. Kimura and H. Yasui, *J. Chem. Soc. Japan, Pure Chem. Sec.* (*Nippon Kagaku Zasshi*), **74**, 555 (1953).
16) S. Kimura and H. Yasui, ibid., **75**, 163 (1954).
17) H. Yasui, ibid., **78**, 82 (1957).
18) S. Kimura and H. Yasui, ibid., **75**, 300 (1954).
19) H. Yasui, ibid., **78**, 85 (1957).
20) H. Yasui, ibid., **78**, 1213 (1957).

crude saturated hydrocarbon, which has b. p. 85~105°C, $d_4^{20}=0.7711$ and $n_D^{20}=1.430$. Now 300 ml. of this oil was submitted to fractional distillation with metallic sodium and 120 ml. of 78~90°C fraction ($d_4^{20}=0.8059$, $n_D^{20}=1.458$), and 150 ml. of 90~103°C fraction ($d_4^{20}=0.7290$, $n_D^{20}=1.406$) were obtained. But, in the 78~90°C fraction, residual benzene was still expected from its physical constants and ultraviolet spectrum[17]. The residual benzene in this fraction, therefore, was again removed with a mixture of conc. sulfuric acid and conc. nitric acid, and the residual oil and 90~103°C fraction were fractionated by Podbielniak distillation equipment, and 4 per cent by weight of 78~90°C fraction ($d_4^{20}=0.7067$, $n_D^{20}=1.398$) and 96 per cent by weight of 96~100°C fraction ($d_4^{20}=0.7170$, $n_D^{20}=1.405$), were obtained.

Saturated Hydrocarbons Contained in Toluene Fraction.—In an iron-pot provided with a stirrer, toluene contained in 169 kg. of toluene fraction, was extracted with 361.7 kg. of conc. sulfuric acid and 2.1 kg. of crude saturated hydrocarbon oil, and about 1.2% by weight of toluene fraction was obtained. Residual toluene in 756 g. of this oil was again removed completely with conc. sulfuric acid. 709 g. of saturated hydrocarbon oil, amounting to about 1.1% of toluene fraction, was obtained. This oil was distilled with metallic sodium and 120~126°C fraction, which has $d_4^{20}=0.7234$ and $n_D^{20}=1.406$, was obtained.

Saturated Hydrocarbons Contained in Solvent Naphtha.—In an iron-pot provided with a stirrer, aromatic hydrocarbons contained in 200 kg. of the material, were extracted four times with conc. sulfuric acid (total of 197.34 kg.), and 6.44 kg. of crude saturated hydrocarbon oil, was obtained. Moreover, the residual aromatic hydrocarbon in 760 g. of this oil was removed with conc. sulfuric acid repeatedly and 708 g. of saturated hydrocarbon oil, amounting to about 3% by weight of the material, was obtained. This oil has b. p. 132~198°C, $d_4^{20}=0.7632$ and $n_D^{20}=1.425$. 616 g. of this oil was submitted to the fractional distillation with metallic sodium and six fractions shown in Table I, were obtained.

Total of 118~147°C and 147~161°C fractions were fractionated by Podbielniak distillation equipment, and five fractions shown in Table II were obtained.

Moreover, total of 155~162°C fraction in Table II and 161~172°C, 172~177°C fractions in Table I, were fractionated and three fractions shown in Table III were obtained.

Analyses were carried out on the main fractions of 143.5~155°C in Table II and of 165~174°C in Table III.

TABLE I. FRACTIONS OBTAINED BY FRACTIONAL DISTILLATION OF 616 g. OF 132~198°C FRACTION

Frac. °C	g.	d_4^{20}	n_D^{20}
118~147	126	0.7492	1.419
147~161	180	0.7551	1.421
161~172	97	0.7629	1.424
172~177	73	0.7705	1.428
177~184	54	0.7749	1.431
184~	—	0.7889	1.439

TABLE II. FRACTIONS OBTAINED BY FRACTIONAL DISTILLATION OF A TOTAL OF 118~147°C AND 147~161°C FRACTIONS

Frac. °C	g.	d_4^{20}	n_D^{20}
111.5~132.5	19	0.7368	1.412
132.5~139	20	0.7461	1.416
139 ~143.5	8	0.7486	1.416
143.5~155	156	0.7502	1.418
155 ~162	28	0.7605	1.422

TABLE III. FRACTIONS OBTAINED BY FRACTIONAL DISTILLATION OF A TOTAL OF 155~162°C IN TABLE II AND 161~172°C, 172~177°C FRACTIONS IN TABLE I

Frac. °C	g.	d_4^{20}	n_D^{20}
145~147	7.5	0.7571	1.420
147~165	36	0.7596	1.422
165~174	83	0.7643	1.425

Identification of *n*-Paraffin.—*n*-Paraffin was isolated by means of urea adduct[21]. According to an estimation *n*-paraffin contained was about 30% in each fraction. It was added to urea (about 4 mol.) moistened with methanol (about 1 mol.). The suspension was stirred for 30 min. at 25°C and filtered, removing unreacted oil. The mixture of urea adduct and residual urea, were washed with anhydrous ether, which was removed under reduced pressure, and decomposed with water, and oil (*n*-paraffin) was obtained. And, unreacted oil was added to urea moistened with methanol, and treated as mentioned above, repeatedly until oil (*n*-paraffin) was no longer obtained by decomposition with water of urea adduct.

78~90°C and 96~100°C Fractions.—These fractions were treated as mentioned above, but oil was not obtained by decomposition with water of the urea adduct[17], suggesting difficulty by means of urea adduct, to separate *n*-paraffin expected to be contained in these fractions as stated by Kuwata and co-workers previously[22].

TABLE IV. ISOLATION OF *n*-PARAFFINS BY MEANS OF UREA ADDUCTS IN 120°~126C, 143.5~155°C AND 165~174°C FRACTIONS

Frac.		Oil isolated by means of urea adduct				Residual oil	
°C	g.	g.	% for frac.	b. p. °C	d_4^{20}	g.	% for frac.
120 ~126	100	30	30	124~125.5	0.7035	51	51
143.5~155	30	7.6	25	149~151	0.720	18	60
165 ~174	30	12	40	165~178	0.7306	12	40

21) J. Zimmerschied, R. A. Dinerstein, A. W. Weitkamp and R. F. Marschner, *Ind. Eng. Chem.*, **42**, 1300 (1950).

22) T. Kuwata, Y. Mizutani and E. Tamura, *J. Chem. Soc. Japan, Ind. Chem. Sec.* (*Kogyo Kagaku Zasshi*), **55**, 799 (1952).

120~126°C[18], 143.5~155°C[19] and 165~174°C[20] Fractions.—*n*-Paraffin contained in the three fractions were isolated by means of urea adduct and the result was shown in Table IV.

Oil Isolated by Means of Urea Adduct in 120~126°C Fraction.—Physical constants (Table IV) of this oil are identical with those of *n*-octane[23] (b. p. 125.6°C, d_4^{20}=0.703, n_D^{20}=1.397). IR spectrum bands[15] (wavelengths; 7.68, 7.87, 8.16, 8.33, 8.8, 9.27, 9.65, 9.95, 10.34, 10.92, 11.4, 11.84, 12.6, 13.08, 13.32, 13.85 μ) of this oil are analogous to those of *n*-octane.

Oil Isolated by Means of Urea Adduct in 149~151°C Fraction.—Physical constants (Table IV) of this oil are identical with those of *n*-nonane[23] (b. p. 150.7°C, d_4^{20}=0.718, n_D^{20}=1.406) and IR spectrum bands[19] (wavelengths; 7.67, 7.94, 8.22, 8.41, 8.81, 9.2, 9.41, 9.58, 10.14, 10.29, 10.79, 11.22, 11.84, 12.05, 12.89, 13.29, 13.86 μ) of this oil are analogous to those of *n*-nonane.

Oil Isolated by Means of Urea Adduct in 165~174°C Fraction.—Physical constants (Table IV) of this oil are identical with those of *n*-decane[23] (b. p. 174°C, d_4^{20}=0.7298, n_D^{20}=1.412). IR spectrum bands[20] (wavelengths; 7.67, 8.01, 8.25, 8.42, 8.81, 9.16, 9.29, 9.92, 10.05, 10.86, 11.15, 11.83, 12.28, 13.0, 13.85 μ) of this oil are analogous to those of *n*-decane.

Identification of Cycloparaffin.—Dehydrogenation of the residual oil free from *n*-paraffin, was carried out with Pt-C catalyst at 300~310°C.

Dehydrogenation[24,25] Catalyst.—Pt-C catalyst was prepared by Berl's method[24]. About 10 g. of granulated active carbon was mixed with 1 g. of platinum chloride ($PtCl_2 \cdot 2HCl + 6HCl$) dissolved in 25 ml. of water acidified with hydrochloric acid, and the mixture was dried at 110°C with frequent stirring. These were put in a quartz reaction tube (dia., 2 cm., length, 80 cm.) and kept in position by a stopper of glass wool. They were heated to 200°C by electric furnace and the platinum compound was decomposed. Hydrogen was sent to the tube from the entrance until no more hydrochloric acid was formed and a treatment with hydrogen at 300°C was carried out for 30 min.

Apparatus.—The sample was dropped into one end of a reaction tube from the sample flask, the dropping velocity regulated by the opening of the cock provided at the lower part of the sample flask, and the oil produced was received from the other end by a receiving flask with an ice-cooled condenser and the gas produced was collected in a gas collector, its pressure being controlled by a pressure

Table V. Dehydrogenation

Reac. temp. 300~310°C; Dropping velocity 5~6 g./hr.

Sample	g.	Dehydrogenated oil g.	Gas produced ml. (N. T. P.)	H_2* ml. (N. T. P.)
(a)	7	4.5	828.8	812.2
(b)	10	6	1906.0	1815.2
(c)	11	5.5	1261.1	1171.0
(d)	13	9.5	1330.1	1210.6
(e)	10	8.5	455.4	439.6

* The gas produced by dehydrogenation was analyzed by the Hempel method, and the volume of hydrogen produced by dehydrogenation was calculated from the gas produced.

Table VI. Nitro-compounds obtained by nitration of dehydrogenated oils

	Dehydrogenated oil	Nitro-compound Obtained Crude	Obtained Recrystal.		Referred[26] Comp.	
	g.	g.	g.	m. p. °C		m. p., °C
(a)	0.7	0.5	0.05	88 ~ 90	*m*-Dinitrobenzene	90
			0.18	69 ~ 70	2,4-Dinitrotoluene	70
(b)	0.7	0.7	0.4	69.5~ 70	〃	〃
(c)	2	0.4	0.31	179 ~181	2,4,6-Trinitro-*m*-xylene	180
			0.02	138 ~141	2,3,5-Trinitro-*p*-xylene	140
(d)	1.5	0.8	0.45	169 ~171	3,5-Dinitro-1,2,4-trimethylbenzene	172
			0.05	99 ~100	Dinitro-1,2,3-trimethylbenzene	100
(e)	2	0.3	0.03	230 ~232	2,4,6-Trinitro-1,3,5-trimethlybenzene	232
			0.1	179 ~181	4,6-Dinitro-1,2,3,5-tetramethylbenzene	180

* All melting points are uncorrected.

23) G. Egloff, "Physical Constants of Pure Hydrocarbons", Vol. I, Reinhold Publ. Corp., New York (1939), p. 49.
24) E. Berl and W. Koerber, *Ind. Eng. Chem., Anal. Ed.*, **12**, 175 (1940).
25) S. Komatsu and S. Kimura, *J. Chem. Soc. Japan, Pure Chem. Sec.* (*Nippon Kagaku Zasshi*), **74**, 343 (1953).
26) S. P. Mulliken, "A Method for Identification of Pure Organic Compounds", Vol. I., John Wiley & Sons, Inc. (1959), p. 200.

control device. 78~90°C (a) and 96~100°C fractions (b) and each residual oils (c), (d), (e) free from *n*-paraffin in 120~126°C, 143.5~155°C and 165~174°C fractions were dehydrogenated as mentioned above, and the oil condensed in the receiver were subjected to dehydrogenation repeatedly, and the results, shown in Table V, were obtained.

Identification of Aromatic Hydrocarbons Produced by Dehydrogenation—UV Spectrum of Dehydrogenated Oil[15~20].—UV spectra of dehydrogenated oils dissolved in purified cyclohexane, was measured with a Beckman spectrophotometer, model DU and the aromatic hydrocarbons produced by dehydrogenation were estimated from their UV spectra.

Nitration of Dehydrogenated Oil[15~20].—Dehydrogenated oil was added to a mixture of 1 vol. of conc. nitric acid and 2 vol. of conc. sulfuric acid and the mixture was heated to boil for five minutes and poured into cold water, and crude nitro-compounds were obtained. These compounds were purified or separated by recrystallization from ethyl alcohol solution, obtaining pure nitro-compounds. The results were shown in Table VI.

The aromatic hydrocarbons contained in each dehydrogenated oil, were determined from UV spectra and Table VI, and the original cycloparaffins contained in (a), (b), (c), (d) and (e) were estimated. The result was shown in Table VII.

TABLE VII. CYCLOPARAFFINS CONTAINED IN (a), (b), (c), (d) AND (e)

	Cycloparaffin	Ratio*
(a)	Cyclohexane	1
	Methylcyclohexane	4
(b)	Methylcyclohexane	
(c)	1,3-Dimethylcyclohexane	15
	1,4-Dimethylcyclohexane	1
(d)	1,2,4-Trimethylcyclohexane	9
	1,2,3-Trimethylcyclohexane	1
(e)	1,3,5-Trimethylcyclohexane	1
	1,2,3,5-Tetramethylcyclohexane	3

* The ratio of cycloparaffins contained in each fraction was calculated from weights of nitro-compounds obtained.

TABLE VIII. PHYSICAL CONSTANTS OF OILS, REMOVED AROMATIC HYDROCARBONS CONTAINED IN DEHYDROGENATED OILS

	Dehydrogenated oil	Oil (saturated hydrocarbon)			
	g.	g.	b. p., °C	d_4^{20}	n_D^0
(a)	2.1	1.7	93 ~ 96	0.6865	1.389
(b)	2.2	1.5	98.5~ 99.5	0.6942	1.393
(c)	1.6	1.35	114 ~116	0.7221	1.405
(d)	2.0	1.5	140 ~145	0.7265	1.407
(e)	1.6	1.3	164 ~166	0.7340	1.413

Identification of Isoparaffin.—Aromatic hydrocarbons produced by dehydrogenation were removed from dehydrogenated oils by mixture of 2 vol. of conc. sulfuric acid and 1 vol. of conc. nitric acid or by conc. sulfuric acid[15~20]. The residual oils were washed by water and neutralized with alkaline solution. Similarly rewashed and dried with calcium chloride and distilled with metallic sodium, and the oils, having the physical constants shown in Table VIII were obtained.

IR spectra of these oils were measured with a Baird infrared spectrophotometer and isoparaffins contained in each oil were determined. IR spectrum bands of oil of (a) (wavelengths; 7.45, 7.68, 8.78, 9.30, 9.79, 10.4, 10.74, 11.1, 11.42, 11.57, 12.01, 12.91, 13.54, 13.83 μ) are analogous to those of *n*-heptane. In IR spectrum bands of oil of (b), those of *n*-heptane and 2,2,4-trimethylpentane (wavelengths; 7.7, 8.01, 8.30, 8.56, 9.84, 10.2, 10.82, 11.58, 13.4 μ) were observed. It was observed that IR spectrum bands of oil of (c) contain the bands of the spectrum for 2-methylheptane (wavelengths; 7.45, 7.68, 7.9, 8.55, 9.28, 10.42, 10.56, 10.74, 12.3, 13.06, 13.82 μ) and those of the spectrum for 3-methylheptane (wavelengths; 7.68, 7.9, 9.28, 10.42, 10.95, 11.43, 12.3 μ). In IR spectrum bands of oil of (d), those of 3-methyloctane (wavelengths; 8.7, 9.97, 10.3, 10.48, 10.72, 10.94, 11.22, 11.43, 12.3 μ) and 4-methyloctane (wavelengths; 8.7, 9.26, 10.48, 10.72, 10.94, 11.22, 12.94, 13.5, 13.8 μ) were observed. In IR spectrum of bands of oil of (e), those of 3-methylnonane (wavelengths; 8.6, 9.43, 9.77, 9.96, 10.34, 10.95, 11.2, 13.0, 13.8 μ) and 4-methylnonane (wavelengths; 8.6, 9.24, 10.47, 11.2, 11.86, 12.3, 13.0, 13.6, 13.8 μ) were observed.

Results and Discussion

The saturated hydrocarbons identified from each fraction and the proportion of *n*-paraffin, isoparaffin and cycloparaffin to each fraction, are shown in Table IX.

It is obvious that saturated hydrocarbons contained in benzene fraction consist of *n*-heptane (about 74.5%), cyclohexane (about 0.1%), methylcyclohexane (about 25.4%) and 2, 2, 4-trimethylpentane (trace). In the saturated hydrocarbons contained in toluene fraction, *n*-octane (30%), mixture of 2-methylheptane and 3-methylheptane (42%) and 1, 3-dimethylcyclohexane (9%) and 1, 4-dimethylcyclohexane (0.5%) were determined. Saturated hydrocarbons contained in solvent naphtha fraction were determined to contain *n*-nonane (about 5.4%), *n*-decane (about 4.7%), mixture of 3-methyloctane and 4-methyloctane (about 10.8%), mixture of 3-methylnonane and 4-methylnonane (about 4.3%), 1,2,4-trimethylcyclohexane (about 0.2%), 1, 2, 4-trimethylcyclohexane (about 2%), 1, 3, 5-trimethylcyclohexane (about 0.1%) and 1, 2, 3, 5-tetramethylcyclohexane (about 0.4%).

The following observations are based on a study of the data presented in this research.

TABLE IX. SATURATED HYDROCARBONS IDENTIFIED AND THE PROPORTION OF *n*-PARAFFIN, ISOPARAFFIN AND CYCLOPARAFFIN TO EACH FRACTION

Frac.	*n*-Paraffin (%)	Isoparaffin (%)	Cycloparaffin (%)	Aromatic*
78 ~ 90	*n*-Heptane (87)	None	Cyclohexane (3) Methylcyclohexane (10)	Benzene
96 ~100	*n*-Heptane (74)		Methylcyclohexane (26)	
120 ~126	*n*-Octane (30)	2-Methylheptane (42) 3-Methylheptane	1,3-Dimethylcyclohexane (9) 1,4-Dimethylcyclohexane (0.5)	Toluene
143.5~155	*n*-Nonane (25)	3-Methyloctane (50) 4-Methyloctane	1,2,3-Trimethylcyclohexane (1) 1,2,4-Trimethylcyclohexane (9)	*o*-Xylene *m*-Xylene *p*-Xylene *o*-Ethyltoluene *m*-Ethyltoluene *p*-Ethyltoluene 1,2,4-Trimethylbenzene 1,2,3-Trimethylbenzene 1,3,5-Trimethylbenzene
165 ~174	*n*-Decane (40)	3-Methylnonane (37) 4-Methylnonane	1,3,5-Trimethylcyclohexane (1) 1,2,3,5-Tetramethylcyclohexane (3)	

* Aromatic hydrocarbons in high-temperature coal carbonization light oil prepared at Yawata Iron & Steel Co., Ltd. as identified previously by S. Kimura, H. Suzumura and the author[3].

1) The saturated hydrocarbons contained in benzene, toluene and solvent naphtha fractions are all composed of saturated aliphatic hydrocarbon, about 85%, and cycloparaffinic hydrocarbon, about 15%.

2) The saturated aliphatic hydrocarbons contained in benzene fraction are nearly all *n*-paraffins and the corresponding isoparaffins are expected to be contained in the forerunnings. In the saturated aliphatic hydrocarbons contained in toluene and solvent naphtha fractions, the proportion of contents of *n*-paraffins and isoparaffins are about 1 : 1.5.

3) The isoparaffins, contained in the three fractions mentioned above, are all monomethylparaffins.

4) Comparing cycloparaffins with aromatics, cyclohexane corresponding to benzene, methylcyclohexane to toluene, dimethylcyclohexane to dimethylbenzene and trimethylcyclohexane to trimethylbenzene, are present respectively. In dimethylbenzene isomer, *m*-xylene is the highest in contents, *p*-xylene, half as much as *m*-xylene and *o*-xylene is of trace[3]. Similar tendency is observed in the contents of dimethylcyclohexane isomers, but 1, 2-dimethylcyclohexane can not be identified in this investigation. It is recognized that in trimethylbenzene isomers, much of 1, 2, 4- and 1, 3, 5-isomers are contained, and almost equally[3]. But it has become clear that in trimethylcyclohexane, the content of 1, 2, 4-isomer is more than that of 1, 3, 5-isomer and 1, 2, 3-isomer is of trace. Thereafter a presence of 1, 2, 3, 5- and 1, 2, 3, 4-isomers[15] in tetramethylcyclohexane isomer is observed. They cannot be compared, however, with the corresponding tetramethylbenzene since it is not analyzed yet by the author. It was reported[27] that 1, 2, 4, 5-tetramethylcyclohexane is contained in high-temperature carbonization tar, but the result obtained in this research presents a different result. Moreover, *p*- and *m*-methylethylcyclohexane[3], which correspond to ethyltoluene isomers, are not found.

The author wishes to express his hearty thanks to Professor Sakujirô Kimura of Kyoto University, Professor Tamon Matsu'ura and Professor the late Bunkichi Masumoto of Hiroshima University and Professor Shôzô Tanaka of Kyoto University for their kind guidance and valuable advice throughout this study.

Thanks are also due to Yawata Iron & Steel Co., Ltd. for donation of the materials used

27) K. E. Schulze, *Ber.*, **18**, 3032 (1885).

for this investigation. The author is indebted to Dr. Kenji Kuratani of the University of Tokyo and Sumitomo Chemical Industries Co., Ltd. for the measurement of IR spectra.

Department of Chemistry
Faculty of Science
Kyoto University
Sakyô-ku, Kyoto

Studies on Constituents of Coal Carbonization Light Oil. II. On Saturated Hydrocarbons Contained in Low-temperature Coal Carbonization Light Oil

By Hiroshi YASUI

(Received January 6, 1960)

Apparently, constituents of high-temperature coal carbonization light oil are mainly aromatic hydrocarbons and those of low-temperature coal carbonization light oil, are mainly saturated hydrocarbons[1]. But, resulting data of identification of saturated hydrocarbons in low-temperature coal carbonization light oil, are scanty. In 1955, some of them have been reported by A. Jäger and G. Kattwinkel[2] and the following results have been found. 1) The saturated hydrocarbons, contained in low-temperature coal carbonization light oil, consist mainly of straight-chain paraffins. 2) The branched-chain paraffins contained in this oil are all monomethylparaffins. 3) Contents of cycloparaffins are scanty.

Ohyama[3] reported that the neutral oil contained in low-temperature coal carbonization light oil, Ube Kôsan Co., Ltd. production, amounted to about 90 per cent and also the contents of the saturated hydrocarbon in the neutral oil to about 40 per cent. However, the constituents of the individual saturated hydrocarbons in this light oil and their contents have never been ascertained. Therefore, the author has studied on the constituents of the saturated hydrocarbons contained in this oil and found five straight-chain hydrocarbons (*n*-hexane, *n*-heptane, *n*-octane, *n*-nonane and *n*-decane) and five branched-chain hydrocarbons (2-methylhexane, 2-methylheptane, 2-methyloctane, 2-methylnonane and 3-methylnonane) and four cycloparaffins (cyclohexane, methylcyclohexane, 1, 3-dimethylcyclohexane and 1, 3, 5-trimethylcyclohexane) and determined their contents approximately and compared them with the result obtained in a previous paper[4].

Experimental

Materials.—Residual oil after extraction of acidic and basic oils in low-temperature coal carbonization light oil (carbonization temperature, 780°C) manufactured by Ube Kôsan Co., Ltd. in August, 1954, with dilute sulfuric acid and alkaline solution, brown colored, was used. This oil kept in a glass reagent bottle for some years and precipitation, amounting to about 1.5 per cent of this oil, was produced. The oil, removing the precipitation by filtration, had a boiling range of 92~265°C, $d_4^{25}=0.8062$ and $n_D^{25}=1.456$. The contents of olefinic, aromatic and saturated hydrocarbons in this oil, were determined to be olefins 9.5 per cent (volume absorbed by 80% H_2SO_4), aromatics 49 per cent (volume absorbed by 98% H_2SO_4) and saturated hydrocarbons 41.5 per cent (residue) by sulfuric acid absorption method.

Separation of the Saturated Hydrocarbon Oil.—Olefinic and aromatic hydrocarbons contained in 320 g. of the material, were removed by extracting with concentrated sulfuric acid. The residual oil was washed by water, neutralized with 10 per cent sodium hydroxide solution, rewashed similarly and dried with calcium chloride to obtain 148 g. of crude saturated hydrocarbon oil (46.2 per cent by weight of the material). This oil was fractionated and 100 g. of 98~220°C fraction, which had $d_4^{25}=0.7403$ and $n_D^{25}=1.417$, and 45 g. of residual oil, were obtained. Residual aromatic hydrocarbons in 100 g. of 98~220°C fraction, were again removed completely with concentrated sulfuric acid and washed with water and neutralized with alkaline solution and rewashed similarly and dried with calcium chloride and 89 g. (27.8 per cent by weight of the material) of saturated hydrocarbon oil

1) M. Vahrman, *J. Appl. Chem.*, **2**, 532 (1952).
2) A. Jäger und G. Kattwinkel, *Erdöl und Köhle*, **9**, 629, 706 (1955).
3) G. Ohyama, "Studies on Ube Coal (Ube-tan no Seijô to Gôsei-yô Gasu oyobi Teion-târu no Seizô to Shori)", Ube Kôsan Co., Ltd., Japan (1951), p. 200.
4) H. Yasui, This Bulletin, **33**, 1493 (1960).

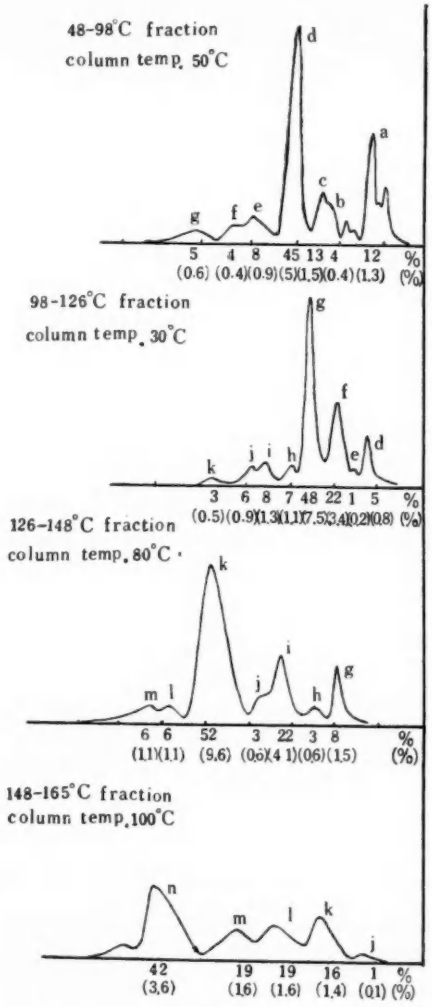

Fig. 1. Gas chromatograms of each fraction.
H_2 flow rate 100 ml./min.

a ····· *n*-Hexane
b ····· Cyclohexane
c ····· 2-Methylhexane
d ····· *n*-Heptane
e ····· Methylcyclohexane
f ····· 2-Methylheptane
g ····· *n*-Octane
h ····· 1,3-Dimethylcyclohexane
i ····· 2-Methyloctane
j ····· 1,3,5-Trimethylcyclohexane
k ····· *n*-Nonane
l ····· 2-Methylnonane
m ····· 3-Methylnonane
n ····· *n*-Decane
% ····· Per cent of contents to each fraction
(%) ··· Per cent of contents to Sample A

(Sample A), which had $d_4^{25}=0.7397$ and $n_D^{25}=1.414$, was obtained. 87 g. (110 ml.) of this oil was submitted to fractional distillation by Podbielniak equipment with metallic sodium and five fractions shown in Table I, were obtained.

TABLE I. FRACTIONS OBTAINED BY FRACTIONAL DISTILLATION OF 87 g. OF SAMPLE A

Frac. °C	Main frac. °C	g.	Wt. %	d_4^{25}	n_D^{25}
48～98	87～98	9.6	11.1	0.6877	1.389
98～126	114～121	13.6	15.6	0.7146	1.401
126～148	135～145	16.2	18.6	0.7340	1.409
148～165	150～164	7.5	8.6	0.7478	1.416
165～184	169～184	4.5	5.1	0.7481	1.422
Residue	—	34.4	39.5	0.7924	1.442

Analyses were carried out on 48～98°C, 98～126°C, 126～148°C and 148～165°C fractions in Table I.

Gas Chromatographic Analysis.—Gas chromatographic analysis of 48～98°C, 98～126°C, 126～148°C and 148°～165°C fractions was performed with a Perkin-Elmer vapor fractometer. Hydrogen was used as carrier gas and di-*n*-decylphthalate was used as liquid substrate. The identification of the peak in the chromatograms was based on synthetic hydrocarbon data. The retention time of hydrocarbons contained in these fractions was obtained from each synthetic hydrocarbon and comparing the retention times of the peak chromatogram of each synthetic hydrocarbon under identical conditions. Contents of the hydrocarbons in these fractions were calculated from the area of each measurable peak.

Identification of *n*-Paraffn.—*n*-Paraffins in these fractions were isolated by means of urea adducts[5]. According to the estimation *n*-paraffin was contained about 50 per cent in each fraction. It was added to urea (about three times in weight of the *n*-paraffin) moistened with methanol (about a fifth of the weight of the urea used). The suspension was stirred for 30 min. at 0°C in 98～126°C, or 20°C in 126～148°C and 148～165°C fractions, and filtered, and unreacted oils were removed. The mixture of urea adduct obtained and the residual urea was washed with anhydrous ether, removed under reduced pressure, decomposed with water, and oil (*n*-paraffin) was obtained. Unreacted oil was once more added to urea moistened with methanol and treated as mentioned above until no more oil (*n*-paraffin) was obtained by decomposition with water of urea adduct. The result was shown in Table II. As stated by the author[4] and Kuwata and co-workers[6] previously, it is difficult to isolate *n*-hexane and *n*-heptane expected to be contained mainly in 48～98°C fraction. Therefore this method was not employed.

IR Spectra of Oils Obtained by Decomposition with Water of Urea Adducts.—IR spectra of 48～98°C fraction and oils isolated by decomposition

5) J. Zimmerschied et al., *Ind. Eng. Chem.*, **42**, 1300 (1950).
6) T. Kuwata, Y. Mizutani and E. Tamura, *J. Chem. Soc. Japan, Ind. Chem. Sec.* (*Kogyo Kagaku Zasshi*) **55**, 799 (1952).

TABLE II. ISOLATION OF *n*-PARAFFIN BY UREA ADDUCTS IN 98～126°, 126～148° AND 148～165°C FRACTION

Fraction		Oil isolated by urea adduct (*n*-paraffin)					Residual oil	
°C	g.	g.	%	b. p., °C	d_4^{25}	n_D^{25}	g.	%
98～126	12	5.5	46	120～124	0.6983	1.396	5	42
126～148	14	6.5	54	142～151	0.7111	1.405	6.5	32
148～165	6.5	3.0	46	152～170	0.7248	1.410	2.2	34

with water of urea adducts of 98～126°C, 126～148°C and 148～165°C fractions, were measured with an Oh'yô Kôken infrared spectrophotometer.

48～98°C Fraction.—In IR spectrum bands of this fraction, those of *n*-hexane (wavelengths; 7.45, 7.73, 8.02, 8.20, 8.6, 8.79, 9.38, 9.46, 9.86, 9.95, 10.29, 11.04, 11.24, 11.31, 11.51, 12.13, 12.6, 12.94, 13.18, 13.78 μ), *n*-heptane (wavelengths; 7.45, 7.68, 7.81, 8.09, 8.27, 8.78, 9.3, 9.79, 10.4, 10.74, 11.1, 11.42, 11.57, 12.01, 12.91, 13.54 13.83 μ), 2-methylhexane (wavelengths; 7.3, 7.41, 7.71, 7.97, 8.18, 8.53, 8.73, 9.3, 9.53, 9.7, 9.85, 10.46, 10.63, 11.0, 11.17, 12.16, 12.81, 13.74 μ), 2-methylheptane (wavelengths; 7.32, 7.46, 7.67, 8.05, 8.28, 8.54, 8.74, 9.22, 9.56, 9.98, 10.41, 10.53, 10.71, 10.88, 11.2, 11.94, 12.31, 13.04, 13.26, 13.81 μ), cyclohexane (wavelengths; 7.4, 7.95, 8.7, 9.1, 9.6, 9.9, 11.1, 11.68 μ) and methylcyclohexane (wavelengths; (7.28, 7.44, 7.69, 8.02, 8.62, 9.06, 9.7, 10.38, 11.02, 11.49, 11.87 μ) were observed.

Oil Isolated by Decomposition with Water of the Urea Adduct of 98～126°C Fraction.—Physical constants (Table II) of this oil were analogous to those of *n*-octane[7] (b. p. 125.6°C, $d_4^{20}=0.703$, $n_D^{20}=1.397$). In IR spectrum bands of this oil, those of *n*-heptane, *n*-octane (wavelengths; 7.46, 7.68, 7.87, 8.16, 8.33, 8.8, 9.27, 9.65, 9.95, 10.34, 10.92, 11.1, 11.21, 11.4, 11.84, 12.6, 13.08, 13.52, 13.85 μ) and *n*-nonane (wavelengths; 7.46, 7.67, 7.94, 8.22, 8.81, 9.2, 9.41, 9.58, 10.29, 10.79, 11.22, 11.4, 11.84, 12.05, 12.89, 13.29, 13.86 μ) were observed.

Oil Isolated by Decomposition with Water of the Urea Adduct of 126～148°C Fraction.—Physical constants (Table II) of this oil were analogous to those of *n*-nonane[7] (b. p. 150.7°C, $d_4^{20}=0.7111$, $n_D^{20}=1.405$), and in IR spectrum bands of this oil, those of *n*-nonane and *n*-octane were observed.

Oil Isolated by Decomposition with Water of the Urea Adduct of 148～165°C Fraction.—Physical constants (Table II) of this oil denoted the values between those of *n*-nonane and *n*-decane[7] (b. p. 174°C, $d_4^{20}=0.7298$, $n_D^{20}=1.412$), and therefore the fraction was expected to be a mixture of *n*-nonane and *n*-decane. In IR spectrum bands of this oil, those of *n*-nonane and *n*-decane (wavelengths; 7.26, 7.45, 7.67, 7.82, 8.01, 8.25, 8.81, 9.16, 9.29, 9.92, 10.05, 10.86, 11.15, 11.83, 12.28, 13.0, 13.85 μ) were observed.

Gas Chromatographic Analysis.—The gas chromatographic analysis of oils, obtained by decomposition with water of urea adducts of 98～126°C, 126～148°C and 148～165°C fraction, was performed and chromatograms of these oils were shown in Fig. 2.

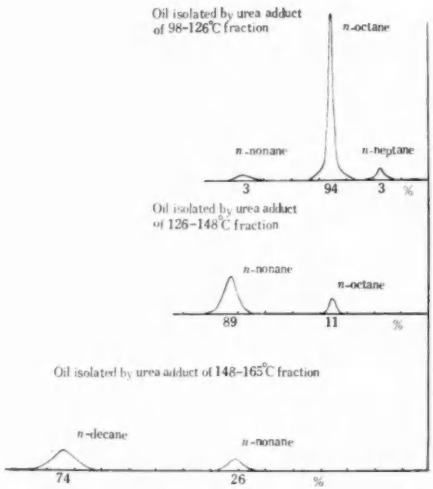

Fig. 2. Gas chromatograms of oils obtained by decomposition with water of urea adducts of each fraction.
Column temp., 100°C; H_2 flow rate, 98.6 ml./min.

Identification of Cycloparaffin and Isoparaffin—IR Spectra.—IR spectra of residual oils, in 98～126°C, 126～148°C and 148～165°C fractions, are measured with an Oh'yô Kôken spectrophotometer.

Residual Oil in 98～126°C Fraction Shown in Table II.—Physical constants of this oil are b. p. 110～125°C, $d_4^{25}=0.7218$, $n_D^{25}=1.404$. In IR spectrum bands of this oil, those of 2-methylheptane, 2-methyloctane (wavelengths; 7.6, 7.67, 7.86, 8.15, 8.33, 8.54, 9.14, 9.3, 9.4, 9.77, 10.18, 10.55, 10.9, 11.25, 11.42, 12.15, 12.7, 13.5, 13.8 μ), 1,3-dimethylcyclohexane (wavelengths; 7.25, 7.66, 7.88, 8.36, 8.6, 8.96, 9.28, 9.45, 10.0, 10.2, 10.53, 10.71, 11.43, 11.72, 12.13 μ) and 1,3,5-trimethylcyclohexane (wavelengths; 7.52, 7.92, 8.53, 8.87, 8.96, 9.35, 9.56, 9.66, 10.0, 10.63, 10.74, 11.84, 11.91, 12.78 μ) were observed.

Residual Oil in 126～148°C Fraction Shown in Table II.—Physical constants of this oil are b. p. 139～151°C, $d_4^{25}=0.7406$ and $n_D^{25}=1.414$. In IR spectrum bands of this oil, those of 2-methyloctane, 1,3-dimethylcyclohexane, 2-methylnonane (wavelengths; 7.67, 7.93, 8.21, 8.40, 8.54, 8.76, 9.12, 9.4, 10.07, 10.4, 10.65, 10.9, 11.1, 11.48, 12.0,

7) G. Egloff, "Physical Constants of Pure Hydrocarbons", Vol. I, Reinhold Publ. Corp., New York (1939), p. 49.

12.32, 13.05, 13.6, 13.81 μ), 3-methylnonane (wavelengths; 7.67, 7.83, 8.16, 8.36, 8.66, 9.12, 9.43, 9.94, 11.28, 11.79, 12.2, 12.78, 12.96, 13.6, 13.8 μ) and 1,3,5-trimethylcyclohexane, were observed.

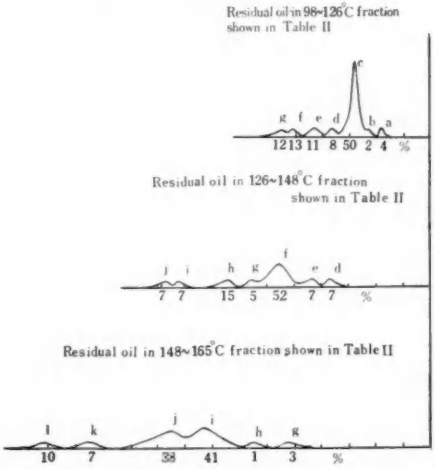
Residual oil in 98~126°C fraction shown in Table II
c
g f e d
h a
12 13 11 8 50 2 4 %
Residual oil in 126~148°C fraction shown in Table II
f
j i h g e d
7 7 15 5 52 7 7 %
Residual oil in 148~165°C fraction shown in Table II
l k j i h g
10 7 38 41 1 3 %

Fig. 3. Gas chromatograms of residual oils in each fraction. Column temp. 100°C; H_2 flow rate 98.6 ml./min.

a ····· *n*-Heptane
b ····· Methylcyclohexane
c ····· 2-Methylheptane
d ····· *n*-Octane
e ····· 1,3-Dimethylcyclohexane
f ····· 2-Methyloctane
g ····· 1,3,5-Trimethylcyclohexane
h ····· *n*-Nonane
i ····· 2-Methylnonane
j ····· 3-Methylnonane
k ····· *n*-Decane

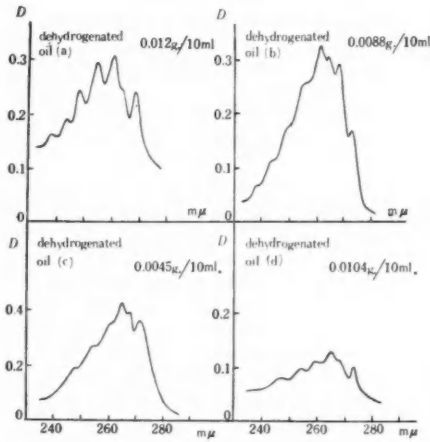

Fig. 4. Ultraviolet spectra of dehydrogenated oils.

Residual Oil in 148~165°C Fraction Shown in Table II.—Physical constants of this oil are b. p. 148~164°C, $d_4^{25}=0.7673$ and $n_D^{25}=1.425$. In IR spectrum bands of this oil, those of 2-methylnonane, 3-methylnonane and 1,3,5-trimethylcyclohexane were observed.

Gas Chromatographic Analysis.—Gas chromatographic analysis of residual oils, in 98~126°C, 126~148°C and 148~165°C fractions was performed and the chromatograms were shown in Fig. 3.

Dehydrogenation[4,8]. — Dehydrogenation of 48~98°C fraction (a) and residual oils (b), (c) and (d) in 98~126°C, 126~148°C and 148~165°C fractions shown in Table II, was carried out with Pt-C catalyst prepared by the method described previously[4], at 290~300°C repeatedly, until no hydrogen was producible and by this method, cycloparaffins contained in these fractions were changed to corresponding aromatic hydrocarbons. The result was shown in Table III.

Table III. Dehydrogenation
Reac. temp. 290~300°C; dropping velocity 5~6 g./hr.

Sample	g.	Dehydrogenated oil g.	Gas produced ml. (N. T. P.)	H_2* ml. (N. T. P.)
(a)	4	2.8	284.8	263.5
(b)	4	3.0	632.9	623.8
(c)	2	1.3	144.1	136.5
(d)	2	1.5	48.1	40.6

* The gas produced by dehydrogenation was analyzed by the Hempel method, and the volume of hydrogen produced was the volume of the gas removed of that of air.

Identification of Aromatic Hydrocarbons Produced by Dehydrogenation. — Ultraviolet Spectra of the Dehydrogenated Oils. — Ultraviolet spectra of dehydrogenated oils, dissolved in purified ethanol, were measured with a Beckman spectrophotometer model DU, and were shown in Fig. 4.

Nitration of Dehydrogenated Oil[9]. — Dehydrogenated oil was added to a mixture of 1 vol. of concentrated nitric acid and 2 vol. of concentrated sulfuric acid and shaken, then boiled for five minutes and poured into cold water, and crude nitro-compounds were obtained. These compounds were separated by fractional recrystallization from ethanol solution, obtaining pure nitro-compounds. The result was shown in Table IV.

From Fig. 3 and Table IV, aromatic hydrocarcons produced by dehydrogenation were confirmed, and their original cycloparaffins and the ratio of their contents were estimated as shown in Table V.

8) E. Berl and W. Koerber, *Ind. Eng. Chem., Anal. Ed.*, 12, 175 (1940).
9) S. P. Mulliken, "A Method for the Identification of Pure Organic Compounds", Vol. I, John Wiley & Sons Inc., New York, p. 200.

TABLE IV. NITRO-COMPOUNDS OBTAINED BY NITRATION OF DEHYDROGENATED OILS

	Dehydrogenated oil	Nitro-compound: Obtained			Nitro-compound: Referred[9]	
		Crude	Recrystallized	M. p.	Compound	M. p.
	g.	g.	g.	°C		°C
(a)	1.0	0.3	0.04	87~ 90	*m*-Dinitrobenzene	90
			0.11	67~ 69	2,4-Dinitrotoluene	70
(b)	1.0	0.2	0.22	66~ 68	〃	〃
			0.04	177~179	2,4,6-Trinitro-*m*-xylene	179
			0.03	228~231	2,4,6-Trinitro-1,3,5-trimethylbenzene	232
(c)	0.75	0.2	0.03	177~180	2,4,6-Trinitro-*m*-xylene	179
			0.04	228~232	2,4,6-Trinitro-1,3,5-trimethylbenzene	232
(d)	1.0	0.04	0.02	230~232	〃	〃

TABLE V. CYCLOPARAFFINS CONTAINED IN (a), (b), (c) AND (d)

	Cycloparaffin	Ratio*
(a)	Cyclohexane : Methylcyclohexane	1 : 3
(b)	Methylcyclohexane : 1,3-Dimethylcyclohexane : 1,3,5-Trimethylcyclohexane	2 : 4 : 3
(c)	1,3-Dimethylcyclohexane : 1,3,5-Trimethylcyclohexane	3 : 4
(d)	1,3,5-Trimethylcyclohexane	

* The ratio of cycloparaffins contained in each fraction was calculated from weights of nitro-compounds obtained.

Results and Discussion

Saturated hydrocarbons identified from the low-temperature coal carbonization light oil produced at Ube Kôsan Co. Ltd. in this research are given below.

It has become clear, that the constituents of the saturated hydrocarbons, contained in this oil, consist of five straight-chain hydrocarbon (*n*-hexane, *n*-heptane, *n*-octane, *n*-nonane and *n*-decane) and five branched-chain hydrocarbon (2-methylhexane, 2-methylheptane, 2-methyloctane, 2-methylnonane and 3-methylnonane) and four cycloparaffins (cyclohexane, methylcyclohexane, 1, 3-dimethylcyclohexane and 1, 3, 5-trimethylcyclohexane). Moreover, percentage of their contents in the saturated hydrocarbon oil (Sample A) separated from the material, is given in the gas chromatograms shown in Fig. 1, and Table VI.

The following observation is based on a study of the data presented in Table VI.

1) Saturated hydrocarbons, contained in the low-temperature coal carbonization light oil, are composed of about 91 per cent of saturated aliphatic hydrocarbon and about 9 per cent of cycloparaffinic hydrocarbon.

2) Saturated aliphatic hydrocarbons contained in this oil, are composed of two parts of *n*-paraffins and one part of isoparaffins.

3) The isoparaffins are all monomethylparaffins and these monomethylparaffins are nearly all 2-methylparaffins.

Comparing the saturated hydrocarbons, contained in high-temperature coal carbonization

TABLE VI. SATURATED HYDROCARBONS IDENTIFIED AND PERCENTAGE OF THEIR CONTENTS IN SAMPLE A

n-Paraffin		Isoparaffin		Cycloparaffin	
Compound	%	Compound	%	Compound	%
n-Hexane	1.3	2-Methylhexane	1.5	Cyclohexane	0.4
n-Heptane	5.8	2-Methylheptane	3.8	Methylcyclohexane	1.1
n-Octane	9.6	2-Methyloctane	5.4	1,3-Dimethylcyclohexane	1.7
n-Nonane	11.5	2-Methylnonane	2.7	1,3,5-Trimethylcyclohexane	1.6
n-Decane	3.6	3-Methylnonane	2.7		
Total	31.8	Total	16.1	Total	4.8

light oil produced at Yawata Iron & Steel Co. Ltd., and identified by the author[4], with those identified in this investigation, the following observations are made.

1) Saturated hydrocarbons identified from both low-temperature and high-temperature coal carbonization light oils, consist mainly of saturated aliphatic hydrocarbons of 90 per cent saturated hydrocarbons in low-temperature coal carbonization light oil, and about 85 per cent in high-temperature coal carbonization light oil.

2) In low-temperature coal carbonization light oil, the ratio of contents of *n*-paraffins and isoparaffins is about 2 : 1. In high-temperature coal carbonization light oil, about 1 : 1.5.

3) Isoparaffins, contained in low- and high-temperature coal carbonization light oils, are all monomethylparaffins, and those contained in low-temperature coal carbonization light oil are all 2-methylparaffins, except 3-methylnonane, and the monomethylparaffins contained in high-temperature coal carbonization light oil, consist of 3-methylparaffins and 4-methylparaffins except 2-methylheptane.

F. D. Rossini and B. J. Mair[10] studying the saturated hydrocarbons contained mainly in U. S. A. Mid-Continent, Ponca petroleum concluded that the saturated hydrocarbons consisted mainly of saturated aliphatic hydrocarbons, which contains a large quantity of *n*-paraffin and monomethylparaffin and a trace of branched paraffin which has many branchings. This conclusion is analogous to that of the present studies on saturated hydrocarbons contained in coal carbonization light oil.

The author wishes to express his hearty thanks to Professor Sakujirô Kimura of Kyoto University, Professor Tamon Matsu'ura and the late Professor Bunkichi Masumoto of Hiroshima University and Professor Shôzô Tanaka of Kyoto University for their kind guidance and valuable advice throughout this study.

Thanks are also due to Ube Kôsan Co. Ltd. for donation of the materials used for this investigation. The author is indebted to Yawata Chemical Industries Co. Ltd. for the measurement of gas chromatograms.

Dapartment of Chemistry
Faculty of Science
Kyoto University
Sakyô-ku, Kyoto

10) F. D. Rossini and B. J. Mair, *Ind. Eng. Chem. D. S.*, 3, 141 (1958).

*Thermodynamic Studies on Cobalt Complexes. VI. Solubility of Nitropentamminecobalt(III), cis- and trans-Dinitrotetramminecobalt(III) and Trinitrotriamminecobalt(III) Complexes**

By Motoshichi MORI, Ryokichi TSUCHIYA and Hiroshi FUKUDA

(Received May 11, 1960)

Thermodynamic discussion of the monoacidopentamminecobalt(III) complexes which have Cl^-, NO_3^- or Br^- as the anionic ligand was carried out in the preceding paper[1]. In the present study the discussion is extended to the cobalt(III) complexes which have one, two or three nitro groups in the coordination sphere. Solubilities of nitropentamminecobalt(III) chloride, nitrate, bromide and perchlorate, *cis*- and *trans*-dinitrotetramminecobalt(III) chlorides and trinitrotriamminecobalt(III) complex were measured, and the standard free energies of their formation were calculated. The thermodynamic stability of the complexes formed by the substitution of ammonia by one, two or three nitro groups was also discussed.

Experimental

Nitropentamminecobalt(III) chloride was prepared by the method of Jörgensen[2]. The nitrate, bromide and perchlorate were precipitated by nitric acid ammonium bromide and perchloric acid respectively from the aqueous solution of the

* Read at the 13th Annual Meeting of the Chemical Society of Japan, Tokyo April, 1960.

1) M. Mori and R. Tsuchiya, This Bulletin, 33, 841 (1960).

2) S. M. Jörgensen, *Z. anorg. Chem.*, 17, 463 (1898).

chloride. *cis*- and *trans*-Dinitrotetramminecobalt (III) chlorides and trinitrotriamminecobalt(III) were also prepared by the method of Jörgensen[2-4].

The solubility in the saturated aqueous solution was measured colorimetrically by means of a Hitachi EPU-2 spectrophotometer. Since these nitro-complexes are unstable towards light, equilibrium of the solution was attained in a brown flask immersed in the thermostat to prevent the photo-decomposition.

Results and Calculation

Solubility of Nitropentamminecobalt(III) Complexes. — The results obtained for nitropentamminecobalt(III) chloride, nitrate, bromide and perchlorate are listed in Tables I—IV.

The equilibrium of nitropentamminecobalt-(III) complex in water is expressed by,

$$[Co(NH_3)_5NO_2]X_2(s) = [Co(NH_3)_5NO_2]^{2+}(aq.) + 2X^-(aq.)$$

where X is an anion. If the activities of the cation, the anion and their activity coefficients are expressed by $a_{[Co(NH_3)_5NO_2]^{2+}}$, a_{X^-}, $\gamma_{[(Co(NH_3)_5NO_2]^{2+}}$ and γ_{X^-} respectively, the equilibrium constant, K, is given by

$$K = a_{[Co(NH_3)_5NO_2]^{2+}} \cdot a^2_{X^-} = (m\gamma_{[Co(NH_3)_5NO_2]^{2+}})(2m\gamma_{X^-})^2 = 4m^3\gamma_{[Co(NH_3)_5NO_2]^{2+}} \cdot \gamma^2_{X^-}$$

where m is the solubility in molality. When the mean activity coefficient is expressed by $\gamma_\pm$, the equilibrium constant is given by

$$K = 4m^3\gamma^3_\pm \quad (1)$$

The mean activity coefficient is calculated by the following formula[5] which gives the activity

Table I. Equilibrium of solution for nitropentamminecobalt(III) chloride

Temp. (°C)	Solubility (Molality m)	$1/T\times10^3$	$\gamma_\pm$	$K\times10^4$	log K
10.8	0.0902	3.521	0.514	3.99	$\bar{4}.601$
15	0.107	3.471	0.497	6.02	$\bar{4}.780$
20	0.117	3.412	0.489	7.49	$\bar{4}.874$
25	0.145	3.355	0.471	12.74	$\bar{3}.105$
30	0.160	3.299	0.461	16.05	$\bar{3}.205$

Table II. Equilibrium of solution for nitropentamminecobalt(III) nitrate

Temp. (°C)	Solubility (Molality m)	$1/T\times10^3$	$\gamma_\pm$	$K\times10^5$	log K
10.8	0.0301	3.521	0.623	2.64	$\bar{5}.422$
15	0.0345	3.471	0.600	3.55	$\bar{5}.550$
20	0.0419	3.412	0.590	6.04	$\bar{5}.781$
25	0.0531	3.355	0.566	10.86	$\bar{4}.036$
30	0.0591	3.299	0.555	14.12	$\bar{4}.150$

Table III. Equilibrium of solution for nitropentamminecobalt(III) bromide

Temp. (°C)	Solubility (Molality m)	$1/T\times10^3$	$\gamma_\pm$	$K\times10^4$	log K
10.8	0.0360	3.521	0.605	4.13	$\bar{5}.616$
15	0.0421	3.471	0.589	6.10	$\bar{5}.785$
20	0.0495	3.412	0.573	9.13	$\bar{5}.960$
25	0.0587	3.355	0.556	13.91	$\bar{4}.143$
30	0.0693	3.299	0.540	20.96	$\bar{4}.321$

Table IV. Equilibrium of solution for nitropentamminecobalt(III) perchlorate

Temp. (°C)	Solubility (Molality m)	$1/T\times10^4$	$\gamma_\pm$	$K\times10^4$	log K
10.8	0.0762	3.521	0.537	2.74	$\bar{4}.438$
15	0.101	3.471	0.511	5.50	$\bar{4}.740$
20	0.128	3.412	0.494	10.11	$\bar{3}.005$
25	0.168	3.355	0.469	19.57	$\bar{3}.292$
30	0.202	3.299	0.452	30.45	$\bar{3}.484$

3) S. M. Jörgensen, ibid., **17**, 473 (1898).
4) S. M. Jörgensen, ibid., **17**, 469 (1898).
5) J. Kielland, *J. Am. Chem. Soc.*, **59**, 1675 (1937).

coefficient of an ion,

$$\log \gamma_{ion} = \frac{-0.358 z^2 \sqrt{2\omega}}{1+0.2325\times 10^8 a\sqrt{2\omega}} - \log(1+0.018\,\nu m)$$

where z is the charge of the ion, ω, the ionic strength of the solution, a, the closest distance between an ion and another one and ν, the number of ions dissociated from one molecule of the salt.

The logarithm of the equilibrium constant of the solution calculated by Eq. 1 is plotted in Fig. 1 against the reciprocal of the absolute temperature. A straight line is obtained. By the method of least squares the equations of these lines are calculated as follows:

$\log K = 6.243 - 2734/T$ for the chloride

$\log K = 7.636 - 3473/T$ for the nitrate

$\log K = 6.732 - 3156/T$ for the bromide

$\log K = 13.080 - 4715/T$ for the perchlorate

The free energy changes of solution are given as

$$\begin{aligned} \Delta G^\circ &= -RT \ln K = 12510 - 28.56\,T \\ \Delta G^\circ_{298} &= 3991 \text{ cal. for the chloride} \\ \Delta G^\circ &= 15890 - 34.93\,T \\ \Delta G^\circ_{298} &= 5477 \text{ cal. for the nitrate} \\ \Delta G^\circ &= 14440 - 30.79\,T \\ \Delta G^\circ_{298} &= 5262 \text{ cal. for the bromide} \end{aligned} \quad (2)$$

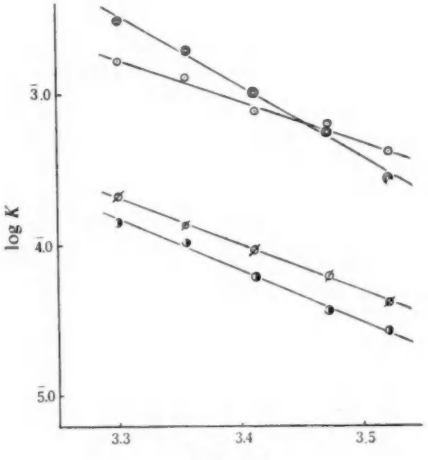

Fig. 1. The relationship between the equilibrium constant of solution and the temperature for nitropentamminecobalt-(III) chloride (⊙), nitrate (◑), bromide (∅) and perchlorate(◎).

$$\Delta G^\circ = 21570 - 59.84\,T$$

$\Delta G^\circ_{298} = 3728$ cal. for the perchlorate

From these equations the heats of solution of the chloride, nitrate, bromide and perchlorate are obtained as $\Delta H = 12.51$, 15.89, 14.44 and 21.57 kcal. respectively. The entropy changes for each salt are calculated as $\Delta S^\circ =$ 28.6, 34.9, 30.8 and 59.8 e. u., respectively.

Since the standard free energy of formation of nitropentamminecobalt(III) ion in unit activity is known as $\Delta G^\circ_{f\,298} = -108.9$ kcal[6]. and the heat of formation as $\Delta H_f = -153.1$ kcal.[7], the relationship between the former and the absolute temperature is calculated as

$$\Delta G^\circ_f = -153100 + 148.3\,T \quad (3)$$

The free energies of formation Cl^-, NO_3^-, Br^- and ClO_4^- in unit activity were already obtained in the second paper[8] of this series as follows:

$$\begin{aligned} \Delta G^\circ_f &= -40020 + 29.1\,T \text{ for } Cl^- \\ \Delta G^\circ_f &= -49370 + 77.03\,T \text{ for } NO_3^- \\ \Delta G^\circ_f &= -28900 + 14.51\,T \text{ for } Br^- \\ \Delta G^\circ_f &= -31410 + 96.75\,T \text{ for } ClO_4^- \end{aligned} \quad (4)$$

Therefore the standard free energy of formation of nitropentamminecobalt(III) chloride in the solid state is calculated by Eqs. 3, 6 and 4 as

$$\begin{aligned} \Delta G^\circ_f &= -245700 + 235.1\,T \\ \Delta G^\circ_{f\,298} &= -175.6 \text{ kcal.} \end{aligned}$$

The values for the nitrate, bromide and perchlorate of the same complex were calculated by combining respective equations:

$\Delta G^\circ_f = -267700 + 337.3\,T$,

$\Delta G^\circ_{f\,298} = -167.2$ kcal., for the the nitrate

$\Delta G^\circ_f = -225300 + 208.1\,T$,

$\Delta G^\circ_{f\,298} = -163.3$ kcal., for the bromide

$\Delta G^\circ_f = -237500 + 401.6\,T$,

$\Delta G^\circ_{f\,298} = -117.8$ kcal., for the perchlorate

Solubility of Dinitrotetramminecobalt(III) Complexes.—The results obtained for *cis*- and *trans*-dinitrotetramminecobalt(III) chlorides are listed in Tables V and VI.

The process of solution of dinitrotetramminecobalt(III) chloride is represented by the following equation,

6) A. B. Lamb and A. T. Larson, *J. Am. Chem. Soc.*, **42**, 2038 (1920).

7) K. B. Yatsimirskii and L. L. Pankowa, *Zhur. Obshchei Khim.*, **18**, 2051 (1948); K. B. Yatsimirskii, "Thermochemie von Komplexverbindungen", Akademie-Verlag, Berlin (1956), p. 179.

8) M. Mori, R. Tsuchiya and Y. Okano, This Bulletin, **32**, 462 (1959).

Table V. Equilibrium of solution for *cis*-dintrotetramminecobalt(III) chloride

Temp. (°C)	Solubility (Molality m)	$1/T\times10^3$	$\gamma_\pm$	$K\times10^2$	log K
10	0.164	3.533	0.737	1.46	$\bar{2}$.164
15	0.189	3.471	0.726	1.88	$\bar{2}$.274
20	0.213	3.412	0.717	2.33	$\bar{2}$.367
25	0.263	3.355	0.701	3.40	$\bar{2}$.531
30	0.321	3.299	0.685	4.83	$\bar{2}$.684

Table VI. Equilibrium of solution for *trans*-dinitrotetramminecobalt(III) chloride

Temp. (°C)	Solubility (Molality m)	$1/T\times10^3$	$\gamma_\pm$	$K\times10^4$	log K
10	0.0319	3.533	0.847	7.30	$\bar{4}$.863
15	0.0357	3.471	0.840	8.99	$\bar{4}$.954
20	0.0437	3.412	0.828	13.09	$\bar{3}$.117
25	0.0521	3.355	0.817	18.12	$\bar{3}$.258
30	0.0627	3.299	0.805	25.48	$\bar{3}$.407

$$[Co(NH_3)_4(NO_2)_2]Cl(s) = [Co(NH_3)_4(NO_2)_2]^+(aq.) + Cl^-(aq.)$$

When the activities of the cation, the anion and their activity coefficients are expressed by $a_{[Co(NH_3)_4(NO_2)_2]^+}$, a_{Cl^-}, $\gamma_{[Co(NH_3)_4(NO_2)_2]^+}$ and γ_{Cl^-} respectively, the equilibrium constant of solution, K, is given as

$$K = a_{[Co(NH_3)_4(NO_2)_2]^+}\cdot a_{Cl^-} = (m\gamma_{[Co(NH_3)_4(NO_2)_2]^+})(m\gamma_{Cl^-}) = m^2\gamma_{[Co(NH_3)_4(NO_2)_2]^+}\cdot\gamma_{Cl^-} = m^2\gamma_\pm^2,$$

m and $\gamma_\pm$ being the solubility in molality and the mean activity coefficient.

The plots of the logarithm of the above equilibrium constant against the reciprocal of the absolute temperature are given in Fig. 2 as straight lines for both salts. The straight lines are expressed by the following equations:

$$\log K = 5.970 - 2215/T \quad \textit{cis}\text{-}[Co(NH_3)_4(NO_2)_2]Cl$$

$$\log K = 5.234 - 2376/T \quad \textit{trans}\text{-}[Co(NH_3)_4(NO_2)_2]Cl$$

The free energy changes of solution are given as for the cis salt,

$$\Delta G^\circ = 9111 - 23.87\,T, \quad \Delta G^\circ_{298} = 1995 \text{ cal.} \quad (5)$$

and for the trans salt,

$$\Delta G^\circ = 9556 - 19.42\,T, \quad \Delta G^\circ_{298} = 3767 \text{ cal.} \quad (6)$$

From these equations $\Delta H = 10.13$ kcal. and $\Delta H = 10.87$ kcal. are obtained as the heats of solution of the cis and trans salts respectively and $\Delta S^\circ = 27.3$ e. u. and $\Delta S^\circ = 23.9$ e. u. are obtained as the entropy changes of the cis and trans salts respectively.

Since the energies of formation of *cis*- and *trans*-dinitrotetramminecobalt(III) ions in unit activity are known as $\Delta G^\circ_{f298} = -164.7$ kcal. and $\Delta G^\circ_{f298} = -161.4$ kcal[6]. and their heat of formation as $\Delta H_f = -159.9$ kcal. and $\Delta H_f = -159.1$ kcal[9]. respectively, the relationships between the free energies of formation and the absolute temperature are calculated for the cis salt as,

$$\Delta G_f^\circ = -159900 - 16.10\,T \quad (7)$$

and for the trans salt as,

$$\Delta G_f^\circ = -159100 - 7.72\,T \quad (8)$$

Then the free energy of formation of *cis*-dinitrotetramminecobalt(III) chloride in the solid state is calculated by Eqs. 4, 5 and 7 as

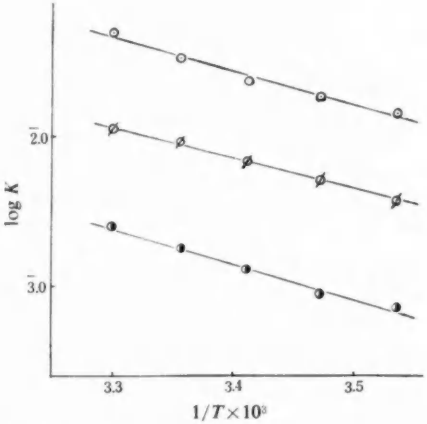

Fig. 2. The relationship between the equilibrium constant of solution and the temperature for *cis*-dinitrotetramminecobalt(III) chloride (⊙), corresponding *trans*-chloride (◑) and trinitrotriamminecobalt(III) complex (∅).

9) K. B. Yatsimirskii and L. L. Pankowa, *Zhur. Obshchei Khim.*, **19**, 623 (1949); K. B. Yatsimirskii, "Thermochemie von Komplexverbindungen", Akademie-Verlag, Berlin (1956), pp. 179, 180.

TABLE VII. EQUILIBRIUM OF SOLUTION FOR TRINITROTRIAMMINECOBALT(III) COMPLEX

Temp. (°C)	Solubility (Molality $m\times10^3$)	$1/T\times10^3$	$K\times10^3$	log K
10	3.88	3.533	3.88	$\bar{3}.588$
15	5.18	3.471	5.18	$\bar{3}.714$
20	6.96	3.412	6.96	$\bar{3}.843$
25	9.15	3.355	9.15	$\bar{3}.961$
30	11.19	3.299	11.19	$\bar{2}.049$

$$\Delta G_f^\circ = -210100 + 40.3\,T,$$
$$\Delta G_{f\,298}^\circ = -198.0 \text{ kcal.}$$

and that of *trans*-dinitrotetramminecobalt(III) chloride by Eqs. 4, 6 and 8 as

$$\Delta G_f^\circ = -210000 + 45.3\,T,$$
$$\Delta G_{f\,298}^\circ = -196.5 \text{ kcal.}$$

Solubility of Trinitrotriamminecobalt(III) Complex. — The results obtained for trinitrotriamminecobalt(III) complex is listed in Table VII.

When the solubility in molality of this complex is expressed by m, the equilibrium constant of the solution, K, is given by $K=m$. The relationship between the logarithm of K and temperature is shown in Fig. 2 and it is expressed by the equation as below:

$$\log K = 4.696 - 2008/T.$$

The heat of solution is $\Delta H = 9.19$ kcal. The free energy change of solution is given as,

$$\Delta G^\circ = 9186 - 21.44\,T,$$
$$\Delta G_{298}^\circ = 2795 \text{ cal.} \qquad (9)$$

The entropy change at 25°C is $\Delta S^\circ_{298} = 21.44$ e. u.

The entropy of formation of hexamminecobalt(III) ion, nitropentamminecobalt(III) ion, *trans*- and *cis*-dinitrotetramminecobalt(III) ions were obtained as -306.9[8], -148.3[10], 7.72[10] and 16.10 e. u.[10], respectively. From these values it is found that the entropy of formation increases by 160 e. u., when every one gram equivalent of ammonia is replaced by one gram equivalent of nitro group. Therefore, if it is assumed that the entropy of formation of trinitrotriamminecobalt(III) complex in unit activity in aqueous solution is larger by three times 160 e. u. than that of hexamminecobalt(III) ion in unit activity, the entropy of the former is obtained as $\Delta S^\circ = 172$ e. u. As the heat of formation of trinitrotriamminecobalt(III) complex in unit activity in aqueous solution is known as $\Delta H = -160$ kcal.[9], the free energy of formation is obtained as

$$\Delta G_f^\circ = -160000 - 172\,T,$$
$$\Delta G_{f\,298}^\circ = -211300 \text{ cal.} \qquad (10)$$

By Eqs. 9 and 10 the free energy of formation of trinitrotriamminecobalt(III) complex in the solid state is obtained as

$$\Delta G_f^\circ = -169200 - 150.6\,T,$$
$$\Delta G_{f\,298}^\circ = -214.1 \text{ kcal.}$$

10) See Eqs. 6, 11 and 10, in this paper.

Discussion

Thermodynamic Stability of Nitropentamminecobalt(III) Complexes. — The solubility, the free energy of solution, the heat of solution and the free energy of formation of nitropentamminecobalt(III) complexes 25°C obtained above are summarized in Table VIII together with the radius of anions[11] forming these complexes. The lattice energy, U_k, required for the dissociation of solid complexes into gaseous ions is calculated by using the heat of solution and the heat of hydration of ions[11] which constitute complexes, and the values are shown in Table VIII.

From this table, the order of decrease of the solubility, the free energy of solution, the heat of solution, the lattice energy, the free energy of formation and the thermochemical and thermodynamic stability are found and shown in Table IX.

The same order was found for the solubility, the free energy of solution and the heat of solution of hexamminecobalt(III) complexes[8]. The order of the thermochemical and thermodynamic stability for the above nitropentamminecobalt(III) chloride, nitrate, bromide and perchlorate is in agreement with the order for the corresponding hexamminecobalt(III)[8], aquopentamminecobalt(III)[1] or acidopentamminecobalt(III) complexes[1]. The above order of the thermodynamic quantities may suggest that the ionic bond character between the complex cation and the anions generally diminishes as the ionic radius of the latter decreases, although several cases of reversal between the nitrate and the bromide are found as shown in Table VIII.

Entropy of Solution of *cis*- and *trans*-Dinitrotetramminecobalt(III) Chlorides. — The solubility, the free energy of solution, the heat of solution and the entropy of solution

11) K. B. Yatsimirskii, "Thermochemie von Komplexverbindungen", Akademie-Verlag, Berlin (1956), pp. 38—40.

Table VIII. Thermodynamic functions of nitropentamminecobalt(III) complexes at 25°C

Complex	Solubility in Molality m	Free energy of solution ΔG° cal.	Heat of solution ΔH kcal.	Free energy of formation ΔG_f° kcal.	Radius of anion (Å)	Lattice energy U_k kcal.
$[Co(NH_3)_5NO_2]Cl_2$	0.145	3991	12.51	−175.6	1.81	390
$[Co(NH_3)_5NO_2](NO_3)_2$	0.0531	5477	15.89	−167.2	1.89	376
$[Co(NH_3)_5NO_2]Br_2$	0.0587	5262	14.44	−163.3	1.96	374
$[Co(NH_3)_5NO_2](ClO_4)_2$	0.168	3728	21.57	−117.8	2.36	340

Table IX. Order of decrease of the thermodynamic quantities

Solubility	Chloride>Bromide>Nitrate
Free energy of solution	Nitrate>Bromide>Chloride
Heat of solution	Nitrate>Bromide>Chloride
Lattice energy	Chloride>Nitrate>Bromide>Perchlorate
Free energy of formation	Perchlorate>Bromide>Nitrate>Chloride
Thermochemical and thermodynamic stability	Chloride>Nitrate>Bromide>Perchlorate

Table X. Thermodynamic functions of *cis*- and *trans*-dinitrotetramminecobalt(III) chlorides

Complex	Solubility m	Free energy of solution ΔG° cal.	Heat of solution ΔH kcal.	Entropy of solution ΔS° e. u.
cis-$[Co(NH_3)_4(NO_2)_2]Cl$	0.263	1990	10.13	27.3
trans-$[Co(NH_3)_4(NO_2)_2]Cl$	0.0521	3731	10.87	23.9

of these two isomers at 25°C are summarized in Table X.

As shown in Table X, the cis chloride is more soluble than the trans chloride and the free energy of solution of the former is much lower than that of the latter. The large difference between the free energies of solution is attributed to the fact that the entropy of solution of the cis salt is considerably larger than that of the trans salt, since the heat of solution is approximately the same. In other words, the free energy changes of solution of these two isomers are affected much more by the entropy effect rather than the enthalpy effect.

Relationship between the Free Energy of Formation and the Number of Coordinated Nitro-groups. — The free energies of formation of nitropentamminecobalt(III), dinitrotetramminecobalt(III) and hexamminecobalt(III) complexes are plotted against the number of coordinated nitro-groups in Fig. 3. Straight lines were obtained for the chlorides, nitrates, bromides and perchlorates. These four lines all converge at a point which corresponds to the free energy of formation of trinitrotriamminecobalt(III) complexes. It shows that an additivity rule holds between the free energy of formation and the number of nitrogroups.

When the free energy of formation of these complexes and the number of nitrogroups are expressed by ΔG_f° and n respectively, these straight lines are expressed by

$$\Delta G_f^\circ = an + c, \qquad (11)$$

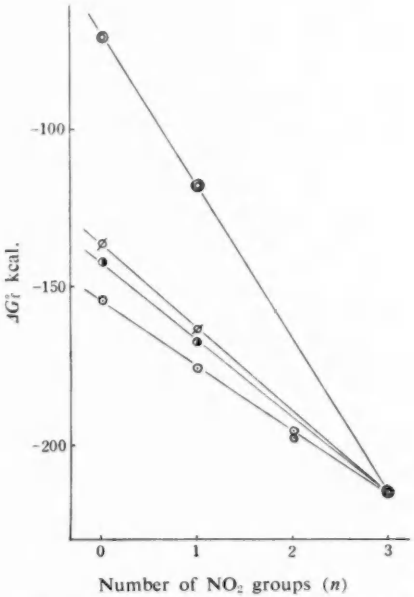

Fig. 3. The relationship between the free energy of formation and the number of nitro-groups coordinated in the series of cobalt(III) nitroammine complexes, that is
$[Co(NH_3)_{6-n}(NO_2)_n]Cl_{3-n}$ (⊙),
$[Co(NH_3)_{6-n}(NO_2)_n](NO_3)_{3-n}$ (◑),
$[Co(NH_3)_{6-n}(NO_2)_n]Br_{3-n}$ (⌀)
and $[Co(NH_3)_{6-n}(NO_2)_n](ClO_4)_{3-n}$ (◎).
(⊗) is trinitrotriamminecobalt(III) complex.

where c is the free energy of formation of a hexamminecobalt(III) complex[8] and a a constant. The constant a gives the difference between the free energy of formation of $[Co(NH_3)_{6-n}(NO_2)_n]X_{3-n}$ and that of $[Co(NH_3)_{6-n-1}(NO_2)_{n+1}]X_{3-n-1}$, which is obtained from Fig. 3 as:

$a=-19.9$ kcal. for chloride

$a=-24.1$ kcal. for nitrate

$a=-26.0$ kcal. for bromide

$a=-47.6$ kcal. for perchlorate

Free Energy Required for the Dissociation of the Anion from Nitroamminecobalt(III) Complexes. — The value of a in Eq. 11 for the chlorides is assumed as the sum of the changes of the free energy of formation in two processes such as:

(a) $[Co(NH_3)_6]Cl_3(s) \rightarrow [Co(NH_3)_6]Cl_2(s) \quad \Delta(\Delta G_f^\circ)_a$

(b) $[Co(NH_3)_6]Cl_2(s) \rightarrow [Co(NH_3)_5NO_2]Cl_2(s) \quad \Delta(\Delta G_f^\circ)_b$

that is,

$$a=\Delta(\Delta G_f^\circ)_a+\Delta(\Delta G_f^\circ)_b$$

If it is assumed that the change of the free energy of formation in process (b) is approximately equal to that in the following process,

$[Co(NH_3)_6]^{3+}(aq.) \rightarrow [Co(NH_3)_5NO_2]^{2+}(aq.) \quad \Delta(\Delta G_f^\circ) = -54.4$ kcal.[6]

that is,

$$\Delta(G_f^\circ)_b \fallingdotseq \Delta(G_f^\circ) = -54.4 \text{ kcal.}$$

then the value in the above process (a) is calculated as $\Delta(\Delta G_f^\circ)_a=34.5$ kcal. by using the value $a=-19.9$ kcal. for the chloride. The value $\Delta(\Delta G_f^\circ)_a$ is the free energy required for the elimination of one gram equivalent of chloride ion in the outer coordination sphere frome nitroammin cobalt(III) chloride.

In the same way, the free energies required for eliminating one gram equivalent of NO_3^-, Br^- or ClO_4^- in the outer sphere from the respective complexes are calculated as below:

$\Delta(\Delta G_f^\circ)_a=30.3$ kcal. for nitrate

$\Delta(\Delta G_f^\circ)_a=28.4$ kcal. for bromide

$\Delta(\Delta G_f^\circ)_a=6.8$ kcal. for perchlorate

These values show that the dissociation of the anion from cobalt(III) nitroammine complexes becomes more difficult in the order: perchlorate <bromide<nitrate<chloride. This also indicates that the thermodynamic stability of these complexes increases in the same order.

Summary

1. From the solubility of cobalt(III) nitroammine complexes the thermodynamic stability was found to decrease in the order, chloride> nitrate>bromide>perchlorate.

2. The free energy of solution of *cis*-dinitrotetramminecobalt(III) chloride is lower than that of the trans chloride. This fact is attributed to the abnormally large value of the entropy of solution of the former compared with the latter.

3. Between the free energy of formation of cobalt(III) nitroammine complexes and the number of coordinated nitro-groups there exists a linear relationship.

Department of Chemistry
Faculty of Science
Kanazawa University
Kanazawa

*Thermodynamic Studies on Cobalt Complexes. VII. Solubility of Erdmann's Salt and Related Complexes**

By Motoshichi MORI, Ryokichi TSUCHIYA, Eishin KYUNO and Takashi NISHIDE

(Received May 11, 1960)

Although there have been several investigations[1] on the structure of Erdmann's salt, ammonium tetranitrodiamminecobaltate(III), no thermodynamic study has ever been made on it. In the preceding paper[2] we determined the solubility of nitropentamminecobalt(III), *cis*- and *trans*-dinitrotetramminecobalt(III) and trinitrotriamminecobalt(III) complexes and calculated the standard free energy of formation of solid cobalt(III) ammine complexes containing one, two or three nitrogroups. In the present paper the solubility of the cobalt-(III) ammine complexes containing four nitrogroups, i. e., tetranitrodiamminecobaltate(III) complexes was measured. The solubilities of some of these salts have already been reported[3,4]. In the present study the measurement was extended to several other salts and to different temperatures.

Experimental

The complexes studied were the following: [I] the so called Erdmann's salt, namely ammonium tetranitrodiamminecobaltate(III) $NH_4[Co(NH_3)_2(NO_2)_4]$, [II] the corresponding potassium salt $K[Co(NH_3)_2(NO_2)_4]$, [III] *cis*-dinitrotetramminecobalt(III) - tetranitrodiamminecobaltate(III) *cis*-$[Co(NH_3)_4(NO_2)_2][Co(NH_3)_2(NO_2)_4]$, and [IV] the corresponding trans isomer among 1-1 valency type salts, [V] nitropentammincobalt(III)-tetranitrodiamminecobaltate(III) $[Co(NH_3)_5NO_2][Co(NH_3)_2(NO_2)_4]_2$ and [VI] chloropentamminecobalt(III)-tetranitrodiamminecobaltate(III) $[Co(NH_3)_5Cl][Co(NH_3)_2(NO_2)_4]_2$ among 1-2 valency type salts and [VII] hexamminecobalt(III) - tetranitrodiamminecobaltate(III) $[Co(NH_3)_6][Co(NH_3)_2(NO_2)_4]_3$ among 1-3 valency type salts.

Erdmann's salt [I] was prepared by the method of Jörgensen[5] and the potassium salt [II] was precipitated from the aqueous solution of I with potassium nitrate. III and IV were prepared by the double decomposition of I and *cis*-dinitrotetramminecobalt(III) nitrate[6] and the trans form chloride[7] respectively. V, VI and VII were prepared by the double decomposition of I and nitropentamminecobalt(III) chloride[8], chloropentamminecobalt(III) chloride[9] and hexamminecobalt(III) chloride[10], respectively.

The measurement of the solubility was made by measuring the cobalt content or the absorbancy of the saturated aqueous solution. The former was carried out by iodometry and the latter with a Hitachi EPU-2 spectrophotometer.

Results and Calculation

The results of measurement are listed in Tables I—VII. The solubilities are expressed in molality, m. The mean activity coefficients $\gamma_\pm$ given for I and II are the values obtained in the first paper of this series[11] and those for the other salts are the values calculated by Debye-Hückel's limiting formula,

$$\log \gamma_\pm = -0.505\, z_+ z_- \sqrt{\mu}$$

where z_+ and z_- are the charges of each cation and anion and μ is the ionic strength of each solution.

Equilibrium Constant of Solution and Standard Free Energy of Formation of Erdmann's Salt.— When Erdmann's salt is dissolved in water, the change is expressed by

$$NH_4[Co(NH_3)_2(NO_2)_4]\,(s) = NH_4^+\,(aq.) + [Co(NH_3)_2(NO_2)_4]^-\,(aq.)$$

The equilibrium constant of the solution, K, is given as in the preceding paper[2] by $K = m^2\gamma^2_\pm$.

A plot of the logarithm of K against the reciprocal of the absolute temperature is given in Fig. 1 as a straight line, the equation being calculated by the method of least squares as

$$\log K = 0.8981 - 771.8/T$$

The free energy change of solution is given by

$$\Delta G^\circ = 3530 - 4.108\,T, \quad \Delta G^\circ_{293} = 2305\ \text{cal.} \qquad (1)$$

* Read at the 12th Annual Meeting of the Chemical Society of Japan Tokyo April, 1959.

1) Y. Komiyama, This Bulletin, **30**, 13 (1957). Other references in the past were cited in this paper.

2) M. Mori, R. Tsuchiya and H. Fukuda, This Bulletin, **33**, 1503 (1960).

3) J. N. Brönsted and A. Petersen, *J. Am. Chem. Soc.* **43**, 2265 (1921).

4) E. Kyuno, *J. Chem. Soc. Japan, Pure Chem. Sec.* (*Nippon Kagaku Zasshi*), **78**, 1494 (1957).

5) S. M. Jörgensen, *Z. anorg. Chem.*, **17**, 477 (1898).

6) S. M. Jörgensen, ibid., **17**, 473 (1898).

7) S. M. Jörgensen, ibid., **17**, 469 (1898).

8) S. M. Jörgensen, ibid., **17**, 463 (1898).

9) W. A. Hynes, L. K. Yanowsky and M. Schiller, *J. Am. Chem. Soc.*, **60**, 3053 (1938).

10) W. C. Fernelius, "Inorganic Syntheses", Vol. II, McGraw-Hill Book Co., Inc., New York, N. Y. (1946), p. 216.

11) M. Mori and R. Tsuchiya, *J. Chem. Soc. Japan, Pure Chem. Sec.* (*Nippon Kagaku Zasshi*), **79**, 1164 (1958).

Table I. Solubility of Erdmann's salt

Temp. (°C)	Solubility (Molality m)	$1/T\times10^3$	$\gamma_\pm$	K	log K
15	0.186	3.471	0.690	0.0164	$\bar{2}.215$
20	0.199	3.412	0.686	0.0186	$\bar{2}.270$
25	0.209	3.355	0.681	0.0203	$\bar{2}.308$
30	0.224	3.299	0.675	0.0228	$\bar{2}.358$
35	0.233	3.246	0.671	0.0244	$\bar{2}.387$

Table II. Solubility of $K[Co(NH_3)_2(NO_2)_4]$

Temp. (°C)	Solubility (Molality m)	$1/T\times10^3$	$\gamma_\pm$	$K\times10^4$	log K
0	0.0107	3.662	0.914	1.23	$\bar{4}.869$
15	0.0364	3.471	0.847	3.08	$\bar{4}.736$
20	0.0516	3.412	0.821	4.23	$\bar{4}.627$
25	0.0684	3.355	0.796	5.45	$\bar{4}.488$
30	0.0969	3.299	0.763	7.39	$\bar{4}.090$

Table III. Solubility of *cis*-$[Co(NH_3)_4(NO_2)_2][Co(NH_3)_2(NO_2)_4]$

Temp. (°C)	Solubility (Molality $m\times10^3$)	$1/T\times10^3$	$\gamma_\pm$	$K\times10^5$	log K
15	4.49	3.471	0.925	1.73	$\bar{5}.237$
20	6.49	3.412	0.911	3.49	$\bar{5}.543$
25	8.99	3.355	0.896	6.49	$\bar{5}.812$
30	11.39	3.299	0.883	10.12	$\bar{4}.005$

Table IV. Solubility of *trans*-$[Co(NH_3)_4(NO_2)_2][Co(NH_3)_2(NO_2)_4]$

Temp. (°C)	Solubility (Molality $m\times10^4$)	$1/T\times10^3$	$\gamma_\pm$	$K\times10^7$	log K
15	4.56	3.471	0.975	1.97	$\bar{7}.295$
20	6.05	3.412	0.972	3.46	$\bar{7}.539$
25	8.38	3.355	0.967	6.56	$\bar{7}.817$
30	11.09	3.299	0.962	11.38	$\bar{6}.056$

Table V. Solubility of $[Co(NH_3)_5NO_2][Co(NH_3)_2(NO_2)_4]_2$

Temp. (°C)	Solubility (Molality $m\times10^3$)	$1/T\times10^3$	$\gamma_\pm$	$K\times10^9$	log K
10	0.670	3.532	0.906	0.892	$\bar{10}.950$
15	0.928	3.471	0.887	2.24	$\bar{9}.349$
20	1.12	3.412	0.879	3.81	$\bar{9}.581$
25	1.46	3.355	0.865	8.07	$\bar{8}.907$
30	1.62	3.299	0.857	10.71	$\bar{8}.030$

Table VI. Solubility of $[Co(NH_3)_5Cl][Co(NH_3)_2(NO_2)_4]_2$

Temp. (°C)	Solubility (Molality $m\times10^3$)	$1/T\times10^3$	$\gamma_\pm$	$K\times10^9$	log K
15	0.501	3.471	0.914	0.383	$\bar{10}.584$
20	0.731	3.412	0.896	1.16	$\bar{9}.066$
25	1.00	3.355	0.880	2.73	$\bar{9}.436$
30	1.32	3.299	0.864	5.97	$\bar{9}.776$
35	1.76	3.246	0.845	13.03	$\bar{8}.115$

Table VII. Solubility of $[Co(NH_3)_6][Co(NH_3)_2(NO_2)_4]_3$

Temp. (°C)	Solubility (Molality $m\times10^4$)	$1/T\times10^3$	$\gamma_\pm$	$K\times10^{14}$	log K
15	1.55	3.471	0.899	1.02	$\bar{14}.010$
20	2.25	3.412	0.880	4.17	$\bar{14}.620$
25	2.84	3.355	0.866	9.88	$\bar{14}.995$
30	4.09	3.299	0.841	37.94	$\bar{13}.579$

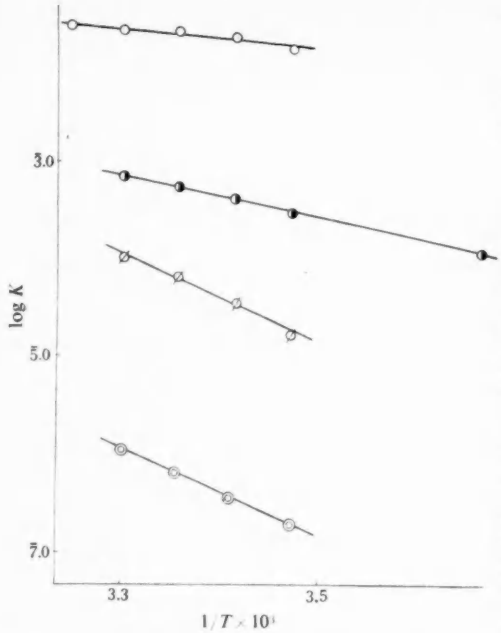

Fig. 1. The relationship between the equilibrium constant of solution and the temperature for Erdmann's salt, $NH_4[(Co(NH_3)_2(NO_2)_4]$ (○), $K[Co(NH_3)_2(NO_2)_4]$ (◑), *cis*-$[Co(NH_3)_4(NO_2)_2][Co(NH_3)_2(NO_2)_4]$ (⊘), and *trans*-$[Co(NH_3)_4(NO_2)_2][Co(NH_3)_2(NO_2)_4]$ (◎).

The heat of solution and the entropy change of solution at 25°C are obtained as $\Delta H = 3530$ cal. and $\Delta S^\circ = 4.108$ e. u., respectively.

As described in the preceding paper[2], it is found that the entropy of formation of cobalt (III) nitroammine complexes increases by 160 e. u. for each replacement of one gram equivalent of ammonia by one gram equivalent of nitrogroup. Therefore the sum of this value and the entropy of formation of trinitrotriamminecobalt(III) complex in unit activity in aqueous solution, $\Delta S^\circ = 172$ e. u., may be regarded as that of tetranitrodiamminecobaltate (III) anion in unit activity in aqueous solution, i. e. $\Delta S^\circ = 332$ e. u. Since the heat of formation of the latter is $\Delta H = -164.9$ kcal.[12], the free energy of formation is given by the equation:

$$\Delta G_f^\circ = -164900 - 332\,T, \quad \Delta G_{f\,298}^\circ = -263.9 \text{ kcal.} \tag{2}$$

The free energy of formation of NH_4^+ in unit activity is given as[13]

$$\Delta G_f^\circ = -31740 - 42.74\,T \tag{3}$$

From Eqs. 1, 2 and 3, the free energy of formation of Erdmann's salt in the solid state is calculated as

$$\Delta G_f^\circ = -200200 - 288.9\,T,$$

$$\Delta G_{f\,298}^\circ = -286.3 \text{ kcal.}$$

Free Energy of Formation of Potassium Tetranitrodiamminecobaltate(III).—The equilibrium constant of the solution of potassium tetranitrodiamminecobaltate(III) is given by $K = m^2\gamma^2_\pm$ in the same way as that of Erdmann's salt described above. The relationship between $\log K$ and $1/T$ is given by a straight line in Fig. 1, which is expressed by the equation,

$$\log K = 3.917 - 2138/T$$

The free energy change of solution is given as

$$\Delta G^\circ = 9777 - 17.92\,T, \quad \Delta G_{298}^\circ = 4436 \text{ cal.} \tag{4}$$

and the heat of the solution is $\Delta H = 9777$ cal., and the entropy change of the solution at 25°C is $\Delta S^\circ = 17.92$ e. u. The free energy of formation of K^+ in unit activity in aqueous solution is given as

$$\Delta G_f^\circ = -60040 - 24.91\,T \tag{5}$$

From Eqs. 2, 4 and 5, the free energy of formation of potassium tetranitrodiamminecobaltate(III) in the solid state is calculated as below:

$$\Delta G_f^\circ = -234700 - 339\,T, \quad \Delta G_{f\,298}^\circ = -335.8 \text{ kcal.}$$

Free Energy of Formation of *cis*- and *trans*-Dinitrotetramminecobalt(III)-Tetranitrodiamminecobaltates(III).—The equilibrium constants of solution of these salts are given by $K = m^2\gamma_\pm^2$ as above and the relationships between $\log K$ and $1/T$ are given by two straight lines for both salts in Fig. 1, which are expressed for the cis salt by

$$\log K = 10.71 - 4450/T$$

and for the trans salt by

$$\log K = 9.014 - 4532/T$$

The free energy change of solution of the cis salt is obtained as

$$\Delta G^\circ = 20350 - 48.98\,T, \quad \Delta G_{29}^\circ = 5751 \text{ cal.} \tag{6}$$

and that of the trans salt is obtained as

$$\Delta G^\circ = 20730 - 41.23\,T, \quad \Delta G_{298}^\circ = 8438 \text{ cal.} \tag{7}$$

The heat of solution and the entropy change of solution of the above cis salt are $\Delta H = 20350$ cal. and $\Delta S^\circ = 48.98$ e. u. and those of the above trans salt are $\Delta H = 20730$ cal. and $\Delta S^\circ = 41.23$ e. u., respectively.

12) K. B. Yatsimirskii and L. L. Pankowa, *Zhur. Obshchei Khim.*, **19**, 623 (1949); K. B. Yatsimirskii, "Thermochemie von Komplexverbindungen", Akademie-Verlag, Berlin (1956), p. 180.

13) C. C. Stephenson, *J. Am. Chem. Soc.*, **66**, 1436 (1944).

14) A. E. Hill and J. E. Ricci, *J. Am. Chem. Soc.*, **53**, 4305 (1931).

In the preceding paper[2] the free energy of formation of *cis*- and *trans*-dinitrotetramminecobaltate(III) ions was obtained respectively as

$$\Delta G_f^\circ = -159900 - 16.10\,T \quad (8)$$

$$\Delta G_f^\circ = -159100 - 7.72\,T \quad (9)$$

From Eqs. 2, 6 and 8, the free energy of formation of the cis salt in the solid sate is obtained as

$$\Delta G_f^\circ = -345200 - 299.1\,T,$$

$$\Delta G_{f\,298}^\circ = -434.4 \text{ kcal.}$$

and from Eqs. 2, 7 and 9, that of the trans salt in the solid state is obtained as

$$\Delta G_f^\circ = -344700 - 298.5\,T,$$

$$\Delta G_{f\,298}^\circ = -433.7 \text{ kcal.}$$

Free Energy of Formation of Nitropentamminecobalt(III)-Tetranitrodiamminecobaltate(III). —The equilibrium constant of solution of this complex is given by $K = 4\,m^3\gamma^3_\pm$ and a plot of $\log K$ against $1/T$ gives a straight line in Fig. 2, which is expressed by the equation:

$$\log K = 7.530 - 4667/T$$

The free energy change of solution is given by

$$\Delta G^\circ = 21390 - 34.44\,T,$$

$$\Delta G_{298}^\circ = 11130 \text{ cal.} \quad (10)$$

The heat of solution and the entropy change of solution are obtained as $\Delta H = 21.39$ kcal. and $\Delta S^\circ = 34.44$ e. u., respectively.

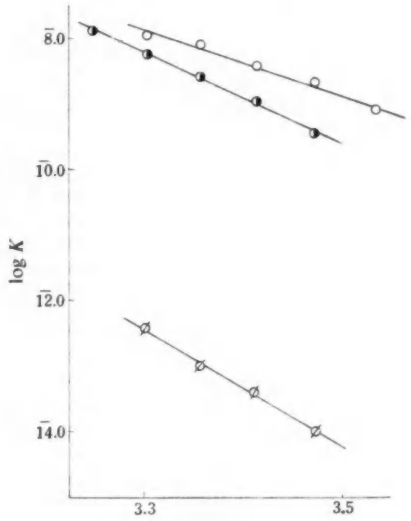

Fig. 2. The relationship between the equilibrium constant of solution and the temperature for $[Co(NH_3)_5NO_2][Co(NH_3)_2(NO_2)_4]_2$ (○), $[Co(NH_3)_5Cl][Co(NH_3)_2(NO_2)_4]_2$ (◑) and $[Co(NH_3)_6][Co(NH_3)_2(NO_2)_4]_3$ (⊘).

The free energy of formation of nitropentamminecobalt(III) ion was obtained in the preceding paper[2] as

$$\Delta G_f^\circ = -153100 + 148.3\,T \quad (11)$$

From Eqs. 2, 10 and 11, that of nitropentamminecobalt(III)-tetranitrodiamminecobaltate(III) is obtained as below:

$$\Delta G_f^\circ = -504300 - 481.3\,T,$$

$$\Delta G_{f\,298}^\circ = -647.8 \text{ kcal.}$$

Free Energy of Formation of Chloropentamminecobalt(III)-Tetranitrodiamminecobaltate(III). —The equilibrium constant of solution of this complex is also given by $K = 4\,m^3\gamma^3_\pm$ in the same way as the above. A plot of $\log K$ against $1/T$ gives a straight line in Fig. 2 and its equation is calculated as

$$\log K = 13.93 - 6714/T$$

The free energy change of solution is given by

$$\Delta G^\circ = 30710 - 63.72\,T,$$

$$\Delta G_{f\,298}^\circ = 11710 \text{ cal.} \quad (12)$$

The heat of solution is $\Delta H = 30710$ cal. and the entropy change of solution, $\Delta S^\circ = 63.72$ e. u.

The free energy of formation of chloropentamminecobalt(III) ion is obtained from the solubility data[5] and given by the equation,

$$\Delta G_f^\circ = -156100 + 270.9\,T \quad (13)$$

From Eqs. 2, 12 and 13, the free energy of formation of chloropentamminecobalt(III)-tetranitrodiamminecobaltate(III) in the solid state is calculated as

$$\Delta G_f^\circ = -516600 - 329.4\,T,$$

$$\Delta G_{f\,298}^\circ = -614.8 \text{ kcal.}$$

Free Energy of Formation of Hexamminecobalt(III)-Tetranitrodiamminecobaltate(III). —The equilibrium constant of solution of this complex is given by $K = 27\,m^4\gamma^4_\pm$ in the same way as that of the hexamminecobalt(III) salts already reported[15]. The logarithm of K is plotted against $1/T$ in Fig. 1 as a straight line, the equation being

$$\log K = 16.83 - 8873/T$$

The free energy change of solution is given by

$$\Delta G^\circ = 40590 - 76.98\,T,$$

$$\Delta G_{298}^\circ = 17640 \text{ cal.} \quad (14)$$

The heat of solution is obtained as $\Delta H = 40590$ cal. and the entropy change of solution as $\Delta S^\circ = 76.98$ e. u.

15) M. Mori, R. Tsuchiya and Y. Okano, This Bulletin, 32, 462 (1959).

TABLE VIII. THERMODYNAMIC FUNCTIONS OF NITROAMMINECOBALT(III) COMPLEXES AT 25°C

Complex	Solubility	Heat of solution	Equivalent free energy of solution	Entropy change of solution	Lattice energy	Standard free energy of formation
	m	ΔH cal.	ΔG° cal.	ΔS° e.u.	U kcal.	ΔG_f° kcal.
$NH_4[Co(NH_3)_2(NO_2)_4]$	0.209	3530	2305			−286.3
$K[Co(NH_3)_2(NO_2)_4]$	0.0684	9777	4436			−335.8
cis-$[Co(NH_3)_4(NO_2)_2]\cdot[Co(NH_3)_2(NO_2)_4]$	8.99×10^{-3}	20350	5751	48.98	101.4	−434.4
trans-$[Co(NH_3)_4(NO_2)_2]\cdot[Co(NH_3)_2(NO_2)_4]$	8.38×10^{-4}	20730	8438	41.23	101.7	−433.7
$[Co(NH_3)_5NO_2][Co(NH_3)_2(NO_2)_4]_2$	1.46×10^{-3}	21390	5565		321.4	−647.8
$[Co(NH_3)_5Cl]\cdot[Co(NH_3)_2(NO_2)_4]_2$	1.00×10^{-3}	30710	5857		323.7	−614.8
$[Co(NH_3)_6][Co(NH_3)_2(NO_2)_4]_3$	2.84×10^{-4}	40590	5880		664.6	−863.7

In the second paper[15] of this series the free energy of formation of hexamminecobalt(III) ion was already obtained as

$$\Delta G_f^\circ = -146000 + 307\,T \qquad (15)$$

Therefore, from Eqs. 2, 14 and 15, the free energy of formation of hexamminecobalt(III)-tetranitrodiamminecobaltate(III) in the solid state is given by

$$\Delta G_f^\circ = -681300 - 612\,T,$$
$$\Delta G_{f\,298}^\circ = -863.7 \text{ kcal.}$$

Discussion

The thermodynamic functions of the nitroamminecobalt(III) complexes at 25°C calculated above are summarized in Table VIII. In this table the free energy of solution is the value for one gram equivalent of each complex, i. e., equivalent free energy of solution.

As shown in this table, the solubilities of these complexes decrease in the order of 1-1, 1-2 and 1-3 valency type salts. In these respects *trans*-$[Co(NH_3)_4(NO_2)_2][Co(NH_3)_2(NO_2)_4]$ presents a single exception. The equivalent free energies of solution lie within the region between 5500 and 5900 cal. except for *trans*-$[Co(NH_3)_4(NO_2)_2][Co(NH_3)_2(NO_2)_4]$, $K[Co(NH_3)_2(NO_2)_4]$ and Erdmann's salt. This corresponds to the free energy required for breaking a bond between the cation and the anion and hydrating each of the ions when the salt is dissolved.

The free energy of solution of *cis*-dinitrotetramminecobalt(III)-tetranitrodiamminecobaltate(III) is remarkably less than that of the corresponding trans salt. This is due to the fact that the entropy change of solution of the former is much greater than that of the latter. In other words, the entropy effect plays an important role when the cis and trans salts are dissolved in water just as in the case of the *cis*- and *trans*-dinitrotetramminecobalt(III) chloride reported in the preceding paper[2].

The heats of hydration of the complex ions concerned are listed in Table IX[16].

TABLE IX. HEAT OF HYDRATION OF COMPLEX IONS

Complex ion	Heat of hydration (kcal.)
$[Co(NH_3)_4(NO_2)_2]^+$	−40
$[Co(NH_3)_5NO_2]^{2+}$	−218
$[Co(NH_3)_5Cl]^{2+}$	−211
$[Co(NH_3)_6]^{3+}$	−501
$[Co(NH_3)_2(NO_2)_4]^-$	−41

By using these values and the heats of solution of the cobalt(III) nitroammine complexes described above, their lattice energies are computed. These are also shown in Table VIII.

The standard free energies of formation of four cobalt(III) nitroammine complexes in the solid state are given by:

$$2Co(s) + 6N_2 + 9H_2 + 6O_2 = cis\text{-}[Co(NH_3)_4(NO_2)_2][Co(NH_3)_2(NO_2)_4] \quad \Delta G_f^\circ = -434.4 \text{ kcal.} \qquad (a)$$

$$2Co(s) + 6N_2 + 9H_2 + 6O_2 = trans\text{-}[Co(NH_3)_4(NO_2)_2][Co(NH_3)_2(NO_2)_4] \quad \Delta G_f^\circ = -433.7 \text{ kcal.} \qquad (b)$$

$$3Co(s) + 9N_2 + 27/2H_2 + 9O_2 = [Co(NH_3)_5NO_2][Co(NH_3)_2(NO_2)_4]_2 \quad \Delta G_f^\circ = -647.8 \text{ kcal.} \qquad (c)$$

$$4Co(s) + 12N_2 + 18H_2 + 12O_2 = [Co(NH_3)_6][Co(NH_3)_2(NO_2)_4]_3 \quad \Delta G_f^\circ = -863.7 \text{ kcal.} \qquad (d)$$

16) K. B. Yatsimirskii, "Thermochemie von Komplexverbindungen", Akademie-Verlag, Berlin (1956), p. 38.

By dividing a and b by two, c by three and d by four the following values are obtained:

$$Co(s)+2N_2+9/2H_2+3O_2 = 1/2\ cis\text{-}[Co(NH_3)(NO_2)_2]\cdot[Co(NH_3)_2(NO_2)_4]$$
$$\Delta G_f^\circ = -217.2\ \text{kcal.}$$

$$Co(s)+3N_2+9/2H_2+3O_2 = 1/2\ trans\text{-}[Co(NH_3)_4(NO_2)_2]\cdot[Co(NH_3)_2(NO_2)_4]$$
$$\Delta G_f^\circ = -216.9\ \text{kcal.}$$

$$Co(s)+3N_2+9/2H_2+3O_2 = 1/3\ [Co(NH_3)_5NO_2][Co(NH_3)_2(NO_2)_4]_2$$
$$\Delta G_f^\circ = -215.9\ \text{kcal.}$$

$$Co(s)+3N_2+9/2H_2+3O_2 = 1/4\ [Co(NH_3)_6][Co(NH_3)_2(NO_2)_4]_3$$
$$\Delta G_f^\circ = -215.9\ \text{kcal.}$$

From these values it is found that the free energy of formation of the above-mentioned cobalt(III) nitroammine complexes is proportional to the number of cobalt atoms contained in one molecule of these complexes.

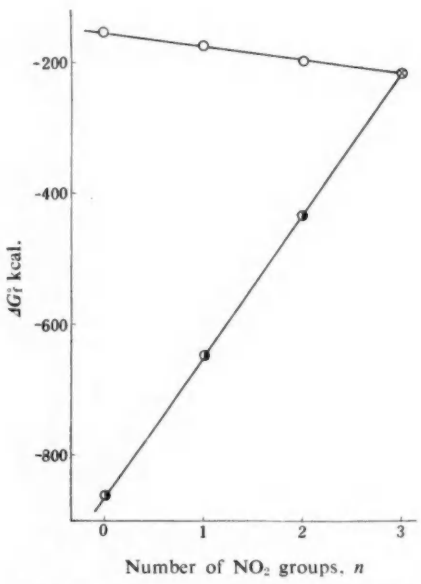

Fig. 3. The relationship between the free energy of formation and the number of nitrogroups co-ordinated in the series of several tetranitrodiamminecobaltates-(III), that is $[Co(NH_3)_{6-n}(NO_2)_n][Co(NH_3)_2(NO_2)_4]_{3-n}$ (◑) and $[Co(NH_3)_{6-n}(NO_2)_n]Cl_{3-n}$ (○). (⊗) is trinitrotriamminecobalt(III) complex.

When the free energies of formation of the series consisting of $[Co(NH_3)_6][Co(NH_3)_2(NO_2)_4]_3$—$[Co(NH_3)_5NO_2][Co(NH_3)_2(NO_2)_4]_2$—$[Co(NH_3)_4(NO_2)_2][Co(NH_3)_2(NO_2)_4]$ are plotted against the number of NO_2 contained in their cations in Fig. 3, a straight line is obtained. This line passes through a point giving the free energy of formation of $[Co(NH_3)_3(NO_2)_3]$. The line for the free energy of formation of the series, $[Co(NH_3)_6]Cl_3$—$[Co(NH_3)_5NO_2]Cl_2$—$[Co(NH_3)_4(NO_2)_2]Cl$, against the number of NO_2 also converges to the same point as shown in Fig. 3.

It can be expected that the free energies of formation of $[Co(NH_3)_6][Co(NO_2)_6]$, $[Co(NH_3)_5NO_2][Co(NH_3)(NO_2)_5]$, $[Co(NH_3)_4(NO_2)_2][Co(NH_3)_2(NO_2)_4]$ and $2[Co(NH_3)_3(NO_2)_3]$, are almost equal. The latter three are produced by the successive replacement of NH_3 in cation and NO_2 in anion of $[Co(NH_3)_6][Co(NO_2)_6]$ with NO_2 and NH_3 respectively, thus forming a set of coordination isomers. Thus the free energy of formation of $2[Co(NH_3)_3(NO_2)_3]$ is $\Delta G_f^\circ = -428.2$ kcal., that of *cis*-$[Co(NH_3)_4(NO_2)_2][Co(NH_3)_2(NO_2)_4]$ $\Delta G_f^\circ = -434.4$ kcal. and that of the trans salt $\Delta G_f^\circ = -433.7$ kcal., although those of $[Co(NH_3)_6][Co(NO_2)_6]$ and $[Co(NH_3)_5NO_2][Co(NH_3)(NO_2)_5]$ have not been found. These facts mean that the free energy of formation cobalt(III) nitroammine complexes is additive with respect to the NO_2 group.

Furthermore, it is also found that the thermodynamic stability of $[Co(NH_3)_5NO_2][Co(NH_3)_2(NO_2)_4]_2$ is greater than that of $[Co(NH_3)_5Cl][Co(NH_3)_2(NO_2)_4]_2$, since the free energy of formation of the former is less than that of the latter.

Summary

The solubilities of Erdmann's salt, $NH_4[Co(NH_3)_2(NO_2)_4]$, and the following complexes which have the same complex anion, $K[Co(NH_3)_2(NO_2)_4]$, *cis*- and *trans*-$[Co(NH_3)_4(NO_2)_2][Co(NH_3)_2(NO_2)_4]$, $[Co(NH_3)_5NO_2][Co(NH_3)_2(NO_2)_4]_2$, $[Co(NH_3)_5Cl][Co(NH_3)_2(NO_2)_4]_2$ and $[Co(NH_3)_6][Co(NH_3)_2(NO_2)_4]_3$ were measured. Based upon the thermodynamic functions calculated from the above measurement, the free energy of solution, the lattice energy and the free energy of formation of these complexes were calculated and discussed.

Department of Chemistry
Faculty of Science
Kanazawa University
Kanazawa

Oxidizing Action of Hydroperoxides. IV. On the Oxidation of Aryl Alkyl Ketones

By Kazuhiro MARUYAMA

(Received March 23, 1960)

This research was started with a view to studying the liquid phase autoxidation of *p*-cymene some years ago. In the liquid phase autoxidation of *p*-cymene in the presence of alkali hydroxide, no resinous product was produced and 8-hydroxy-*p*-cymene, cumic acid and *p*-toluic acid were found, accompanied by a negligibly small amount of *p*-methylacetophenone—an interesting contrast to the autoxidation in the absence of alkali hydroxide. From the studies on the autoxidation of some hydrocarbons, it was observed[1] that alkylhydroperoxides act as a strong oxidizing agent on alkylbenzene and also on some carbonyl compounds*, e.g., the primary carbon atom at α-position of the side chain is oxidized to alcohol, to aldehyde and finally to carboxylic acid, the secondary carbon is oxidized to carbonyl group and finally decomposes to yield a mixture of acids and the tertiary carbon atom is oxidized to alcohol and/or decomposes to ketone having a fewer number of carbon atoms. Especially, aryl alkyl ketones are easily split by these oxidizing agents into aromatic carboxylic acid and aliphatic alcohol. Further, in all these oxidation reactions, in contrast to peracid oxidation, no phenolic substances are produced. Also diaryl ketones are not affected by these oxidizing agents—an outstanding difference as compared with the case of the cleavage of ketones by peracids**—, whereas aryl alkyl ketones are affected with great ease. In this paper are reported only the oxidation of aryl alkyl ketones.

Experimental

Materials.—*p*-Methylacetophenone was prepared by the action of acethyl chloride on toluene using anhydrous aluminium chloride as a catalyst. The resulting *p*-methylacetophenone was distilled under reduced pressure using Hempel's column, b. p. 94~95°C/12 mmHg: semicarbazone, m. p. 205°C. Propiophenone was prepared by the action of propionyl chloride on benzene suspending anhydrous aluminum chloride. The resulting propiophenone was completely freed from aluminum ions by shaking with acid and alkali, and was distilled under reduced pressure. B. p. 105°C/20 mmHg, m. p. 21°C. *tert*-Butyl phenyl ketone was synthesized from isopropyl phenyl ketone, following Halle's method[2]. B. p. 220~222°C, 104~106°C/17 mmHg, 2,4-dinitrophenylhydrazone; m. p. 166~168°C. Benzophenone was prepared by the action of benzoyl chloride on benzene suspending anhydrous aluminum chloride. M. p. 47~48°C. Fluorenone was synthesized by the oxidation of commercial grade fluorene, following Fanto's method[3]. M. p. 83~84°C. *p*-Nitrobenzophenone was synthesized by the action of *p*-nitrobenzoyl chloride on benzene suspended with anhydrous aluminum chloride, following Schroeter's method[4]. M. p. 138°C. *tert*-Butylhydroperoxide was synthesized by the action of 30% hydrogen peroxide on *tert*-butanol, following Milas and Surgenor's method[5]. The obtained mixture of *tert*-butylhydroperoxide and di-*tert*-butylperoxide was fractionally distilled under reduced pressure. For the purpose of obtaining highly purified hydroperoxide, this process was repeated four times. B. p. 36°C/19 mmHg. n_D^{25}: 1.3967. Cumylhydroperoxide was synthesized by the autoxidation of cumene, following Armstrong, Hall and Quin's method[6]. The obtained cumylhydroperoxide was purified by the fractionation under a high vacuum. B. p. 53~54°C/0.0005 mmHg.

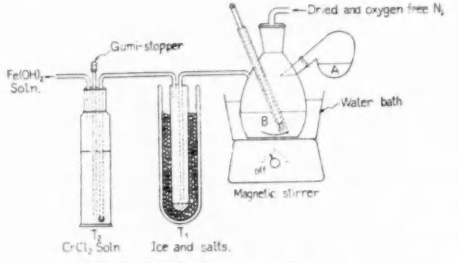

Fig. 1. Reaction apparatus.

Reaction Apparatus and Procedure.—The reaction apparatus is shown in Fig. 1. Ketone, monochlorobenzene and finely powdered analytical grade

1) Unpublished work.

* M. S. Kharasch et al. reported that alkylhydroperoxides act as an oxidizing agent on the primary as well as secondary alcohols in alkaline solution (*J. Org. Chem.*, **17**, 207 (1952).

** W. H. Saunders, *J. Am. Chem. Soc.*, **77**, 4679 (1957); W. v. E. Doering and E. Dorfman, ibid., **75**, 5595 (1953); W. G. Dauben and E. Hoerger, ibid., **73**, 1504 (1951), etc.

2) M. A. Haller and Ed. Bauer, *Compt. rend.*, **148**, 72 (1909).

3) R. Fanto, *Monatsh.*, **19**, 584 (1898).

4) G. Schroeter., *Ber.* **42**, 3360 (1909).

5) N. A. Milas and D. Surgenor, *J. Am. Chem. Soc.*, **68**, 1938 (1946).

6) G. P. Armstrong, R. Hall and D. C. Quin, *Nature*, **164**, 834 (1949).

potassium hydroxide were charged in B and hydroperoxide in A. After the air in the reaction vessel (A and B) was substituted completely with dried and purified nitrogen gas and the temperature of the reaction mixture was made to reach 80°C, and then the hydroperoxide was poured into the reaction mixture by rotating the part A by hand. A flow of the nitrogen gas was maintained constantly to 30 cc./min. during the reaction. A vigorous reaction occurred and the temperature of the reaction mixture was raised to about 90°C. Trap T_1 was cooled with ice and salt for condensing therein low boiling substances. The oxygen evolved during the reaction was determined at Trap T_2 charged with chromous chloride hydrochloric acid solution[7].

Oxidation.—*Acetophenone.*—10 g. of acetophenone were dissolved in 150 cc. monochlorobenzene in which 1.3 g. of finely powdered special grade potassium hydroxide were suspended. As an oxidizing agent, 2.0 g. of *tert*-butylhydroperoxide were used. The reaction mixture was agitated by a magnetic stirrer. After the temperature of the reaction mixture reached 80°C, A was gradually rotated to pour the peroxide into B. Then, a vigorous reaction occurred and a white precipitate appeared immediately. Almost all the peroxide was decomposed in the first hour, but about 6 hr. were required to complete the decomposition. After the end of the reaction, the reaction mixture was extracted with a total of 300 g. of water three times. The water extract was acidified with 2 N sulfuric acid and the precipitated benzoic acid was collected, dried and weighed. The filtrate was neutralized with concentrated ammonia water and concentrated to 10 cc., and then subjected to a paperchromatographic analysis. However, no appreciable amount of formic acid was observed. The substances condensed in Trap T_1 were gaschromatographically tested and methanol and *tert*-butanol were found to be the main components.

p-Methylacetophenone. — 50 g. of *p*-methylacetophenone suspending 1.3 g. of finely powdered potassium hydroxide were charged in B. As an oxidizing agent, 2.0 g. of *tert*-butylhydroperoxide were used. The reaction procedure was in manner similar to that of the acetophenone. The water extract was acidified. Then, *p*-toluic acid was the main reaction product. *p*-Acetylbenzoic acid and formic acid were paperchromatographically detected in the filtrate, but the amounts of acids were too small to be estimated. *p*-Toluic acid (m. p. 176°C) was confirmed by recrystallization and paperchromatography. The condensate of the Trap T_1 was analyzed gaschromatographically to find methanol and *tert*-butanol as the main components.

Propiophenone.—10 g. of propiophenone were dissolved in 150 cc. monochlorobenzene in which finely powdered 1.7 g. potassium hydroxide suspended. As an oxidizing agent, 2.0 g. of *tert*-butylhydroperoxide were used. After the temperature of the reaction mixture reached 80°C, A was rotated to pour the peroxide into the mixture and a vigorous reaction took place. Then the temperature of the reaction mixture reached as high as 95°C in a few minutes. Almost all the amount of the peroxide was decomposed in the first half hour, but the reaction continued for 6 hr. to complete the decomposition of the peroxide. The water extract was acidified with 2 N sulfuric acid and the acid precipitated was filtrated, dried and weighed. The filtrate was steamdistilled. Acetic acid was found in the distillate. This was estimated by titration. The acetaldehyde and acetone were also detected as 2,4-dinitrophenylhydrazone on a silicagel chromatostrip, but not estimated. From the condensate in Trap T_1, ethanol, *tert*-butanol and methanol were respectively detected gaschromatographically (see Fig. 2), but not estimated. A trace of oxygen was detected in Trap T_2.

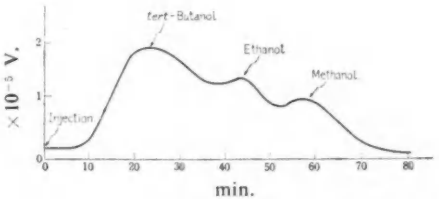

Fig. 2. Gaschromatographic analysis of oxidation products of propiophenone.
Propiophenone $\xrightarrow{tert\text{-}C_4H_9OOH,\ KOH}$ Products
Condition: Sample used: 0.02 ml.
Column temp.: 83°C
Flow rate: N_2 40 ml./min.
Column: Glycerol-Kunirait (20 : 100 w/w)

tert-Butyl Phenyl Ketone.—Eight grams of *tert*-butyl phenyl ketone were dissolved in 150 cc. monochlorobenzene suspending 2.8 g. of finely powdered potassium hydroxide. As an oxidizing agent, 10g. of cumylhydroperoxide were used. Cumylhydroperoxide was used to afford facilities for an analysis of low boiling substances, because thermal decomposition products of cumylhydroperoxide will be methanol, aceto-

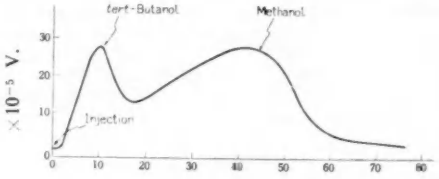

Fig. 3. Gaschromatographic analysis of oxidation products of *tert*-butylphenylketone.
tert-Butylphenylketone $\xrightarrow[KOH]{cumylhydroperoxide}$ products
Condition: Sample: 0.03 ml.
Column temp.: 85°C.
Flow rate: N_2 60 ml./min.
Column.: Glycerol-Kunirait (20 : 100 w/w)

7) J. Meis, *Chem. Abstr.*, 8748*d* (1955); H. Karl, *Paliva*, 35, 8 (1955); *Chem. Abstr.*, 13019g (1955); von Pferdton, *Ann.*, 228, 112 (1885).

TABLE I. OXIDATION OF KETONES BY HYDROPEROXIDES AT 80°C, 6 hr.

Ketone g.		Hydroperoxide g.	Recovered ketone g.	Reaction products, g.		Oxygen
				Acid	Alcohol	
Acetophenone	10	*tert*-Butyl 2.0	9.1	Benzoic acid 0.50	(*tert*-Butanol), methanol	None
〃	10	*tert*-Butyl 2.0	8.5	Benzoic acid 0.71	(*tert*-Butanol), methanol	None
p-Methyl-acetophenone	50	*tert*-Butyl 2.0	45	*p*-Toluic acid 1.0, *p*-acetylbenzoic acid (trace), formic acid (trace)	(*tert*-Butanol),	None
〃	50	*tert*-Butyl 2.0	42	*p*-Toluic acid 1.5, *p*-acetylbenzoic acid (trace), formic acid (trace)	(*tert*-Butanol), methanol	Trace
Propiophenone	10	*tert*-Butyl 2.0	8.3	Benzoic acid 1.13, acetic acid 0.34, formic acid (trace)	(*tert*-Butanol), ethanol, methanol	None
Propiophenone	17	*tert*-Butyl 2.0	—	Benzoic acid 1.13, acetic acid —, formic acid (trace)	(*tert*-Butanol), ethanol, methanol	None
tert-Butylphenyl ketone	10	Cumyl 10	9.5	Benzoic acid 2.5	(*tert*-Butanol), methanol, (α,α-dimethyl-benzylalcohol)	None
tert-Butylphenyl ketone	0.5	*tert*-Butyl 1.0	—	Benzoic acid 0.05	(*tert*-Butanol), methanol	Trace
Benzophenone	10	*tert*-Butyl 2.0		None reaction		O_2-evolute
p-Nitrobenzo-phenone	10	*tert*-Butyl 2.0		None reaction		O_2-evolute
Fluorenone	10	*tert*-Butyl 2.0		None reaction		O_2-evolute

(*tert*-Butanol and α,α-dimethylbenzylalcohol are reduction products of *tert*-butylhydroperoxide and cumylhydroperoxide.)

phenone and α,α-dimethylbenzylalcohol, if the thermal decomposition would occur. On the other hand, the reduction product which could be expected through the reduction of cumylhydroperoxide by ketone, is α,α-dimethylbenzylalcohol. Treatment of the reaction mixture was almost the same as in the case of propiophenone. From the water extract was obtained benzoic acid which was confirmed by recrystallization and paperchromatography. *tert*-Butanol was detected and estimated as the main component of low boiling substances condensed in the Trap T_1. This was confirmed as phenylurethane (m. p. 136°C; Found: C, 67.4; H, 7.4. Calcd. for $C_{11}H_{16}O_2N$: C, 68.3; H, 7.7%) and also gaschromatographic analysis was made. Besides *tert*-butanol, a small amount of methanol was also found.

Benzophenone, p-Nitrobenzophenone and Fluorenone. —10 g. of each of all the ketones were dissolved separately in 100 cc. monochlorobenzene in which 2.8 g. of finely powdered potassium hydroxide were suspended. 5 g. of *tert*-butylhydroperoxide were used as an oxidizing agent. Oxidation was carried out in the same apparatus as shown in Fig. 1. After the reaction had finished, the same procedure as before was repeated. None of the oxidation products of the ketones was found and the greater part of unchanged ketones were completely recovered during the reaction. Only oxygen—one of the decomposition products of the hydroperoxide—evolved vigorously in all the cases. *tert*-Butanol, acetone and methanol—the remaining decomposition products of the hydroperoxide itself—were found in the reaction mixture. The experimental results were summarized in Table I.

Discussion

It is likely that for the oxidizing action of hydroperoxides their anions are responsible, because the hydroperoxides themselves can cleave aryl alkyl ketone very slowly or can not do so at all in the absence of alkali hydroxide. Furthermore, in the course of oxidation of alkylbenzenes[8] (*p*-xylene, cumene, ethylbenzene, *p*-cymene and tetralin) by alkali hydroperoxide, the author has observed that potassium hydroxide suspended in alkylbenzene at the beginning of the reaction dissolves nearly completely after the hydroperoxide added and then the oxidation occurs immediately. The alkylbenzenes are oxidized to alcohols, ketones and carboxylic acids. In contrast to this, hydroperoxide alone can not oxidize a side chain of the alkylbenzene in the absence of alkali hydroxide. It may, therefore, be induced

8) K. Maruyama and R. Goto, *Wood Research*, **21**, 12 (1959).

that the anion of hydroperoxide acts as an oxidizing agent. Kharasch et al.[9] asserted that the anion of hydroperoxide is an oxidizing agent in the oxidation of alcohol by hydroperoxide in alkaline solution.

In the oxidation of the above aryl alkyl ketones, the first oxidation products are arylcarboxylc acid and aliphatic alcohol. For example, when propiophenone is oxidized in the above conditions, benzoic acid, ethanol, acetaldehyde and acetic acid are obtained, and it may be seen easily that the latter two products are the second oxidation products. *tert*-Butyl phenyl ketone is also decomposed to benzoic acid and *tert*-butanol (peroxide used, cumylhydroperoxide). Oxidation of both acetophenone and *p*-methylacetophenone yields benzoic acid, *p*-toluic acid and methanol as the main reaction products. However, the methanol provides no direct evidence of alcoholic cleavage originating in the methyl-group of acetophenone or *p*-methylacetophenone, because methanol can be a thermal decomposition product of *tert*-butylhydroperoxide. In spite of the above misgivings, it may be possible to deduce that the methanol would be a cleavage product of acetophenone and also of *p*-methylacetophenone from the estimation of the results of cleavage of propiophenone and *tert*-butyl phenyl ketone; that is, the propiophenone produces ethanol and the *tert*-butyl phenyl ketone produces *tert*-butanol. On the other hand, it seems reasonable to deduce from the experimental results of benzophenone, *p*-nitrobenzophenone and fluorenone that in general diaryl ketones resist the oxidizing agent. This is noticeably different from the cleavage of ketones by peracids, because diaryl ketones are easily cleft by peracids—e.g., peracetic acid—to produce phenols and carboxylic acids[10]. In the cleavage of alkyl aryl ketones by peracids with the exception of cycloalkyl aryl ketones[11], a migration of the aryl group generally occurs, resulting in the formation of phenol.

On the contrary, acetophenone, *p*-methylacetophenone, propiophenone and *tert*-butyl phenyl ketone do not undergo such a cleavage as to yield phenols and carboxylic acids as anticipated from the phenolic cleavage of ketones, that is, the C–C linkage between the carbon atom of benzene and the carbonyl carbon atom resists the attack of hydroperoxide anion and the C–C linkage between the carbonyl carbon atom and the alkyl carbon atom is selectively attacked. For the above reasons, it may be assumed that the oxidation mechanism of ketones by hydroperoxide anion must be kept separated from that of ketones by peracids. Recently, House et al.[12] have reported the cleavage of ketones by alkaline hydrogen peroxide with a poor yield. Based upon the fact that butyrophenone does not cleave to phenol and butyric acid but does cleave to benzoic acid and propionic acid and/or corresponding propanol, they suggest a partly revised oxidation mechanism based on the peracid oxidation mechanism. However, the oxidation mechanism imagined by them hardly explains the results obtained by the present author in the oxidation of diaryl ketones. The author proposes a new oxidation scheme as follows:

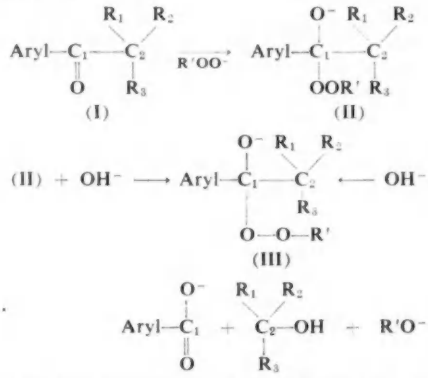

In the above assumption, hydroxide anion plays in III a most important role, that is a "pushing action" which is indispensable to the cleavage of ketones. In the case of action of hydroperoxide anion to diaryl ketones resulting in no cleavage, the pushing action of hydroxide anion on C_2 which is the benzene ring carbon atom, would not effectively affect it owing to the high potential energy of the transition state represented by IV.

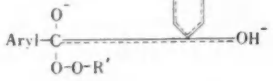

(IV)

Moreover, the fact that with aromatic halides the S_N2 type substitution reaction can not easily proceed appears to support a new mechanism, mentioned above. In future, the author has the intention to perform an experiment of oxidation of ketones having an asymmetric carbon atom at C_2.

9) M. S. Kharasch et al., *J. Org. Chem.*, **17**, 207 (1952).
10) W. H. Saunders, *J. Am. Chem. Soc.*, **77**, 4679 (1957).
11) S. L. Fries and N. Farnham, ibid., **72**, 5518 (1950).
12) H. O. House and R. L. Wasson, *J. Org. Chem.*, **22**, 1157 (1957).

The author is indebted to Professor R. Goto for his encouragement and discussion throughout this research.

Department of Chemistry
Faculty of Science
Kyoto University

Préparation de l'Emulsion à Grand Contraste pour l'Usage Lithographique

Par Shinichi KIKUCHI et Hirozo UEDA

(Reçu le 13 Février, 1960)

Récemment les pellicules à grand contraste comme Kodalith, Reprolith ont commencé à remplacer les plaques humides dans l'usage lithographique. Les émulsions de cette espèce doivent avoir un grand contraste, une forte densité maximum et une partie inférieure courte de la courbe caractéristique. D-85, dit révélateur contagieux[1] est recommandé pour rendre l'image à grande contraste. Nous avons préparé les émulsions qui s'adaptent à ce révélateur spécial et examiné les conditions de préparation de l'émulsion qui paraissent avoir une influence sur le contraste[2]. Avant d'aborder le développement par D-85 qui est spécial, nous avons essayé de développer les émulsions avec les révélateurs N.S.G. et D-11 dont les formules seront données plus tard.

Méthode Adoptée

Nous avons pensé qu'un des points les plus importants pour rendre l'image à grand contraste était d'uniformiser les dimensions des grains d'halogénure d'argent. Pour atteindre ce but, nous avons procédé à varier les conditions suivantes:

1. Le mode d'addition du nitrate d'argent dans la solution de bromure de potassium.
2. La concentration en ions argent dans la solution de nitrate d'argent.
3. La vitesse d'addition du nitrate d'argent.
4. L'excès des ions halogènes.
5. Le rapport des concentrations en ions Cl^-, Br^- et I^-.
6. Le rapport de la concentrations en ions argent à la concentration de gélatine.
7. La concentration de la gélatine.
8. La température.

Nous avons employé dans cette expérience la méthode statistique pour déterminer si quelques-unes de ces conditions ont une influence sur le contraste. La corrélation entre les les conditions et le gamma est jugée par le degré de confiance à 95 et 97%.

Partie Expérimentale

Examen des Gélatines Utilisées.—Dans la première partie de cette étude nous avons examiné les propriétés physico-chimiques et chimiques des gélatines destinées à la préparation de l'émulsion. La teneur en eau de la gélatine a été mesurée par la diminution de poids de la gélatine laissée dans une étuve sèche maintenue à la température constante de 105 ± 5°C. Le point de fusion et le point de congélation ont été mesurés d'après la méthode* recommandée par l'Association des Compagnies Photographiques du Japon. La réaction de Feigl a été examinée de la manière suivante. Environ 1 ml. de la solution de gélatine à 10% qui contient 0.02 g. d'azoture de soude pour 5 ml. de la solution de gélatine, est étendu sur une plaque de verre 2×2 cm. puis laissé à se solidifier. Une heure après, une goutte de solution d'iode (1.268 g. d'iode et 2.5 g. de l'iodure de potassium sont dissous dans 1 litre d'eau distillée) est mise sur la gélatine et cela donne des bulles d'azote suivant la formule: $2NaN_3+I_2=3N_2+2NaI$.

Le nombre de bulle de gaz est compté pendant un quart d'heure et la quantité de bulles est classée entre les valeurs relatives 1 et 10. Cette méthode n'est que qualitative et peut donner une erreur assez élevée quand le nombre de bulles dépasse 40 par 0.5 cm^2.

La réaction de Vogel a été examinée de la manière suivante pour montrer le pouvoir réducteur de gélatine. 10 ml. de nitrate d'argent ammoniacal à 6% et 10 ml. de la solution de gélatine à 2% sont mélangés à 32°C et laissés à cette température pendant 24 heures. La couleur de la gélatine est comparée à l'aide d'un colorimètre de Dubosque et le degré de coloration est classé entre les valeurs relatives 1 et 10. Des propriété physico-chimiques des gélatines essayées sont données dans Tableau I.

1) J. A. Yule, *J. Frankl. Inst.*, **239**, 221 (1945).
2) E. J. Wall, "Photographic Emulsions", (1929) pp. 35, 48 et 67; Eder, "Handb. d. Photogrphie", (1927), Bd. 3 Teil I, 3 Aufl; A. Steigmann, "IX e Congré Intern. Photo. Paris", (1936), pp. 372—386.

* Cette méthode est semblable à celle de PAGI qui a paru dans *Bull. Soc. Phot. Sci. Japon*, No. 6, 34 (1956).

TABLEAU I. PROPRIÉTÉS PHYSICO-CHIMIQUES ET CHIMIQUES DES GÉLATINES

Espèces d'échantillons	Eau %	Point de fusion, °C	Point de congélation, °C	Valeur Feigl	Valeur Vogel
Nitta No. 3	17.7	31.9	26.0	1	1
Nippi process	17.1	31.9	26.6	1	2
Nippi ammonia	16.4	30.4	25.5	10	1
Takarazuka 179-5	16.5	32.5	28.5	4	5

Procédé de Préparation de l'Emulsion.—*a. Les solutions de réactifs.*—Nous avons préparé les solutions de nitrate d'argent, d'halogénure et de gélatine à température déterminée (45°C). La gélatine est dissoute à 45°C, après d'avoir gonflé dans l'eau. La quantité des solutions est en général de 50 ml.

b. Addition des solutions et première maturation.—Les solutions maintenues à 45°C sont mélangées brusquement dans un vase porcelaine et mises à la maturation pendant 20 min. avec agitation. L'appareil d'addition et de maturation est représenté par Fig. 1.

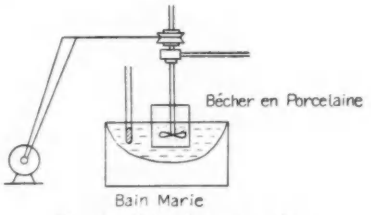

Fig. 1. Bain de maturation.

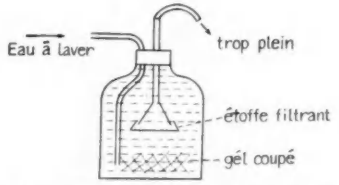

Fig. 2. Appareil de lavage de gél.

c. Congélation de l'émulsion et son coupage en morceaux.—Après la première maturation, l'émulsion est mise dans la glace pour la congélation et elle est laissée pendant une nuit dans un frigorifique. Le lendemain matin l'émulsion est coupée par un réseau encadré de bois et formé d'amylan (résine synthétique) dont la maille est de 3 mm. carré. Les émulsions coupées en morceaux sont lavées à l'eau courante dans l'appareil comme dans Fig. 2. La température de l'eau de lavage est maintenue à 14~16°C. La fin de lavage est contrôlée à l'aide du réactif de Nessler qui permet de vérifier s'il reste de l'ammoniaque. Pour 50 ml. d'émulsion une demi-heure de lavage est nécessaire.

d. 2e Maturation.—Après le lavage, l'émulsion est mise de nouveau dans un bécher de porcelaine où le gel doit se dissoudre en 1 min. à 45°C. En maintenant l'émulsion à cette température, le plus haut gamma est attteint avec une maturation de 40~70 min. L'agitation mécanique pendant la 2e maturation donne naissance à des bulles quand l'émulsion est étendue sur le verre. On agite donc lentement à la main.

e. Coulage de l'émulsion sur le verre.—Le verre de format 119×146 mm. est préalablement lavé, enduit d'une solution d'alun de chrome à 20% et desséché. Avant de coulage, il est porté à 35°C. Le prélèvement de 5 ml. d'émulsion est fait avec une pipette et le coulage est effectué. La couche est nivelée par une tige de verre. La plaque de verre est trans portée sur une planche de verre placée horizontalement et laissée à sécher à l'air à 35°C.

f. Sensitométrie.—La sensitométrie se fait par le sensitomètre type I de N.S.G. qui est muni d'un coin ayant une différence de densités successives de 0.15. Les révélateurs employés sont N.S.G. et D-11 à 20°C et ils sont appliqués pendant 4 minutes.

Résultats

Propriétés Physico-chimiques et Chimiques des Gélatines Utilisées. — Les propriétés physico-chimiques et chimiques des gélatines utilisées sont données dans Tableau I. Dans ce tableau les valeurs relatives de Feigl se réfèrent à 1 de Nitta No 3 et 10 de Nippi ammonia et les valeurs de Vogel à 2 de Nippi 61-i et 10 de Nippi FAG 4.

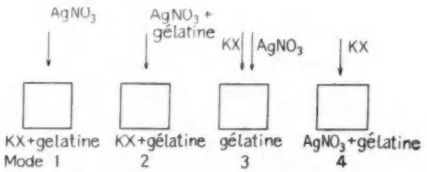

Fig. 3. Différents modes d'addition.

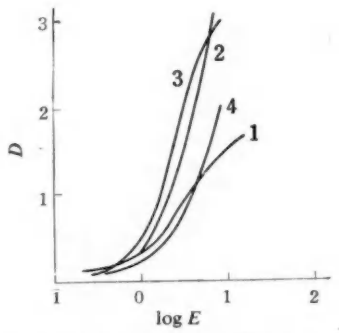

Fig. 4. Courbes caractéristiques.

Différents Modes d'Addition. — Nous avons employé quatre différents modes d'addition comme dans Fig. 3. Les résultats sont indiqués dans Tableau II. Prenons un exemple pour illustrer la signification des nombres donnés dans ce tableau. 25 ml. (0.025 g. mole) de la solution de nitrate d'argent 1 M (conc.) sont ajoutés à une solution de gélatine contenant 23.8 ml. de KBr 1.2 M et 1.2 M ml. de KI 1.2 M. Le repport de KBr/KI est de 23.8/1.2=19.8. Cette solution dissout 2.0575 g. de gélatine, ce qui donne le rapport gélatine en gramme/AgX en g. mole 2.0575/0.025=82.3. Dans les conditions où l'iodure est totalement précipité, le rapport AgBr/AgI est 23.56/1.43=16.3. La quantité totale d'émulsion devient 50 ml. après l'addition.

Dans le mode 2, la quantité de gélatine est divisée en deux parties égales. Les courbes caractéristiques sont données dans Fig. 4 où l'ont voit que c'est le mode 2 qui donne la mailleure courbe avec un gamma élevé.

Variation de l'Excès d'Halogénure, Rapport des Halogénures et Quantité de Gélatine.— Dans cette série d'expériences, nous avons fait varier deux facteurs en même temps entre trois qui peuvent influencer les caractéristiques de l'émulsion (Tableaux III et IV). En comparant les résultats, nous avons trouvé qu'une valeur élevée du rapport halogénure d'argent gélatine et un petit excès d'halogénure favorisaient un gamma élevé. La variation du rapport AgCl/AgBr a peu d'effet dans les conditions de ces essais. Si l'on diminue la quantité de gélatine au-delà d'une limite, les grains d'halogénure d'argent sont susceptibles de s'aggroméler avec certaines sortes de gélatine. Nippi Process donne le meilleur résultat. Comme excès

TABLEAU II. RÉSULTATS DE QUATRE MODES D'ADDITION (GÉLATINE, NITTA NO. 3)

No. d'essais	Mode d'addition	$AgNO_3$ g. mole	Conc. M	KX conc. M	KBr/KI	AgBr/AgI
1	1	0.025	1	1.20	19.8	16.3
2	2	〃	〃	〃	〃	〃
3	3	〃	1.43	1.71	〃	〃
4	4	〃	1	1.20	〃	〃

No.	Conc. de gélatine gél/AgX	Conc.	2e Maturation	γ (degré de confiance à 95%)	Sensibilité N. S. G.	Voile
1	82.3	82.3	45°C, 50 min.	1.58～1.36	0.43	0.07
2	〃	41.2	〃 〃	4.93～3.77	0.24	0.10
3	〃	137	〃 〃	3.72～3.40	0.53	0.05
4	〃	82.3	〃 〃	2.76～2.52	0.22	0.09

TABLEAU III. RÉSULTATS DES EXPÉRIENCES OÙ L'ON FAIT VARIER L'EXCÈS D'HALOGÉNURE, LE RAPPORT DES HALOGÉNURES ET LA QUANTITÉ DE GÉLATINE (NITTA NO. 3, GÉLATINE)

No. d'essai	$AgNO_3$ g. mole	$AgNO_3$ Conc. M	KX Excès g. mole	KX Conc. M	Rapport KCl/KBr	Rapport AgCl/AgBr
5	0.016	0.64	0.20	0.77	1.97	1.5
6	〃	〃	0.90	1.24	3.74	〃
7	〃	〃	0.20	0.77	4.74	4
8	〃	〃	0.90	1.24	8.29	〃

No. d'essai	Gélatine g. / AgX g. mole	Gélatine Conc.	2è Maturation	γ	Sensibilité N. S. G.	Voile
5	101	33 33	45°C, 50 min.	5.42～4.98	0.42	0.15
6	151	49.8 49.8	〃 〃	1.51～1.39	0.43	0.13
7	151	49.8 49.8	〃 〃	1.98～1.70	0.65	0.12
8	101	33 33	〃 〃	3.95～2.05	0.43	0.14

TABLEAU IV. RÉSULTATS DES EXPERIENCES OÙ L'ON FAIT VARIER L'EXCÈS D'HALOGÉNURE, LE RAPPORT DES HALOGÉNURES DANS LES ENVIRONS DE NO. 5 (GÉLATINE NIPPI PROCESS)

No. d'essai	$AgNO_3$ g. mole	$AgNO_3$ Conc. M	KX Excès g. mole	KX Conc. M	Rapport KCl/KBr	Rapport AgCl/AgBr
9	0.20	1	0.15	0.77	1.54	1.2
10	〃	〃	0.25	0.84	1.76	〃
11	〃	〃	0.15	0.77	2.23	1.8
12	〃	〃	0.25	0.84	2.51	〃
13	〃	〃	0.20	0.80	2.00	1.5
14	〃	〃	0.25	0.84	2.12	〃
15	〃	〃	0.30	0.87	2.25	〃

No. d'essai	Gélatine g. / AgX g. mole	Gélatine Conc.	2è Maturation	γ	Sensibilité N. S. G.	Voile
9	100	33.5 44.5	45°C, 80 min.	2.58～1.94	0.55	0.29
10	〃	〃	〃 70	3.30～2.48	0.50	0.14
11	〃	〃	〃 60	2.54～2.14	0.35	0.21
12	〃	〃	〃 70	3.08～2.68	0.35	0.18
13	〃	〃	〃 60	3.08～2.72	0.45	0.20
14	〃	〃	〃 65	2.94～1.90	0.90	0.08
15	〃	〃	〃 60	3.11～2.15	0.91	0.16

TABKEAU V. BASES DE CALCUL

No. de coin	Log $E=x_i$	Densités observées, D_i					
11	0.25	2.22	2.23	2.15	2.15	2.27	2.25
12	0.10	1.52	1.52	1.44	1.46	1.35	1.33
13	−0.05	0.63	0.65	0.63	0.64	0.66	0.68

x_i	$(x_i-\bar{x})$ $\times 10^{-2}$	$(x_i-\bar{x})^2$ $\times 10^{-4}$	D_i	$(D_i-\bar{D})$ $\times 10^{-2}$	$(x_i-\bar{x})\times(D_i-\bar{D})$ $\times 10^{-4}$	$\hat{\beta}(x_i-\bar{x})$ $\times 10^{-2}$	$\{(D_i-\bar{D})-\hat{\beta}(x_i-\bar{x})\}^2$ $\times 10^{-4}$
0.25	15	225	2.22	79	1185	78	1
		〃	2.23	80	1200		4
		〃	2.15	72	1080		36
		〃	2.15	72	1080		36
		〃	2.27	84	1260		36
		〃	2.25	82	1230		16
0.10	0	0	1.52	9	0	0	81
		〃	1.52	9			81
		〃	1.44	1			1
		〃	1.46	3			9
		〃	1.35	− 8			64
		〃	1.33	−10			100
−0.05	−15	225	0.63	−80	1200	78	4
		〃	0.65	−78	1130		0
		〃	0.63	−80	1200		4
		〃	0.64	−79	1185		1
		〃	0.66	−77	1155		1
		〃	0.68	−75	1125		9
$\bar{x}=0.10$		$\Sigma=2700$	$\Sigma=25.78$		$\Sigma=14030$		$\Sigma=484$

d'halogénure, 25% est le meilleur.

Manière de traitement des valeurs.—Pour obtenir les résultats ci-dessus, nous avons employé la manière statistique pour obtenir le gamma probable.

Supposons qu'une relation linéaire existe entre deux valeurs x et y comme suit:

$$y=a_0+b_0x \tag{1}$$

où a_0 et b_0 sont constants. Les valeurs $y=y_i$ sont obtenues pour $x=x_i$ et $i=1, 2, \cdots\cdots n$. Si Y_i est la valeur obtenue par la méthode de minimum de carrés des valeurs observées,

$$Y_i=a+bx_i$$

L'addition des carrés de déviation entre y_i et Y_i soit minimum:

$$y=\bar{y}+[\Sigma(x_i-\bar{x})(y_i-\bar{y})/\Sigma(x_i-\bar{x})^2](x_i-x)$$

$$=\bar{y}+\hat{\beta}(x_i-\bar{x}) \tag{2}$$

où $\bar{y}$ est le moyen de y_i, $\bar{x}$ est celui de x_i et $\hat{\beta}$ correspond au gamma. Si l'on prend S_y comme dispersion de y et n, comme degré de liberté.

$$S_y=(1/n)\Sigma[y_i-\{\bar{y}+(\Sigma(x_i-\bar{x})(y_i-\bar{y})/\Sigma(x_i-\bar{x})^2)(x_i-\bar{x})\}]^2\equiv\hat{c} \tag{3}$$

Si la fonction $\hat{c}$ (la dispersion du groupe mère) suit la répartition χ^2 du système ayant le degré de liberté n, la répartition t est induite de la répartition χ^2 comme suit:

$$t=\sqrt{(n-2)}S_x^2(\hat{\beta}-\gamma)/\sqrt{\hat{c}} \tag{4}$$

d'où

$$\gamma=\hat{\beta}\pm t\sqrt{\hat{c}}/\sqrt{(n-2)}S_x^2 \tag{5}$$

où γ est le gamma probable et

$$S_x^2=\Sigma(x_i-\bar{x})^2/n$$

Les auteurs citent un exemple de calcul dans Tableau V.

$$S_x^2=(x_i-\bar{x})/n=2700\times10^{-4}/18=150\times10^{-4}$$

$$\bar{y}=\bar{D}=1.43$$

$$\hat{\beta}=(x_i-\bar{x})(y_i-\bar{y})/(x_i-\bar{x})^2$$

$$=14030\times10^{-4}/2700\times^{-4}=5.20$$

$$\hat{c}=26.9$$

$$n-2=16$$

$t=2.12$ (pour le degré de confiance de 95%)

$$=5.20\pm\frac{2.12\sqrt{26.9}}{\sqrt{16\times150}}=5.20\pm0.22$$

$$=5.42\sim4.98$$

Par cette expérience nous avons voulu examiner l'effet sur gamma en faisant varier la quantité d'excès d'halogénure, du rapport d'ions halogène et la quantité de gélatine. Pour savoir l'effet de trois facteurs il faut faire au moins huit expériences. Mais nous avons fait l'application partielle en employant la méthode du carré latin avec deux niveaux de chaque condition. Le système est schématisé comme Tableau VI.

TABLEAU VI. SYSTÈME DE L'APPLICATION PARTIELLE DU CARRÉ LATIN

Expérience	Facteurs 1	2	3
I	A	C	E
II	A	D	F
III	B	C	F
IV	B	D	E

Nous avons employé deux niveaux A, B du facteur 1, deux niveaux C, D du facteur 2 et E, F du facteur 3. La valeur obtenue, Val. I de l'équation (6) montre la variation de la différence entre A et B du facteur 1. D'autres facteurs se sont compensés les uns les autres.

TABLEAU VII. RÉSULTATS DES EXPÉRIENCES OÙ L'ON FAIT VARIER LES CONCENTRATIONS DE LA SOLUTION D'ARGENT ET DE LA SOLUTION D'HALOGÉNURE

No.	$AgNO_3$ g. mole	Conc.	KX Excès g. mole	Conc.	2e Maturation Rapport KCl/KBr	Rapport AgCl/AgBr
13	0.020	1	0.20	0.80	2.00	1.5
16	0.022	1.09	〃	0.87	〃	〃
17	0.024	1.20	〃	0.96	〃	〃
18	0.027	1.34	〃	1.07	〃	〃
19	0.030	1.50	〃	1.20	〃	〃

No.	Gélatine g. / AgX g. mole	Gélatine conc.	2e Maturation	γ	Sensibilité	Voile
13	100	33.5	45°C, 60 min.	3.08∼2.72	0.45	0.20
16	92	〃	〃 75	3.22∼2.72	0.54	0.20
17	83.5	〃	〃 60	3.64∼3.20	0.70	0.18
18	75	〃	〃 60	2.73∼1.97	1.00	0.15
19	66.7	〃	〃 70	2.61∼2.13	0.91	0.23

TABLEAU VIII. RÉSULTATS DES EXPÉRIENCES OÙ L'ON FAIT VARIER LA QUANTITÉ D'AMMONIAQUE (GÉLATINE WINTERTHUR N4625)

No.	$AgNO_3$ mole	$AgNO_3$ conc. M	NH_3 par 0.025 mole de $AgNO_3$	KX Excès	KX Conc. M	Rapport KCl/KBr	Rapport AgCl/AgBr
20	0.016	0.73	1 ml.	0.20	0.67	2.0	1.5
21	〃	0.88	9.5	〃	0.59	〃	〃
22	〃	0.88	1	〃	0.59	〃	〃
23	〃	0.73	9.5	〃	0.67	〃	〃

No.	Gélatine g. / AgX mole	Gélatine conc.	2e Maturation	γ	Sensibilité	Voile
20	101	38.5 28.9	45°C, 55 min.	3.47～2.37	0.90	0.43
21	〃	46.2 25.6	〃 65	3.78～3.32	2.22	0.30
22	〃	〃	〃 45	4.30～3.54	1.33	0.29
23	〃	38.5 28.9	〃 70	2.89～2.57	1.17	0.43

TABLEAU IX. RÉSULTATS DES EXPÉRIENCES FAITES AVEC DIVERSES ESPÈCES DE GÉLATINE

No.	$AgNO_3$ mole	$AgNO_3$ Conc. M	KX Excès	KX Conc. M	Rapport KCl/KBr	Rapport AgCl/AgBr
24	0.20	1	0.20	0.80	2.0	1.5
25	〃	〃	〃	〃	2.38	1.8
26	0.16	0.88	〃	0.59	2.00	1.5
27	0.24	1.20	〃	0.96	2.00	1.5
5	0.16	0.64	〃	0.77	2.00	1.5

No.	Gélatines Espèces	Gélatine g. / AgX mole	Conc.	2e Maturation	γ	Sensibilité	Voile
24	British gélatine	92.4	29.3	45°C, 60 min.	3.37～2.35	0.60	0.28
25	〃	100.5	38.5	〃 55	3.92～2.54	0.25	0.32
26	Winterthur N4625	101	46.2	〃 60	4.30～3.54	1.33	0.29
27	Nippi process	83.5	33.5	〃 60	3.64～3.20	0.70	0.18
5	Nitta No. 3	101	33	〃 50	5.42～4.98	0.42	0.15

$$\text{Val. I} = (\text{Résultat I} + \text{Résultat II})/2 - (\text{Résultat III} + \text{Résultat IV})/2 \quad (6)$$

Total des carrés moyens :

$$\text{C. F.} = (5.20+3.00+1.84+1.45)^2/4 = 11.49^2/4 = 33.005$$

Influence du facteur 1 :

$$S_1 = \{(5.20+3.00)^2+(1.84+1.45)^2\}/2 - \text{C. F.} = 6.027$$

d'où s'obtient le rapport de dispersion 602.7.
Influence du facteur 2 :

$$S_2 = \{(5.20+1.84)^2+(3.00+1.45)^2\}/2 - \text{C. F.} = 1.627$$

Influence du facteur 3 :

$$S_3 = \{(5.20+1.45)^2+(3.00+1.84)^2\}/2 - \text{C. F.} = 0.819$$

D'où les rapports de dispersion des facteurs 2 et 3 sont respectivement 162.7 et 81.9.

D'après le tableau de répartition de F, S_1 et S_2 montrent que les facteurs 1 et 2 sont significatifs et que S_3 ne l'est pas pour varier gamma.

Variation de Concentration de la Solution.— Nous avons également essayé de faire varier la concentration de la solution d'argent et de la solution d'halogénure. Les résultats sont donnés dans Tableau VII.

Plus la concentration est grande, plus la sensibilité est grande et le gamma est petit. Au-dessus d'une certaine concentration, le voile

TABLEAU X. FORMULES DES RÉVÉLATEURS* D-11 ET N.S.G.

	D-11	N. S. G.
Métol	1 g.	3 g.
Na_2SO_3	75	50
Hydroquinone	9	6
Na_2CO_3	25	25
KBr	5	1
Eau q.s.p.f.	1000 ml.	1000 ml.

* à diluer pour double volume

TABLEAU XI. GAMMAS OBTENS PAR D-11 ET PAR N. S. G.

No. des essais	9	10	11	12	13	14	15	16	17	18	19
N. S. G.	2.26	2.89	2.34	2.88	2.90	2.42	2.63	3.11	3.42	2.35	2.37
D-11	4.65	4.02	3.09	3.47	3.36	3.71	3.71	3.22	3.84	3.56	4.12

augmente sensiblement trandis que la sensibilité et le gamma diminuent.

Cas où l'on Ajoute un Excès d'Ammoniaque. Nous avons essayé d'ajouter un excès d'ammoniaque. Les résultats sont présentés dans Tableau VIII. Dans cette série d'expériences on a également fait varier la quantité de gélatine. Le voile était assez sensible et nous n'avons pas pu obtenir de résultats significatifs et utiles.

Espèces de Gélatine.—Nous avons essayé la formule No. 9 avec quatre espèces de gélatine. Nitta No. 3 donne le moindre voile et elle est considérée comme la meilleure parmi ces gélatines (Tableau IX).

Emploi de Différents Révélateurs.—Tous les résultats mentionnés jusqu'ici ont été obtenus par le révélateur NSG. D I I donne toujours un gamma plus élevé que le révélateur NSG. Les formules de de deux révélateurs sont données dans Tableau X. La différence entre ces deux gammas dans certains échantillons est donnée dans Tableau XI.

Conclusion

Dans les conditions que nous avons essayées, le mode 2 d'addition du nitrate d'argent dans KBr avec division de la gélatine en deux parties a donné les résultats les plus conformes au but que nous avous visé proposés. L'observation à microscope électronique semble indiquer que ce mode donne les grains de grandeurs homogènes. Il est préférable de choisir l'excès d'halogénure entre 20 et 30%. Un rapport de la concentration de gélatine à la concentration d'halogénure d'argent voisin de 101 (en unité de gélatine gramme au g. mole de AgX). L'influence de certains autres facteurs n'est pas encore bien déterminée.

Institut des Sciences Industrielles
Université de Tokio
Chiba

Graft Polymerization by Pre-heating Method Applied to Polyethylene Containing Benzoyl Peroxide

By Seizo OKAMURA and Tomonobu MANABE

(Received March 28, 1960)

It has been found by G. Oster that some solid polymers containing photo-sensitizer such as benzophenone could initiate graft polymerization with irradiation by ultra-violet as well as by ionizing rays[1-3]. In those cases, the primary action will be not on the polymer but on the photo-sensitizer, and the decomposed sensitizer fragment may abstract hydrogen atoms from the polymer molecules. The polymer radicals thus formed can initiate graft polymerization or cross-linking reaction.

The ultraviolet pre-irradiation method for graft polymerization or cross-linking reaction cannot be generally applied to thick films or a bundle of fibers because the penetrating power of the rays may be fairly low.

It is found here that some solid polymers containing initiator of radical polymerization of vinyl monomers such as benzoyl peroxide or azobisisobutyronitrile can initiate graft polymerization. This grafting method may be easily applied to thick films or to a bundle of fibres.

Experimental

A commercial low density polyethylene film of $0.0017\,g.\cdot cm^{-2}$ thickness is soaked for 60 min. in the benzene solution of benzoyl peroxide ($20\,g.\,l^{-1}$) at 50°C, the surface is washed with benzene, and dried. The sample thus obtained contains benzoyl peroxide about 0.2 wt. %. The sample is then heated in air. The sample is sealed with purified methyl methacrylate monomer in a glass tube, and

1) G. Oster and O. Shibata, *J. Polymer Sci.*, **26**, 233 (1957).
2) G. Oster, G. K. Oster and H. Moroson, *J. Polymer Sci.*, **34**, 671 (1959).
3) S. Okamura and T. Manabe, *Isotopes and Radiation*, in press.

then heated in vacuum. After the treatment for graft polymerization, the sample is washed with benzene for about 20 hr. at room temperature in order to extract the homopolymer already formed. The complete extraction, however, will be very hard in such a condition, but some comparison between the graft polymerization conditions may be possible. The sample is then dried and weighed. The amount of graft polymerization will be defined here by

$$\text{graft polymerization } \% = \left(\frac{\text{weight of sample after graft polymerization}}{\text{weight of sample before graft polymerization}} - 1 \right) \times 100$$

The values of grafting thus obtained are rather scattered according to the inhomogeneity of the benzoyl peroxide content and of the sample thickness. Therefore kinetical discussion is omitted here.

Results

Time of Pre-heating.—The effect of time of pre-heating on the graft polymerization is shown in Fig. 1, where the temperature of pre-heating is maintained at 110°C, and the polymerization temperature is 60°C.

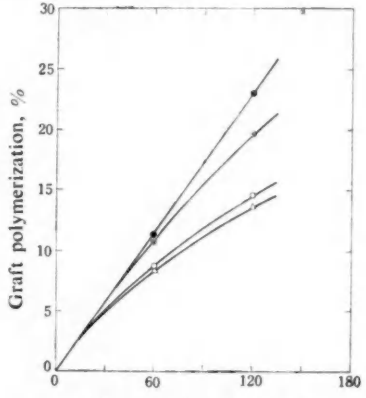

Fig. 1. Effect of time of pre-heating on graft polymerization.
Pre-heating temperature: 110°C
Polymerization temperature: 60°C
Time of pre-heating: -△- 15 min., -○- 30 min., -⊙- 45 min., -●- 60 min.

From the results shown in Fig. 1, it is recognized that the rate of graft polymerization increases with an increase of the time of pre-heating.

Temperature of Pre-heating.—The effect of temperature of pre-heating on the graft polymerization is shown in Fig. 2, where the time

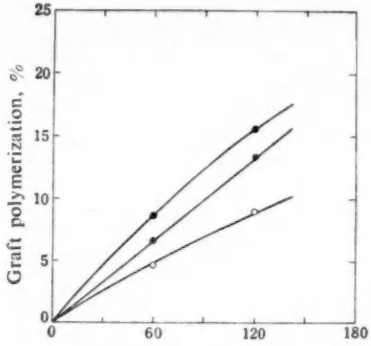

Fig. 2. Effect of temperature of pre-heating on graft polymerization.
Pre-heating time: 30 min.
Polymerization temperature: 60°C
Temperature of pre-heating: -○- 90°C, -⊙- 110°C, -●- 120°C.

of pre-heating is maintained at 30 min., and the polymerization temperature is 60°C.

From the results shown in Fig. 2, it is found that the rate of graft polymerization increases with the rise of temperature of pre-heating.

Polymerization Temperature.—The influence of polymerization temperature on the graft polymerization is represented in Fig. 3, where the pre-heating temperature is maintained at 110°C, and the pre-heating time is 30 min.

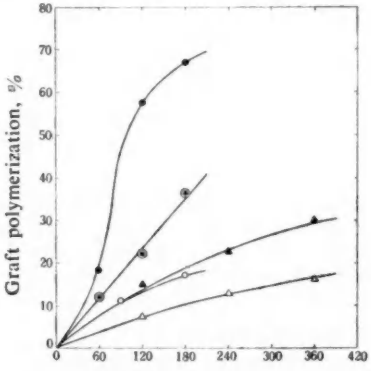

Fig. 3. Effects of polymerization temperature, pre-heating and benzoyl peroxide sensitization on graft polymerization.
Pre-heating: 110°C, 30 min.
-●- -⊙- No pre-heating -○- No BPO sensitization } Polymerization temperature: 70°C
-▲- -△- No BPO sensitization } Polymerization temperature: 50°C

After-effect of Pre-heating.—The after-effect of pre-heating is shown in Fig. 4, where the pre-heating temperature is maintained at 110°C, the pre-heating time is 30 min. and the polymerization temperature is 60°C.

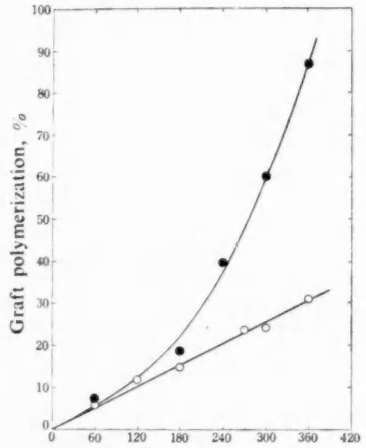

Fig. 4. After effect of pre-heating on graft polymerization.
Pre-heating: 110°C, 30 min.
Polymerization temperature: 60°C
Time interval after pre-heating until polymerization: -○- 4,300 min., -●- 300 min.

From the results represented in Fig. 4, it is shown that the rate of graft polymerization decreases with an increase of time interval after pre-heating until polymerization. And also, the difference of rates between two experiments having different intervals increases with an increase of polymerization time.

Discussion

The mechanism of graft polymerization reported here may be as follows. I represents the initiator of radical polymerization, P the polymer, M the monomer, and O_2 the oxygen respectively.

Reaction in Pre-heating.

$I \rightarrow R\cdot$ (1) decomposition of initiator

$R\cdot + P \rightarrow P\cdot + RH$ (2) radical transfer to polymer, production of polymer radical

$P\cdot + O_2 \rightarrow POO\cdot$ (3) production of polymer peroxide radical

$P\cdot + R\cdot \rightarrow$ product (4) disappearence of polymer radical

$P\cdot + P\cdot \rightarrow PP$ (5) cross-linking reaction

$P\cdot + POO\cdot \rightarrow POOP$ (6) production of polymer diperoxide

$POO\cdot + R\cdot \rightarrow POOR$ (7) production of polymer peroxide

Reaction in Graft Polymerization.

$I \rightarrow R\cdot$ (8) decomposition of initiator

$POOP \rightarrow PO\cdot + PO\cdot$ (9) decomposition of polymer diperoxide

$POOR \rightarrow PO\cdot + RO\cdot$ (10) decomposition of polymer peroxide

$R\cdot + M \rightarrow RM\cdot$ (11) polymerization by initiator fragment

$PO\cdot + M \rightarrow POM\cdot$ (12) polymerization by polymer diperoxide fragment

$RO\cdot + M \rightarrow ROM\cdot$ (13) polymerization by polymer peroxide fragment

$P\cdot + M \rightarrow PM\cdot$ (14) polymerization by frozen polymer radical at the inside of polymer

$POO\cdot + M \rightarrow POOM\cdot$ (15) polymerization by frozen polymer peroxide radical

The increasing of time and the rise of temperature of pre-heating increase the initiator fragment $[R\cdot]$, and then the increase of graft polymerization may be expected (Figs. 1 and 2). The increase of time interval after pre-heating until polymerization results in the decrease of the concentration of frozen polymer radical (reactions 4 and 5), and then the decrease of graft polymerization may also be expected (Fig. 4). Reaction 14 is expected at the inside of polymer molecule, for the reaction of oxygen with radical (reaction 3) will be very fast.

Summary

Some solid polymers containing initiator of radical polymerization of vinyl monomers can initiate graft polymerization by heating in air or in vacuo prior to polymerization. In the experiment on polyethylene film containing benzoyl peroxide (monomer: methyl methacrylate), the increase of time (from 0 to 60 min.) and the rise of temperature (from 20 to 120°C) in pre-heating procedure increase the graft polymerization rate. And also, the increase of time interval after pre-heating until polymerization results in the decrease of the graft polymerization rate.

Department of Textile Chemistry
Faculty of Engineering
Kyoto University
Sakyo-ku, Kyoto

Synthesis of a,α'-Diaminodicarboxylic Acids

By Koji Toi, Kan Mori and Yoshiharu Izumi

(Received April 11, 1960)

A systematic study of the synthesis of a series of α,α'-diaminodicarboxylic acids, containing a number of biologically and biochemically important amino acids, was made, mainly by amination of the corresponding α,α-dibromo-compounds using succinimide as an aminating reagent (Method I) and by condensation of diethyl acetamidomalonate with α,α'-dibromo-paraffin (Method II).

Among the compounds of this type, of particular interest is α,α'-diaminopimelic acid because of its presence in bacterial products[1,2], and because of its role as a precursor in the biosynthesis of lysine[3,4]. α,α'-Diaminosuccinic acid, with a chemical structure analogous to aspartic acid, asparagine, C_4-dicarboxylic acid and other biologically important substances, has recently been isolated from a natural source[5]. The other amino acids in this series have not yet been found in nature. However, α,α'-diaminoglutaric acid is regarded as a precursor in the biosynthesis of α,γ-diaminobutyric acid.[6] Therefore the availability of these amino acids for biological investigations is desirable.

Method I:

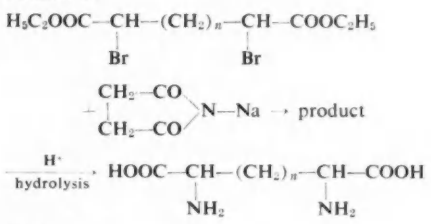

Method II:

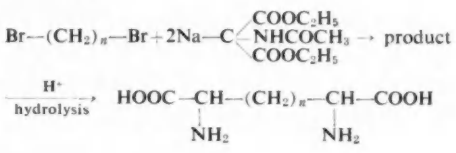

Succinimide was first used successfully as an aminating reagent by Akabori, Izumi and Fujiwara for the synthesis of α,α'-diaminopimelic acid (D. A. Pim.)[7]. In the present work this method was tried for the preparation of α,α'-diaminosuccinic (D. A. Suc.), glutaric (D. A. Glu.) and adipic acid (D. A. Adi.). However it was only successful for D. A. Adi. The diethyl acetamidomalonate method was tested in the preparation of D. A. Adi., D. A. Pim., α,α'-diaminosuberic (D. A. Seb.), azelaic (D. A. Aze.), and sebacic acid (D. A. Seb.). It was satisfactory for the synthesis of the three last named. Table I shows the results of the above synthesis.

D. A. Suc. has been prepared by reduction of sodium dihydroxytartarate osazone with sodium amalgam.[8-12] Wenner[13,14] and Mckennis et al.[15] prepared it in high yield by hydrolysis of the corresponding bisbenzylamino compound in the presence of Pd-C and hydrogen at high or atmospheric pressure. In the present work a 44 per cent yield of D. A. Suc. was readily obtained by amination of *meso*-α,α'-dibromosuccinate, obtained easily by bromination of diethyl fumarate in sunlight, using succinimide as an aminating reagent.

D. A. Glu. has been prepared by Carter et al.[16] by hydrogenolysis of diethyl pyrazoline-3, 5-dicarboxylate at a high pressure. Hellmann et at.[17] prepared it by reacting diethyl α-acetamido - α - dimethylaminomethylmalonateiodomethylate with sodium salt of acetamidomalonate, and by hydrolysis of α,α'-diphosphiminoglutaric acid. The final product could not be obtained by amination of diethyl α,α'-dibromoglutarate with succinimide. Therefore the method of Carter et al. was reinvestigated. A modification of their procedures

1) E. Work, *Biochem. J.*, **49**, 17 (1951).
2) E. Work and D. L. Dewey, *J. Gen. Microbiol.*, **9**, 394 (1953).
3) D. L. Dewey and E. Work, *Nature*, **169**, 533 (1952).
4) B. D. Davis, ibid., **169**, 534 (1952).
5) F. A. Hochstein, *J. Org. Chem.*, **24**, 679 (1959).
6) H. Hellmann, F. Lingens and E. Frolz, *Chem. Ber.*, **89**, 2433 (1956).
7) S. Akabori, Y. Izumi and T. Fujiwara, *J. Chem. Soc. Japan, Pure Chem. Sec.* (*Nippon Kagaku Zasshi*), **75**, 993 (1954).
8) J. M. Raecgy and J. Tafel, *Chem. Ber.*, **26**, 1980 (1893).
9) J. Tafel, ibid., **20**, 244 (1887).
10) J. Tafel and H. Stern, ibid., **38**. 1589 (1905).
11) J. Tamura, *J. Biochem.*, **27**, 335 (1938).
12) R. Kuhn and F. Zumstein, *Chem. Ber.*, **58**, 1429 (1925).
13) W. Wenner, *J. Org. Chem.*, **13**, 26 (1948).
14) W. Wenner, U. S. Patent, 2,389,099, Nov. 13, 1945.
15) H. Mckennis and A. S. Yard, *J. Org. Chem.*, **23**, 980 (1958).
16) H. E. Carter, F. R. Van Abeel and J. W. Tothrock, *J. Biol. Chem.*, **178**, 325 (1949).
17) H. Hellmann, F. Lingens and E. Frolz, *Chem. Ber.*, **89**, 2433 (1956).

Table I

Compounds to be synthesized	Method I: Starting material	Method I: Yield of product	Method II: Starting material	Method II: Yield of product
D. A. Suc.	*meso*-Diethyl α,α'-dibromosuccinic acid	44%	—	—
D. A. Glu.	Diethyl α,α-dibromoglutaric acid	Trace	—	—
D. A. Adi.	Diethyl α,α'-dibromoadipic acid	73%	Ethylene dibromide	Trace
D. A. Pim.	Diethyl α,α'-dibromopimelic acid	81%[7]	Trimethylene dibromide	Trace
D. A. Sub.	—	—	Tetramethylene dibromide	62%
D. A. Aze.	—	—	Pentamethylene dibromide	66%
D. A. Seb.	—	—	Hexamethylene dibromide	79%

was employed and D. A. Glu. was synthesized in a yield of 33 per cent from glycine ethyl ester hydrochloride without separation of the individual intermediates. The method was as follows: to an aqueous solution of glycine ethyl ester hydrochloride was added an aqueous solution of sodium nitrite. An ethereal solution of methyl acrylate was added without separation of ethyl diazoacetate. Since the product could not be crystallized, the substance was reduced in ethereal solution at a high pressure of hydrogen in the presence of Raney's nickel. It was then hydrolyzed in hydrochloric acid.

Simmonds[18] reported the synthesis of D. A. Adi. and D. A. Pim. by the reaction of phthalimide with the corresponding α,α'-dibromo-compounds. Using succinimide instead of phthalimide, these two α,α'-dibromo-compounds were converted to D. A. Adi. and D. A. Pim. with comparatively good yields of 73 and 81 per cent, respectively. However, the use of diethyl acetamidomalonate resulted in very poor yields.

D. A. Sub., D. A. Aze., and D. A. Seb. were prepared by Neuberg[19] and Abderhalden et al.[20] from the corresponding α,α'-dibromo-compounds and ammonia. Simmonds[19] also reported the preparation of D. A. Seb. by a similar method and of D. A. Seb. and D. A. Aze. in 44 and 39 per cent yields, using acetamidomalonate. In the present work the use of acetamidomalonate resulted in yields of 62, 66, and 79 per cent for D. A. Sub., D. A. Aze. and D. A. Seb., respectively. This method seems the most suitable for these three amino acids, since the starting materials are readily available and the required operations are simple.

It is considered that the low yields of D. A. Suc. and D. A. Glu. in the succinimide method, and of D. A. Adi. and D. A. Pim. in the acetamidomalonate method are probably caused by an inhibition of the reaction by steric hindrance.

18) D. H. Simmonds, *Biochem. J.*, **58**, 520 (1954).
19) C. Neuberg, *Z. phys. Chem.*, **45**, 99 (1905).
20) E. Abderhalden and W. Zeisset; *Fermentforschung*, **9**, 336 (1928).

Table II. The chromatographic behavior of synthetic diaminodicarboxylic acids

	R_f-value: Fee-form	R_f-value: Hydrochloride
D. A. Suc.	0.0312	0.0402
D. A. Glu.	0.0406	0.0522
D. A. Adi.	0.0455	0.0600
D. A. Pim.	0.0570	0.0715
D. A. Sub.	0.0691	0.0878
D. A. Aze.	0.109	0.127
D. A. Seb.	0.157	0.186

The above seven amino acids and their hydrochlorides prepared as described above have R_f-values shown in Table II on paper chromatography using acetic acid-butanol-water (1 : 4 : 1) as solvent.

Experimental

D. A. Suc. — To a solution of 5.5 g. (0.24 mol.) of sodium in 100 ml. of absolute ethanol was added 30 g. (0.30 mol.) of succinimide. This was heated on a water bath to dissolve the succinimide. To this mixture were added 0.5 g. of potassium iodide and 33 g. (0.10 mol.) of *meso*-α,α'-dibromosuccinic acid. The mixture was refluxed on an oil bath for 1 hr. It was cooled and filtered. The filtrate was concentrated in vacuo and the residue was hydrolyzed by refluxing in 100 ml. of concentrated hydrochloric acid and 50 ml. of water for 4 hr. The precipitated succinic acid was removed by filtration and the supernatant was concentrated under reduced pressure. The residual material was dissolved in 70 ml. of methanol and filtered to remove sodium chloride. On neutralization with aniline, D. A. Suc. crystallized immediately as paste or block. This crude solid was washed with 90 per cent methanol. It was dissolved in 100 ml. of warm 20 per cent hydrochloric acid and decolorized. The solution was adjusted to pH 6 with aqueous ammonia and 100 ml. of methanol was added to complete crystallization. White crystalline D. A. Suc. decomposing at 305~310°C was obtained in a yield of 6.0 g. (44 per cent).

Found: C, 32.10; H, 5.62; N, 18.54. Calcd. for $C_4H_8O_4N_2$: C, 32.43; H, 5.44; N, 18.91%.

D. A. Glu.—A solution of 12 g. (0.15 mol.) of nitrite and 0.5 g. of sodium acetate in 15 ml. of

water was cooled to 0°C and a cold solution containing 14 g. (0.1 mol.) of glycine ethyl ester hydrochloride was added with stirring, external cooling being used to keep the temperature at 0~2°C. After 30 min. 13 g. (0.15 mol.) of methyl acrylate in 25 ml. of ether was added, and rapid stirring was continued for 1 hr. Then 4 ml. of acetic acid was added to the mixture dropwise, and stirring was continued for 1 hr. The ethereal layer was separated. The aqueous layer was extracted with 70 ml. of ether, and the combined ethereal solutions were dried over sodium sulfate. The ether was slowly removed by distillation until the total volume became 40 ml. This solution was then reduced at 80 kg./cm² by hydrogen in the presence of Raney's nickel for 3 hr. at 60°C and for a further 3 hr. at 120°C. After removal of the catalyst, the filtrate was concentrated under reduced pressure. The residue was hydrolyzed for 3 hr. in 50 ml of boiling concentrated hydrochloric acid. The hydrolysate was decolorized with charcoal and concentrated in vacuo. The residual material was dissolved in 50 ml. of 50 per cent methanol and then 20 ml. of aniline was added with vigorous shaking. D. A. Glu. was crystallized. After storing in a refrigerator, the product was filtered and washed with 10 ml. of water, and then twice with 10 ml. of methanol. The dried product weighed 5.3 g. or 33 per cent of the theoretical yield from glycine ethyl ester hydrochloride. It decomposed at 300~310°C without melting.

Found: C, 36.68 H, 6.40; N, 16.54. Calcd. for $C_5H_{10}O_4N_2$: C, 37.03; H, 6.22; N, 17.28%.

D. A. Adi. — This was prepared in a manner similar to that of D. A. Suc. using 5.5 g. (0.24 mol.) of sodium, 30 g. (0.3 g. mol.) of succinimide, and 36 g. (0.1 mol.) of diethyl α,α'-dibromoadipate. The white crystalline product, reprecipitated from hydrochloric acid and aqueous ammonia, weighed 13.6 g. (73 per cent) and decomposed at 275~277°C without melting.

Found: C, 38.99; H, 7.02; N, 15.49. Calcd. for $C_6H_{12}O_4N_2$: C, 40.90; H, 6.87; N, 15.90%.

D. A. Pim.—The preparation of this compound was reported in a previous paper.[1] The yield was 81 per cent, and the decomposition point was 307~310°.

D. A. Sub.—To 800 ml. of absolute alcohol containing 19 g. (0.825 mol.) of sodium was added 184 g. (0.85 mol.) of diethyl acetamidomalonate. The mixture was dissolved by heating on a water bath. Then 70 g. (0.324 mol.) of tetramethylenedibromide was added and the mixture was refluxed for 10 hr. The hot reaction mixture was filtered, the residue being washed with hot alcohol. The filtrate and the washings were combined and evaporated in vacuo. The residue was hydrolyzed in 1000 ml. of boiling hydrochloric acid for 5 hr. The mixture was concentrated in vacuo and the dry residue was taken up in 100 ml. of water, and again concentrated to dryness. This operation was repeated once more. Then the dry residue was dissolved in 300 ml. of methanol. A mixture of 80 ml. of pyridine and 300 ml. of methanol was added with shaking and the resulting mixture was let stand overnight to precipitate the crude D. A. Sub. This precipitate was washed with methanol and ether and dried. The yield was 53.5 g. This crude compound was suspended in 1000 ml. of water and dissolved by the addition of 10 per cent sodium hydroxide. An aqueous solution containing 100 g. of copper sulphate was added and the mixture was adjusted to pH 5.4 with 10 per cent sodium hydroxide. The precipitate was washed thoroughly with water and was dissolved in 500 ml. of 3 N hydrochloric acid. It was then treated with hydrogen sulfide to remove the copper. The black precipitate was filtered off, and the filtrate was concentrated in vacuo. The residue was taken up in 400 ml. of methanol. A mixture of 80 ml. of pyridine and 200 ml. of methanol was added with shaking and the resulting mixture allowed to stand. After washing with methanol and ether and drying, 41 g. (62 per cent yield) of white crystalline D. A. Sub. were obtained. This did not decompose below 360°C. Paper chromatography showed a single spot with the R_f-value given in Table II.

Found: C, 46.89; H, 7.86; N, 13.79. Calcd. for C, 47.05; H, 7.90; N, 13.72%.

D. A. Aze.—This was prepared as above by condensation of 160 g. (0.74 mol.) of diethyl acetamidomalonate with 65 g. (0.283 mol.) of pentamethylenedibromide using 16.8 g. (0.73 mol.) of sodium in 700 ml. of absolute alcohol. The crude product (55.5 g.) was dissolved in 2000 ml. of hot water and 80 g. of basic copper carbonate monchydrate was added. The mixture was heated at boiling point for some time. The precipitate was collected on a suction funnel and thoroughly washed with water. It was dissolved in diluted hydrochloric acid. The solution was saturated with hydrogen sulfide to precipitate the copper sulfide completely. The precipitate was removed by filtration and the filtrate was concentrated in vacuo. The residue was dissolved in 300 ml. of methanol. Neutralization with a mixture of 80 ml. of pyridine and 450 ml. of methanol gave a white crystalline product. This was collected on a suction filter, washed with water, methanol and ether, and dried. 40.5 g. (66 per cent yield) of D. A. Aze. was obtained. This decomposed above 320°C without melting. Paper chromatography of this compound gave a single spot with the R_f-value given in Table II.

Found: C, 49.74; H, 8.31; N, 12.81. Calcd. for $C_9H_{15}O_4N_2$: C, 49.53; H, 8.31; N, 12.84%.

D. A. Seb.—This compound was prepared in the same way as D. A. Sub. from 23 g. (0.106 mol.) of diethyl acetamidomalonate, 10 g. (0.041 mol.) of hexamethylene dibromide, and 2.3 g. (0.10 mol.) of sodium. The yield was 7.5 g. (79 per cent). It did not decompose below 360°C and gave a single spot on paper chromatography with the R_f-value given in Table II.

Found: C, 51.73; H, 8.70; N, 11.96. Calcd. for $C_{10}H_{20}O_4N_2$: C, 51.70; H, 8.68; N, 12.06%.

Summary

A systematic study was made on the synthesis of α,α'-diaminodicarboxylic acids mainly by amination of the corresponding α,α'-dibromodicarboxylic acids using succinimide as an

aminating reagent and by condensation of diethyl acetamidomalonate with α,ω-dibromoparaffin.

The authors wish to express their sincere thanks to Professor Shiro Akabori for encouragement and valuable advice throughout this work.

Division of Organic Chemistry
Institute for Protein Research
Osaka University Nishi-ku,
Osaka (K. T. & Y. I.)

Department of General Education
Osaka Prefectural University
Nakamozu, Sakai (K. M.)

The Ion-Exchange Behavior of Some Neutral Amino Acids

By Manabu SENŌ and Takeo YAMABE

(Received May 12, 1960)

In many practical works on the separation of amino acids by means of ion-exchangers, some successful procedures using the ion-exchange chromatography have been established. Above all, the displacement development method has been applied with success to the separation by Partridge et al., and Moore and Stein pointed out that the elution method possessed higher resolving power for analytical purposes[1]. However, few fundamental researches have been carried out on the exchange behavior of amino acids on ion-exchange resins[2]. This problem is interesting, since it is expected that weak amphoteric electrolytes such as amino acids exhibit some characteristic behavior concerning the ion-exchange reaction.

In the present paper, the experimental resuls are described on the ion-exchange behavior of some neutral amino acids, particularly the influence of pH on the ion-exchange reaction and some general remarks are presented in this respect. The behavior of the acidic and the basic amino acids toword the ion-exchange resins will be given in the succeeding paper.

Experimental

Through the present investigation the following reagents were used; amino acids are glycine, DL-alanine and L-leucine, which are commercial special-grade and were used without further purification. The dissociation constants and the isoelectric points of these amino acids are as follows.

	pK_1	pK_2	pI
Glycine	2.34	9.60	5.97
Alanine	2.34	9.69	6.00
Leucine	2.36	9.60	5.98

The ion-exchange resins used were Amberlite resins, IR-120 (4.24) IRC-50 (10.0), IRA-400 (2.15) IR-4B (8.0), the exchange capacities of these resins being given in parentheses in the unit, meq./g. dry resin.

All the experiments were carried out batch-wise. Through a run of measurements, a constant volume, 50 ml., of a solution containing a constant amount, about 2 meq., of amino acid and being adjusted to a desired pH by adding hydrochloric acid or sodium hydroxide, was added onto a constant quantity, about 1 meq., of the ion-exchange resin. The details for each system are given in the following table.

Amino acids	Total amounts[a] mmol.	H- or OH-form resins, w g. dry resin			
		IR-120	IRC-50	IRA-400	IR-4B
Glycine	1.95	0.169	0.094	0.330	0.101
Alanine	1.98	0.166	0.111	0.331	0.180
Leucine	2.02	0.175	0.103	0.343	0.134

After being allowed to stand for a few days, which were long enough for the attaining of the ion-exchange equilibrium, the pH and the remaining amount of the amino acid in the solution phase were measured and the adsorbed amount of the amino acid was estimated herefrom.

Amino acids were measured colorimetrically with ninhydrin[3] and pH of the solutions was measured with a glass-electrode pH-meter, model HM-5, Toa Dempa Kogyo Co., Ltd. All the measurements were made at room temperature, 5~15°C.

1) P. B. Hamilton, "Ion Exchangers in Organic and Biochemistry" Ed. by C. Calmon and T. R. E. Kressman, Interscience Publishers, Inc., New York (1957), p. 255.
2) D. T. Englis and H. A. Fiess, *Ind. Eng. Chem.*, **36**, 604 (1944); C. S. Cleaver, R. A. Hardy, Jr. and H. G. Cassidy, *J. Am. Chem. Soc.*, **67**, 1343 (1945); M. E. Carsten and K. Cannan, ibid., **74**, 5950 (1952).
3) K. Satake et al., "Biochemistry I (Seibutu Kagaku I)", Zikken Kagaku Koza, Vol. 23. Maruzen Co., Tokyo (1957), p. 124.

Results and Discussion

Experimental results were shown in Figs. 1–3, in which the adsorbed amounts of amino acids were plotted against the pH of the equilibrium external solution. As anticipated from the amphoteric nature of amino acids, these are adsorbed by the cation-exchange resins in the pH range lower than its isoelectric point and by the anion-exchange resins in the higher pH range.

As seen in these figures, it was revealed that the maximum adsorption of the neutral amino acids by hydrogen- or hydroxyl-form ion-exchange resins takes place in a rather broad pH range near the isoelectric points, while the acidic and the basic amino acid are extensively adsorbed in a relatively narrow pH range near the isoelectric points, as will be presented in the succeeding paper. Furthermore, it was noticed that, in the case of the sodium or chloride form resins, the amounts of amino acids are remarkably diminished in the pH range near the isoelectric point, compared to the case of the hydrogen- or hydroxyl-form resins. In the lower and the higher pH ranges, the adsorbed amounts of all the amino acids decrease sharply owing to the competitive adsorption of hydrogen or hydroxyl ions.

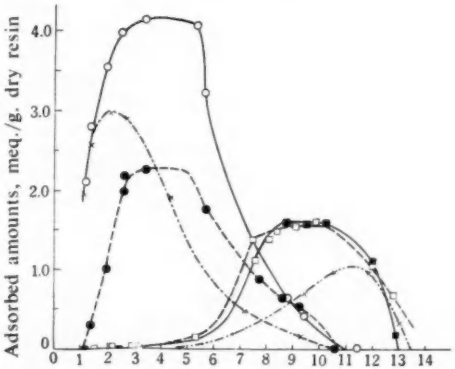

Fig. 1. Adsorption of glycine on ion-exchange resins.
—○— IR-120, H-form
--●-- IRC-50, H-form
--□-- IRA-400, OH-form
—■— IR-4B, OH-form
—·×—· IR-120, Na-form
— ×—·· IRA-400, Cl-form

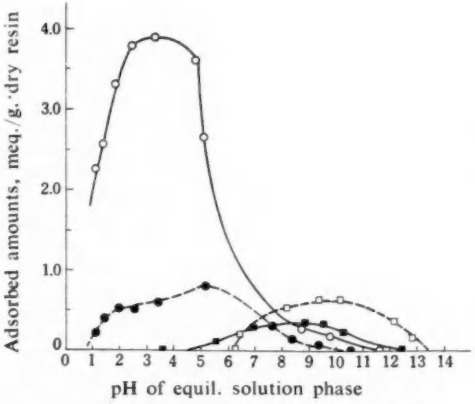

Fig. 2. Adsorption of DL-alanine (symbols are the same as those in Fig. 1).

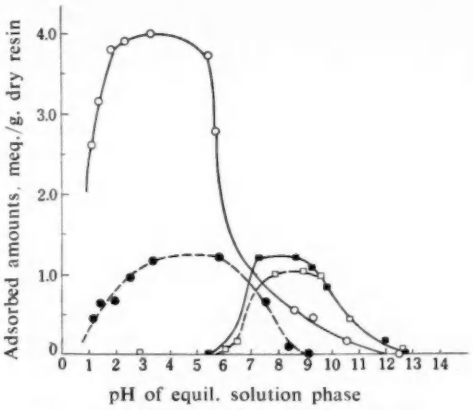

Fig. 3. Adsorption of L-leucine (symbols are the same as those in Fig. 1).

Adsorption Mechanism of Amino Acids on Ion-Exchange Resins.—The apparent equilibrium constants defined by

$$\left.\begin{aligned} K_{H}' &= \frac{[A]_r[H^+]_s}{[A]_s[H^+]_r} \\ K_{OH}' &= \frac{[A]_r[OH^-]_s}{[A]_s[OH^-]_r} \end{aligned}\right\} \quad (1)$$

are not constant but depend on pH in the solution phase; K_H' decreases and K_{OH}' increases, with increase of pH, where $[A]_s$, $[H^+]_s$ or $[OH^-]_s$ is concentration in meq./ml. of amino acid, hydrogen or hydroxyl ions in the equilibrium external solution, respectively, and $[A]_r$, $[H^+]_r$ or $[OH^-]_r$ is concentration in meq./(g. dry resin) of amino acid, hydrogen or hydroxyl ions in the resin phase at equilibrium, respectively. It seems that this constancy does not hold, because the dissociation equilibrium of amino acids in the solution is not taken into consideration.

When the neutral amino acid is adsorbed on cation-exchange resin of hydrogen-form,

the amino acid cations that exist in the following equilibrium state,

$$AH^+ \rightleftarrows A^\pm + H^+ \quad \text{(i)}$$

$$A^\pm \rightleftarrows A^- + H^+ \quad \text{(ii)}$$

exchange for hydrogen ions in the ion-exchange resin,

$$RH + AH^+ \rightleftarrows RAH + H^+ \quad \text{(iii)}$$

and the hydrogen ions are liberated from the cation-exchange resin, resulting in production of more amino acid cations and further exchange of the amino acid cations for the hydrogen ions. The exchange reaction attains the equilibrium through such a repeating process[4].

This adsorption mechanism would be supported by the following empirical facts.

(1) The pH of the external solution remains nearly constant through the adsorption process of amino acids as shown in Table I, in which pH's of the solution phase before and after equilibration of ion-exchange were given in the case of glycine as an example.

TABLE I. pH OF THE SOLUTION PHASE BEFORE AND AFTER EQUILIBRATION OF ION-EXCHANGE OF GLYCINE

pH of orig. soln.	pH of equil. soln.	pH of orig. soln.	pH of eqil. soln.
Amberlite IR-120, H-form.		Amberlite IRC-50, H-form.	
1.20	1.19	1.20	1.20
1.35	1.38	1.35	1.40
1.90	1.90	1.98	1.98
2.50	2.42	2.50	2.58
3.37	3.32	3.37	3.40
6.60	5.30	6.60	5.60
8.72	5.60	8.72	7.65
9.72	8.70	9.72	8.55
10.80	9.39	10.80	9.20
12.55	12.50	12.55	12.45
Amberlite IRA-400, OH-form.		Amberlite IR-4B, OH-form.	
1.35	1.48	1.35	1.52
2.50	2.93	2.50	3.02
3.37	7.40	3.37	5.24
6.60	8.00	6.60	7.45
8.72	8.30	8.72	8.60
9.72	9.05	9.72	9.40
10.80	9.80	10.80	10.10
12.55	11.89	12.55	11.90
12.89	12.75	12.89	12.80
Amberlite IR-120, Na-form.		Amberlite IRA-400, Cl-form.	
1.10	1.12	1.92	1.94
1.38	1.42	3.37	3.60
1.92	2.09	6.60	5.25
2.48	2.70	9.80	9.40
3.37	4.37	10.72	10.51
6.60	7.16	11.98	11.81
9.80	9.33	13.19	13.02
13.49	13.42	13.49	13.41

(2) The amino acids are adsorbed remarkably on the hydrogen- or hydroxyl-form ion-exchanger in the pH range near the isoelectric points, while the amino acid adsorbed on the salt-form ion-exchanger is small in quantity in this pH range.

It should be noticed that the completion of the above-mentioned two processes, i and iii, lead to the same result as the following mechanism[2],

$$RH + A^\pm \rightleftarrows RAH \quad \text{(iv)}$$

However, there is not any evidence that such a process takes place actually.

Relations between the Adsorbed Amount of Amino Acid and the pH of the External Solution.—In a case when the neutral amino acid is adsorbed on the hydrogen-form cation-exchanger, the selectivity coefficient is defined as follows:

$$K_H = \frac{[AH^+]_r[H^+]_s}{[AH^+]_s[H^+]_r} \quad (2)$$

where $[A^+]_s$ is the concentration of ion A in the equilibrium external solution in the unit, meq./ml., and $[A^+]_r$ is that in the resin phase in the unit, meq./g. dry resin. Strictly, the activity should be used instead of the concentration in these equations but was not used in the present paper to avoid the troublesome procedure.

The dissociation constants of the neutral amino acids are given as

$$K_1 = \frac{[A^\pm]_s[H^+]_s}{[AH^+]_s}$$

$$K_2 = \frac{[A^-]_s[H^+]_s}{[A^\pm]_s} \quad (3)$$

where the term arising from activity coefficient is also neglected.

Under the present experimental condition, that is;

(1) the total amount of amino acid in the system is constant, a meq.,

(2) the amount of the exchangeable ions in the ion-exchange resin is constant, c meq.,

4) Amino acids are taken up from the solution phase into the resin phase by the other processes, such as Donnan adsorption and physical or chemical adsorption, besides the ion-exchange process. Although it is difficult to estimate the contributions of these processes experimentally, it would be safely said on the basis of the preceding reports listed in Ref. 1, that the ion-exchange is the primary process and the other ones have a small contribution to be neglected to a first approximation, excepting for the case of amino acids with benzene rings.

$c=Cw$, where C is the exchange capacity (meq./g. dry resin) of the resin and w is the weight of the resin used,

(3) the volume of the external solution is constant, v ml., the following relationship holds between the exchanged amount of the amino acid, $[AH^+]_r=y$, and the hydrogen ion concentration in the external solution, $[H^+]_s=x$,

$$\frac{(a-wy)(c-wy)}{y}=\frac{vw}{K_H}\cdot\frac{x^2+K_1x+K_1K_2}{x} \quad (4)$$

The similar relation is gained in a case when the neutral amino acid is adsorbed on the hydroxyl-form anion-exchanger, where the selectivity coefficient K_{OH} is defined by

$$K_{OH}\frac{[A^-]_r[OH^-]_s}{[A^-]_s[OH^-]_r} \quad (5)$$

The exchanged amount of the amino acid anion, $[A^-]_r=y$, is related to the hydroxyl ion concentration in the equilibrium external solution, $[OH^-]_s=x'$, by the formula

$$\frac{(a-wy)(c-wy)}{y}=\frac{vw}{K_{OH}}\cdot\frac{K_1K_2x'^2+K_1K_wx'+K_w^2}{K_1K_2x'} \quad (6)$$

where K_w is the dissociation constant of water.

It must be noted that these relationships are valid for the two-component systems that contain only hydrogen or hydroxyl ions besides amino acid ions.

$f(x)$ or $f(x')$ Functions. — It is found that, in the ion-exchange behavior of the weak amphoteric electrolytes such as amino acids, a function of only the concentration of the hydrogen or the hydroxyl ion in the equilibrium solution phase, $f(x)$ or $f(x')$, which appears in the right hands of the Eqs. 4 and 6, gives the characteristic behavior. This function is, for cation exchange,

$$f(x)=\frac{x^2+K_1x+K_1K_2}{x} \quad (7)$$

and for anion exchange

$$f(x')=\frac{K_1K_2x'^2+K_1K_wx'K_w^2}{K_1K_2x'} \quad (8)$$

The numerical values of these functions for amino acids under investigation are given in Table II and shown against pH of the solution phase in Fig. 4[5,6].

The $f(x)$ or $f(x')$ of each amino acid has a minimum at its isoelectric point. At the minimum of $f(x)$ or $f(x')$, the adsorbed amount of the amino acid is the maximum. This can be shown directly by differentiating the Eqs. 4 and 6. It is supported by the present experiment that the adsorbed amount of the amino acid is the maximum at the isoelectric point.

The adsorbed amount of the amino acid is related inversely to the $f(x)$ or $f(x')$. For

TABLE II. $f(x)$ AND $f(x')$ FUNCTIONS

pH	log $f(x)$		
$(-\log x)$	Glycine	Alanine	Leucine
0	0.002	0.002	0.002
1	$\bar{1}$.021	$\bar{1}$.021	$\bar{1}$.017
2	$\bar{2}$.164	$\bar{2}$.164	$\bar{2}$.155
3	$\bar{3}$.746	$\bar{3}$.746	$\bar{3}$.729
4	$\bar{3}$.669	$\bar{3}$.669	$\bar{3}$.649
5	$\bar{3}$.661	$\bar{3}$.661	$\bar{3}$.641
6	$\bar{3}$.660	$\bar{3}$.660	$\bar{3}$.640
7	$\bar{3}$.661	$\bar{3}$.661	$\bar{3}$.641
pH	log $f(x')$		
$(-\log K_w/x')$	Glycine	Alanine	Leucine
6	$\bar{5}$.600	$\bar{5}$.691	$\bar{5}$.600
7	$\bar{5}$.601	$\bar{5}$.692	$\bar{5}$.601
8	$\bar{5}$.611	$\bar{5}$.700	$\bar{5}$.611
9	$\bar{5}$.697	$\bar{5}$.772	$\bar{5}$.697
10	$\bar{4}$.146	$\bar{4}$.173	$\bar{4}$.146
11	$\bar{3}$.017	$\bar{3}$.020	$\bar{3}$.017
12	$\bar{2}$.002	$\bar{2}$.002	$\bar{2}$.002
13	$\bar{1}$.000	$\bar{1}$.000	$\bar{1}$.000
14	0.000	0.000	0.000

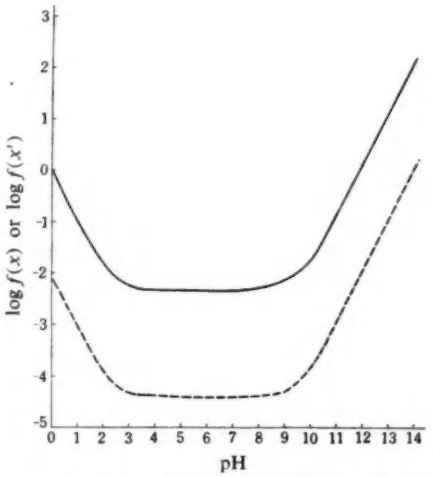

Fig. 4. $f(x)$ and $f(x')$ for glycine, which are shown by a full line and a dotted line, respectively.

5) $f(x)$ is related to $f(x')$ by the formula,
$$K_wf(x)=K_1K_2f(x')$$
Then, for amino acid of which isoelectric point is 7, in this case $K_1K_2=K_w$, $f(x)$ is identical with $f(x')$.

6) $f(x)$ has a practical meaning in the pH range lower than the isoelectric point and $f(x')$ in the higher pH range.

example, the following formula is derived from Eq. 4,

$$y=\frac{ac}{w\left(a+c+\frac{v}{K_H}f(x)\right)}+\frac{a^2c^2}{w\left(a+c+\frac{v}{K_H}f(x)\right)^3}+\cdots\cdots \quad (9)$$

and the similar relation is obtained in another system. From these relations and the dependence of $f(x)$ or $f(x')$ on pH, it is concluded that the maximum adsorption of the neutral amino acids on the hydrogen- or hydroxyl-form exchanger takes place in the broad pH range near the isoelectric point, and this conclusion is also supported experimentally.

Selectivity Coefficients.—The selectivity coefficients K_H and K_{OH} were estimated using the above-mentioned experimental data and the formulas and are given in Table III. As for three kinds of neutral amino acids, glycine, alanine and leucine, K_H is very large in comparison with K_{OH}. This is partly because the carboxyl group of these amino acids is dissociated more strongly than the amino group and, on this account, the ratio of the concentration of the hydrogen ion to that of the amino acid cation is larger than the ratio of the concentration of the hydroxyl ion to that of the amino acid anion in the equilibrium solution phase[7].

Table III. Selectivity coefficients for ion-exchange of amino acids for hydrogen or hydroxyl ions

	log K_H		log K_{OH}	
	IR-120	IRC-50	IRA-400	IR-4B
Glycine	0.56	$\bar{2}.52$	$\bar{2}.00$	$\bar{3}.03$
Alanine	0.41	$\bar{2}.29$	$\bar{4}.73$	$\bar{5}.52$
Leucine	0.53	$\bar{2}.43$	$\bar{3}.24$	$\bar{4}.38$

The order of the selectivity coefficient does not agree with that of the chain length of the amino acid molecule and alanine has smaller K value than that of leucine. This was already reported[8] and it might be considered that a simple adsorption makes a contribution to the uptake of amino acids by ion-exchange resins to some extent in the case of amino acid as glycine which is small in size, and as leucine, which has a long nonpolar chain.

Summary

The ion-exchange behavior of three kinds of neutral amino acids was examined and the following results were obtained.

1) The ion-exchange behavior of amino acids can be explained when the dissociation equilibrium of amino acids in the solution was taken into account.

2) The maximum adsorption of neutral amino acids on the ion-exchange resins takes place in a rather broad pH range at the isoelectric point.

3) The neutral amino acids are adsorbed more extensively on cation-exchangers than on anion-exchangers. Glycine is adsorbed most extensively and leucine is more adsorbed than alanine.

Institute of Industrial Science
The University of Tokyo
Yayoi-cho, Chiba

7) These ratios are given by
$[H^+]_s/[AH^+]_s=f(x)/[A]_s$
$[OH^-]_s/[A^-]_s=f(x')/[A]_s$
where $[A]_s$ is the concentration of amino acid remaining in the equilibrium solution phase, and, for example, $f(x')=0.087\times10^{-2}\ f(x)$ for glycine.

8) K. Narita, S. Fujiwara and S. Murasawa, This Bulletin, **31**, 381 (1958).

Syntheses of Peptides Containing Proline. I. Syntheses of Glycyl-L-prolyl-L-leucyl-glycyl-L-proline and its Related Compounds

By Shumpei SAKAKIBARA and Yutaka NAGAI*

(Received April 1, 1960)

Collagenase is a proteinase with a very high degree of substrate specificity, and its nature has been the object of keen interest of workers both in the fields of biochemistry and medicine. Very recently several preliminary reports[1-4] have been published and we seem to have some clue to look into the whole picture of the action of collagenase.

It had already been shown by several workers[3,5-8] that when collagen was digested with collagenase, most of the *N*-terminal groups belonged to glycine and several amino acids were found at the *C*-terminal ends. Nagai and Noda[2] found that poly-(L-prolyl-L-leucyl-glycyl)[9] was entirely hydrolyzed by collagenase, mostly into tripeptides, glycyl-prolyl-leucine and peptides from both the ends, prolyl-leucyl-glycyl-prolyl-leucine and glycyl-prolyl-leucyl-glycine. Tripeptides similar to the above were also isolated from collagenase digested collagen[7,10]. From these results and also from the accumulated informations[4,6,11-13] of oligopeptides unsusceptible to the action of collagenase, it was contemplated that the substrate specificity of collagenase requires the presence of two proline residues at a proper distance.

The syntheses of peptides containing two proline residues in the sequence of X-Pro-Leu-Gly-Pro-Y which would be a possible good substrate were carried out in our laboratory. The pentapeptide amide, glycyl-L-prolyl-L-leucyl-glycyl-L-proline amide was split by collagenase into two peptides, glycyl-prolyl-leucine and glycyl-proline amide[2]. This pentapeptide amide was the first example of the synthetic oligo-peptide as a good substrate of collagenase, and furnished a good starting inertia for us to elucidate the substrate specificity of the enzyme. Subsequently, many kinds of peptide containing proline, hydroxyproline or sarcosine were synthesized along this line and a preliminary report on an enzymatic test of those peptides has already been published[14].

In the present series of reports, the synthetic studies of those peptides containing proline will be described successively.

Syntheses of Peptides

In the planning of the synthetic routes of the pentapeptide, a precaution was taken not to use routes passing through dipeptide esters containing proline because free esters of proline dipeptides are considered to have a great tendency for diketopiperazine formation[15]. In the present study, almost all of the possible routes which conformed with the above precaution, as indicated befow, were tried, and the yield, crystallizability and specific rotation of products were compared for each route. The synthetic routes tested were as follows*:

(1) **a.** Z-Gly-N_3 + H-Pro-OEt
$\longrightarrow$ {Z-Gly-Pro-OEt}
$\longrightarrow$ Z-Gly-Pro-OH (I)

b. Z-Gly-OH + H-Pro-OEt
M.A.
$\longrightarrow$ {Z-Gly-Pro-OEt}
$\longrightarrow$ Z-Gly-Pro-OH (I)

* On leave from Department of Biophysics and Biochemistry, Faculty of Science, the University of Tokyo.

1) W. Harrington and P. H. von Hippel, cited by S. Seifter et al., *J. Biol. Chem.*, **234**, 285 (1959).
2) Y. Nagai and H. Noda, *Biochim. Biophys. Acta*, **34**, 298 (1959).
3) K. Heyns and G. Legler, *Z. physiol. Chem.*, **315**, 288 (1959).
4) W. Grassmann, H. Hörmann, A. Nordwig and E. Wünsch, ibid., **316**, 287 (1959).
5) V. O. Kazakova, V. N. Orekhovich and V. O. Shpikiter, *Doklady Akad. Nauk., S. S. S. R.*, **122**, 657 (1958).
6) S. Michaels, P. M. Gallop, S. Seifter and E. Meilman, *Biochim. Biophys. Acta*, **29**, 450 (1958); *J. Biol. Chem.*, **234**, 285 (1959).
7) S. Akabori, H. Noda, S. Sakakibara and Y. Nagai, *Abstr. 11th Symposium on Enz. Chem. (Japan)*, 109 (1959).
8) I. Mandl, personal communication.
9) H. Kitaoka, S. Sakakibara and H. Tani, This Bulletin, **31**, 802 (1958).
10) R. E. Schrohenloher, J. D. Ogle and M. A. Logan, *J. Biol. Chem.*, **234**, 58 (1959).
11) E. Bidwell and W. E. Van Heyningen, *Biochem. J.*, **42**, 140 (1948).
12) R. Monier, G. Litwack, M. Somlo and B. Labouesse, *Biochim. Biophys. Acta*, **18**, 71 (1955).
13) I. Mandl, H. Zipper and L. T. Ferguson, *Arch. Biochem. Biophys.*, **74**, 465 (1958).
14) Y. Nagai, S. Sakakibara, H. Noda and S. Akabori, *Biochim. Biophys. Acta*, **37**, 567 (1960).
15) J. S. Fruton, *Advances in Protein Chemistry*, **5**, 67 (1949).

* Z = Carbobenzoxy; M. A. = isovaleroyl mixed anhydride method; { } shows a material failed to crystallize, the purity of which is not confirmed by elementary analysis; [ ] shows a material failed to crystallize but obtained as a powder, the purity of which is confirmed by elementary analysis.

(2) Z-Leu-OH + H-Gly-OEt
$\xrightarrow{\text{M.A.}}$ Z-Leu-Gly-OEt (II)
$\longrightarrow$ Z-Leu-Gly-NH-NH_2 (III)
II $\longrightarrow$ Z-Leu-Gly-OH (IV)

(3) a. Z-Leu-Gly-N_3 ($\longleftarrow$ III)
+ H-Pro-OEt
$\longrightarrow$ Z-Leu-Gly-Pro-OEt (V)

b. IV + H-Pro-OEt $\xrightarrow{\text{M.A.}}$ V

(4) Z-Pro-OH + H-Leu-Gly-OEt ($\longleftarrow$ II)
$\xrightarrow{\text{M.A.}}$ Z-Pro-Leu-Gly-OEt (VI)
VI $\longrightarrow$ Z-Pro-Leu-Gly-NH-NH_2 (VII)

(5) a. Z-Pro-OH + H-Leu-Gly-Pro-OEt
($\longleftarrow$ V)
$\xrightarrow{\text{M.A.}}$ {Z-Pro-Leu-Gly-Pro-OEt} (VIII)

b. Z-Pro-Leu-Gly-N_3
($\longleftarrow$ VII) + H-Pro-OEt
$\longrightarrow$ {Z-Pro-Leu-Gly-Pro-OEt} (VIII)
VIII $\longrightarrow$ [Z-Pro-Leu-Gly-Pro-OH]
(IX) $\longrightarrow$ [H-Pro-Leu-Gly-Pro-OH] (X)

(6) a. Z-Gly-N_3 + H-Pro-Leu-Gly-OEt
($\longleftarrow$ VI)
$\longrightarrow$ Z-Gly-Pro-Leu-Gly-OEt (XI)

b. I + H-Leu-Gly-OEt ($\longleftarrow$ II) $\xrightarrow{\text{M.A.}}$
XI $\longrightarrow$ Z-Gly-Pro-Leu-Gly-OH (XII)
XI $\longrightarrow$ Z-Gly-Pro-Leu-Gly-NH-NH_2 (XIII)

(7) a. Z-Gly-N_3 + H-Pro-Leu-Gly-Pro-OEt
($\longleftarrow$ VIII)
$\longrightarrow$ {Z-Gly-Pro-Leu-Gly-Pro-OEt} (XIV)

b. I + H-Leu-Gly-Pro-OEt ($\longleftarrow$ V)
$\xrightarrow{\text{M.A.}}$ {Z-Gly-Pro-Leu-Gly-Pro-OEt} (XIV)

c. XII + H-Pro-OEt
$\xrightarrow{\text{M.A.}}$ {Z-Gly-Pro-Leu-Gly-Pro-OEt} (XIV)

d. Z-Gly-Pro-Leu-Gly-N_3
($\longleftarrow$ XIII) + H-Pro-OEt
$\longrightarrow$ {Z-Gly-Pro-Leu-Gly-Pro-OEt} (XIV)

XIV $\longrightarrow$ Z-Gly-Pro-Leu-Gly-Pro-OH (XV)
$\longrightarrow$ [H-Gly-Pro-Leu-Gly-Pro-OH] (XVI)
XIV $\longrightarrow$ [Z-Gly-Pro-Leu-Gly-Pro-NH_2] (XVII)
$\longrightarrow$ [H-Gly-Pro-Leu-Gly-Pro-NH_2] (XVIII)

Methods of peptide-bond formation employed in the present study, were the azide method and the isovaleroyl mixed anhydride method[16]. The azide method is well known to be suitable for keeping the optical purity of peptides in the course of the reaction[17]. The mixed anhydride method is a comparatively simple method of the activation of the carboxyl component, and had been used successfully by Ressler and du Vigneaud[18] for the coupling reaction of carbobenzoxy-L-proline and L-leucyl-glycine ethylester. In every case of the azide procedure used in our present study, it was to be noted that carbobenzoxypeptide azide containing proline residue was insoluble in ether, and chloroform was the most suitable solvent for extracting the azide formed. In regard to the acylation of the proline imino group, the azide method was superior to the mixed anhydride method in view of the synthetic yield, crystallizability and melting point of the products. For example, carbobenzoxyglycyl-L-proline (I) which was prepared by the azide method from carbobenzoxyglycine hydrazide and L-proline ethylester was sufficiently pure without recrystallization, and the yield was also satisfactory (m. p. 155°C, yield 75%). On the other hand, the mixed anhydride method gave the substance I with a lower melting point (153°C) in poorer yield (42%). Similar results were obtained in cases of coupling reactions of carbobenzoxy-L-leucyl-glycine with L-proline ethylester, and of carbobenzoxyglycyl-L-prolyl-L-leucyl-glycine with L-proline ethylester. Recently, Bodanszky and du Vigneard[19] have published an interesting communication, in which they proposed the use of carbobenzoxyamino acid *p*-nitrophenylesters for acylation of peptide esters. If their new procedures would be employed in parts of our procedures, better results might be obtained.

Among the synthetic routes for the carbobenzoxypentapeptide ester (XIV), the best result was obtained by route 7-d. Since the

16) J. R. Vaughan, Jr. and R. L. Osato, *J. Am. Chem. Soc.*, **73**, 5553 (1951).
17) M. B. North and G. T. Young, *Chemistry & Industry*, 1567 (1955).
18) C. Ressler and V. du Vigneaud, *J. Am. Chem. Soc.*, **76**, 3107 (1954).
19) M. Bodanszky and V. du Vigneaud, ibid., **81**, 5688 (1959).

substance XIV has not been heretofore crystallized, the synthetic yields for those procedures, 7-b, c and d, were compared with each other on the saponified product XV. The route 7-a was eliminated, since the substance VIII which was used as the intermediate in the route was not crystallized, and purification of which was unsuccessful. Substance XV prepared by route 7-d was readily crystallized under the presence of ethyl acetate, but the same substance XV prepared by route 7-b or 7-c was hard to crystallize. The route 7-b was abandoned for the reason that the crystallizability of the intermediate V was poor and of which yield was rather low. Although both intermediate substances XII and XIII were easily crystallized and were obtained from XI in good yields, mixed anhydride route 7-c was somewhat inferior to azide route 7-d as described above. The intermediate XI was prepared through two routes 6-a and 6-b, and the former was somewhat superior to the latter in synthetic yield. In regard to the optical purity, every preparations (XV) obtained by routes 7-b, c and a showed the same specific rotation after recrystallization.

Carbobenzoxy-L-prolyl-L-leucyl-glycyl-L-proline ethylester (VIII) was prepared not only as an intermediate for the substance XIV, but also as a substrate for collagenase. In the synthesis of the substance VIII, two routes, mixed anhydride procedure (5-a) and azide procedure (5-b), were taken into consideration. Since the substances VIII and its saponified product IX were not crystallized, formation of by-products, separation of which seemed to be difficult, was particularly undesirable. In the similar cases of 7-b and 7-d, which corresponded respectively to 5-a and 5-b, it was observed previously that the former was inferior to the latter in the purity and yield of the product. Then, the route 5-a was not explored in this case. Carbobenzoxy-L-prolyl-L-leucyl-glycine hydrazide (VII), which was used in route 5-b, was water-soluble substance and it was very interesting, that this substance was crystallizable only from toluene and this crystal contained crystallization toluene, which could be removed completely when the compound was heated at 50°C in vacuo.

Peptides or their derivatives containing proline residue in general are hydrophilic and peptides containing two or more proline residues, especially, were hard to be crystallized because of the effect of humidity. It was, however, found that carbobenzoxyglycyl-L-prolyl-L-leucyl-glycyl-L-proline (XV) was an exceptional example of readily crystallizable substance as described above. In this case, both ethyl acetate and water were indispensable for crystallization. When the peptide XV was recrystallized from ethyl acetate which contains equimolar amount of water to the peptide, it formed prisms. The crystal contained one mole each of water, and ethyl acetate per mole of the peptide as crystallization solvent and was fairly stable even when it was kept in the open air. In turn, when the same peptide was recrystallized from water-saturated ethyl acetate, different crystals (plates) were obtained, and they were unstable in the open air and gradually transformed into opaque crystals. A crystallographic study on these phenomena is now in progress by Sasada and Kakudo in our laboratory with X-ray diffraction technique.

As described above, the interesting phenomenon that some kinds of peptide derivatives (VII and XV) have affinity with specific substances (toluene or ethyl acetate) seemed to suggest a possible mode of combination in the enzyme-substrate complex formation. Similarly, the penta-peptide amide (XVIII) which was dried azeotropically by using toluene or ethanol occluded the solvents firmly, and complete removal of the solvents was very hard.

The above mentioned carbobenzoxypentapeptide XV was the best substrate for collagenase as described in the previous communication[14]. The substances IX, XV, XVI and XVIII were all hydrolyzed completely by collagenase within a comparatively short period of time. Studies on the enzymatic digestion of these peptides will be published elsewhere in the near future.

Experimental*

Carbobenzoxyglycyl-L-proline (I). — a. Carbobenzoxyglycine hydrazide (11.2 g., 0.05 mol.) was dissolved in a mixture of acetic acid (40 ml.) and water (80 ml.), and 6 N hydrochloric acid (17 ml., 0.1 mol.) was added into the solution. The mixture was cooled to −5°C, shaken well with a small amount of chloroform and carefully treated with sodium nitrite (3.8 g., 0.055 mol.). The carbobenzoxyglycine azide formed was extracted three times with cold chloroform (total 150 ml.). The combined extract was washed with ice water (50 ml.) and acids for a short time over anhydrous sodium sulfate at −5°C. The dried solution was filtered into a mixture of proline ethylester hydrochloride (10 g., 0.055 mol.) and triethylamine (5.6 g., 0.055 mol.) in chloroform (50 ml.) at −5°C, and allowed to stand overnight at 0~4°C. The reaction mixture was washed successively with 0.5 N hydrochloric acid, water and 5% sodium bicarbonate solution and dried over anhydrous magnesium sulfate. The dried solution was concentrated to syrup under reduced pressure and the residue was redissolved in methanol (100 ml.), and then 2 N sodium hydroxide (25 ml., 0.05 M) was added. After the solution was kept for 2 hr. at room temperature, it was neutralized with 6 N hydrochloric acid, and the methanol

* All melting points were uncorrected.

was removed under reduced pressure. As soon as methanol was removed, colorless prisms appeared. After being stored overnight in a refrigerator, the crystals were filtered off, washed with water and ethyl acetate, and dried in a desiccator. The yield of I with m. p. 154.5~155°C was 75% (11.5 g.). This substance was pure enough without recrystallization for preparing higher peptides. Recrystallization from ethyl acetate of the product (1.4 g.) gave prisms (1.2 g.); m. p. 154.5~155°C, $[\alpha]_D^{15}$ −70.4° (c. 6, ethanol); Bergmann et al.[20] reported m. p. 156°C (corr.).

b. Carbobenzoxyglycine (2.1 g., 0.01 M) was dissolved in chloroform (40 ml.) by adding triethylamine (1.0 g., 0.01 M), and then toluene (40 ml.) was added into the solution. The mixture was cooled to −10°C and isovaleroyl chloride (1.2 g., 0.01 M) was added slowly into the solution under stirring. After about 1.5 hr. a solution of proline ethylester hydrochloride (2.16 g., 0.012 M) and triethylamine (1.2 g., 0.012 M) in chloroform (40 ml.) was added into the mixed anhydride solution, and the mixture was allowed to stand overnight at 4°C. The reaction mixture was treated as described above. Yield of I was 42% (1.3 g.); m. p. 152~154°C. Recrystallization from ethyl acetate of the product (1.3 g.) gave fine prisms (1.1 g.); m. p. 153~154°C, $[\alpha]_D^{15}$ −70.2° (c. 5, ethanol).

Carbobenzoxy-L-leucyl-glycine Ethylester (II).—This substance was prepared according to the procedures of Vaughan and Osato[16]; yield 70%, m. p. 102~104°C, $[\alpha]_D^{15}$ −26.8° (c. 5.5, ethanol).

Carbobenzoxy-L-leucyl-glycine Hydrazide (III).—Into a solution of II (10 g.) in ethanol (40 ml.) was added hydrazine hydrate (8 ml.), and then the mixture was allowed to stand overnight at room temperature. The reaction mixture was concentrated to dryness under reduced pressure and the residual crystalline mass was recrystallized from ethanol and ether to give needles; m. p. 130~132°C, yield 89% (8.5 g.).

Found: C, 56.97; H, 7.29; N, 16.71. Calcd. for $C_{16}H_{24}O_4N_4$: C, 57.13; H, 7.19; N, 16.66%.

Carbobenzoxy-L-leucyl-glycine (IV).—This substance was prepared from II according to procedures of Bergmann et al.[21]; m. p. 114~115°C, yield 90%, $[\alpha]_D^{15}$ −26.3° (c. 8, ethanol).

Carbobenzoxy-L-leucyl-glycyl-L-proline Ethylester (V).—a. A solution of carbobenzoxy-L-leucyl-glycine azide in chloroform, which was prepared from III (3.4 g.) as in the case of I-a was added into a mixture of proline ethylester hydrochloride (2 g.) and triethylamine (1.1 g.) in chloroform (20 ml.) at −5°C, and the mixture was allowed to stand overnight. The reaction mixture was washed successively with water, 1 N hydrochloric acid, water, 5% sodium bicarbonate and water again, and dried. The dried solution was concentrated to syrup and the residue was crystallized in a refrigerator after treatment with petroleum benzine. The crude crystals formed were triturated with a small amount of ethyl acetate and carefully recrystallized with a small amount of petroleum benzine. The crystals were filtered off, washed with ether and dried in a desiccator in vacuo to give fine needles; m. p. 81~85°C, yield 80% (3.6 g.). Recrystallization of the product from ethyl acetate-petroleum benzine gave needles with m. p. 89~91°C; yield 44% (2.0 g.), $[\alpha]_D^{17}$ −78.0° (c. 6, ethanol). A second crop of the recrystallization was obtained in 11% yield (0.5 g.); m. p. 88~91°C.

Found: C, 61.75; H, 7.25; N, 9.64. Calcd. for $C_{23}H_{33}O_6N_3$: C, 61.72; H, 7.43; N, 9.36%.

b. Carbobenzoxy-L-leucyl-glycine (IV) (3.2 g.) was dissolved in chloroform (50 ml.) by adding triethylamine (1 g.) and then toluene (50 ml.) was added to the solution. The mixture was cooled to −10°C and isovaleroyl chloride (1.2 g.) was added slowly to the solution under stirring. After about 1.5 hr. a solution of proline ethylester hydrochloride (2.16 g.) and triethylamine (1.2 g.) in chloroform (40 ml.) was added to the mixed anhydride solution, and then the mixture was allowed to stand overnight at 4°C. The reaction mixture was treated as described above to give a crude product; yield 67% (3 g.). Recrystallization from ethyl acetate-petroleum benzine gave fine needles; m. p. 88~91°C, yield 46% (2.1 g.), $[\alpha]_D^{17}$ −77.8° (c. 4, ethanol).

Carbobenzoxy-L-prolyl-L-leucyl-glycine Ethylester (VI).—This substance was prepared according to the procedures of Ressler and du Vigneaud[15]; m.p. 148.5~150.5°C, yield 88~90%. Recrystallization from ethanol-water gave 70% yield, m. p. 150~151.5°C, $[\alpha]_D^{15}$ −81.9° (c. 2, ethanol); second crop from the mother liquor gave 13% yield, m. p. 149~150°C.

Carbobenzoxy-L-prolyl-L-leucyl-glycine Hydrazide (VII).—Hydrazine hydrate (2 ml.) was added to a solution of VI (2.24 g.) in ethanol (30 ml.) and then the mixture was allowed to stand overnight at room temperature. The reaction mixture was concentrated to syrup under reduced pressure and the residual syrup was dried by the addition of benzene followed by evaporation under reduced pressure. After the drying procedures were repeated, the residue was crystallized by trituration with toluene (about 10 ml.) and dried over sodium hydroxide at room temperature to give fine needles; yield 91% (2.4 g.), m. p. 76~80°C. This substance contained about one mole of crystallization toluene.

Found: C, 62.82; H, 7.44; N, 14.14. Calcd. for $C_{21}H_{31}O_5N_5 \cdot 3/4C_7H_8$: C, 62.73; H, 7.42; N, 13.94%.

After dryness in vacuo at 50°C, the crystallization toluene was removed.

Found: C, 58.27; H, 7.26; N, 16.40. Calcd. for $C_{21}H_{31}O_5N_5$: C, 58.18; H, 7.21; N, 16.16%.

Carbobenzoxy-L-prolyl-L-leucyl-glycyl-L-proline (IX).—b. A carbobenzoxy-L-prolyl-L-leucyl-glycine azide solution, which was prepared from VII (toluene-free 2.15 g.) as in the case of I-a, was added to a mixture of proline ethylester hydrochloride (1 g.) and triethylamine (0.56 g.) in chloroform (20 ml.) at −5°C. After being kept overnight at 4°C, the solution was washed successively with water, 1 N hydrochloric acid, water, 5% sodium bicarbonate solution and again with water, and dried. The dried solution was concentrated to syrup under reduced pressure and the residue was

20) M. Bergmann et al., *Ber.*, **65**, 1192 (1932); *Z. physiol. Chem.*, **212**, 72 (1932).
21) M. Bergmann et al., *J. Biol. Chem.*, **111**, 225 (1935).

redissolved in methanol (30 ml.). 1 N Sodium hydroxide (8 ml.) was added into the methanol solution and the mixture was allowed to stand for about 3 hr. at room temperature. After neutralizing the reaction mixture with 6 N hydrochloric acid, it was concentrated to syrup under reduced pressure and the remaining oily material was dissolved in 5% sodium bicarbonate solution. The bicarbonate solution was washed well with ethyl acetate and then acidfied with 6 N hydrochloric acid. The separated oil was extracted with chloroform. On evaporation of the solvent a syrup was obtained and was solidified by trituration with petroleum benzine. After dryness in vacuo at 80°C, the amorphous powder amounted to 54% yield (1.4 g.); m.p. 90~120°C (sintered at 90°C), $[\alpha]_D^{17}$ −106.1° (c. 5.5, ethanol).

Found: C, 61.20; H, 7.29; N, 10.38. Calcd. for $C_{26}H_{36}O_7N_4$: C, 60.45; H, 7.02; N, 10.85%.

L-Prolyl-L-leucyl-glycyl-L-proline (X).—Palladium-charcoal (5%, 1 g.) was added to a solution of IX (1 g.) in a mixture of methanol (20 ml.) and water (30 ml.), and hydrogen was introduced into the suspension for 3 hr. under stirring. The catalyst was filtered off and washed three times with hot water (total 30 ml.), and then the combined filtrate was concentrated under reduced pressure. The residual syrup was dissolved in small amount of water, and the solution was filtered. The clear solution was concentrated to syrup and the residue was dried by the addition of benzene followed by evaporation under reduced pressure, and then pulverized. After dryness in vacuo at 110°C for about 3 hr., the product amounted to an 80% yield (0.6 g.); deliquescent powder, m. p. 170~180°C (sintered at 147~150°C), $[\alpha]_D^{15}$ −121.5° (c. 5, water).

Found: C, 55.94; H, 7.86; N, 14.32. Calcd. for $C_{14}H_{30}O_5N_4 \cdot 1/6H_2O$: C, 56.09; H 7.93; N, 14.54%.

Complete dryness of this substance failed because the substance was partially charred when heated at 135°C for 3 hr. in vacuo.

Carbobenzoxyglycyl-L-prolyl-L-leucyl-glycine Ethylester (XI).—**a.** Palladium-charcoal (5%, 5 g.) and 6 N hydrochloric acid (6 ml.) was added to a solution of VI (13.4 g.) in ethanol (200 ml.), and hydrogen was introduced into the suspension for 3 hr. under stirring. The catalyst was filtered off and washed three times with ethanol (total 60 ml.), and then the combined filtrate was concentrated under reduced pressure. The residual syrup was dried by the addition of toluene followed by evaporation under reduced pressure. A carbobenzoxyglycine azide solution, which was prepared from carbobenzoxyglyciues hydrazide (6.7 g.) according to the procednre in the case of I-a was added into a mixture of the prolyl-leucyl-glycine ethylester hydrochloride and triethylamine (3 g.) in chloroform (100 ml.). After storage overnight in a refrigerator at 4°C, the reaction mixture was washed successively with 1 N hydrochloric acid, water, 5% sodium bicarbonate solution and water again, and dried. Evaporation of the solvent gave a syrupy material which was crystallized by the addition of chloroform and petroleum benzine. The yield of the crude product was 80% (12 g.); m. p. 96~101°C (after dryness in vacuo at 80°C). This substance was used for the preparation of XII and XIII without recrystallization. Melting point of this substance rose to 101~104°C after two recrystallization from chloroform and petroleum benzene; $[\alpha]_D^{15}$ −69.9° (c. 5, ethanol).

Found: C, 59.47; H, 7.10; N, 11.15. Calcd. for $C_{25}H_{36}O_7N_4$: C, 59.51; H, 7.19; N, 11.10%.

b. The substance II (10 g.) was hydrogenated in ethanol (50 ml.) containing 6 N hydrochloric acid (5 ml.) with 5% palladium-charcoal (4 g.). The catalyst was filtered off and washed three times with ethanol, and then the combined filtrate was concentrated under reduced pressure. The residual syrup was dried by the addition of toluene followed by evaporation under reduced pressure. A mixture of the leucyl-glycine ethylester hydrochloride and triethylamine (3 g.) in chloroform (30 ml.) was added to a mixed anhydride solution at −10°C, which was prepared from I (8 g.), triethylamine (2.65 g.) and isovaleroyl chloride (3.15 g.) in a mixture of chloroform (100 ml.) and toluene (100 ml.) as in the case of I-b. After being kept overnight at 4°C, the reaction mixture was treated in a similar manner to the case of XI-a and a crude product was obtained in a 78% yield (10.3 g.); m. p. 96~101°C (dried in vacuo at 80°C). After several recrystallizations from chloroform-petroleum benzine, this substance melted at 101~105°C; $[\alpha]_D^{15}$ −70.5° (c. 5, ethanol).

Carbobenzoxyglycyl-L-prolyl-L-leucyl-glycine (XII).—The crude product of XI-a (5 g.) was dissolved in methanol (50 ml.) and 1 N sodium hydroxide (11 ml.) was added into the solution, and then the mixture was allowed to stand at room temperature for 2 hr. The mixture was neutralized with 6 N hydrochloric acid, and the methanol was distilled under reduced pressure. The crystals formed were filtered off, washed with water and ethyl acetate, and dried; m. p. 184~187°C. yield 87% (4.1 g.). After recrystallization from ethanol-water (1:1), this substance melted at 185~188°C; $[\alpha]_D^{15}$ −60.4° (c. 6.5, pyridine).

Found: C, 58.14; H, 6.90; N, 11.76. Calcd. for $C_{23}H_{32}O_7N_4$: C, 57.97; H, 6.77; N, 11.76%.

This substance was prepared from XI-b (3.2 g.) in a yield of 86% (2.6 g.); m. p. 184~188°C, $[\alpha]_D^{15}$ −60.3° (c. 5, pyridine).

Carbobenzoxyglycyl-L-prolyl-L-leucyl-glycine Hydrazide (XIII).—The crude XI-a (10.1 g.) was dissolved in ethanol (50 ml.) and hydrazine hydrate (5 ml.) was added to the solution. After being kept overnight at room temperature, the reaction mixture was concentrated to dryness, and the residual syrup was crystallized from ethanol and ether to give long needles; m. p. 155~157°C, yield 97% (9.5 g.). Recrystallization from ethanol and petroleum benzine gave a 94% yield (9.2 g.); m. p. 157~159°C.

Found: C, 56.34; H, 7.04; N, 17.24. Calcd. for $C_{23}H_{34}O_6N_6$: C, 56.31; H, 6.99; N, 17.13%.

This substance was prepared from XI-b (8.8 g.) in a yield of 94% (8.1 g.); m. p. 157~159°C.

Carbobenzoxyglycyl-L-prolyl-L-leucyl-glycyl-L-proline (XV).—**d.** An azide solution which was prepared from XIII (8 g.) as in the case of I-a,

was added to a solution of proline ethylester hydrochloride (3.2 g.) and triethylamine (1.8 g.) in chloroform (20 ml.) at −5°C. The reaction mixture was allowed to stand overnight at 4°C, and was then washed successively with water, 1 N hydrochloric acid, water, 5% sodium bicarbonate solution and water again, and dried. The dried solution was concentrated to syrup under reduced pressure and the residue was redissolved in methanol (100 ml.). 1 N sodium hydroxide (20 ml.) was added into the methanol solution and the mixture was allowed to stand for about 3 hr. at room temperature. After neutralizing the reaction mixture with 6 N hydrochloric acid, it was concentrated to dryness under reduced pressure and the remaining syrup was dissolved in saturated sodium bicarbonate solution. The bicarbonate solution was washed with ethyl acetate and then acidified with 6 N hydrochloric acid. The separated oil was extracted with chloroform and the extract was concentrated to syrup, which was crystallized by trituration with ethyl acetate containing a small amount of water. After storage overnight in a refrigerator, the crystals were filtered off and dried in vacuo at 80°C for about 3 hr. to give 5.0 g. of the first crop. On evaporation of the ethyl acetate washing described above, a slight amount of residue was obtained. The residue was again saponified in the same manner and a second crop (0.6 g.) was obtained. The total yield was 60%. Recrystallization of the product from ethyl acetate containing an equimolar amount of water to the peptide, gave prisms (6 g.) with m. p. 72°C (dec. at 75~77°C), which were dried in the open air. This material contained one mole of ethyl acetate and one mole of water as crystallization solvents.

Found: C, 56.55; H, 7.44; N, 10.39. Calcd. for $C_{28}H_{39}O_8N_5 \cdot C_4H_8O_2 \cdot H_2O$: C, 56.54; H, 7.27; N, 10.30%.

The crystallization solvents could be removed at 80°C in vacuo to give an amorphous powder; m. p. 130~135°C, $[\alpha]_D^{15}$ −128.2° (c. 4, ethanol).

Found: C, 58.49; H, 6.84; N, 12.23. Calcd. for $C_{28}H_{39}O_8N_5$: C, 58.62; H, 6.85; N, 12.21%.

The route XIV-b-XV gave 35% yield of the amorphous powder; $[\alpha]_D^{15}$ −128.2° (c. 4, ethanol). The route XIV-c-XV gave a 45% yield of the same substance; $[\alpha]_D^{15}$ −128.2° (c. 4, ethanol).

Glycyl-L-prolyl-L-leucyl-glycyl-L-proline (XVI).—Palladium-charcoal (5%, 1 g.) was added to a solution of XV (1.7 g.) (amorphous powder) in methanol (20 ml.) and water (30 ml.), and hydrogen was introduced into the suspension for 3 hr. under stirring. The catalyst was filtered off and washed three times with hot water (total 30 ml.), and then the combined filtrate was concentrated under reduced pressure. The residual syrup was dissolved in a small amount of water, and the solution was filtered. The clear solution was concentrated to syrup and the residue was dried by the addition of toluene followed by evaporation under reduced pressure, and then pulverized. After dryness in vacuo at 110°C for about 3 hr., the product amounted to a 51% yield (0.8 g.) of deliquescent powder; m. p. 160~167°C, $[\alpha]_D^{15}$ −160.1° (c. 5.5, water.)

Found: C, 53.72; H, 7.65; N, 15.71. Calcd. for $C_{20}H_{33}O_6N_5 \cdot 1/2H_2O$: C, 53.56; H, 7.64; N, 15.62%.

Carbobenzoxyglycyl-L-prolyl-L-leucyl-glycyl-L-proline Amide (XVII).—The syrupy material XIV which was prepared from XIII (4.9 g.) according to the procedure XV-d was dissolved in methanol (40 ml.). After being saturated with dry ammonia gas at 0°C, the solution was allowed to stand one week at room temperature in a sealed tube. The reaction mixture was concentrated to syrup under reduced pressure and the residue was dried by the addition of benzene followed by evaporation under reduced pressure. The dried residue was dissolved in hot ethyl acetate and reprecipitated by the addition of petroleum benzine, and dried over phosphrous pentoxide in vacuo at 80°C; yield 63% (3.6 g.), m. p. 118~128°C (sintered at 102~118°C), $[\alpha]_D^{17}$ −117° (c. 4.5, ethanol).

Found: C, 58.73; H, 7.23; N, 14.60. Calcd. for $C_{28}H_{40}O_7N_6$: C, 58.72; H, 7.04; N, 14.68%.

Glycyl-L-prolyl-L-leucyl-glycyl-L-proline Amide (XVIII).—Palladium-charcoal (5%, 1 g.) was added to a solution of XVII (1.5 g.) in ethanol (20 ml.) and water (20 ml.), and hydrogen was introduced into the suspension for 3 hr. under stirring. The catalyst was filtered off and washed three times with hot water (total 30 ml.), and then the combined filtrate was concentrated under reduced pressure. The residual syrup was dissolved in a small amount of water, and the solution was filtered. The clear solution was concentrated to syrup and the residue was dried by the addition of ethanol followed by evaporation under reduced pressure, and then pulverized. This material was dried at 110°C in vacuo for 3 hr. before analysis; deliquescent powder, yield of 82% (0.95 g.), m. p. 135~155°C (sintered at 110~115°C), $[\alpha]_D^{17}$ −147.2°C (c. 3.3, ethanol).

Found: C, 54.25; H, 7.76; N, 19.04. Calcd. for $C_{20}H_{34}O_5N_6$: C, 54.78; H, 7.82; N, 19.17%.

Summary

Glycyl-L-prolyl-L-leucyl-glycyl-L-proline and its related compounds were synthesized for elucidating the substrate specificity of collagenase. In the synthetic study, almost all of the possible routes were tried and the yield, crystallizability and specific rotation of products were compared for each route. Peptides or their derivatives containing two proline residues in general were hydrophilic and hard to be crystallized, but it was found, that carbobenzoxyglycyl-L-prolyl-L-leucyl-glycyl-L-proline was an exceptional example of a readily crystallizable substance and a good substrate for collagenase.

The authors should like to express their thanks to Professor Shiro Akabori of the Institute and Professor Haruhiko Noda of the University of Tokyo for helpful suggestions and guidance in the course of this work.

Institute for Protein Research
Osaka University
Joan-cho-36, Kita-ku, Osaka

Crystal Habit Modification of Strontium Sulfate. I. Habit-Modifying Action of Foreign Substances

By Sadaichi OTANI

(Received March 23, 1960)

Crystals having spherical forms are often found in mineral spherulite which is recognized as a type of radiated crystals. Spherulites have also been prepared artificially by many workers. Popoff[1] studied the two-dimensional spherulites of resorcinol and malonamide, while Lengyel[2] investigated those of several inorganic substances. Three-dimentional spherulites of various inorganic substances were prepared by Morse and others[3] by allowing the reacting solutions to be mixed through diffusion avoiding convection; their best spherulites having spherical forms were obtained in a gelatinous medium. Hence they considered the high viscosity of the medium to be one of the favorable conditions for spherulitic growth. From an ordinary solution, instead of the viscous medium, Patterson[4] obtained spherulitic aggregates of calcium phosphate in the presence of the citrate ion, but the shape of the aggregate was far from being spherical. Recently Miura and his co-workers[5] have succeeded in preparing fine spherical crystals of barium sulfate having nearly uniform size, from an aqueous solution containing citrate ion, and they pointed out the effective utilizations of such crystals in the fundamental study of colloid science and also in the industrial field.

The present author has been interested in the preparation of spherical crystals as well as in the mechanism of their formation, and several attempts have been made regarding these problems. The results obtained will be presented in two parts, of which the first deals with the habit-modifying effect of various substances upon the crystal of strontium sulfate, and the second with the characteristic behavior of the triphosphate ion in the course of deposition and dissolution of strontium sulfate, as well as the mechanism of spherulite formation.

Experimental

Reagents.—Strontium chloride of the reagent grade was purified by repeating three times the alternate crystallization of the dihydrate from a hot solution and then of the hexahydrate from a cold solution. Both potassium sulfate and sodium citrate of the analytical grade were recrystallized from their aqueous solutions. Sodium triphosphate (STP) was prepared by Bell's method[6] and recrystallized from an aqueous solution by adding methanol. Both the EDTA and glycerol used were of the analytical grade. The polyvinyl alcohol (PVA) used had an average molecular weight of 8.5×10^4. Both oleylpyridinium chloride and polyethyleneglycol monostearate were furnished by the courtesy of Daiichi Kogyo Seiyaku Co. Ltd. Aerosol OT was of the commercially highest grade.

Procedure.—The crystals to be examined were precipitated by mixing a solution of strontium chloride with one of potassium sulfate, in the presence or absence of a third substance in a glass-stoppered flask. To diminish the influence of the container wall upon crystallization, the inside surface of the flask was coated with silicone by the diethyldichlorosilane-treatment. This prevented the precipitate from adhering to the container wall, and thus the crystal growth was not troubled with any steric disturbance of the wall. During mixing and crystallizing, the solutions were violently and continuously shaken with a motor-driven shaker, and the temperature was kept constant within the limits of ±0.1°C.

Foreign substances whose effects were to be examined were added either to the solution of strontium chloride or to one of potassium sulfate, prior to the mixing of these. Sodium citrate, EDTA or condensed phosphates, anyone of which was a complexing agent for metallic cations, was always added to the solution of strontium chloride.

Results

Crystals Grown from Mixtures of Strontium Chloride and Potassium Sulfate Solutions.—First of all, crystals deposited from the solutions prepared by mixing strontium chloride and potassium sulfate solutions without foreign substance were examined. Quite a number of samples were prepared by varying the concentrations and the mixing proportions of the solutions. The concentration range of strontium and sulfate, immediately after mixing, was 0.002~0.1 M.

According to the crystal forms of these samples, they could be classified roughy into

1) B. Popoff, *Latv. Farm. Zurn.*, **1934**, 1.
2) E. v. Lengyel, *Z. Krist.*, **97**, 67 (1937).
3) H. W. Morse, C. H. Warren and J. D. H. Donnay, *Am. J. Sci.*, **23**, 421 (1932).
4) D. Patterson, *Nature*, **173**, 75 (1937).
5) M. Miura, T. Nagakane and S. Masaki, *J. Sci. Hiroshima Univ., Ser. A*, **19**, 513 (1956).
6) R. N. Bell, "Inorganic Syntheses", Vol. 3, McGraw-Hill Inc., New York (1950), p. 101.

two large groups. Two microphotographs are shown in Fig. 1 for reference. Fig. 1a represents the crystals of a type obtainable from solutions containing a large excess of sulfate ion and Fig. 1b those of another type from the equivalent mixtures or solutions containing strontium ion in excess. By observing the extinction and retardation of polarized light between the crossed nicols, the orientations of the crystallographic axes were determined, and indicated in the photographs.

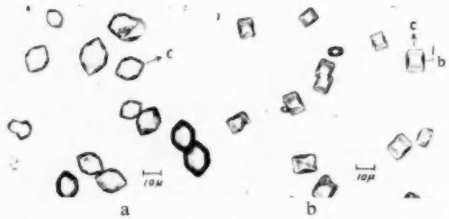

a b

Fig. 1. Two samples of crystals grown from mixtures of $SrCl_2$ and K_2SO_4 solutions.

a: 0.017 M $SrCl_2$, 0.10 M K_2SO_4
b: 0.10 M $SrCl_2$, 0.017 M K_2SO_4

Effect of Several Additives. — To inquire whether the viscosity of the medium is an essential factor to the habit modification as reported by Morse and others[2], the effects of glycerol and PVA were tested. In the concentration ranges up to 27% with glycerol and up to 0.4% with PVA, none of these gave any significant influence on the habit of crystals formed.

Then the effects of some surface active agents were examined. Addition of oleylpyridinium chloride or polyethylene glycol monostearate caused a slight increase in the size of the crystals deposited, but the crystal form was hardly influenced by these surface active agents within the concentration limit of 1.0% in each case. Anionic surface active agent Aerosol OT, however, produced a voluminous white precipitate which might be its strontium salt.

Effect of Sodium Citrate.—Sodium citrate, even at a very low concentration, has a remarkable effect on the deposition rate and the shape of the crystals. The larger the amount of sodium citrate added, the slower was the deposition rate and the smaller the size of the crystals formed. The shape of the crystals was altered by the addition of sodium citrate in such a way that the edges and corners of the polyhedrons shown in Fig. 1 gradually vanished as the amount of citrate was increased, resulting finally in thin ellipsoids. However, because of the low solubility of strontium citrate, there was a limit to the concentration of the citrate ion in solution, above which the voluminous needle-shaped precipitate appeared.

In Fig. 2 the microphotographs of two samples are shown. These were obtained at 25°C from two separate solutions containing equal amounts of sodium citrate. Both of the solutions from which these crystals were deposited had the same concentration with respect to either of the essential salts as in the previous case (Fig. 1). The electron micrographs of these samples are shown in Fig. 3. Several slenderer figures appearing in Fig. 3a represent the oblique projections of thin ellipsoids (cf. Fig. 7b). Fig. 3b was taken after chromium shadowing at an angle of approximately 22° to the plane of the supporting

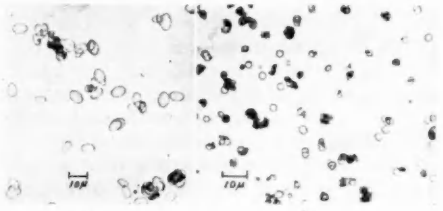

a b

Fig. 2. Two samples of crystals grown from samples solutions containing sodium citrate.

a: 0.071 M $SrCl_2$, 0.10 M K_2SO_4, 0.003 M sodium citrate
b: 0.10 M $SrCl_2$, 0.017 M K_2SO_4, 0.003 M sodium citrate

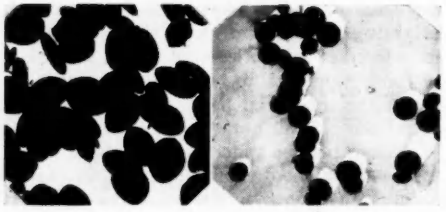

a b

Fig. 3. Electron micrographs of the two a and b shown in Fig. 2.

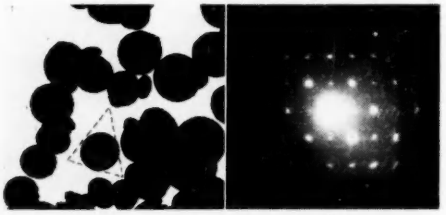

a b

Fig. 4. Electron micrograph (a) of the sample as one shown in Fig. 2b, and the diffraction pattern (b) of the selected crystal in (a) (surrounded with the triangle).

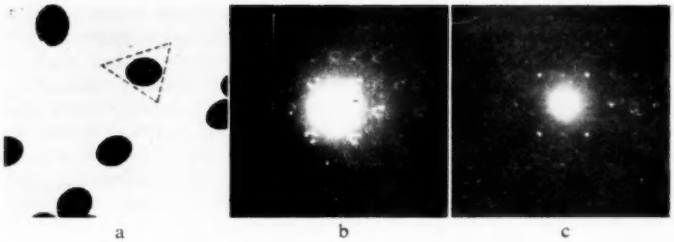

a b c

Fig. 5. Electron micrograph (a) of the same sample as one shown in Fig. 2a, and the diffraction pattern (b and c) of the selected crystal in (a) (surrounded with the triangle).

film. This micrograph shows that the crystals are flat and nearly disk-shaped (cf. Fig. 7a).

These crystals were then examined by means of an electron microdiffraction technique. The selected-area diffraction of any particle examined gave always an N-pattern as one shown in Fig. 4b or 5c, indicating that these individual crystals are single crystals. For the analysis of the diffraction patterns, the interplanar spacings were determined by comparing these patterns with the Debye-Scherrer rings of magnesium oxide which were taken under a similar condition. For this purpose, the sample crystals and magnesium oxide smoke were mounted together on a supporting film. That is to say, the film on which the sample crystals had already been mounted was exposed to the smoke of burning magnesium. Fig. 6a represents the diffraction pattern of the selected area where both a sample crystal and a large number of fine crystals of magnesium oxide are involved. The Miller indices corresponding to these spots and rings are indicated in Fig. 6b. From this result it is ascertained that the direction of the electron beam in this case was parallel to the *c* axis of the crystal.

Fig. 4b represents the diffraction pattern of the selected crystal shown in Fig. 4a which shows the electron micrograph of the same sample as the one in Fig. 2b. Fig. 5a represents the electron micrograph of the same sample as the one shown in Fig. 2a, and Fig. 5c shows the diffraction pattern of the selected crystal shown in Fig. 5a. Fig. 5b was taken at a current of the intermediate lens which was a little larger than in the case of Fig. 5c. Comparing these three photographs in Fig. 5 with each other, one can easily understand the relation between the orientation of the particle shown in the electron micrograph and that of the same particle in the diffraction pattern. From the fact that the patterns shown in Figs. 4b and 5c coincide with the N-pattern appearing in Fig. 6a, it is revealed that the nearly flat surfaces of these thin ellipsoidal crystals are parallel to the (001) plane. The direction of the largest

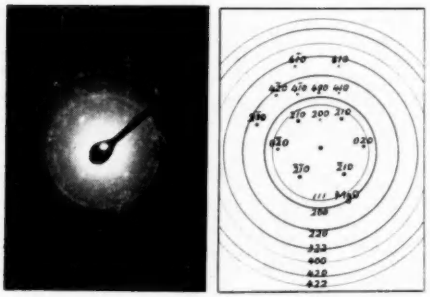

a b

Fig. 6. Diffraction pattern of a selected area where a sample crystal and MgO smoke are mounted together.

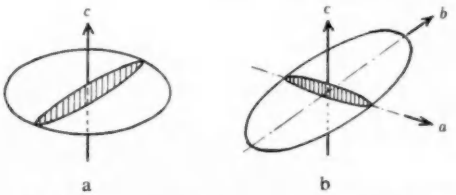

a b

Fig. 7. Shapes and crytsallographic axes of ellipsoidal crystals obtained from solutions containing sodium citrate. Shaded parts indicate the cross sections.

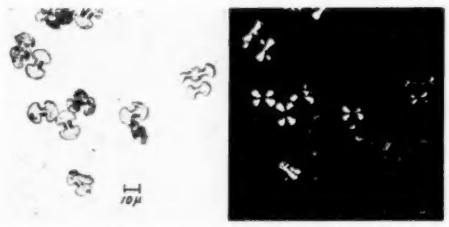

a b

Fig. 8. Crystals grown from a solution containing EDTA. (0.013 M $SrCl_2$, 0.05 M K_2SO_4, 0.025 M EDTA.)

a: with lower nicol only
b: with crossed nicols

diameter of the crystals shown in Fig. 5a or 2a coincides with that of *b* axis. The axial directions of these crystals are illustrated in Fig. 7.

Effect of EDTA.—The crystal habit of strontium sulfate was significantly influenced by EDTA, and it was found that spherulitic aggregates were obtained from a solution containing a relatively large amount of EDTA. One of the remarkable examples is shown in Fig. 8. These photographs were taken with a polarizing microscope with lower nicol only (a) and with the crossed nicols (b). From these photographs, the crystals are seen to be nearly two-dimentional spherulites.

Effect of Condensed Phosphates.—The effects of sodium triphosphate (STP) and sodium hexametaphosphate (SHMP) were examined at 25°C. A quite minute amount of these phosphates exerted a great influence on the deposition rate and the crystal habit.

The relation between the composition of the solution and the habit of the crystals obtained in the presence of STP are illustrated in Figs. 9 and 10. Small circles in Fig. 9 indicate the initial concentrations of the three components, strontium chloride, potassium sulfate and STP, the ionic product $[Sr^{2+}][SO_4^{2-}]$ being fixed at 0.001 M^2. After examining many solutions having various compositions plotted in the figure, the whole area of the diagram can be divided roughly into six regions A, B,……F. The characteristic behavior of the solution falling in each of these regions is described as follows.

Region A.—The effect of STP is insignificant on both the deposition rate and the crystal habit.

Region B.—Deposition is retarded noticeably and crystalline aggregates having irregular shapes make their appearance among remarkably modified single crystals (Fig. 10a).

Region C.—Retardation of the deposition becomes more significant, and a relatively small number of larger aggregates having irregular shapes (*primary product*) appear in the earlier stage of the process, and later the solution becomes intensely turbid with the deposition of fine single crystals (*secondary product*). Fig. 10b illustrates the primary product.

Region D.—Crystal deposition is retarded as well, and crystallization occurs stepwise as in Region C, but the primary product is composed of nearly spherical aggregates as shown in Fig. 10c.

Region E.—Spontaneous crystallization is inhibited for a long period of time. However, if the solution was seeded with the crystals obtained from a solution falling in Region D, the seed crystals grow up to larger spheres. The secondary fine crystals also are deposited later.

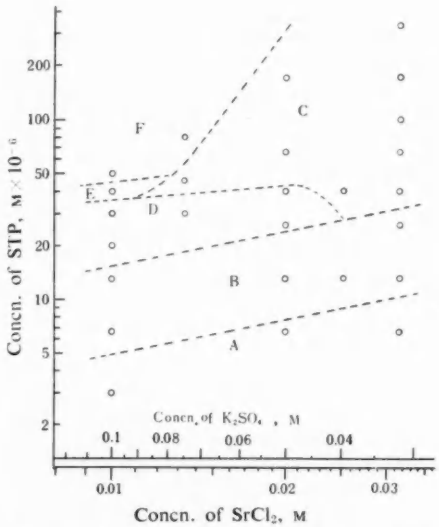

Fig. 9. Composition diagram of $SrCl_2$–K_2SO_4–STP–H_2O system.
$[Sr^{2+}][SO_4^{2-}] = 0.001$ M^2

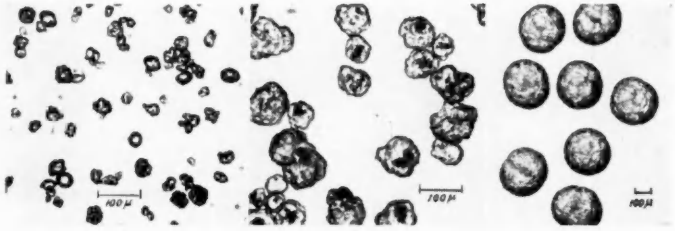

Fig. 10. Crystals grown from solutions containing STP.
a: 0.01 M $SrCl_2$, 0.1 M K_2SO_4, 1.3×10^{-5} M STP (Region B)
b: 0.032 M $SrCl_2$, 0.032 M K_2SO_4, 6.3×10^{-5} M STP (Region C)
c: 0.01 M $SrCl_2$, 0.1 M K_2SO_4, 3.0×10^{-5} M STP (Region D)

Region F.—Both spontaneous crystallization and the growth of the seed added are inhibited almost completely.

As the present author was interested in the preparation of spherical crystals, the favorable compositions of the solutions were inquired into for the purpose of examining this process, and it was found that there were the following restrictions on the selection of available compositions. (a) The concentration of STP must be high enough to cause marked habit modification, though there is an upper limit above which no crystallization occurs. (b) The favorable concentration of strontium sulfate is limited to a certain narrow range; below this range crystallization is prevented by so small an amount of STP that the habit-modifying effect does not come into question, while above this range it is impossible to maintain the concentration of STP of sufficiently large value because of the precipitation of sparingly soluble strontium triphosphate. It may be concluded, therefore, that the solution containing a large excess of sulfate ion and a sufficient amount of STP should be recommended for the preparation of well-formed spherical crystals.

Fig. 11, which shows the splinters obtained by crushing the spherical crystal between a pair of microscope slides, makes it clear that the spherical crystal is a kind of spherulite. The arrangement of crystallites can be visualized from microscopic observation of a thin section of the spherulite. Fig. 12a shows a section of a spherulite grown by treating a seed spherulite several times successively with newly prepared solutions of the composition falling in Region E. Fig. 12b illustrates the central portion of the same section in a larger magnification. Fig. 12c shows a micrograph taken with the crossed nicols.

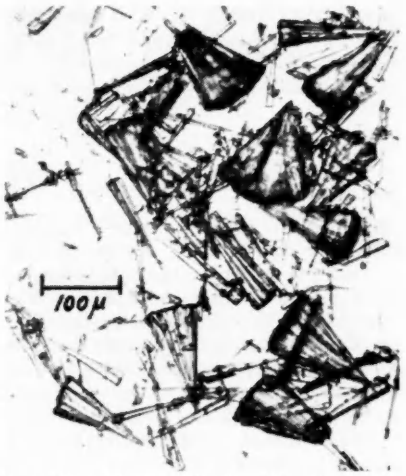

Fig. 11. Splinters of spherulite shown in Fig. 10c.

By certain X-ray examination, it was ascertained that the spherulite was constructed of needle- or wedge-shaped crystallites, each of which was elongated in the direction of *c* axis. The X-ray study was reported in another paper[7].

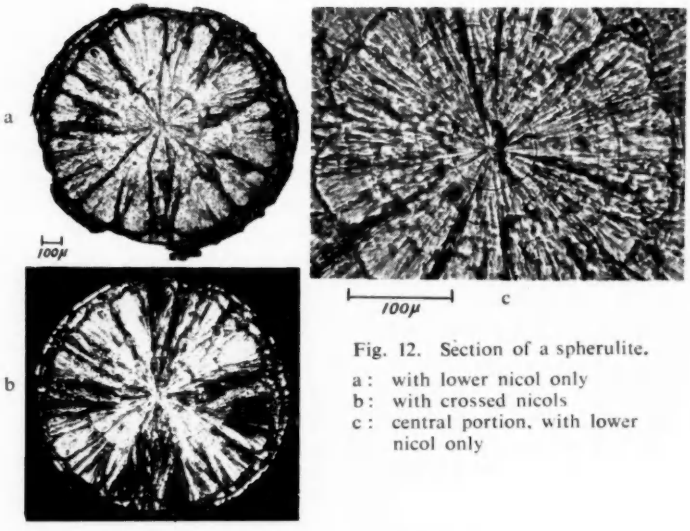

Fig. 12. Section of a spherulite.
a: with lower nicol only
b: with crossed nicols
c: central portion, with lower nicol only

7) Y. Takano and S. Otani, *J. Sci. Hiroshima Univ., Ser. A*, 23, 109 (1959).

The effect of SHMP was also significant and similar to that of STP, and spherulite was obtained from solutions containing a large excess of sulfate and an appropriate amount of SHMP in its concentration range $(3\sim6)\times10^{-5}$ M.

Discussion

Lambert and Hume-Rothery[8] studied the crystal habit of strontium sulfate precipitated by mixing the strontium chloride solution with sulfuric acid at various concentrations and temperatures. They also investigated the effect of various foreign ions on the precipitation rate, but did not mention the effect on the habit modification. The crystal habits of their products are somewhat different from what was noticed in the present experiments. This discrepancy may be attributed to the difference in the composition of solutions; particularly the difference in acidity may play a dominant role.

From many experimental evidences which have been reported and those of the present work, it is known that the effect of a foreign substance on the crystal habit is very complicated. For example, the citrate ion caused the formation of spherical crystals of barium sulfate[5] on the one hand, and of nearly disk-shaped single crystals of strontium sulfate on the other hand. Another example is the case of spindle-shaped crystals of barium sulfate obtained by Takiyama[9] in the presence of EDTA, which, in the case of strontium sulfate, caused the formation of nearly two-dimensional spherulites.

It is self-evident that the shape of a crystal depends on the relative growth rate in one direction to that in another direction. The growth rate may be affected by the adsorption of foreign substances on crystal faces. According to the peculiarity of each crystal face, the nature and the degree of adsorption may be varied from face to face. Thus a peculiar habit modification might be interpreted by the relation between the crystal structure of the substance to be crystallized and the molecular or ionic structure of the foreign substance added.

The effect of viscosity itself on the crystal habit seems to be insignificant from the experimental results obtained with glycerol or PVA. Referring to the evidence that spherulite can be obtained from ordinary solutions in the presence of a certain impurity, the adsorption, but not the high viscosity, may be the dominant factor for the spherulitic growth. Morse and others' results[3] that the gelatinous medium favored the spherulitic growth may also be attributed to the adsorption of the gelatin itself or of some other impurities possibly involved in it. The mechanism of the spherulitic growth will be discussed in detail in the following paper.

Summary

The effect of various impurities on the crystal habit of strontium sulfate were investigated. Solutions containing citrate ion produced a nearly disk-shaped single crystal whose nearly flat surface was parallel to the (001) plane. Nearly two-dimensional spherulite is obtainable from a solution containing EDTA. A minute amount of sodium triphosphate or sodium hexametaphosphate caused the deposition of a relatively large spherulite having a spherical form, which is composed of numerous needle- or wedge-shaped crystallites elongated in the direction of *c* axis. The habit-modifying action of impurities is discussed in detail.

The author wishes to express his sincere thanks to Professor M. Miura of Hiroshima University for his kind guidance and encouragement throughout this work, and to Professor T. Fujiwara of Hiroshima University for his helpful advice. The author is also indebted to Professor T. Sasaki of Tokyo Metropolitan University, Professor M. Shinagawa of Hiroshima University and Dr. M. Kobayashi of Kobe University for their interest in this work and their kindness in furnishing him with various refined condensed phosphates.

Department of Chemistry
Faculty of Science
Hiroshima University
Hiroshima

8) B. Lambert and W. Hume-Rothery, *J. Chem. Soc.*, 1926, 2937.
9) K. Takiyama, This Bulletin, **31**, 950 (1958).

Crystal Habit Modification of Strontium Sulfate. II. Characteristic Effect of Sodium Triphosphate on Crystallization and Mechanism of Spherulite Formation

By Sadaichi OTANI

(Received March 23, 1960)

In the preceding paper[1] it was reported that the crystal habit of strontium sulfate was remarkably affected by a quite minute amount of sodium triphosphate (STP) added to the solution from which the crystals were deposited, and that the crystallization was retarded and finally came to be practically inhibited, as the amount of STP was increased, provided the concentration of the strontium ion was not over a given value.

Concerning the similar effect of condensed phosphates on the precipitation of various inorganic salts, many works have been published, mostly from the industrial point of view. For example, the effect of metaphosphates on the deposition of calcium carbonate was studied by several workers[2], and the action of triphosphate, metaphosphate, or Quadrafos on the precipitation of gypsum by Burcik[3]. Because of the minuteness of the amount of the phosphates effective in these cases, the prevention of the precipitation could not be ascribed to the sequestration of the component cations by complex formation. Some of the above authors, therefore, attributed the action of these phosphates to the adsorption of them on the crystal nuclei or the growing crystals.

However, the experimental evidences hitherto reported seem to be still insufficient for the reasonable interpretation of the mechanism of these phenomena, and concerning the effect of pure STP on the deposition of strontium sulfate, no work seems to be available in the literature. For the purpose of studying systematically the peculiar effect of STP on the deposition and the crystal habit of strontium sulfate, measurements were made in the present work on the following: (a) deposition rate and (b) dissolution rate of strontium sulfate at various STP contents, (c) surface adsorption of STP on strontium sulfate crystals, and (d) coprecipitation of STP with strontium sulfate. From the results of these experiments, the mechanisms of the habit modification, of the prevention of crystallization and of the spherulite formation will be discussed.

Experimental and Results

Inhibition of Crystallization by STP.—To estimate quantitatively the retardation of the crystal deposition by STP, the rate of crystallization was measured by a conductance method. The reagents used were the same as those in the preceding work[1]. The solution to be examined was prepared

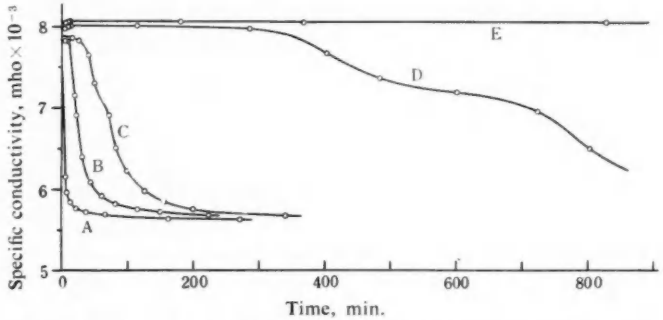

Fig. 1. Conductivity—time curves of 0.02 M $SrSO_4$ solutions containing (A) no STP, (B) 1.0×10^{-5} M STP, (C) 1.5×10^{-5} M STP, (D) 2.0×10^{-5} M STP and (E) 3.0×10^{-5} M STP.

1) S. Otani, This Bulletin, 33, 1543 (1960).
2) L. Rosenstein, U. S. Pat., 2038316 (1936); G. B. Hatch and O. Rice, *Ind. Eng. Chem.*, 31, 51 (1939); R. F. Reitemeier and T. F. Buehrer, *J. Phys. Chem.*, 44, 535, 552 (1940).
3) E. J. Burcik, *Producers Monthly*, 19, No. 1, p. 42 (1954).

in a conductivity cell by mixing equal volumes of potassium sulfate and strontium chloride solutions of equivalent concentration, the latter containing an appropriate amount of STP. Being continuously shaken, the solution was put to the test as to its conductivity at intervals. The results of five runs with different concentrations of STP are illustrated in Fig. 1. The initial concentration of strontium sulfate was fixed at 0.02 M in all cases.

This figure shows how the deposition rate is reduced by a minute amount of STP. Indeed, when the initial concentration of STP amounted to 3.0×10^{-5} M, no change could be detected for a period more than 70 hr. Even if some fine crystals of strontium sulfate were added to this solution, its conductivity remained unchanged for a long period. These facts show that not only the spontaneous crystallization but also the growth of the crystals added was inhibited by STP at this concentration.

The irregularities seen on curves C and D are caused by the stepwise deposition of crystals of two quite different types, one being spherulite and the other fine single crsytals. The comparatively steep decrease in conductivity in the earlier stage corresponds to the growth of the spherulites and that in the later stage to the deposition of fine single crystals.

Effect of STP on Dissolution. — The rates of dissolution of strontium sulfate into water and dilute STP solutions of various concentrations were measured by the conductance method at 25°C. The conductivity of the solvent was first measured with a glass-stoppered conductivity cell with 30.0 ml. of the solvent. Then 1.00 ml. of a solution containing 1.00 mg. of strontium sulfate was pipetted into the cell, and the resultant change in conductivity was traced, the solution being shaken continuously. The result is illustrated graphically in Fig. 2.

Adsorption of STP on Strontium Sulfate.—The adsorption of STP on strontium sulfate was measured by a radio tracer method with the aid of STP labeled with ^{32}P.

The labeled STP was prepared, referring to the result of Edward and Herzog[4], by a thermal treatment of the orthophosphate mixture to which radioactive orthophosphate had been added. The product was then recrystallized from an aqueous solution by adding ethanol, and purity was found to be satisfactory for the purpose from a paper chromatographic test. The strontium sulfate used as the adsorbent was precipitated from an equivalent mixture of strontium chloride and potassium sulfate solutions, washed thoroughly with distilled water by decantation, and dried in an oven at 150°C. The particle size of strontium sulfate thus obtained was 3~5 μ in diameter.

The adsorbed amount of STP was determined by shaking 30.0 ml. of its solution of a known concentration with 0.1000 g. of the adsorbent for an appropriate period and by measuring the radioactivity of the solution before and after treatment. To avoid the dissolution of the adsorbent during the treatment, the STP solution used was prepared by diluting a measured small volume, say 0.1~1 ml., of a rather concentrated stock solution with a given large volume, say 100~500 ml., of a saturated solution of strontium sulfate.

The adsorption rate was estimated by measuring the radioactivity of the solution under investigation at intervals during the shaking. One of the results obtained at 1.0×10^{-5} M of the initial STP concentration at 30°C is shown in Fig. 3, in which the radioactivity is plotted against the time of shaking. The adsorption isotherm obtained at 30.0°C is also illustrated graphically in Fig. 4. It is ascertained

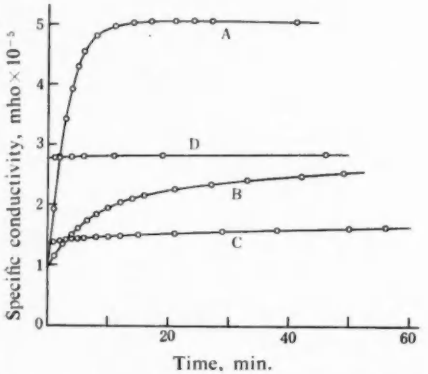

Fig. 2. Conductivity—time curves, showing the dissolution rate of $SrSO_4$ into water and STP solutions.
A: H_2O, B: 0.20×10^{-5} M STP, C: 1.0×10^{-5} M STP, D: 4.0×10^{-5} M STP

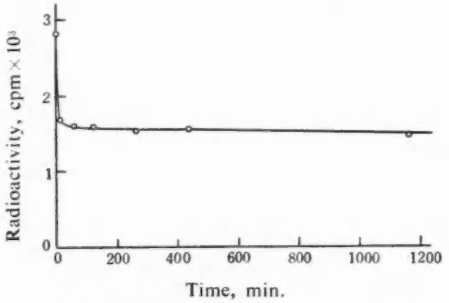

Fig. 3. Radioactivity—time curve, showing adsorption rate of STP on $SrSO_4$ at 30°C.

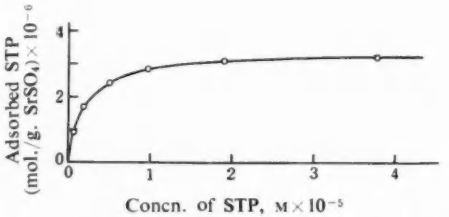

Fig. 4. Adsorption isotherm of STP on $SrSO_4$ at 30.0°C.

4) J. W. Edwards and A. H. Herzog, *J. Am. Chem. Soc.*, 79, 3647 (1957).

that this isotherm is in good agreement with Langmuir's equation.

Coprecipitation of STP with Strontium Sulfate. —The coprecipitation was studied with the aid of both the conductance method and the radiotracer technique. The procedures were as follows. Appropriate volumes of strontium chloride, labeled STP, and potassium sulfate solutions, all at 25°C, were pipetted into the conductivity cell in the order just mentioned, and shaken. The decrease in the concentration of strontium sulfate in the solution was traced by conductivity measurement. The radioactivity of the supernatant liquid was measured at intervals during precipitation to trace the decrease in STP concentration. Thus, both amounts of the strontium sulfate and STP precipitated within any desired period were determined simultaneously. One of the results obtained at 25°C is shown with curve A in Fig. 5. This curve illustrates how the amount of coprecipitated STP increases as the crystallization proceeds in a solution where the initial concentrations are 0.02 M with respect to both strontium chloride and potassium sulfate and 1.50×10^{-5} M with respect to STP. In this experiment the solution was constantly shaken during crystallization.

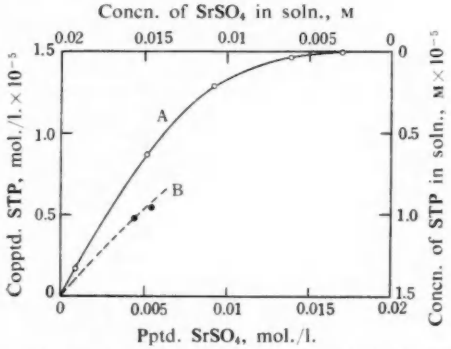

Fig. 5. Coprecipitation of STP with $SrSO_4$.
A: with continuous shaking
B: without shaking

A few measurements were made when solutions were kept unstirred during crystallization. In this case, however, the above-mentioned procedures could not be employed to trace the change in the amount coprecipitated, because the growing crystals were all sedimented at the bottom of the container, thus making the solution inhomogeneous. Therefore, the crystals deposited were filtered off at an appropriate time in the course of crystallization, and weighed after drying. The amount of coprecipitated STP was determined from the radioactivity of the filtrate. The two solid circles in Fig. 5 indicate the values obtained from two runs with solutions having the same composition as that mentioned above.

The mole ratios of STP to strontium sulfate both in the precipitate and the solution were calculated from the data given on curve A in Fig. 5, and are plotted in Fig. 6. The upper curve

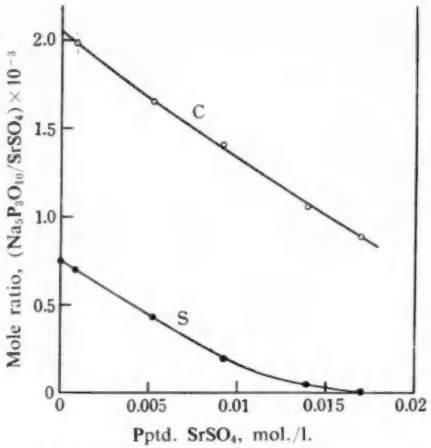

Fig. 6. Mole ratio of STP to $SrSO_4$ during crystallization.
C: in crystal S: in solution

indicates the value in the precipitate and the lower that in the solution.

Discussion

From the measurements on the crystallization rate, a striking effect of STP was well noticed. As is seen in Fig. 1, an extremely small amount of STP (3.0×10^{-5} M in its concentration) is quite sufficient to prevent the deposition of crystals from the 0.02 M solution of strontium sulfate. This fact can not be attributed to the complex formation between strontium and triphosphate, in view of the extremely small mole ratio of triphosphate to strontium, namely, 1 : 670.

From the measurements on the dissolution rate, another striking effect of STP was observed. As is seen in Fig. 2, the dissolution of strontium sulfate was retarded by STP even when its concentration was as small as the one in the above-mentioned case. This evidence may possibly be attributed to the adsorption of STP on the crystal surface, because the dissolution can not be hindered directly by the STP existing in the bulk of the solution.

From the measurement of adsorption, the amount of STP adsorbed on strontium sulfate was found to be up to saturation at an extremely low concentration, namely $(2\sim4)\times10^{-5}$ M. Comparison of Fig. 4 with Figs. 1 and 2 reveals the fact that the concentration range within which the amount of adsorbed STP tends to be saturated agrees roughly with the one within which the retardation of crystallization and of dissolution becomes significant. The retardation or prevention of crystallization may accordingly be attributed to the adsorption of STP on the

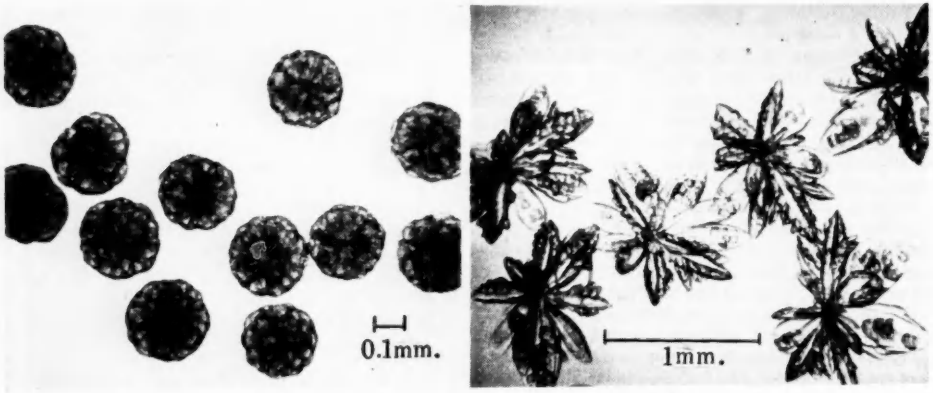

a b

Fig. 7. Products grown from solutions of $SrSO_4$(0.02 M) containg STP (1.5×10^{-5} M).
a: with continuous shaking. b: without shaking

crystal nuclei or the growing crystals, and the following mechanism may be considered. The triphosphate ion may be adsorbed preferentially at the active centers of growth on the crystal nuclei or the growing faces of crystals, and the adsorbed triphosphate ion may act as a poison to the layer growth of the crystal faces. The larger the concentration of STP is, the more the active centers will be poisoned and the slower the growth rate will become, and finally, when the concentration of STP exceeds a given value, namely $(3\sim4)\times10^{-5}$ M, at which the adsorption comes to be nearly saturated, all the active centers will be poisoned, and crystallization may be completely inhibited.

Strong interaction between STP and strontium sulfate may be reasonably recognized also from the measurements on coprecipitation. Fig. 6 shows that STP is coprecipitated almost completely with strontium sulfate, the mole ratio of STP to strontium sulfate in the crystal being several times as great as that in the solution.

As is seen from Figs. 5 and 7, agitation of the solution during crystallization has a considerable influence not only on the amount of coprecipitation but also on the crystal habit. Fig. 7a shows the spherulite obtained from a solution with continous shaking (corresponding to curve A in Fig. 5), and Fig. 7b the star-like aggregate from another solution of the same initial composition without shaking (corresponding to curve B in Fig. 5). The difference between the habits of these crystals may be due to the difference in the amount of coprecipitated STP, which can be possibly traced back to the difference in the mode of supply—one by agitation and the other merely by diffusion—of STP from the bulk on the crystal interface.

As already reported[5], the component crystallite of the spherulite or the star-like aggregate is elongated in the direction of c axis. This fact means that STP makes the growth rate predominant in the direction of c axis. From the above-mentioned poisoning action of the adsorbed STP upon the regular layer growth, it may be concluded that the adsorption of STP is at its minimum on the (001) face as compared with all the other faces, and accordingly the layer growth on this face is least retarded.

Next, the mechanism of spherulite formation will be considered. If radiating fibrillar growth starts from a common center in all directions with an equal growth rate, the growing aggregate will always be spherical. For this to occur, it is necessary to postulate the existence of a cluster of nuclei which has the ability to emit fibrillar crystallites in all directions. In practice, however, the formation of such a cluster of nuclei seems to be improbable, and it may be more acceptable to assume the branching of growing crystallite.

Keller and Waring[6] assumed a periodic branching of fibrils occurring at constant distances with a constant acute angle to explain the "sheaf" formation in the course of spherulitic growth of synthetic high polymers. They proved that the periodicity of branching is a necessary condition for the formation of Popoff's "Zweiblatt"[7] or Morse and Donnay's "sheaf"[8]. Keller and Waring's illustration of

5) Y. Takano and S. Otani, *J. Sci. Hiroshima Univ., Ser. A*, **23**, 109 (1959).
6) A. Keller and J. R. S. Waring, *J. Polymer Sci.*, **17**, 447 (1955).
7) B. Popoff, *Latv. Farm. Zurn.*, **1934**, 1.
8) H. W. Morse and J. D. H. Donnay, *Am. Mineralogist*, **21**, 392 (1936).

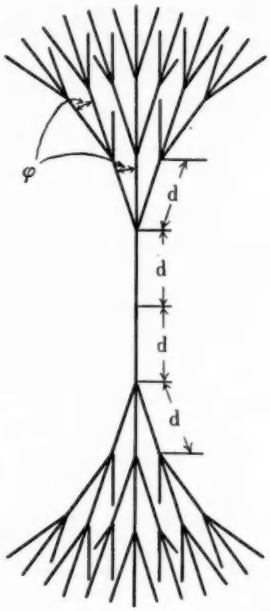

Fig. 8. Schematic diagram showing the sheaf formation through periodic branchings (after Keller and Waring).

the sheaf formation through the periodic branching is reproduced in Fig. 8.

In the present case, the branching of crystallite were recognized from a microscopic observation of the growth process. Fig. 9 shows the development of a seed in a solution containing an appropriate amount of STP. Fig. 9a shows the seed which is one of the splinters obtained by crushing a well-developed spherulite, and Fig. 9b and 9c illustrate the successive stages of its growth. By crushing the product (Fig. 9c), a large number of wedge-shaped smaller crystallites resulted. These are shown in Fig. 9d. By comparing these photographs with each other, it may be seen that radiating crystallization started everywhere on the surface of the seed. This fact may certify that branching of crystallite is induced by STP.

No indication of sheaf formation was observed either in this experiment or in many others mentioned before. However, the formation of spherulite can be interpreted on the basis of the above-mentioned evidence that, under the influence of STP, branchings are accompanied by the growth of strontium sulfate crystal and its growth rate is highly predominant in the direction of *c* axis. Under this condition, the crystal growth must proceed as follows. Starting from a single nucleus, an aggregate crystallites will be formed as a result of successive branchings during the growth, and the number of the crystallites will increase acceleratedly as the growth proceeds. On the other hand, the growth of each crystallite must inevitably be restricted by the steric hindrance of the adjacent ones, and, as a result, only those crystallites of which the direction of the fastest growth happened to coincide nearly with the radial direction may survive. Thus, sooner or later, the aggregate changes to be constructed of a great number of crystallites directed radially, at least near the periphery. Hereafter, the

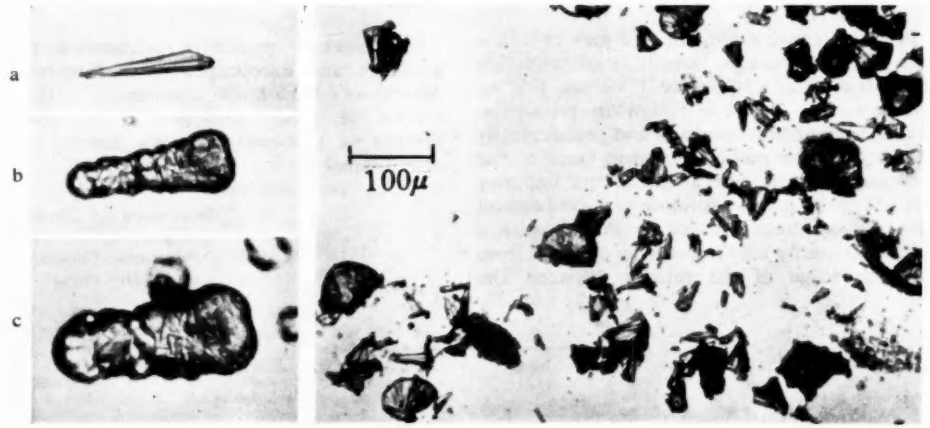

Fig. 9. Spherulitic growth from a seed.
a: seed, b: after 48 min., c: after 190 min., d: splinters obtained by crushing c

shape of the aggregate must gradually approach a sphere, because the growth rate is uniform in all directions in the radial growth.

The above-mentioned concept may explain why such a star-like aggregate as that shown in Fig. 7b is produced, when the solution is kept unstirred. For a moment just after a crystal nucleus begins to grow, it may be supplied with enough STP to cause frequent branchings regardless of the solution being stirred or not. However, as the growth proceeds, the concentration of STP at the immediate vicinity of the growing aggregate may be reduced rapidly because of the consumption of STP due to the selective adsorption (cf. Fig. 6). If the solution is not stirred, STP is supplied merely by diffusion, and hence the branching may occurr less frequently. Accordingly the resultant aggregate, being composed of a relatively small number of radiated crystallites, gives a star-like appearance.

As to the mechanism of the branching of crystallite, Keller and Waring[6] mentioned twinning and rupture of distorted crystal as possible causes. In the present work, branching is induced by STP, and may be attributed to the adsorption of the latter onto the crystallite. The mechanism of branching may be considered as follows. The adsorbed triphosphate ion could hardly enter into the regular crystal lattice of strontium sulfate because of the unfitness of the size and ionic charge. The crystal lattice may be distorted in the vicinity of the adsorbed triphosphate ion. As the amount of adsorbed triphosphate increases, many ruptures of lattice may appear on the crystal faces owing to the distortions of the lattice. These ruptures may cause branchings of crystallite.

From the above discussion, we may conclude that we shall have a possibility of preparing spherulites of any substance, if we can find an impurity that has the following properties. (1) The impurity is intensely and preferentially adsorbed by the particular crystal faces of the substance in question and (2) the impurity can not make a solid solution or mixed crystal with the substance. A clue to finding such a suitable impurity may possibly be obtained from the knowledge of the relation between the molecular or ionic structure of the impurity and the crystal structure of the substance in question. For the preparation of a spherulite of an inorganic salt, there may be found some suitable impurities among those polyatomic complex ions which have a strong affinity to either of the component ions of the salt.

Summary

1) The peculiar effect of sodium triphosphate (STP) on the crystallization and the crystal habit of strontium sulfate was studied systematically by measuring (a) the deposition rate and (b) the dissolution rate of strontium sulfate at various STP concentrations, (c) the surface adsorption of STP on strontium sulfate crystal, and (d) the coprecipitation of these salts.

2) The inhibiting action of STP on the deposition and dissolution of strontium sulfate is attributed to the adsorption of STP.

3) The fact that STP makes the growth rate predominant in the direction of *c* axis of strontium sulfate is ascribed to the small adsorption of STP on the (001) faces compared with that on the other faces.

4) The occurrence of the branching of crystallite was ascertained experimentally, and attributed to the ruptures appearing on the crystal faces as a result of the unfitness in the size and ionic charge of the adsorbed triphosphate.

5) The formation process of the spherulite can be interpreted from the fact that the frequent branchings are accompanied by the nearly one-dimentional growth of crystallite.

6) Possibilities of preparing spherulites from other substances are discussed.

The author gratefully acknowledges the guidance and encouragement of Professor M. Miura of Hiroshima University. He also wishes to thank Professor T. Ichikawa of Hiroshima University for his helpful advice and discussions.

Department of Chemistry
Faculty of Science
Hiroshima University
Hiroshima

The Structure of the Yellow Pigment from Drosophila

By Saburo NAWA

(Received May 9, 1960)

It has been known that the wild type eye-color of *Drosophila melanogaster* is due to the presence of two pigments, the red and the brown. It is of particular interest to study the chemistry of the eye pigments in order to clarify the relationship between genes and biochemical processes, since the various genetic interrelationships are well established in the group of eye-color mutants of *Drosophila*. Hadorn and Mitchell[1] have mentioned for the first time the presence of a yellow pigment, which was later named Sepiapterin by Ziegler-Günder and Hadorn[2], in *Drosophila* by a simple chromatographic technique and that the mutant *sepia* contained much greater amounts of Sepiapterin in comparison with the wild type. In 1954 Nawa and Taira[3] have reported that the yellow pigment, Xanthopterin-B[4], found in the epidermis of the mutant *lemon* of silkworm is a derivative of 2-amino-4-hydroxypteridine and is indistinguishable from Sepiapterin. In the same year Forrest and Mitchell[5] have isolated Sepiapterin as a crystalline form and proposed the structure I for it, although I was later modified to structure II by Forrest et al.[6] In the light of some new experiments on Sepiapterin, however, its structure will be discussed in this paper. And we now wish to propose the structure III for Sepiapterin on the basis of the following findings.

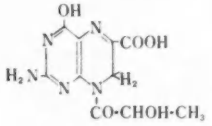

I

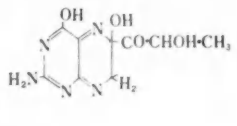

II

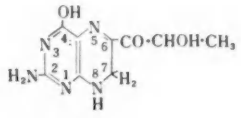

III

Experimental

Isolation of Sepiapterin. — One handred grams (wet) of flies (*D. melanogaster*, mutant *sepia*) were homogenized in a Waring Blender in 30% ethanol (500 ml.). The suspension was heated at 80°C for 5 min. and allowed to stand overnight in an ice box. The reddish yellow supernatant obtained by centrifugation was concentrated in vacuo to a small volume (about 50 ml.) and then spread on 8 sheets (40×40 cm.) of heavy filter paper (Toyo Roshi Co. Ltd., No. 26). These were then chromatographed with water. The yellow band was cut off and eluted with water. The eluate was then concentrated and chromatographed again on the heavy filter paper (4 sheets) with a mixture of *n*-butanol, acetic acid and water (4 : 1 : 1). After allowing the chromatogram to dry, the appropriate band corresponding to Sepiapterin was eluted with water. The concentrated solution was applied to a column (6×40 cm.) of cellulose powder and developed with water. The fraction of yellow pigment was collected and evaporated to dryness in vacuo. The residue was dissolved in hot water (8 ml.) and allowed to stand overnight in an ice box, when the product (13 mg.) crystallized as orange needles. All the above procedure was carried out in the dark to avoid photolysis. Eight handred gram of flies gave 105 mg. of crystals in repetition of this procedure.

Found: C, 45.9; H, 4.5; N, 29.2. Calcd. for $C_9H_{11}N_5O_3$: C, 45.6; H, 4.7; N, 29.5%.

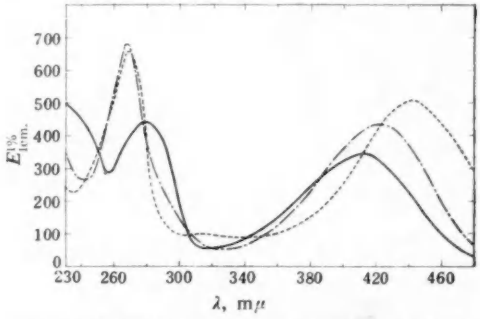

Fig. 1. The ultraviolet absorption of Sepiapterin: ——, at pH 1.0; — — —, at pH 5.0; and – – –, at pH 11.0.

1) E. Hadorn and H. K. Mitchell, *Proc. Nat. Acad. Sci. U. S.*, **37**, 650 (1951).
2) Ziegler-Günder and E. Hadorn, *Z. Vererbungslehre*, **89**, 235 (1958).
3) S. Nawa and T. Taira, *Proc. Japan Acad.*, **30**, 632 (1954).
4) Y. Hirata, K. Nakanishi and H. Kikkawa, This Bulletin, **23**, 76 (1950).
5) H. S. Forrest and H. K. Mitchell, *J. Am. Chem. Soc.*, **76**, 5656, 5658 (1954).
6) H. S. Forrest, D. Hatfield and C. V. Baalen, *Nature*, **183**, 1269 (1959).

The ultraviolet absorption spectra are shown in Fig. 1. (At pH 1, λ_{max} 281, 410 mμ, $E^{1\%}_{1cm.}$ 440, 340. At pH 11, λ_{max} 268, 440 mμ, $E^{1\%}_{1cm.}$ 665, 510.)

Air Oxidation in Borax Solution. — Sepiapterin (25 mg.) was dissolved in 5% borax (50 ml.) and shaken at 35°C for 5 hr. in the dark to avoid photodecomposition, when the yellow color of the solution gradually disappeared and the yellow fluorescence changed to green.

a) Estimation of 7,8-Dihydroxanthopterin (IV). —When this reaction mixture was allowed to stand overnight in an ice box, the product (14.6 mg.) precipitated. The compound was recrystallized from 0.25 N sulfuric acid as the sulfate (10.7 mg.).

Found: C, 30.0; H, 3.9; N, 29.2. Calcd. for $C_6H_7N_5O_2 \cdot 1/2H_2SO_4 \cdot H_2O$: C, 29.0; H, 4.0; N, 28.2%.

The ultraviolet absorption curves as shown in Fig. 2a. (At pH 1, λ_{max} 276, 305 mμ, $E^{1\%}_{1cm.}$, 535, 310. At pH 11, λ_{max} 276 mμ, $E^{1\%}_{1cm.}$ 515.) This compound was readily oxidized to xanthopterin (V) with manganese dioxide in alkaline solution. In neutral solution, moreover, the compound was oxidized to V accompanied by consumption of one mole of iodine. These properties, absorption spectra and R_f values of the compound are perfectly identical with those of the authentic 7,8-dihydroxanthopterin (IV)[7-9]. Some R_f values compared with those for authentic IV (in parentheses) are: *n*-propanol, 1% ammonia (2:1), 0.16 (0.16); 2% K_2HPO_4, 0.32 (0.32), 3% sodium citrate, 0.35 (0.35). The absorption curves of IV obtained from the catalytic hydrogenation of xanthopterin (Nutritional Biochemicals Co., U. S. A.) are shown in Fig. 2b.

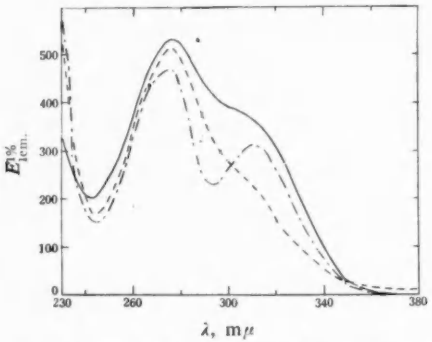

Fig. 2a. The ultraviolet absorption of the product from decomposition of Sepiapterin: ——, at pH 1.0; — — —, at pH 5.0; and - - -, at pH 11.0.

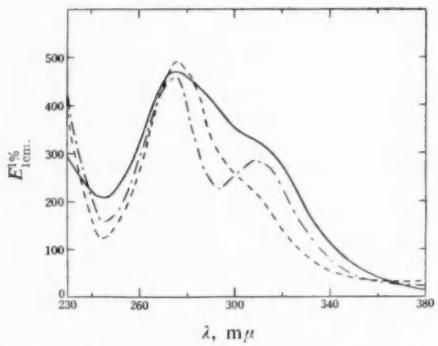

Fig. 2b. The ultraviolet absorption of 7,8-dihydroxanthopterin (IV) obtained from catalytic reduction of xanthopterin: ——, at pH 1.0; — — —, at pH 5.0; and - - -, at pH 11.0.

b) Characterization of Lactic Acid. — The supernatant from the reaction mixture mentioned above showed the color reaction[10] characteristic of lactic acid. The supernatant (0.01 ml.) was withdrawn and heated at 100°C for 5 min. with 3 ml. of sulfuric acid and 0.05 ml. of 2% $CuSO_4$. After cooling,, 0.05 ml. of 1.5% *p*-hydroxydiphenyl reagent was added and allowed to stand at 30°C for 30 min. And then the color developed was estimated at 570 mμ in a Beckman spectrophotometer. From a standard curve obtained from known amounts of lithium lactate, 5 μg. of Sepiapterin (0.01 ml. of the reaction mixture) was estimated to give 1.5 μg. of lactic acid (with a molecular weight of 237, the theory for one mole of lactic acid per mole of Sepiapterin is 1.57 μg.). The remained supernatant was concentrated to a small volume and paper chromatographed in various solvent systems. Some R_f values compared with those for lactic acid (in parentheses) are: *n*-butanol, acetic acid, water (4:1:1), 0.75 (0.75); ethanol,10% ammonia (4:1), 0.77 (0.77); *n*-butanol, pyridine, water (1:1:1), 0.39 (0.39).

c) Relationship of Oxygen Uptake, and IV and Lactic Acid Production. — Sepiapterin (4.7 mg.) was dissolved in 5% borax solution (20 ml.) and each aliquots (2 ml., 0.47 mg.) were shaken in Warburg flasks at 35°C in the dark. At various

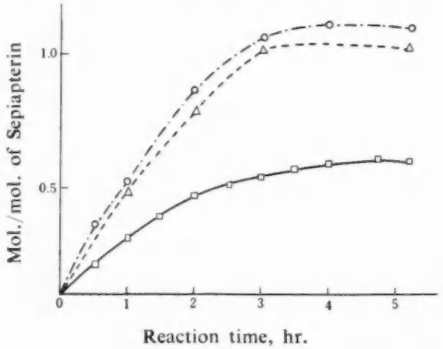

Fig. 3. Air oxidation of Sepiapterin in the presenc of borax: -□-, oxygen consumed; -○-, lactic acid produced; and -△-, 7,8-dihydroxanthopterin produced.

7) B. L. O'Dell, J. M. Vandenbelt, E. S. Bloom and J. J. Pfiffner, *J. Am. Chem. Soc.*, **69**, 250 (1947).
8) W. R. Boon and T. Leigh, *J. Chem. Soc.*, **1951** 1497.
9) G. B. Elion and G. H. Hitchings, *J. Am. Chem. Soc.*, **74**, 3877 (1952).
10) S. B. Barker and W. H. Summerson, *J. Biol. Chem.*, **138**, 535 (1941).

time intervals, oxygen uptake was measured, the amounts of IV produced were calculated using the known extinction constant at 310 mμ at pH 7 and the amounts of lactic acid were determined by the procedure described previously. As shown in Fig. 3, the molar ratio of oxygen consumed, and IV and lactic acid produced was 0.5 : 1 : 1 at all reaction intervals. This reaction did not occur in the absence of oxygen. It should be noted that the rate of reaction is variable. Since the reaction is accerelated by addition of small amounts of heavy metal ions and inhibited by chelating agents, it is concluded that the variable rate is due to the presence of metal-ion impurities.

Periodate Oxidation.—A solution of Sepiapterin (2.0 mg.) in 2% sodium bicarbonate (1.2 ml.) was treated with 1% sodium metaperiodate (0.8 ml.) in an ice bath. At various intervals the undestroyed periodate was estimated. Aliquots (0.1 ml.) were withdrawn and quenched in 0.001 N sodium arsenite (1.0 ml.) containing potassium iodide (10 mg.). After 15 min. the samples were titrated with standard potassium iodide-iodine (0.002 N) to a starch end-point. Acetaldehyde was determined by the color development[11] with *p*-hydroxydiphenyl in sulfuric acid. To aliquots (0.01 ml.) was added 0.1% sodium arsenite (0.5 ml.). After 15 min. the solution was treated with sulfuric acid (3 ml.), 2% $CuSO_4$ (0.05 ml.) and 1.5% *p*-hydroxydiphenyl reagent (0.05 ml.) at 30°C for 30 min. The color developed was estimated at 570 mμ. As shown in Fig. 4, the

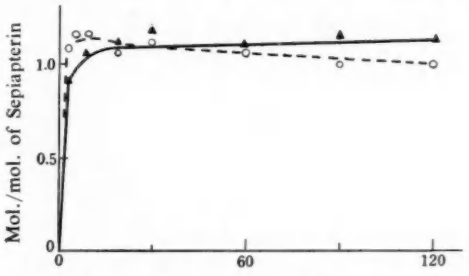

Fig. 4. Periodate oxidation of Sepiapterin: -▲-, periodate consumed; --○--, acetaldehyde produced.

curves of the acetaldehyde production and periodate consumption reached to plateaus as soon as periodate was added to the solution of Sepiapterin. In the reaction the yellow color of the solution rapidly disappeared and the yellow fluorescence changed to green.

2-Amino-4-hydroxy-7, 8-dihydropteridine-6-carboxylic Acid (VI).—To a solution of Sepiapterin (20 mg.) in 2% sodium bicarbonate (12 ml.), 1% sodium metaperiodate (8 ml.) was added. After standing 30 min. at 0°C, the reaction mixture was diluted with cold water (20 ml.), applied immediately to a column (5×40 cm.) of cellulose powder and developed with 0.002% ammonia. During the development of the column, the fluorescent products were separated into two bands, major greenish yellow and minor blue fluorescent. The minor blue fluorescent compound (1.6 mg.) was 2-amino-4-hydroxypteridine-6-carboxylic acid (VII) with identity of ultraviolet absorption and its paper chromatographic behavior. The main greenish yellow fluorescent band was collected and a pale greyish residue (7.4 mg.) was obtained by freeze-drying. For convenience, this compound is henceforth referred to as Compound-A.

Found: C, 40.78; H, 3.21; N, 32.75. Calcd. for $C_7H_7N_5O_3$: C, 40.19; H, 3.37; N, 33.48%.

The ultraviolet absorption spectra are shown in Fig. 5. (At pH 1, λ_{max} 280, 380 mμ. At pH 11,

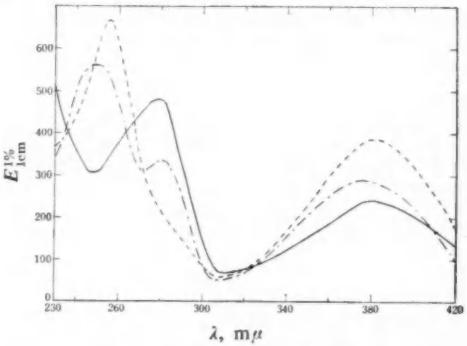

Fig. 5. The ultraviolet absorption of pteridine (VI) obtained from periodate oxidation of Sepiapterin: ——, at pH 1.0; — — — —, at pH 5.0; and - - -, at pH 11.0.

λ_{max} 255, 380 mμ.) Some R_f values compared with those for VII (in brackets) are: *n*-propanol, 1% ammonia (2 : 1), 0.11 (0.14); *n*-butanol, acetic acid, water (4 : 1 : 1), 0.09 (0.14); 3% sodium citrate. 0.37 (0.53); 5% acetic acid, 0.30 (0.47); 2% K_2HPO_4, 0.35 (0.44). Compound-A was comparatively stable to auto-oxidation in neutral solution when stored at 0°C in the dark, but it was readily converted to VII on exposure to light and at that time consumed 0.5 mol. of oxgen. In alkaline solution Compound-A was oxidized into VII with manganese dioxide. In neutral or acidic solution, furthermore, Compound-A consumed 1 mol. of iodine and gave VII. From these results, it is concluded that Compound-A is a dihydro-form of VII, i. e. 2-amino-4-hydroxy-7, 8-dihydropteridine-6-carboxylic acid (VI). This is also confirmed by the following findings.

a) Reduction of Compound-A with Sodium Borohydride.—A solution of Compound-A (0.1 mg.) in 0.01 N acetic acid (10 ml.) was treated with sodium borohydride (1 mg.), when the greenish yellow fluorescence of the solution immediately dissappeared. Aliquots of the reaction mixture were adjusted to various pH and the absorption spectra were recorded as shown in Fig. 6. The curves are characteristic of tetrahydropteridies[7,12,13].

11) R. J. Block and D. Bolling, *J. Biol. Chem.*, **130**, 365 (1939).

12) M. Viscontini and H. R. Weilenmann, *Helv. Chim. Acta.*, **41**, 2170 (1958).

13) S. Kaufman, *J. Biol. Chem.*, **234**, 2677 (1959).

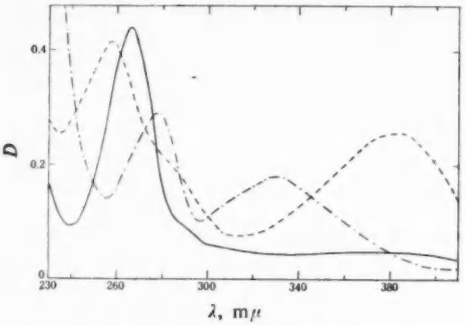

Fig. 6. The absorption of the product resulting from $NaBH_4$ reduction of VI: ——, at pH 1.0; — — —, at pH 5; and – – –, at pH 11.0.

Upon shaking the reaction mixture in air, its fluorescence became blue. Paper chromatography of this solution showed the presence of two blue fluorescent compounds. The major spot was VII and the weaker was 2-amino-4-hydroxypteridine (VIII). Neither VII nor VIII was attacked by $NaBH_4$.

b) Conversion of Compound-A to 2,6-Diamino-4-hydroxypteridine (IX).—A solution of compound-A (0.5 mg.) in 1% ammonia (1 ml.) was heated at 80°C for 30 min. The reaction mixture was applied to a column of cellulose powder and developed with 0.002% ammonia. The main bright green fluorescent band was eluted. The absorption spectra of this eluate in various pH (Fig. 7) correspond to these of 2,6-diamino-4-hydroxypteridine (IX)[14], which were obtained from the catalytic reduction of VIII in dilute ammonia, and the identity of this compound was confirmed by paper chromatographic comparison with the authentic sample. When the compound was incubated with milk xanthine oxidase at pH 8, it was oxidized to a purplish blue

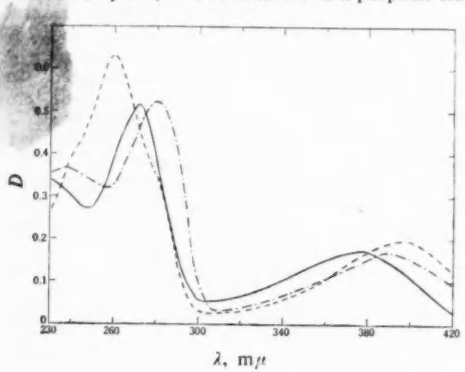

Fig. 7. The absorption of pteridine (IX) obtained from VI by treating with ammonia: ——, at pH 1.0; — — —, at pH 5.0; and – – –, at pH 11.0.

14) C. V. Baalen and H. S. Forrest, *J. Am. Chem. Soc.*, **81**, 1770 (1959).

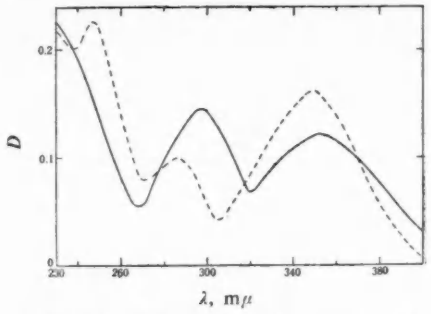

Fig. 8. The absorption of pteridine (X) obtained from IX by treatment with milk xanthine oxidase: ——, at pH 1.0; – – –, at pH 11.0.

fluorescent substance. Its absorption spectra (Fig. 8) resemble those of isoxanthopterin (2-amino-4,7-dihydroxypteridine)[15]. From the evidence[16,17] that milk xanthine oxidase attacks the 7-position of the pteridine skeleton, it is probable that the substance is 2,6-diamino-4,7-dihydroxypteridine(X).

Photodecomposition.—Sepiapterin (0.47 mg., 2.0 μmol.) dissolved in water (2 ml.) was exposed to sunlight in a Warburg flask at 35°C. An oxygen uptake of 50 μl. was observed, when the yellow color of the solution had disappeared. Acetaldehyde (0.086 mg., 1.95 μmol.) was ascertained by the procedure described above. VII (0.39 mg., 1.88 μmol.) was determined using the known optical density for this acid, after separating by paper chromatography.

Discussion

It has been known that both photodecomposition[3,5] and permanganate oxidation[5] of Sepiapterin gave 2-amino-4-hydroxypteridine-6-carboxylic acid (VII). This shows that Sepiapterin is a 6-substituted pteridine. In connection with the result by Forrest et al.[5], who obtained VII and acetaldehyde from periodate oxidation of Sepiapterin, the present observation that one mole of lactic acid is quantitatively obtained from decomposition of Sepiapterin suggests that the substituent is a lactyl group ($CH_3 \cdot CHOH \cdot CO-$). Since the analytical data indicate that Sepiaterin has three carbon atoms other than its pteridine skeleton, the lactyl group seems to be a sole side chain. The isolation of 7,8-dihydroxanthopterin (IV) from air oxidation of Sepiapterin suggest whether the 6-hydroxy group of IV is an integral part of the molecule of Sepiapterin or a hydroxylation at the 6-position occurs at

15) A. Albert and H. C. S. Wood, *J. Appl. Chem.* (London), **3**, 521 (1953).
16) O. H. Lowry, O. A. Bessey and E. J. Crawford, *J. Biol. Chem.*, **180**, 389 (1949).
17) F. Bergmann and H. Kwietny, *Biochem. et Biophys. Acta*, **26**, 613 (1958).

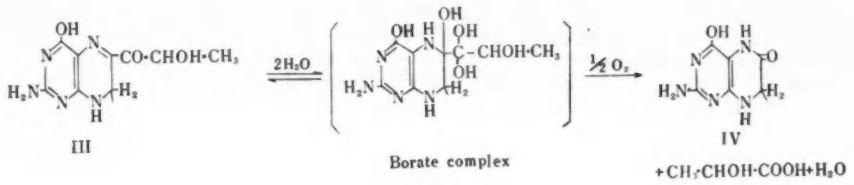

Fig. 9.

the same time as the lactyl side chain is split off. Since this reaction did not occur in the absence of oxygen (0.5 mol. of oxygen were consumed), it is sure that the side chain is split off oxidatively. In this connection, Blakley[18] has reported the production of xanthopterin in aerated solution of dihydro- or tetrahydrofolic acid. It seems reasonable to assume, therefore, that the oxygen atom in the 6-position of IV is oxidatively introduced and then Sepiapterin has no OH group in its 6-position. The finding that the decomposition of Sepiapterin give one mole each of IV and lactic acid accompanied by consumption of 0.5 mol. of oxygen, therefore, suggests that Sepiapterin has the structure 2-amino-4-hydroxy-7, 8-dihydro-6-lactylpteridine (III). From the evidence[19] that polyhydroxy compounds form borate complexes and from the experimental result that 0.5 mol. of oxygen are consumed in the reaction of sepiapterin with borax, the schema shown in Fig. 9 is postulated.

The formation of 2-amino-4-hydroxypteridine-6-carboxylic acid (VII) and acetaldehyde by periodate oxidation of Sepiapterin has been reported by Forrest et al.[5]. However, when in alkaline solution Sepiapterin was treated with periodate, it consumed one mole of periodate to give acetaldehyde and a pteridine different from VII. The pteridine seems to be a dihydro form of VII, i. e. 2-amino-4-hydroxy-7, 8-dihydropteridine-6-carboxylic acid (VI), since it is readily oxidized to VII accompanied by consumption of 0.5 mol. of oxygen or one mole of iodine. Furthermore, the finding that pteridine was converted to 2, 6-diamino-4-hydroxypteridine (IX) by treating with ammonia again supports it to be hydropteridine, in connection with the evidence[14] that the catalytic reduction of 2-amino-4-hydroxypteridine (VIII) in the presence of ammonia gave IX. In progress of our studies, Viscontini and Möhlmann[20] reported that the reduction of Sepiapterin with sodium borohydride give a tetrahydro form of biopterin (2-amino-4-hydroxy-6-(1, 2-dihydroxypropyl)-pteridine)[21-23]. We observed that the sodium borohydride reduction of VI give a compound with a spectrum characteristic of typical tetrahydropteridine[7,12,13], although neither VII nor VIII is affected. Dihydropteridines, therefore, seems to be reduced to the corresponding tetrahydro form by the action of sodium borohydride. It was also found that Sepiapterin is reduced to a tetrahydro form with the enzyme system from chicken liver, which carries out a reaction of dihydrofolic acid to tetrahydrofolic acid. These observations confirm that Sepiapterin is a dihydropteridine. The present result that photodecomposition of Sepiapterin gave one mole each of acetaldehyde and VII accompanied by consumption of one mole of oxygen, is again in accord with the proposed structure III.

Several different pteridines[3,5,6,20,21,23] have already been isolated from *Drosophila*. It has been assumed[3,5,20] that the red pigment found in the wild type has a structure related closely to the yellow pigment (Sepiapterin) and the latter is an intermediate in the synthesis of the former. It is of particular interest that Sepiapterin is a hydropteridine, in connection with the biological significance[24] of hydrofolic acid. Recently, Kaufman[13] reported the role of hydro-form of simple pteridines in the enzymatic oxidation of phenylalanine to tyrosine. It has been, furthermore, known that the mutant *lemon* of silkworm, which accumulates the yellow pigment identical with Sepiapterin in larval epidermis, shows the inhibition of oxidation of phenolic substances in vivo. From these, it may be expected that in the insect the yellow pigment (Sepiapterin) participates in some oxidation-reduction systems, although its biological significance remains to be determined.

Summary

The yellow pigment (Sepiapterin), occuring in the eyes of *Drosophila melanogaster*,

18) R. L. Blakley, *Biochem. J.*, 65, 331 (1957).
19) J. Böeseken, *Advances in Carbohydrate Chem.*, 4, 189 (1949).
20) M. Viscontini and E. Möhlmann, *Helv. Chim. Acta*, 42, 836, 1679 (1959).
21) H. S. Forrest and H. K. Mitchell, *J. Am. Chem. Soc.*, 77, 4865 (1955).
22) E. L. Patterson, R. Milstrey and E. L. R. Stokstad, ibid., 78, 5868 (1956).
23) M. Viscontini, E. Loeser and P. Karrer, *Helv. Chim. Acta*, 41, 440 (1958).
24) R. L. Blakley, "Current Trends in Heterocyclic Chemistry", A. Albert, editor, Butterworths Scientific Publication, London (1958), p. 140.

decomposed to one mole each of 7, 8-dihydroxanthopterin and lactic acid accompanied by consumption of 0.5 mol. of oxygen. From this and from the results of its photodecomposition and periodate oxidation, it is concluded that the compound has the structure 2-amino-4-hydroxy-7, 8-dihydro-6-lactylpteridine (III).

The author wishes to acknowledge Professor Y. Hirata and Dr. M. Tsujita for their encouragements and criticisms in this work. He is also indebted to Mr. T. Taira for the gift of flies.

National Institute of Genetics
Yata, Mishima, Shizuoka-ken

---

*Total Syntheses of Renieratene and Renierapurpurin**

By Masaru YAMAGUCHI

(Received May 11, 1960)

In the present paper are described the total syntheses of renieratene, I, and renierapurpurin, the chemical constitution of the latter having been hitherto unknown. By these works, therefore, the chemical constitution of renieratene has been established beyond doubt and the chemical constitution of renierapurpurin, II, has also been clearly established without any degradation studies.

The orange coloration of the sponge *Reniera japonica*, which is considered by zoologists to be identical with *Halichondria panicea*, a species of wide distribution, is mainly due to the presence of a complicated mixture of carotenoids. Fifteen different carotenoids have been isolated from the sponge in crystalline states[1]. The main pigments are, however, carotenoid hydrocarbons which are renieratene, isorenieratene (III), β-carotene and renierapurpurin. Among these pigments, the chemical constitution[2,3] of renieratene and isorenieratene

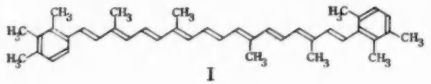

I

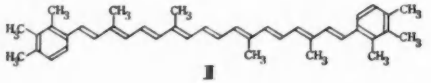

II

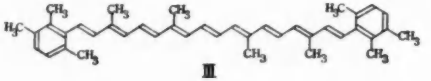

III

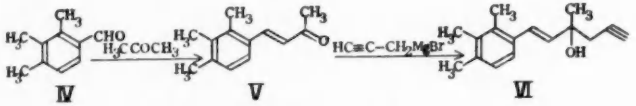

IV V VI

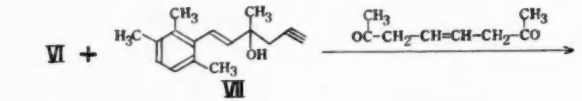

VI + VII

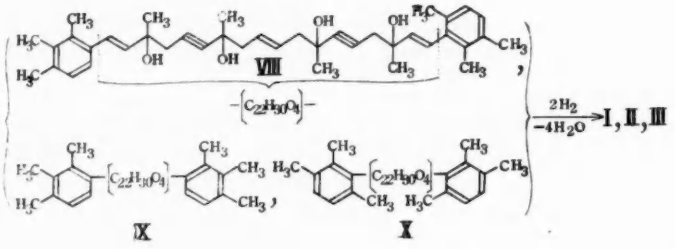

VIII IX X

* Pigments of Marine Animals, Part XI. X of this series; T. Mukai, This Bulletin, 33, 1234 (1960).

1) T. Tsumaki, M. Yamaguchi and T. Tsumaki, *J. Chem. Soc. Japan, Pure Chem. Sec.* (*Nippon Kagaku Zasshi*), 75, 297 (1954); M. Yamaguchi, This Bulletin, 30, 111 (1957).

2) M. Yamaguchi, This Bulletin, 31, 739 (1958).

3) M. Yamaguchi, ibid., 31, 51 (1958).

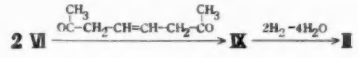

have been elucidated and the total synthesis of the latter has been carried out by the author[4] and later by M. C. Khosla and P. Karrer[5]. On the other hand, however, little progress has been made on the study of the chemical constitution of renierapurpurin because of the limited quantity of the pigment available. It has so far been known that renierapurpurin forms purple plates of m. p. 230°C, exhibits absorption maxima at 544, 504 and 475 mμ in carbon disulfide, and has the formula $C_{40}H_{48}$ (or $C_{40}H_{50}$)[1]. In regard to its constitution, it has been inferred from its absorption maxima and from an analogy to renieratene, etc., that if it contains two triemthylphenyl groups at both ends of the molecule as in renieratene and isorenieratene, the terminal groups should be ones having small steric hindrance between the polyene chain and annular methyl groups. For example 2, 3, 4-trimethylphenyl group satisfies the condition. However, no experiment has been carried out to draw any conclusion on the problem.

The syntheses were carried out according to Karrer's method[6]. 2, 3, 4-Trimethylbenzaldehyde (IV)[2] was condensed with acetone to give 2, 3, 4-trimethylbenzalacetone (V), which was converted into acetylenic alcohol VI by Grignard reaction. A mixture of this acetylenic alcohol and another acetylenic alcohol VII[4] was condensed with octene-2, 7-dione to give a mixture of three isomeric C_{40}-diynetetraols (VIII, IX and X). The mixture was partially hydrogenated and then dehydrated, and the chromatographic separations of the product gave renieratene (I), renierapurpurin (II) and isorenieratene (III) in pure states but in low yields. The identity of these pigments with the natural specimens was verified by mixed melting point determinations, mixed chromatographies, and IR- and UV-determinations.

Renierapurpurin was obtained in a better yield in another experiment starting from acetylenic alcohol VI.

Renierapurpurin is the third carotenoid that is proved to contain benzene rings, and the fact that three possible isomers derivable by combinations of 2, 3, 4-trimethylphenyl and 2, 3, 6-trimethylphenyl groups are all present in the sponge, may be considered to provide an important orientation of the biogenesis of this interesting group of carotenoids.

Furthermore these isomers afford a typical example of steric hindrance, the cause of which has been discussed in the previous paper[3]. The absorption maxima (the longest wavelength, in carbon disulfide solution) of renierapurpurin, renieratene and isorenieratene are at 544, 532 and 520 mμ, respectively[2]. The shifts of maxima (12 and 24 mμ) are proportional to the number of 2, 3, 6-trimethylphenyl group in their molecules.

Experimental

Solutions were evaporated under diminished pressure unless otherwise mentioned. Anhydrous sodium sulfate was employed for drying solutions.

4-(2, 3, 4-Trimethylphenyl)-3-buten-2-one (V).—It was prepared from 2, 3, 4-trimethylbenzaldehyde (IV, 22 g., b. p. 133~135°C/20 mmHg), in the way described in 4-(2, 3, 6-trimethylphenyl)-3-buten-2-one in the previous paper[4]. Colorless solid (17.2 g.), b. p. 125~130°C/3 mmHg. On recrystallization from petroleum benzine it formed thick plates of m. p. 70~71°C.

Found: C, 82.87; H, 8.74. Calcd. for $C_{13}H_{16}O$: C, 82.93; H, 8.57%.

From the residue of the distillation, 1, 5-bis-(2, 3, 4-trimethylphenyl)-1, 4-pentadien-3-one (1.6 g.) was obtained in yellow plates when recrystallized from benzene-ethanol, m. p. 150°C.

Found: C, 86.69; H, 8.33. Calcd. for $C_{23}H_{26}O$: C, 86.74; H, 8.23%.

1-(2, 3, 4-Trimethylphenyl)-3-methyl-1-hexen-5-yn-3-ol (VI).—Operations of the experiment and the proportions of the reagents are similar to those of the synthesis of 1-(2, 3, 6-trimethylphenyl)-3-methyl-1-hexen-5-yn-3-ol in the previous paper[4]. From C_{13}-ketone (V, 13 g.), acetylenic alcohol (VI, 6.1 g.) was obtained as faint colored oil, b. p. 115~120°C (bath temperature)/0.05 mmHg.

Found: C, 84.41; H, 8.92. Calcd. for $C_{16}H_{20}O$: C, 84.16; H, 8.83%.

C_{40}-Diynetetraol Mixture (VIII, IX and X).—An ethereal solution (ca. 30 cc.) of ethylmagnesium bromide prepared from 3.9 g. of ethyl bromide, was added dropwise to a well-stirred mixture of the above acetylenic alcohol (VI, 2 g.), 1-(2, 3, 6-trimethylphenyl)-3-methyl-1-hexen-5-yn-3-ol (VII, 2 g.)[4], cuprous chloride (50 mg.) and dry ether (20 cc.) during one and a half hours, and the mixture was refluxed for an hour. A solution of 4-octene-2, 7-dione (840 mg.) in dry ether (20 cc.) was added dropwise during thirty minutes under stirring. After refluxing for one hour, the mixture was allowed to stand overnight, and decomposed with 1 N sulfuric acid under ice-cooling. The organic layer was extracted with ether and the ethereal solution was washed with dilute sulfuric acid, aqueous sodium hydrogen carbonate and water, dried and evaporated. The residue (4.8 g.) dissolved in benzene (20 cc.) was adsorbed on alumina (Merck, 80 g.) and the column was washed successively with benzene (100 cc., the eluate gave an oily residue 1.95 g.), with ether (60 cc., residue 0.8 g.) and with ether-methanol 10 : 1 (200 cc., residue 1.8 g.). The last fraction was the mixture

4) M. Yamaguchi, ibid., 32, 1171 (1959).
5) M. C. Khosla and P. Karrer, *Helv. Chim. Acta*, 43, 453 (1960).
6) P. Karrer and C. H. Eugster, ibid., 33, 1172 (1950).

of three isomers of C_{40}-diynetetraol and formed a yellowish-colored glass-like mass.

Found: C, 79.91; H, 8.80. Calcd. for $C_{40}H_{52}O_4$: C, 80.50; H, 8.78%.

Renieratene (I), Renierapurpurin (II) and Isorenieratene (III).—A solution of the above tetraol mixture (1.5 g.) in ethyl acetate (40 cc.) was filtered through a column of active charcoal (0.3 g.) and shaken with palladium-barium sulfate catalyst (1%, 50 mg.) in an atmosphere of hydrogen. Occasional additions of the small amount of catalyst were necessary until 2 mol. of hydrogen (ca. 116 cc., 9°C/760 mmHg) was absorbed. The catalyst was filtered and the solution was evaporated to glassy residue. A boiling solution of toluene-*p*-sulfonic acid (180 mg., dehydrated by melting in vacuo) in toluene (30 cc.) was added at a time to a boiling solution of the above residue in toluene (40 cc.) and the mixture was boiled for ca. eighty seconds. The greenish brown solution was, as soon as possible, poured into a mixture of a saturated aqueous solution of sodium hydrogen carbonate (300 cc.) and petroleum ether (200 cc.). The petroleum ether solution was then washed once with water and thrice with 90% methanol, dried and evaporated. The reddish-brown residue was dissolved in petroleum ether and chromatographed on alumina (4×20 cm.), giving the following zone: i) dark brown zone (most strongly adsorbed), ii) a broad zone, its color changing from red to orange, iii) an orange brown zone, and iv) faint yellow. The residue of the zone ii) was boiled several times with methanol, and the insoluble residue was rechromatographed on alumina giving the following main zones; a) purplish red (uppermost), b) red and c) orange. The pigment of the zone b) was further purified by rechromatography. The residue of the eluate of each zone was boiled with methanol. The insoluble parts were treated with petroleum ether and ethanol, and each pigment which separated out, was recrystallized several times from suitable solvents. The zone a) gave glistening purple plates (2.4 mg.) of renierapurpurin (from chloroform-ethanol), m. p. 229~230°C, its identity with natural pigment being confirmed by mixed melting point, 229~230°C, by mixed chromatography, and by IR- and UV-spectra (Fig. 1 and Fig. 2). The zone b) gave purplish red fine needles (1.4 mg.) of renieratene (from benzene-ethanol), m. p. 184~185°C, the identity with natural pigment being confirmed by mixed melting point, 184~185°C, by mixed chromatography, and by IR- and UV-spectra. The zone c) gave purplish red find needles (2.0 mg.) of isorenieratene (from benzene-ethanol), m. p. 199~200°C, the identity with natural pigment being confirmed by mixed melting point, 199~200°C, by mixed chromatography, and by UV-spectrum.

Because of the small yields of these pigments, no elementary analysis was carried out.

C_{40}-Diynetetraol (IX).—It was synthesized from acetylenic alcohol (VI, 3 g.) in the way described above. It formed a faint yellow glass-like mass (1.6 g.).

Found: C, 80.12; H, 8.81. Calcd. for $C_{40}H_{52}O_4$: C, 80.50; H, 8.78%.

Renierapurpurin (II).—Tetraol (IX, 1.5 g.) was

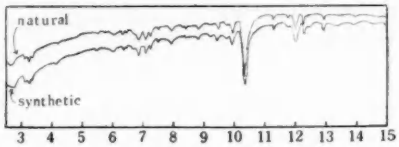

Fig. 1. Infrared spectra of renierapurpurin (KBr disk).

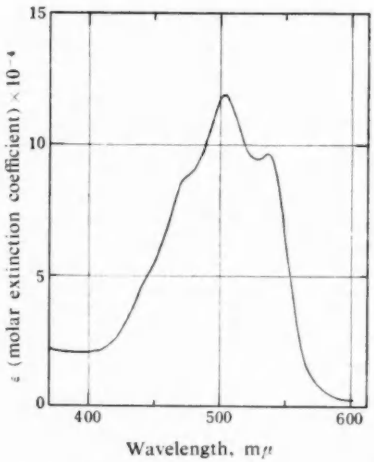

Fig. 2. Absorption curve of renierapurpurin (carbon disulfide).

partially hydrogenated and then dehydrated in the way described above. While petroleum benzine solution of the dehydration product was washed, a part of the pigment was crystallized out, which was filtered off (43 mg.). The mother liquor was chromatographed on alumina from a benzene solution, giving three main zones; i) pink, ii) red and iii) orange. From the zone i), 25 mg. of the pigment was obtained, which was combined with the crystals separated during washing. Several recrystallizations from chloroform-ethanol gave pure renierapurpurin (38 mg.), m. p. 230°C.

Found: C, 90.76; H, 8.99. Calcd. for $C_{40}H_{48}$: C, 90.85; H, 9.15%.

The author wishes to express his thanks to Professor Tokuichi Tsumaki for his exceedingly kind directions throughout this work. The author also thanks Yoshiya Kanda, Assistant Professor of Structural Chemistry, who kindly provided facilities for measurements of infrared and ultraviolet spectra. The cost of this work has been partially covered by the Scientific Research Grant of the Ministry of Education.

Department of Chemistry
Faculty of Science
Kyushu University
Hakozaki, Fukuoka

Flow Properties of Aluminum Soaps-Hydrocarbon Systems

By Sukekuni SHIBA

(Received May 31, 1960)

It has been known that the aluminum soaps dispersed in hydrocarbon oils make stable gels and exhibit a wide variety of flow behaviors. The polymeric natures of the aluminum soaps have been pointed out by many authors[1-3] from the osmotic pressure and viscosity data on aluminum soaps in benzene. These properties indicate that the soap molecules aggregate to form fibrous micelles and are dispersed polymerically with a network structure in hydrocarbon.

Garner, Nissan and Wood[4], studying thermodynamics and rheological behaviors of the aluminum stearate gels in petrol, found that the apparent viscosity at different rates of shear was at first constant, but at higher rates of shear, the apparent viscosity decreased, reaching approximately constant value at very high rates of shear. Weber and Bauer[5], and also Bauer, Weber and Wiberley[6,7], studying the flow properties of aluminum laurate-toluene gels, the effect of peptizers and entrance effects in capillary, by a pressure capillary viscometer over a wide range of mean rates of shear, ranging from 10^{-3} to 10^{+6} sec^{-1}, obtained the shear stress-rate of shear curves, which showed three types of flow: Newtonian flow at low rates of shear, rapid increase in shear rate with shear stress in the region of shear rate above 10^{-2} sec^{-1}, and constant slope in log-log plot at shear rate above 10^{-2} sec^{-1}.

Some of the manifold flow properties were clarified by these investigations; however, many aspects of flow behaviors are not fully explained, due to the variability of flow properties with the nature of soaps, solvents, soap concentrations and physical conditions of measurements especially the rate of shear. Measurements with the capillary type viscometers are liable to be affected by the capillary end effects and the changes in properties during the flow. Therefore, it is desirable to take measures under a uniform rate of shear with specimens not subjected to shear. In this investigation, the flow properties of aluminum soaps of various parent fatty acids in hydrocarbon were measured with a concentric cylinder type rotational viscometer of small clearance; the flow properties and especially the time effects under shear were examined.

Experimental

Materials.—The alminum soaps used in this investigation were prepared from purified fatty acids by an aqueous metathetic process. Stearic and palmitic acids were purified from pure acids (Nihon Yushi Co.) by repeated recrystallization from 80 vol.% ethanol. Myristic and lauric acids were purified from commercial reagents by the same method. Capric and caprylic acids were purified from the commercial reagents by distillation under reduced pressure. The purity of the acids was examined by melting points and neutralization equivalents by titration. The physical constants of fatty acids are shown in Table I.

TABLE I. PHYSICAL CONSTANTS OF FATTY ACIDS

Fatty acid	M. p., °C		Neut. equiv.	
	Found	Lit.[8]	Found	Calcd.
Stearic	69.5	69.6	281.9	284.5
Palmitic	62.2	62.9	258.0	256.4
Myristic	54.5	54.4	229.1	228.4
Lauric	43.3	44.0	201.3	200.3
Capric	30.1	31.3	173.1	172.3
Caprylic	14.3	16.3	143.8	144.2

Fatty acid was treated with a 40~50% excess sodium hydroxide solution and distilled water to yield an approximately 5% solution of sodium soap. The mixture was heated to dissolve the soap and the solution was kept completely transparent at 70~80°C for soaps from stearate to laurate and at 50°C for caprate and caprylate. A hot solution of aluminum sulfate was added slowly while being stirred vigorously, until a slight excess was present and precipitation was complete. The precipitated aluminum soap was filtered and washed with distilled water, until free from sulfate. The test for sulfate ion was made by adding barium chloride solution to the filtrate, which was made slightly acidic with hydrochloric acid. The soaps

1) J. W. McBain and E. B. Working, *J. Phys. Colloid Chem.*, **51**, 974 (1947).
2) H. Sheffer, *Canad. J. Research*, **B-26**, 481 (1948).
3) V. R. Gray and A. E. Alexander, *J. Phys. Colloid Chem.*, **53**, 9 (1949).
4) F. H. Garner, A. H. Nissan and G. F. Wood, *Phil. Trans. Roy. Soc.*, **A-243**, 37 (1950).
5) N. Weber and W. H. Bauer, *J. Phys. Chem.*, **60**, 270 (1956).
6) W. H. Bauer, N. Weber and S. E. Wiberley, ibid, **62**, 106 (1958).
7) W. H. Bauer, N. Weber and S. E. Wiberley, ibid, **62**, 1245 (1958).
8) A. W. Ralston, "Fatty Acids and their Derivatives", John Wiley & Sons, Inc., New York (1948), pp. 23-40.

were then dried to constant weight at 110°C, and stored in a desiccator over phosphorus pentoxide. Dried soaps were analysed for aluminum by ignition to oxide. The composition of the soaps is shown in Table II.

TABLE II. COMPOSITION OF ALUMINUM SOAPS

Aluminum soaps	No. of C atoms in acid	Al wt. % (analysed)	Mole acid per mole Al
Stearate	18	5.04	1.72
Palmitate	16	5.80	1.62
Myristate	14	5.96	1.77
Laurate	12	6.38	1.88
Caprate	10	7.36	1.87
Caprylate	8	9.17	1.72

Nujol was used as a vehicle. It is a liquid paraffin of a commercial grade, a paraffin-rich saturated hydrocarbon. The physical properties are as follows; $d_4^{25}=0.8429$, $n_D^{25}=1.467$, $\eta_{25}=0.217$ poise.

Preparation of Specimen.—Nujol was added to a weighed quantity of aluminum soap, and the mixture was heated slowly while being stirred until it became a transparent solution at 110~120°C. After maintaining this temperature for 15min. the solution was cooled and stored in a desiccator over phosphorus pentoxide.

Apparatus.—A concentric cylinder type rotational viscometer essentially the same as the apparatus developed by Green[9], was used. The outer cylinder was rotated and the torque necessary to keep the inner cylinder stationary was measured by a torsion spring. When the sample is a Bingham body of plastic viscosity η_{pl} and yield value f, the relation of angular velocity ω, troque M, η_{pl} and f is given by the Buckingham-Reiner equation[10];

$$\eta_{pl}\omega=(M/4\pi h)(1/r_i^2-1/r_e^2)-f\ln(r_e/r_i) \qquad (1)$$

where r_i and r_e are the radii of inner and outer cylinders; h is the height of the immersed part of inner cylinder; η_{pl} and f are obtained by the measurement of M corresponding to ω. The shear stress τ and the rate of shear D at radius r from the center of the cylinder are given by

$$\tau=M/2\pi hr^2 \qquad (2)$$

$$D=2\omega/(1/r_i^2-1/r_e^2)r^2 \qquad (3)^{11}$$

The dimensions of the apparatus are as follows: $2r_i=29$ mm., $2r_e=30$ mm., $h=50$ mm. rate of revolution 0~400 rpm, torsion constants of the springs $3\times10^3\sim3\times10^5$ dyn. cm./rad. The apparatus was calibrated with viscosity standard oils. The absolute accuracy of the values obtained from dimensions and force constant of the apparatus was within 2%. The end effect was checked, changing the depth of immersion of the inner cylinder. It was found that the end effect was negligible.

Procedure.—The speicmen was placed between the cylinders and kept for 15 min. at the measuring temperature. The rate of revolution was raised stepwise, and at each step the equilibrium points where the deflexion of the torsion spring became constant were determined[12]. The down curve was obtained by reducing the rate of revolution down to zero to obtain the rate of shear-shear stress relation corresponding to the state. Measurements were made for systems containing 0.5~4 wt. % soaps in nujol at temperatures 15~75°C.

Results and Discussion

The aluminum soap-nujol systems give various types of flow. At room temperature, the system containing soaps above 1% makes a gel, and it changes to paste or liquid state by shear. The more diluted system makes a sol with fluidity, which shows linear or non-linear flow properties. At high temperatures above 80°C, the system becomes a homogeneous transparent elastic solution. Thus, the systems show various flow properties and are unstable in regard to shear and time. Therefore, it is necessary to study the change in properties corresponding to the variables.

Rate of Shear-Shear Stress Curves.—Examples of the curves exhibiting the rate of shear-shear stress relations are shown in Fig. 1. The lower curves are the equilibrium curves, which are obtained with the elevated rate of shear, and the upper curves are the $D-\tau$ curves (or down curves) for the states of the specimens equilibrated under the highest rates of shear. Two curves coincide for the dilute systems which behave as Newtonian liquids or Bingham plastic bodies. When the concentration is increased, the two curves make a loop. Plastic viscosity

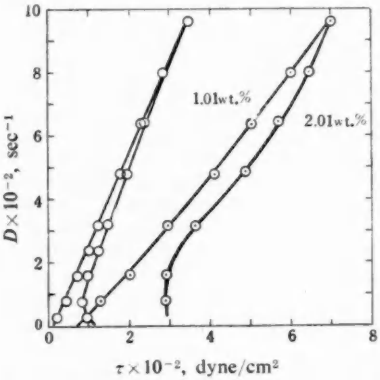

Fig. 1. Rate of shear-shear stress curves for aluminum stearate in nujol at 25°C.

9) H. Green, "Industrial Rheology and Rheological Structures", John Wiley & Sons, Inc., New York (1949), p. 99.

10) M. Reiner, "Deformation and Flow", H. K. Lewis, London (1949), p. 44.

11) For substances which show non-linear flow properties, Eq. 3 can not be used rigorously. In this apparatus, (r_e-r_i) is small enough compared with r, so that approximation with Eq. 3 is possible.

12) The specimen was assumed to reach equilibrium when the change in deflexion angle became less than 1/2 deg./min.

and yield value are obtained from the down curve for the state.

Concerning the equilibrium curves, a rapid decrease in viscosity is observed in the range of rate of shear up to 200 sec^{-1}. This is in agreement with the results of Weber and Bauer[5], who found a sudden viscosity decrease in the range of rate of shear up to 10^2 sec^{-1} for aluminum laurate-toluene gels. The curves which they obtained are likely to correspond to the equilibrium curves in this investigation, because the results by these authors will be subject to the effects of shear softening in capillary.

Ageing.—The flow properties of the system change with time while standing after preparation. The changes in viscosity and yield value at room temperature (20°C) are shown in Fig. 2. Where the viscosity is obtained from the inclination of the down curve at the rate of shear 5×10^2 sec^{-1}, for the specimen equilibrated at 10^{-3} sec^{-1}; the yield values are obtained from the intercepts of the extension of the down curves. Viscosity and yield value increase rapidly with time, exhibiting maximum values at about 4 hr. after preparation, and approach approximately constant values. Therefore, the measurements were carried out between 24~96 hr. after preparation of the specimen. This effect is in agreement with the results of Gray and Alexander[2], and of McBain and Working[1], who obtained the effect of ageing for the benzene solution of aluminum laurate, from flow birefringence and viscosity study. The mechanism of this phenomenon is explained as follows: The system cooled from a hot solution is a metastable jelly containing soap micelles; three dimensional networks of the soap crystallites grow rapidly, and are arranged slowly to the stable state.

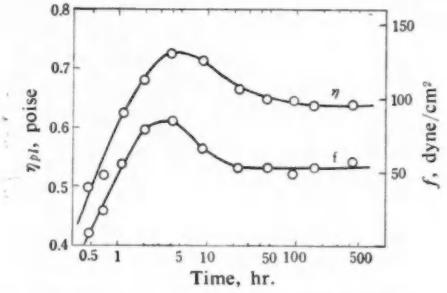

Fig. 2. Ageing of the aluminum stearate in nujol 2.01 wt.%, 25°C.

Change of Flow Properties under Shear.—Decrease of shear stress with time under constant rate of shear is shown in Fig. 3. The curve for each rate is obtained for the specimen equilibrated under lower rates of shear. If it is assumed that the contribution of the rheological structures to the shear stress is proportional to the concentration of the structures, C, and that the rate of breakdown of the structure is also proportional to C, the decrease in shear stress under constant rate of shear is expressed by,

$$\tau-\tau_{eq}=aC \tag{4}$$

$$-\frac{d(\tau-\tau_{eq})}{dt}=-a\frac{dC}{dt}=kC \tag{5}$$

integrating (5)

$$\ln(\tau-\tau_{eq})=\ln(\tau_0-\tau_{eq})-(k/a)t \tag{6}$$

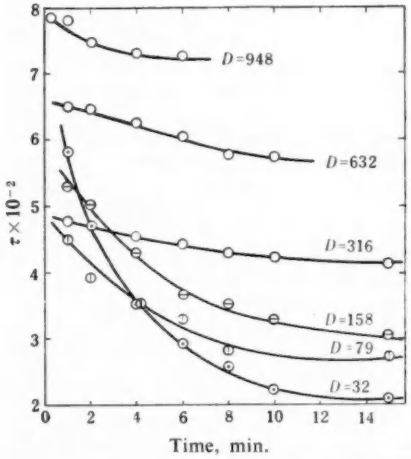

Fig. 3. Decrease of shear stress with time under constant rate of shear.
Aluminum stearate, 2.01 wt.%, 25°C

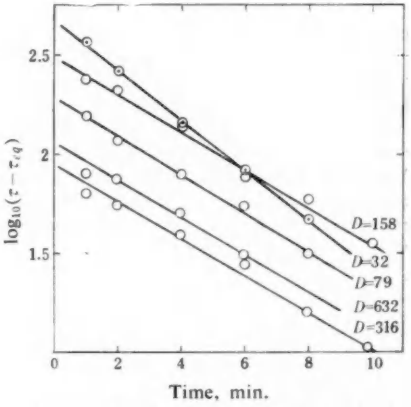

Fig. 4. Rate of degradation of the rheological structure.
Aluminum stearate, 2.01wt.%, 25°C

where τ_{eq} is the shear stress in quilibrium, τ_0 is the value of τ at time $t=0$. The decrease in $\log(\tau-\tau_{eq})$ with t is shown in Fig. 4. These results support the assumptions mentioned above. Rates of breakdown under various rates of shear are not constant in general; the rapid breakdown of weak structures under low rate of shear is recognized.

Examination on Thixotropy[13].—Flow measurements were repeated to examine the thixotropic recovery, after the specimen was kept standing for some time. The results are shown in Fig. 5. If complete recovery is present, the curves should coincide. However, the curves in subsequent measurements resemble the down curve in the first run, and the breakdown of the structures proceeds by repeated shear. Therefore, in these experimental conditions, thixotropy does not exist even after considerable time.

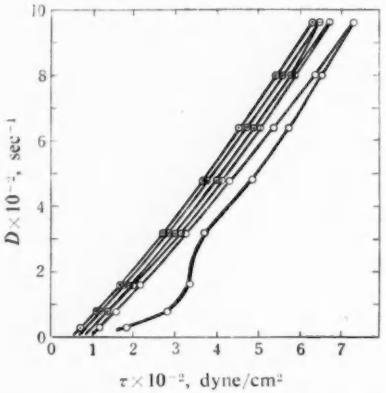

Fig. 5. D-τ curves for repeated shear. Alumium stearate in nujol, 2.01 wt.%, 25°C. ○ 0 hr., ◑ 3 hr., ⊖ 20 hr., • 72 hr.

Agreements in opinions concerning the time effects of flow behaviors on aluminum soap-hydrocarbon systems have not yet been obtained. Complete recovery was reported by Goldberg and Sandvik[14], and Carver and Van Wazer[15]; whereas, absence of thixotropy was pointed out by Evans and Matthews[16]. Evans states for aluminum greases that the change caused by the applied shearing stress is not thixotropic but

13) It will be adequate to give a general definition of thixotropy in rheological terms as follows: "Thixotropy is the property of a body by virtue of which the ratio of shearing stress to rate of deformation is *temporarily* reduced by previous deformation.", E. K. Fischer, "Colloidal Dispersion", John Wiley and Sons, Inc., New York (1950), p. 183.

14) H. Goldberg and O. Sandvik, *Anal. Chem.*, **19**, 123 (1947).

15) E. K. Carver and J. R. Van Wazer, *J. Phys. Colloid Chem.*, **51**, 751 (1947).

16) D. Evans and J. B. Matthews, *J. Colloid Sci.*, **9**, 60 (1954).

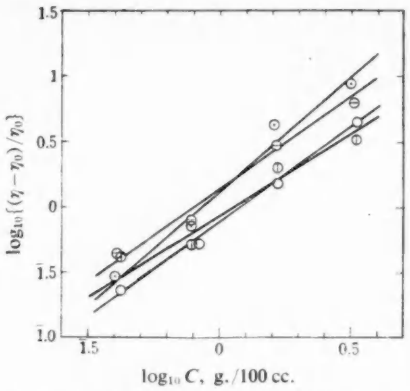

Fig. 6. Concentration dependence of specific viscosity.
○ 15°C, ◑ 25°C ⊖ 50 C, • 75°C

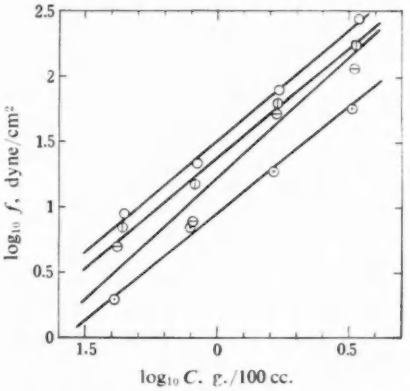

Fig. 7. Concentration dependence of yield values.
○ 15°C, ◑ 25°C, ⊖ 50°C, • 75°C

appears to be a permanent change in the structure of the grease. Results of this experiment appear to support those of Evans and Matthews. However, the discrepancy of the results obtained by many authors will be ascribed mainly to the experimental conditions; for example, the rate of shear, temperature, concentration and properties of soaps which are not always pure substances. At high temperatures or under a very low rate of shear, it will be possible that the system is thixotropic.

Effect of Concentration.—The specific viscosity and yield values for various concentrations and temperatures are shown in Figs. 6 and 7, where the viscosity and yield values are obtained as previously described. These values show an approximately linear relation against $\log C$. That is, the dependence of the viscosity and yield values on concentration is expressed by empirical formulae,

$$\eta=\eta_0(1+aC^m) \quad (7)$$

$$f=bC^n \quad (8)$$

where values of m, a and n calculated from the data at 15, 25, 50 and 75°C are, m=1.47, 1.30, 1.39, 1.73; a=0.73, 0.78, 1.33, 1.33; n= 1.72, 1.64, 1.72 and 1.61, respectively.

The systems are considered essentially as colloidal suspensions of soap crystallites in oil. If the soap crystallites are non-attractive rod-like ellipsoidal particles of axial ratio over 20, specific viscosity is given by Simha[17], as a function of axial ratio and volume fraction of the particles. The formula gives very high values of axial ratio corresponding to the measured viscosity values. These facts indicate that it is more appropriate to consider the interaction between soap particles and the network structures in the system.

Effect of Temperature.—Viscosity-temperature relation is shown in Fig. 8. In this temperature region, approximately linear relations exist. This shows the absence of serious change in rheological structures in this region. Apparent activation energies of flow and constant A, calculated from Andrade equation,

$$\eta=A\exp(\Delta E/RT)$$

are shown in Table III. Decrease in ΔE with increase in concentration is apparent. This tendency, which is in agreement with the results of Carver et al.[15], will be understandable if it is considered that the flow mechanism, is divided into the usual friction and break down of secondary bonding, and the predominance of the latter mechanism in concentrated systems is considered.

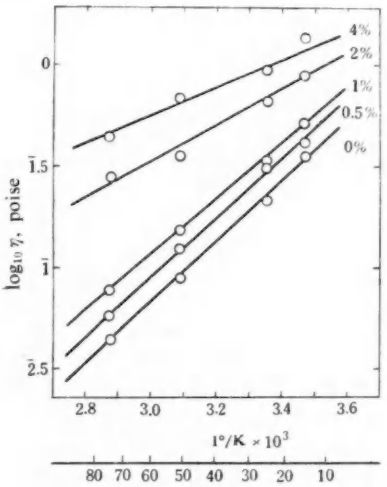

Fig. 8. Viscosity—temperature relations. Aluminum stearate in nujol.

TABLE III. CONSTANTS OF THE ANDRADE FORMULA

(Aluminum stearate in nujol)

Soap conc. wt. %	A	ΔE, kcal./mol.
0.00	2.5×10^{-6}	6.7
0.50	4.3×10^{-6}	6.6
0.99	9.4×10^{-6}	6.2
2.01	4.0×10^{-4}	4.4
3.99	4.7×10^{-3}	3.2

17) R. Simha, *J. Phys. Chem.*, **44**, 25 (1940).

Effect of the Fatty Acids.—Results for soaps from various fatty acids are shown in Fig. 9. Soaps from stearate to laurate show similar flow properties, whereas caprate and caprylate show lower values, This fact correlates many other properties of soaps, which change abruptly for soaps below caprate.

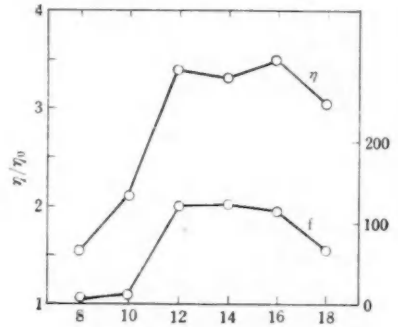

Fig. 9. Viscosity ratio and yield values of various Al soap-nujol gels, 2 wt. %, 25°C.

Summary

Flow properties of aluminum soap-hydrocarbon systems as viscous liquids or plastic bodies are studied with a concentric rotational viscometer. Results are obtained under the rate of shear up to 10^3 sec^{-1}.

(1) The systems behave as dispersions of soap crystallites with network structures combined by secondary interactions of the particles, and they exhibit marked viscosity increase.

(2) The rheological structures suffer shear breakdown under shear, resulting in decrease in viscosity.

(3) Recovery from the broken structures is impossible, that is, this change is not thixotropic but shear breakdown.

(4) Flow properties change with time while standing at rest.

(5) The effects of concentration, temperature and fatty acids constituting soaps are clarified.

The author wishes to express his thank to Professor H. Akamatu and Dr. T. Nakagawa, both of the University of Tokyo, for their interest and encouragement throughout this investigation.

Railway Technical Research Institute
Kunitachi, Tokyo

---

*Stress Relaxation of Thermo-reversible Gels. Molecular Weight Dependence of Relaxation Spectrum. Polyvinyl Alcohol-Congo Red-Water System**

By Kiyoshi ARAKAWA

(Received May 24, 1960)

In the previous paper[1] the author reported the results of the stress relaxation study of the gels of polyvinyl alcohol-congo red-water system, where the experiment was intended to obtain some knowledge on the concentration dependence of the relaxation spectrum of the gel which was taken as a typical example of thermo-reversible gels of polymeric nature. As a part of the series of rheological studies of thermo-reversible gels[1,2] a stress relaxation experiment has been made for the purpose of studying the molecular weight dependence of the relaxation spectrum of the gel, and the result is reported in the present paper.

Experimental

Apparatus. — A chainomatic balance relaxometer was used to measure the relaxation Young's modulus of the cylindrical gel, which was the same one as that used previously[1], and the schematic diagram of it is shown in Fig. 1. A specimen is compressed to a given strain between a plate attached to a bar and a bottom plate in a double jacket connected to a screw gauge by the rotation of it. The stress in the specimen is automatically balanced with a chain weight by means of a relay and a balancing motor, the ralaxation Young's modulus E_r is calculated form the vertical length of the suspended chain, as follows.

$$E_r = \frac{l}{\Delta l} \cdot \frac{adhg}{bs}$$

l is the height of the cylindrical specimen without strain, Δl the amount of the given compression, s the original sectional area of the specimen, a the distance from the fulcrum to the chain, b the distance from the fulcrum to the center of the pressure plate, d the linear density of the chain, h the vertical length of the suspended chain and g is the acceleration of gravity.

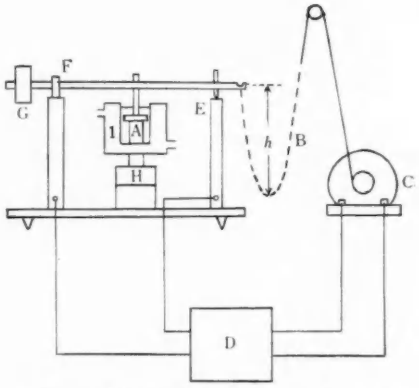

Fig. 1. Chainomatic balance relaxometer.
A: Specimen B: Chain
C: Balancing motor D: Relay
E: Point contact F: Fulcrum
G: Counter weight
H: Micrometer screw
I: Double jacket

Sample. — Commercial samples of polyvinyl alcohol were purified by precipitation from aqueous solutions with addition of acetone. The amount of residual acetyl group was smaller than 0.7% by mole for all samples used in this experiment. The values of the intrinsic viscosity $[\eta]_{30°C}$ determined by a capillary viscometer and the molecular weight calculated from those using the formula of Nakajima et al.[3] are given in Table I. Congo red

1) K. Arakawa, This Bulletin, **32**, 1248 (1959).
2) K. Arakawa, This Bulletin, **31**, 842 (1958); K. Arakawa and K. Atsumi, *J. Chem. Soc. Japan, Pure Chem. Sec.* (*Nippon Kagaku Zasshi*), **80**, 133 (1959).
* Partly presented at the Annual Meeting of the Chemical Society of Japan, Tokyo, April, 1960.

3) A. Nakajima and K. Furutati, *Chem. High Polymers* (*Kobunshi Kagaku*) **6**, 460 (1949).

used was Merck's analytical grade chemical. The preparation of testing specimens was made according the same procedure as described in the previous paper[1], except that in the present work an especially designed vessel with a double jacket was used in the dissolution process instead of a conical beaker and a water bath.

The composition of the prepared gel was maintained to be the same for all specimens: polyvinyl alcohol 17.5% and Congo red 1.75% by weight.

TABLE I. MOLECULAR WEIGHT OF POLYVINYL ALCOHOL

Sample	$[\eta]_{30°C}$(100 cc./g.)	Molecular weight
I	0.54	3.5×10^4
II	0.66	4.9×10^4
III	1.03	9.8×10^4

Results and Discussion

Stress Relaxation Data. — The data of stress relaxation at various temperatures are plotted in the form $(298/T)E_r$ versus $\log t$, where t is time, in Figs. 2a, 2b and 2c. The strain

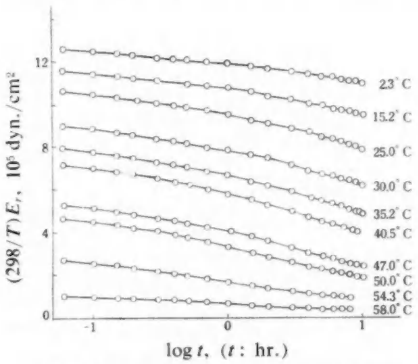

Fig. 2a. Reduced relaxation Young's modulus. Sample I (molecular weight 3.5×10^4).

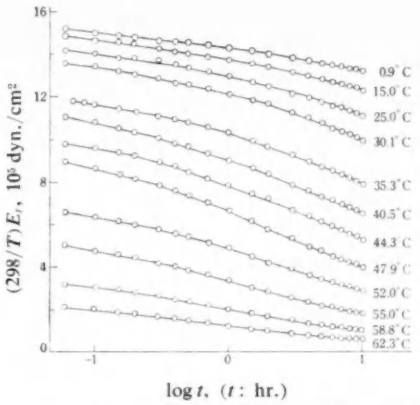

Fig. 2b. Reduced relaxation Young's modulus. Sample II (molecular weight 4.9×10^4).

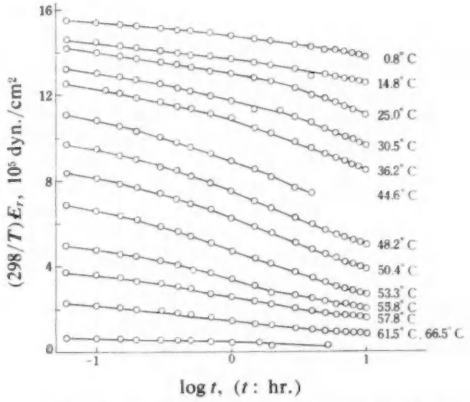

Fig. 2c. Reduced relaxation Young's modulus. Sample III (molecular weight 9.8×10^4).

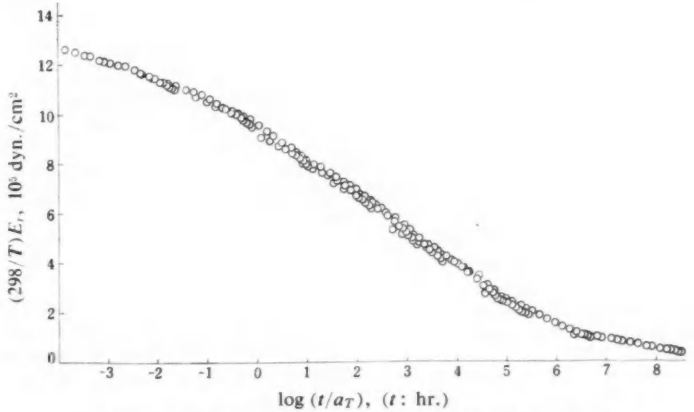

Fig. 3a. Composite relaxation curve at 25°C, Sample I.

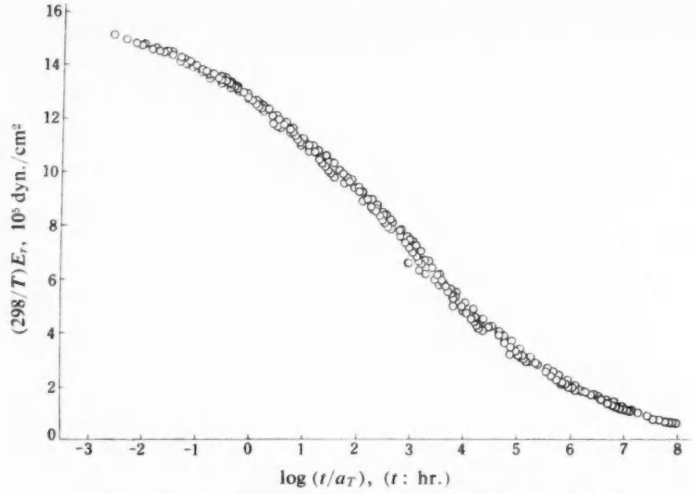

Fig. 3b. Composite relaxation curve at 25°C, Sample II.

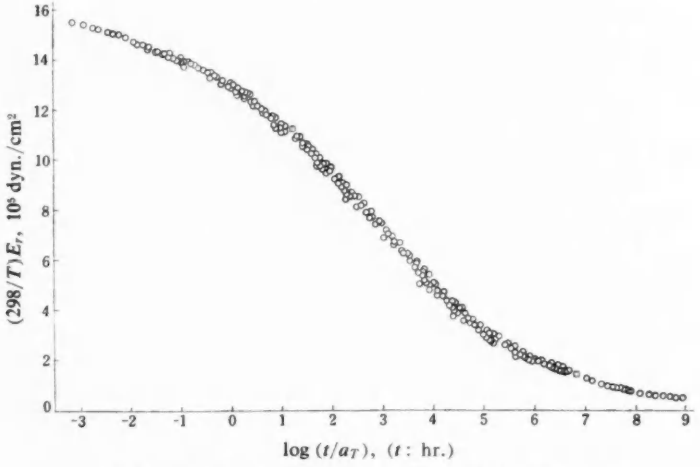

Fig. 3c. Composite relaxation curve at 25°C, Sample III.

applied in this experiment was 15% for all specimens. The data are reduced to 25°C with the multiplication by a factor $298/T$.

According to the time temperature superposition principles[4], each group of relxation curves was superposed to a composite relaxation curve by the horizontal shift of relaxation curves at different temperatures along the $\log t$ axis. The superposition of relaxation curves is good as it is seen in Figs. 3a, 3b and 3c. The density factors was ignored, because its temperature dependence was very small. The shift factors $\log a_T$ are plotted against T in Fig. 4 together with the apparent activation energy H_a, which was calculated from the mean $\log a_T$ versus T curve by the following equation.

$$H_a = R\frac{\partial \ln a_T}{\partial(1/T)} \qquad (1)$$

From the Fig. 4 it is seen that $\log a_T$ versus T relation does not obey the W. L. F. equation[5].

Distribution Functions of Relaxation Times. —The relaxation spectra $H(\log\tau)$ defined by

4) J. D. Ferry, *J. Am. Chem. Soc.*, **72**, 3746 (1950); F. Schwarzl and A. J. Staverman, *J. Appl. Phys.*, **23**, 838 (1952); C. A. Dahlquist and M. R. Hatfield, *J. Colloid Sci.*, **7**, 253 (1952).

5) M. L. Williams, R. F. Landel and J. D. Ferry, *J. Am. Chem. Soc.*, **77**, 3701 (1955).

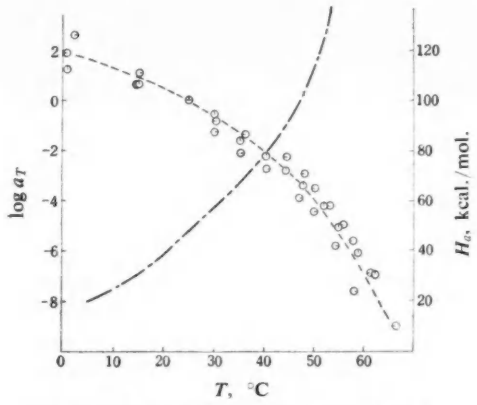

Fig. 4. Temperature dependence of shift factors.
⊖ Sample I, ⊖ Sample II, ⊖ Sample III
----- mean curve of log a_T versus T relation, --- H_a

the following Eq. 2 are calculated from the composite relaxation curves shown in Figs. 3a, 3b and 3c by the second order approximation[6].

$$E_r = \int_0^\infty H(\log\tau)\mathrm{e}^{-(t/\tau)}\,\mathrm{d}\log\tau \qquad (2)$$

$$H\left(\log\frac{\tau}{2}\right) = \left[-\frac{\mathrm{d}E_r}{\mathrm{d}\log t} + \frac{1}{2.303}\frac{\mathrm{d}^2E_r}{\mathrm{d}(\log t)^2}\right]_{t=\tau} \qquad (3)$$

The obtained relaxation spectra are plotted against $\log\tau$ in Fig. 5. Each spectrum shows the typical box type character, except the structure in details, which is expected to follow a wedge type spectrum at the shorter time region.

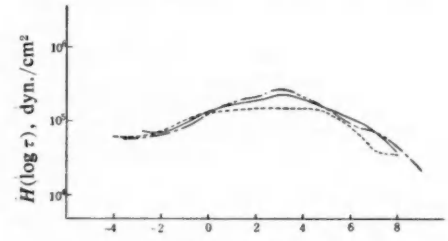

Fig. 5. Relaxation spectra.
----- Sample I
—— Sample II
--- Sample III

They nearly superpose each other at a short time region in Fig. 5. On the longer time side than one hour some difference is seen, and the spectrum goes upwards as the average molecular weight becomes larger, though in the curves of samples II and III the difference is very small and besides, when seen in details, the exchange of the mutual position is found. At the long time end the spectrum of the sample III tends to extend furthest[7].

Summary and Conclusion

A stress relaxation experiment was made for the gels of polyvinyl alcohol-Congo red-water system using the chainomatic balance relaxometer. Three samples of polyvinyl alcohol whose molecular weight were 3.5×10^4, 4.9×10^4 and 9.8×10^4 were used, and the composition of the gels was maintained to be the same for all specimens: polyvinyl alcohol 17.5% and Congo red 1.75%. The measurement was made to ten hours and the temperature was changed from about 1°C to about 66°C.

The obtained relaxation curves were superposed to a composite relaxation curves for each sample according to the time-temperature superposition principle, and the curves ranging from 10^{-4} to 10^9 hours were obtained, and from those the relaxation spectra were calculated by the second order approximation.

It is seen that the three spectra are nearly all superposed on the shorter time side than one hour and that the maximum value becomes larger as the molecular weight increases, and that the two spectra of the larger molecular weight are very close on the whole, except that at the long time end the spectrum of the largest molecular weight tends to extend further.

It is also seen that the box type spectrum of the gel nearly superposes when the molecular weight is larger than a certain value M, where $4.8\times10^4 > M > 3.5\times10^4$, and that the spectrum tends to extend to longer time region as the molecular weight increases.

The author is indebted to Mr. Mineo Watase, Mr. Kokichi Seo and Mr. Hiroshi Osada for their cooperation in carrying out this experiment.

Department of Chemical Industry
Faculty of Engineering
Shizuoka University
Oiwake, Hamamatsu

6) F. Schwarzl and A. J. Staverman, *Physica*, **18**, 791 (1952).
7) A. V. Tobolsky, *J. Appl. Phys.*, **27**, 673 (1956).

*Physical Properties and Crystal Structure of 2-Bromo-2, 3, 3-trimethylbutane**

By Tsutomu KOIDE, Yoshihiro KATO** and Tsutomu ODA

(Received May 23, 1960)

It has been shown that the haloethane derivatives such as 1, 1, 1, 2-tetrachloro-2-methylpropane[1] and other compounds whose molecules are similar to hexamethylethane[2] in shape possess polymorphism and for any temperature range below their melting points they possess molecular orientational or rotational freedom. This freedom in the high temperature modification, which is cubic, seems to be responsible for their relatively high melting points.

Since the van der Waals radius of bromine atom is nearly equal to that of chlorine[3], it is of interest to investigate the behavior of molecules in the solid state for bromo-derivatives of ethane in comparison with the same state of its chloro-derivatives[1,4]. As an example, the authors have studied the crystal structure and the behavior of molecules of 2-bromo-2, 3, 3-trimethylbutane by means of optical, X-ray and differential thermal analysis methods.

Experimental and Results

Materials. — The sample of 2-bromo-2, 3, 3-trimethylbutane was prepared by passing gaseous hydrogen bromide through an ethereal solution of pentamethylethanol, which had been obtained by the Grignard reaction of pinacolone with magnesium bromide in ethereal solution. The final product was twice purified by recrystallization, followed by sublimation in high vacuum (10^{-5} mmHg).

The melting point is found to be 151°C in a sealed capillary tube. The liquid phase vaporizes immediately after melting. The solid is soft and shows plasticity. The density is found to be 1.31 g./cc. at 13°C by the flotation method using an aqueous solution of calcium carbonate.

Optical Observation.—Under the polarized microscope, the room temperature phase was found to be isotropic, indicating the crystal to be cubic. Observations were extended to the liquid air temperature. The cryostat for this purpose is shown in Fig. 1. Cooling was made by heat conduction through a copper rod dipped in liquid air. The temperature was measured with a copper-constantan thermo-couple and a millivoltmeter. By cooling, it was observed that the crystal transformed at about −117°C into a different crystalline phase which was optically anisotropic.

X-ray Measurements.—*The Crystal Structure of the High Temperature Modification.*—Owing to its extremely high volatility, a single crystal of this substance, sealed in a capillary tube for X-ray measurement, sublimes gradually in few days into a number of smaller crystals in the cooler part of the tube. Therefore, in order to prevent this loss of sample due to sublimation, a glass rod just fitting the glass capillary was inserted to make the remaining free space as small as possible.

Using Cu-K_α radiation ($\lambda = 1.54$ Å) filtered through nickel foil, we prepared a series of 20° oscillation photographs covering a range of about 90° with [011] as the axis of rotation.

Laue photographs were taken with X-ray beams parallel to [100], [110] and [111]. All of the Laue spots were split into two or three parts, but the same crystal showed no splitting in its oscillation photographs when rotated through [110]. Thus the crystal used was not a single crystal, but was composed of several crystallites which were slightly different in orientation. All the efforts to get a single crystal have been unsuccessful, as was the case of 2-chloro-2, 3, 3-trimethylbutane[5]. All the Laue spots were successfully indexed, based upon a cubic lattice having holotesseral symmetry. The point group symmetry of the crystal was found to be T_d-$\bar{4}3m$, O-43 or O_h-$m3m$.

The observed spectra in oscillation photographs can be indexed satisfactorily with a body-centered cubic lattice having a unit cell of the side $a = 7.66$ Å. The observed value of density, 1.31 g./cc., is almost equal to the calculated value, 1.32 g./cc., assuming that two molecules are contained in the unit cell.

Differential Thermal Analysis (D. T. A.).—The apparatus used for the D. T. A. was described elsewhere[1]. The temperature range of the measurement was from 90°C to the liquid air temperature. Fig. 2 shows the result of the D. T. A. measurement for warming. The time-temperature curve of Fig. 2 shows the temperature of the used reference substance (sodium chloride) and the differential curve shows the temperature difference between the reference

* Presented at the 11th Annual Meeting of the Chemical Society of Japan, Tokyo, April, 1958.

** Present address,, Daitetsu High School, Matsubara City, Osaka.

1) T. Koide, T. Oda and I. Nitta, This Bulletin, **29**, 738 (1956).

2) D. W. Scott, D. R. Doulsin, M. E. Gross, C. D. Oliver and H. M. Huffman, *J. Am. Chem. Soc.*, **74**, 883 (1954).

3) L. Pauling, "The Nature of the Chemical Bond", Cornell Univ. Press, Ithaca (1948), p. 189.

4) T. Koide, T. Oda and I. Nitta, This Bulletin, **30**, 199 (1957).

5) T. Koide and S. Takeuchi, T. Oda, Y. Yamada and I. Taguchi, ibid., **30**, 680 (1957).

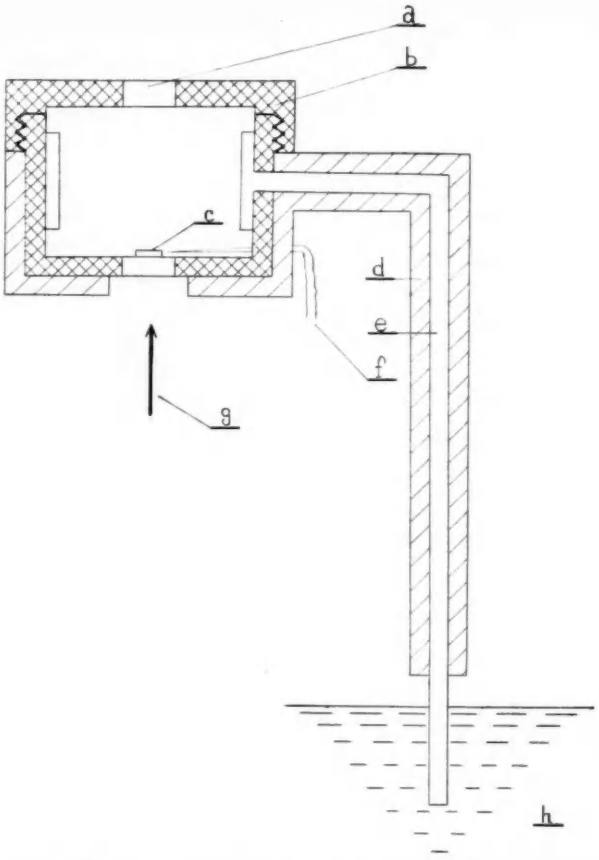

Fig. 1. The cryostat for the optical measurement at low temperature.
a) window (glass), b) bakelite, c) sample, d) thermal insulator, e) copper rod, f) thermocouple, g) polarized light, h) liquid air

substance and the sample. The temperature differences are plotted on an arbitrary scale. There is an anomalous thermal effect at about -114°C (the peak of the differential curve in Fig. 2) for warming and at about -117°C for cooling. This result is in good agreement with the optical observation.

Discussion

Since there are two molecules in each unit cell with the body-centered cubic lattice, it is reasonable to place the centers of mass of the molecules at the lattice points 0, 0, 0 and 1/2, 1/2, 1/2. The proper symmetry of these points is T_d-$\bar{4}3m$, O-43 or O_h-$m3m$, so that the symmetry of the molecule should have one of these cubic point groups. On the other hand, if we assume that the molecule has the skew configuration (Fig. 3), the highest symmetry that the molecule could have is C_s-m, the central C–C bond lying on the plane of symmetry. In order that the molecule, which has the symmetry C_s-m, attains the cubic symmetry, it is necessary to take into consideration some statistical arrangements for explaining the structure of the crystal, as was done in the X-ray studies of other plastic crystals[6].

One of the possibilities that the statistical symmetry of the molecule is as high as T_d-$\bar{4}3m$ is that the molecule orientates its central C–C axis parallel to each one of the four body-diagonals statistically equally, so that the C–C axis acquires at least a statistical symmetry

6) C. D. West, *Z. Krist.*, **88**, 195; C. Finbak, *Tids. Kjem, Bergv.*, **17**, 2 (1937); M. Atoji, T. Oda and T. Watanabe, *Acta Cryst.*, **6**, 868 (1953); I. Nitta and T. Watanabe, This Bulletin, **13**, 28 (1938); T. Oda and T. Watanabe, *J. Chem. Soc. Japan, Pure Chem. Sec.* (*Nippon Kagaku Zasshi*), **65**, 154 (1944); T. B. Reed and W. N. Lipscomb, *Acta Cryst.*, **6**, 108 (1958).

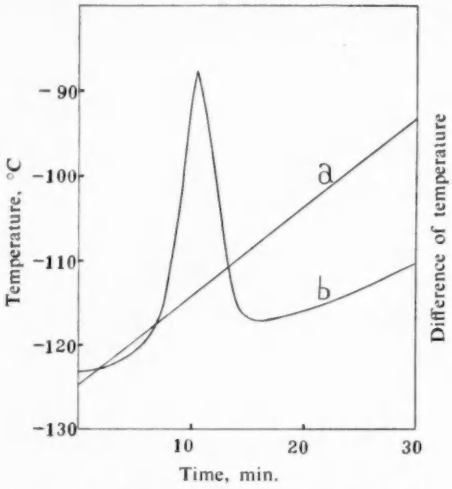

Fig. 2. Differential thermal analysis curve for 2-bromo-2,3,3-trimethylbutane $Br(CH_3)_2C\cdot C(CH_3)_3$.
a) time-temperature curve
b) differential curve

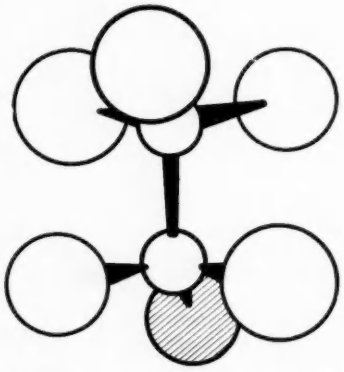

Fig. 3. The assumed model for the free molecule of 2-bromo-2,3,3-trimethylbutane. The small circle represents the carbon atom, the large circle the methyl group and the hatched one the bromine atom.

of $3m$. Following such a statistical configuration, a calculation of structural factors was carried out, using two models, Ia (Fig. 4) and Ib, which are slightly different from each other. Namely in Ia, the two bromine atoms were assumed to lie statistically on the twenty-four equivalent positions, 24 (g)[7] near the three principal axes, and the ten CH_3 groups on another set of the same equivalent positions.

7) "International Tables for X-ray Crystallography", Vol. I, Kynoch Press, Birmingham (1952), p. 326.

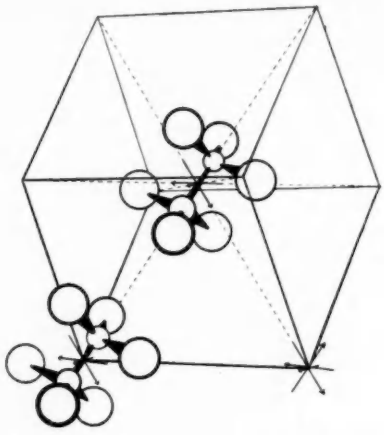

Fig. 4. The model for a statistical configuration, Ia.

In Ib the bromine atoms and the methylic carbon atoms lie separately on two sets of forty-eight equivalent positions, (h) with a weight 1/24 for bromine and 5/24 for C. It is to be added here that in these calculations the molecule was assumed to possess the skew form with the C–C and C–Br bond distances, 1.54 and 1.94 Å, and the tetrahedral valency angle.

If half of the molecules, in a statistical sense, rotate their molecular axes around the principal crystal axes through 90°, then the polar molecular axes will be found in eight different directions parallel to the body-diagonals of the crystal. If we add this operation to model Ia, the symmetry of the crystal will become O^9_h-$Im3m$. We shall call this model IIa. In this model, the polar axes of the molecules will be found in antiparallel orientations, whereas the bromine atoms and methyl groups will remain in almost the same positions as in model Ia. In these two models Ia and IIa, methyl groups and bromine atoms belonging to any two neighbouring molecules are found in trans configuration. By twisting the molecular axis from the positions given by model IIa, we have model IIb (angle of twist ±15°), model IIc (angle of twist ±40°) and model IId (angle of twist ±60°). The symmetry of these three models remains as in IIa.

In addition to these models, which are statistically static, we have also considered model III, in which molecules are rotating spherically around their centers of mass. The crystal will also assume the symmetry of O^9_h-$Im3m$.

The calculated $|F|$-values based on these models are plotted in Fig. 5, together with the observed data. Curve III is quite different

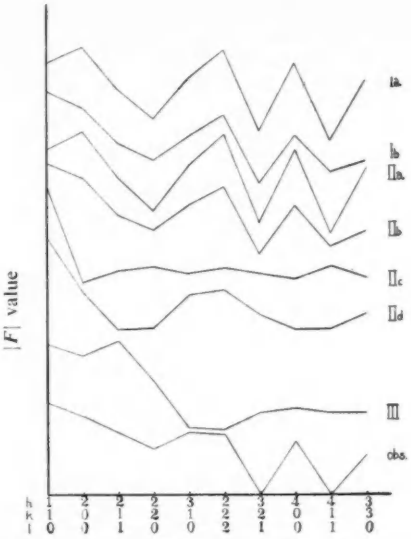

Fig. 5. Observed and calculated values of $|F|$.

from the observed one, suggesting that the free rotation of molecules as a whole in the crystal is ruled out. As a matter of fact, the domain required for the free rotation of the molecules at each lattice point overlaps not only with those of the first neighboring molecules but also with the second neighboring molecules as shown in Fig. 6. The curves for the models IIc and IId also do not agree with the observed one.

The curve Ia agrees fairly well with the observed one. In this model, though there is no appreciable overlap between the first neighboring molecules, there remains the possibility of colliding between the second neighboring molecules (Fig. 6). The agreement between the intensities calculated by model IIb, Ib and the observed ones is the best among all the models so far investigated. In these models, none of the shortest distances between atoms in neighboring molecules exceeds appreciably the sum of the van der Waals radii. It is difficult to decide which one of models, Ib or IIb, is really the case in point. The actual configuration may be expressed by a combination of Ia, Ib, IIa and IIb with appropriate weights.

This statistical structure may throw light on the explanation of the plasticity and rapid decrease of intensity with the increase of diffraction angle.

The orientational disorder of the arrangement of molecules may disappear below the transition temperature. This view is supported by the thermal differential analysis. The change of the optical property from isotropic to anisotropic in passing the transition temperature means that the crystal assumes the lower symmetry. This may imply that the arrangement of the molecules becomes more ordered than that of the room temperature phase.

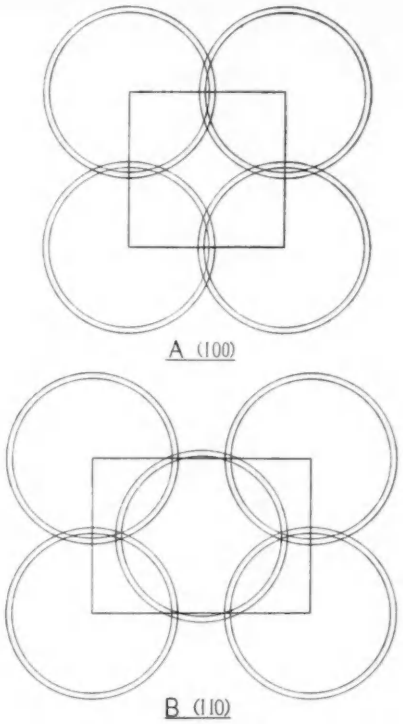

Fig. 6. The required domain for the free rotation of molecule at each lattice point. The radii of these circles are calculated using assumed molecular configuration and van der Waals radii for bromine (outer circles) and methyl groups (inner).
A shows the section parallel to (100).
B shows the section parallel to (110).

It has been reported that 1, 1, 1, 2-tetrachloro-2-methylpropane[1] and 2-chloro-2, 3, 3-trimethylbutane[4] also give plastic crystals at high temperature. Both of these also belong to the body-centered cubic lattice and the fact that their unit cell dimensions (7.4 and 7.62 Å) are close to the value of the present substance indicates that the free volumes of these molecules are similar.

Summary

2-Bromo-2, 3, 3-trimethylbutane gives a plastic crystal, which is optically isotropic and has a density of 1.31 g./cc. at 13°C. The X-ray data

can be interpreted on the bases of a body-centered cubic lattice, having $a=7.66$ Å with two molecules in the unit cell. The symmetry interpretation gives a structure of disordered orientation of molecules. It was found, by means of optical and differential thermal analysis methods, that there is a phase transition at about -114°C, below which the crystal is of a lower symmetry.

The authors express their hearty thanks to Professor Isamu Nitta, Professor Tokunosuke Watanabé and Dr. Syuzo Seki for their interest during this study. They also express their thanks to Dr. Hiroshi Suga for his help in optical measurements, and to Mr. Yoshiyuki Namba for his discussion. A part of the cost of this research was supported by the Ministry of Education, to which their thanks are due.

Laboratory of Chemistry
Osaka University of
Liberal Arts and Education
Tennoji, Osaka

Variation of Radiocarbon Concentration in Modern Wood

By Kunihiko KIGOSHI and Yoshio TOMIKURA

(Received May 27, 1960)

It has recently been pointed out by several authors[1-7] that the atmospheric radiocarbon is increasing because of nuclear tests. The present authors have also detected a remarkable change of the atmospheric radiocarbon concentration after 1953. This recent increase of radiocarbon and the Suess effect[5-10], i.e. the dilution effect of atmospheric radiocarbon by combustion of fossil fuel play an important role in the studies on the carbon dioxide cycle in nature. The present paper presents the results of the measurements on the change of the atmospheric radiocarbon contents in recent years using the carbon in tree rings taken from Honshu Island. We used the tree rings of Japanese cedar (*Crytomeria Japonica*) of which the place of growth and the date of cut were known. The measurements of radiocarbon were made with an acetylene filled proportional counter shielded with iron plates and provided by anticoincidence counters.

1) W. S. Broecker and A. Walton, *Science*, **130**, 309 (1959).
2) G. S. Bien and H. E. Suess, *Z. für Physik*, **154**, 172 (1959).
3) K. O. Munnich and J. C. Vogel, *Naturwiss.*, **45**, 327 (1958).
4) T. A. Rafter and G. J. Fergusson, *Science*, **126**, 557 (1957).
5) T. A. Rafter and G. J. Fergusson, *N. Z. J. Sci. Tech.*, **B38**, 871 (1957).
6) T. A. Rafter and G. J. Fergusson, U. N. Con. on the Peaceful Uses of Atomic Energy, **18**, 526 (1958).
7) Hl. de Vries, *Science*, **128**, 250 (1958).
8) R. Revelle and H. E. Suess, *Tellus*, **9**, 18 (1957).
9) H. R. Brannon, A. C. Daughtry, D. Perry, W. W. Whitaker and M. Williams, *Trans. Am. Geophys. Union*, **38**, 643 (1957).
10) G. J. Fergusson, *Proc. Roy. Soc.*, **A243**, 561 (1958).

Experimental Procedures

Apparatus.—A stainless steel tube proportional counter is placed in the middle of eleven anti-coincidence Geiger counters inside of an iron shield of 23 cm. in thickness. The pulses from the proportional counter are delaye 10 micro second and are mixed with the pulses of the anticoincidence counters. The background of the proportional counter is 5.46 ± 0.3 counts per minute. The proportional counter used for these experiments has the dimensions of 3.5 cm. in inner diameter and of 52 cm. in length. The center anode is stainless steel wire of 0.05 mm. in diameter. The effective volume of the counter is 420 ml.

Preparation of Acetylene from a Wood Sample.—A wood sample is heated in a metal crucible in order to remove the volatile organic substance. This procedure makes the sample charcoal. The charcoal is converted into strontium carbonate by the following procedures; combustion in a current of oxygen, absorption of carbon dioxide in 6 N ammonia water, precipitation of calcium carbonate from an ammonium carbonate solution, evolution of carbon dioxide with hydrochloric acid from the calcium carbonate, absorption of carbon dioxide into ammonia water and precipitation of strontium carbonate. The preparation of acetylene from the strontium carbonate is done in a stainless steel tube which is illustrated in Fig. 1.

The mixture of strontium carbonate (8 g.) and magnesium powder (8 g.) is heated in the stainless steel tube by an electric furnace. The tube is connected to a vacuum line and when the temperature rises to 300~400°C the pumping system is cut by the metal cock. The best way to get a good result is to heat the tube up to 800~900°C for more than 4 hr. Very often a kind of explosion was observed during the heating up to 800°C. The

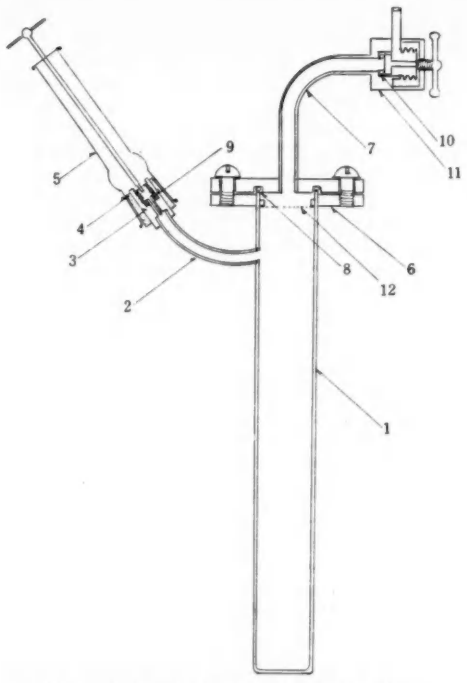

Fig. 1. Tube for preparation of acetylene.
1. Stainless steel tube of 30 mm. in diameter, 780 mm. length
2, 7. Copper tube of 8 mm. in diameter
3. Metal cock for the injection of water
4. Rubber stopper
5. Glass cylinder of 20 mm. in diameter, 150 mm. in length
6. Steel frange
8, 9, 10. O-ring
11. Metal cock
12. Glass filter

explosion can be detected by a sudden temperature rise. The explosion takes place around 450~600°C and if the reaction were stopped just after the explosion, one would get around 60% of acetylene of the calculated value*. Heating up to 800°C after the explosion gives good acetylene yield of 85~95% of the calculated value.

After the preparation of carbide in the stainless steel tube, this is connected to another vacumm line with several cold traps for the purification of acetylene. Acetylene and hydrogen which are evolved by adding water through the side tube to carbide are dried with dry ice in the cold trap. The acetylene is separated from the hydrogen by a trap cooled with liquid nitrogen. The charcoal trap cooled with dry ice removes effectively the contaminated radon from the acetylene. However, since contamination of radon, though it is trace

* When the amount of reaction mixture is large, the temperature rise at the explosion is high enough to produce carbide in fairly good yield.

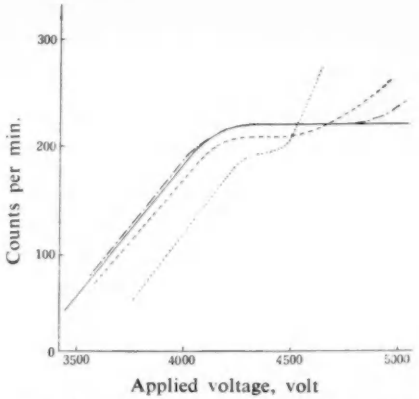

Fig. 2. Characteristic curves of acetylene filled (1 atm.) propertional counter.
——— Pure acetylene
– – – – Acetylene with 0.1% air
– – – 〃 0.2% air
– – – – – – 〃 0.9% air

amount (less than one count per minute), was observed even with these purifications, the acetylene had to be stored in a flask more than three weeks before the activity measurement was made.

Characteristics of the Acetylene Filled Counter.—A solid curve in Fig. 2 shows a typical characteristic curve of an acetylene filled proportional counter. The slope of the plateau is constant over the wide range of acetylene pressure within 2% increase per 100 volts. The starting voltage of the plateau is

$$V=(2100+2.98\times P) \text{ volts}, \quad 200<P<800$$

where P is the pressure of acetylene in mmHg. The counter was used with a voltage higher than the starting voltage by 250 volts.

The characteristic curve of the proportional counter changes with the content of impurity of acetylene as is shown in Fig. 2. The allowable maximun amount of impurities such as moisture or air which gives a serious effect on the characteristic curve is abous 0.2% of the total gas. This amount is large enough to operate the counter in a good condition without any special care such as is necessary for the carbon dioxide filled counter that is seriously affected by contaminated air of 0.001% of filling gas[11].

Effect of the Tritium Activity.—Fig. 3 shows counts per minute for the different amounts of acetylene gases of modern and dead carbon. There is no change in counts per minute in the case of dead carbon. This indicates that the acetylene produced from dead carbon (from coal or lime) has no activity. The extrapolated values of counts per minute at pressure zero for modern and dead carbon agree with each other within the experimental error of 0.06 count per minute. This shows that the observed activity of the acetyene produced from modern carbon is attributed to the carbon and not to the tritium in acetylene.

11) Hl. de Vries and W. Barendsen, *Physica*, **19**, 987 (1953).

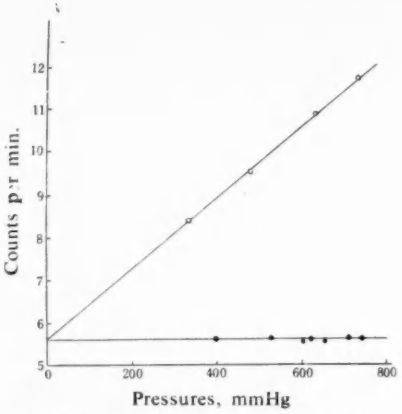

Fig. 3. Relation between counts per minute and pressure of acetylene.
○ Modern carbon, ● Dead carbon

Counting Procedure.—Acetylene gas stored more than three weeks is filled in the proportional counter and its characteristic curve is measured. According to the characteristic curve and the pressure in the counter one sets high voltage to be applied. The counting time is usually 48 hr. and the counts are checked every 5 or 10 hr. Background measurements are made for 24 hr. in every two or four days.

Experimental Results

Table I summarizes the data of the measurements of radiocarbon concentrations in the tree ring samples which were obtained from tree No. 1. Tree No. 1 grew in Akita Prefecture in Honshu Island. This tree has an age of 177 years and was cut in December, 1958. Each tree ring has more than 2 mm. thickness and shows clear boundaries.

The first column of Table I indicates the intervals in which the tree rings grew. The second column shows observed counts per

TABLE I. VARIATION OF C-14 CONCENTRATION IN TREE RINGS GROWN BETWEEN 1789 AND 1950 (Sample tree No. 1)[a]

Intervals of growth of tree ring	Counts per min. g. carbon	C-14 concentration[b]
Aug.1782～Sept.1798	11.69±0.18	0.960±0.015
Aug.1799～Sept.1808	12.02±0.18	0.986±0.015
Aug.1809～Sept.1818	12.19±0.18	1.000±0.015
Aug.1819～Sept.1828	11.90±0.18	0.976±0.015
Aug.1829～Sept.1838	12.10±0.18	0.988±0.015
Aug.1839～Sept.1848	12.19±0.18	0.998±0.015
Aug.1849～Sept.1858	12.14±0.18	0.990±0.015
Aug.1859～Sept.1863	12.24±0.18	1.000±0.015
Aug.1864～Sept.1868	12.24±0.18	1.000±0.015
Aug.1869～Sept.1873	12.39±0.18	1.010±0.015
Aug.1874～Sept.1878	12.47±0.14	1.015±0.011
Aug.1879～Sept.1883	12.49±0.18	1.015±0.015
Aug.1884～Sept.1888	12.18±0.14	0.986±0.011
Aug.1889～Sept.1893	12.63±0.18	1.028±0.015
Aug.1894～Sept.1998	12.40±0.18	1.008±0.015
Aug.1899～Sept.1903	12.47±0.14	1.011±0.011
Aug.1904～Sept.1908	12.47±0.18	1.011±0.015
Aug.1909～Sept.1913	12.52±0.18	1.013±0.015
Aug.1914～Sept.1918	12.47±0.18	1.010±0.015
Aug.1919～Sept.1923	12.02±0.18	0.974±0.015
Aug.1924～Sept.1928	12.20±0.18	0.982±0.015
Aug.1929～Sept.1933	12.39±0.14	1.000±0.011
Aug.1934～Sept.1938	12.60±0.18	1.017±0.015
Aug.1939～Sept.1943	12.02±0.18	0.968±0.015
Aug.1944～Sept.1945	12.42±0.18	1.000±0.015
Aug.1945～Sept.1946	12.52±0.14	1.011±0.011
Aug.1946～Sept.1947	12.10±0.18	0.974±0.015
Aug.1947～Sept.1948	12.04±0.18	0.970±0.015
Aug.1948～Sept.1949	12.38±0.18	0.997±0.015
Aug.1949～Sept.1950	11.78±0.18	0.949±0.015

a) The data are normalized to the concentration of C-14 of the hypothetical modern wood which would not have been affected by industrial effect and nuclear tests.
b) Grown in Akita Prefecture in Honshu Island.

TABLE II. VARIATION OF C-14 CONCENTRATION IN TREE RINGS GROWN AFTER 1950

Intervals of growth of tree rings	C-14 concentration in tree rings		
	Sample No. 1	Sample No. 2[a]	Sample No. 3[b]
Aug. 1950～Sept. 1951	1.010±0.015		
Aug. 1951～Sept. 1952	1.000±0.015		
Aug. 1952～Sept. 1953	0.994±0.014		
Aug. 1953～Sept. 1954	1.012±0.014		
Aug. 1954～Sept. 1955	1.034±0.014		
Aug. 1955～Sept. 1956	1.050±0.011	1.037±0.011	
Aug. 1956～Sept. 1957	1.092±0.015	1.081±0.011	1.084±0.011
Aug. 1957～Sept. 1958	1.122±0.014[c]	1.083±0.011	1.086±0.011
Aug. 1958～Sept. 1959		1.238±0.011	1.240±0.011

a) Grown on the campus of Gakushuin University in Tokyo.
b) Grown in Mie Prefecture in Honshu Island.
c) This sample includes the tree rings up to December, 1958.

minute for one gram carbon of each sample. The third column gives the concentrations of C-14 in tree rings at the year indicated in the first column. The concentrations are normalized to the mean value of 18 measured concentrations between 1782 and 1913 (Table I). This mean value will be referred to as a concentration of C-14 in hypothetical modern wood which would not have been affected by industrial effect and nuclear tests.

Table II gives a summary of our data on the tree ring samples after 1950. The second column shows the concentrations of C-14 in the samples which were obtained from tree No. 1. The third and the fourth columns give the results on the trees which grew in Tokyo and Mie Prefecture. Tree No. 2 (the third column) was cut in September, 1959, and No. 3 (the fourth column) in August, 1959. These three series of measurements agree well, and indicate a remarkable increase after the autumn of 1958. The errors indicated in Tables I and II include only statistical counting errors (standard deviations).

Discussion

The tree ring is a sample formed by constant accumulation of carbon from the atmosphere and is dated by clear boundaries. The examination of the data on the concentration of C-14 in the tree rings gives information on the annual average concentration of C-14 in the atmosphere. Moreover, if samples from the same species of tree were used, the differences of the possible isotopic fractionation among the samples might be negligibly small*. These make the tree ring samples adequate for the studies on the annual variation of C-14 concentration in the atmospheric carbon. However there are some questions about the nature of the sample. First, there is a possibility that the carbon which is taken up through the root could be used for assimilation. Second, the carbon dioxide from the pedosphere might be utilized for assimilation by aerial transport to leaf level. Finally there is a question when the organic substance in a certain part of tree ring was synthesized from the carbon dioxide.

The first and the second question had been discussed by W. Whitaker et al.[12] They suggested a possible influence of the uptake of older carbon by the root system as the most likely explanation of differences in radiocarbon contents of trees from different enviroments. If such an influence plays an important role for a tall tree, the increase in radiocarbon contents in tree rings after 1953 would be less than the increases in atmospheric radiocarbon contents. The authors favor the assumption that this influence is negligibly small because the direct experimental evidences on young pea and barley plants show a small amount of uptake of carbon dioxide through the root system[13]. The experimental results of Whitaker et al. on the effect of the aerial transport for carbon dioxide from pedosphere to leaf level show the absence of any significant amount of old carbon cycling from pedosphere to the leaves of trees.

On the circulation of synthesized organic substances in the tree we have some knowledge which will serve to show when the organic substances in a certain part of the tree ring was synthesized from the atmospheric carbon dioxide. The large cells which are adjacent to the boundary of a tree ring are formed in the spring of the year from the carbon dioxide existing in the atmosphere and from the organic substances, which were synthesized after the summer of the preceding year and have been stored in the older tree rings. The cells which are formed after the middle of the summer of the year become smaller. Finally the smallest cells are formed in September forming the boundary of the tree ring. A large part of the organic substances synthesized during the middle of summer and autumn is stored in a newly formed tree ring[14]. The stored organic substances will be used for the formation of new cells in the next spring. It is therefore desirable to cut down the tree in summer for the measurement.

In general it can be said that the tree ring is made by the atmospheric carbon dioxide during August of the preceding year and September of this year. Although formation of boundaries can be influenced easily by the climate of the place where the sample tree grew, the expected error of the indicated intervals of growth of tree rings in Table I and II may be within one month.

Examination of the results listed in Table I shows a constant concentration of C-14 in the atmosphere between 1782 and 1950 within an error of 2%. Fergusson[10] reported 2% depletion of C-14 concentration in the atmospheric carbon dioxide between 1860 and 1954. Although the limits of statistical counting error of the data are rather broad, the present data seem to support the opinion that the depletion is less than 2% between 1782 and 1950.

* The measurements on the isotopic ratio of $^{13}C/^{12}C$ in tree ring carbon by Fergusson[10] and Broecker et al.[1] show a constant value on the samples from a tree or the trees of same species.

12) W. W. Whitaker, S. Valastro, Jr. and M. Williams, *J. Geophys. Res.*, **64** 1023 (1959).

13) J. A. J. Stolwijk and K. V. Thimann, *Plant Physiol.*, **32**, 513 (1957).

14) J. H. Priestley, *New Phytologist*, **24**, 316 (1930).

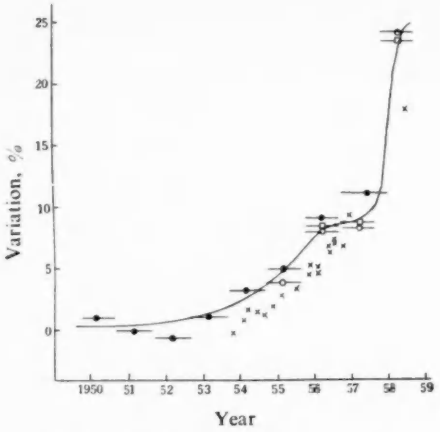

Fig. 4. Variation of C-14 concentration in the atmosphere.

Data of this paper
● Akita
○ Tokyo
□ Mie
—— Interval of growth of tree ring.
Standard deviation; 1.1~1.5%

Data by Rafter and Fergusson, ×

All the data in Table II as are plotted in Fig. 4 show no essential difference among the three samples except the value of sample No. 1, 1957—1958. Since sample No. 1 was cut in December, 1958 and its last tree ring (1957—1958) was very likely to have incorporated the atmospheric carbon in December, 1958, the higher value corresponds to a sudden increase of atmospheric radiocarbon in the autumn of 1958. It could be concluded that there was no local variation along the south east shore line of Honshu Island from the fact that there is no meaningful difference among the values of the three samples. Bien and Suess[2] reported the variation of C-14 concentration in the tree ring samples up to 1957. These values agree with the present data within the experimental errors. It seems very likely that the local variation of the atmospheric radiocarbon contents is very small, at least in the temperate zone of the northern hemisphere.

In Fig. 4 the plot of the variation of C-14 concentration in the southern atmosphere reported by Rafter and Fergusson[5,6] indicates a systematic delay of the variation to that of the present data. Although the limits of error on the time scale of the present data are rather broad, the delay of the variation of the atmospheric C-14 concentration in the southern hemisphere seems to be several months in length. Broecker and Walton[1] discussed the difference of the atmospheric C-14 concentration between the northern and southern hemispheres. The present result seems to agree with that of Broecker and Walton.

Summary

1) Using the tree ring samples, the variation of C-14 concentration in the atmosphere since 1782 has been measured by the use of trees growing in Japan. The results show a constant concentration of C-14 in the atmosphere during 1782 and 1950 within the error of 2%.

2) The depletion of C-14 concentration in the atmospheric carbon dioxide between 1782 and 1950 seems to be less than 2%.

3) The observed annual variations on the samples from Tokyo, Akita and Mie Prefectures show almost the same amount of increase after 1953. There is a good agreement between our data and those on the tree ring samples taken in California by Bien and Suess. The concentration of C-14 in the atmosphere averaged over a year seems to have little difference in the temperate zone of the northern hemisphere.

4) The variation of C-14 concentration in the atmosphere of the southern hemisphere seems to follow that of the northern hemisphere with a time lag of several months.

The cooperation of Mr. T. Tokumoto and other officers of the Government Forest Experiment Station and Mr. T. Iwata of the Ise Shrine who supplied the tree samples is gratefully acknowledged. The authors wish to thank Dr. E. Tajima for valuable advice. A part of the expense for this work has been defrayed by the Ministry of Education.

Department of Physics
and Chemistry
Gakushuin University
Mejiro, Toshima-ku, Tokyo

Spectrophotometric Determination of Bismuth with Xylenol Orange

By Hiroshi ONISHI and Nasumi ISHIWATARI

(Received May 24, 1960)

Xylenol Orange was first proposed by Körbl and Pribil[1] as a metal indicator for the EDTA titration. Cheng recently described photometric methods for the determination of zirconium[2], hafnium[3], and iron[4] using Xylenol Orange. It does not appear, however, that a photometric method for determining bismuth with this reagent has been reported.

The present paper reports the conditions for the spectrophotometric determination of bismuth with Xylenol Orange including the effect of foreign substances. The composition and formation constant of the bismuth complex are also discussed.

Experimental

Apparatus.—Absorbance measurements were made with a Hitachi Model EPU-2A spectrophotometer, using 1 cm. cells.

Solutions. — L-Ascorbic acid, 10 g. in 100 ml. of water, may be used for several days. A 0.1 g. portion of sodium fluoride was dissolved in 100 ml. of water. A 0.10 g. portion of Xylenol Orange, Dotite XO (Dojindo & Co., Ltd., Kumamoto) was dissolved in 100 ml. of water. This solution can be kept for at least one week. Standard bismuth solution was prepared by dissolving 0.500 g. of pure bismuth metal in a few milliliters of nitric acid, evaporating the solution to dryness on a water bath, dissolving the residue in 1 : 9 nitric acid, and making up to 500 ml. From this stock solution (1.00 mg. Bi per ml.) a working standard solution (e. g., 40 p.p.m. Bi) was prepared by dilution.

Procedure.—Transfer the sample solution (dilute nitric acid solution) containing 10~80 μg. of bismuth to 25 ml. volumetric flask and adjust the nitric acid concentration to make the acidity 0.08~0.12 N after diluting to volume. If the acidity of the sample solution is too high, neutralize excess of acid with sodium hydroxide. Dilute the solution to about 15 ml. with water. Add 1 ml. of ascorbic acid solution and allow to stand at room temperature for about 5 min. Next add 1 ml. of sodium fluoride solution, mix, add 1.0 ml. of Xylenol Orange solution. After diluting to the mark with water and mixing, measure the absorbance of the solution in a 1 cm. cell at 530 mμ. Use the reference solution containing the same amounts of Xylenol Orange and other reagents.

1) J. Körbl and R. Pribil, *Chemist-Analyst*, **45**, 102 (1956); J. Körbl, R. Pribil and A. Emr, *Collection Czechoslov. Chem. Communs.*, **22**, 961 (1957).
2) K. L. Cheng, *Talanta*, **2**, 61 (1959).
3) K. L. Cheng, ibid., **3**, 81 (1959).
4) K. L. Cheng, ibid., **3**, 147 (1959).

Results and Discussion

The absorption spectra for Xylenol Orange and its bismuth complex are shown in Fig. 1. When a correction is applied for the reagent blank, an absorption peak is found at about 520 mμ. Because the reagent blank against water at 520 mμ is about twice as much as that at 530 mμ, the wavelength of 530 mμ has been adopted for the determination of bismuth.

The effect of nitric acid concentration on the absorbance of bismuth complex is shown in Fig. 2. The absorbances were measured against respective reagent blanks. It is seen that the acidity of 0.08~0.12 N is suitable. Perchloric acid or sulfuric acid also gives the same results as does the nitric acid.

As shown in Fig. 3, a practically constant

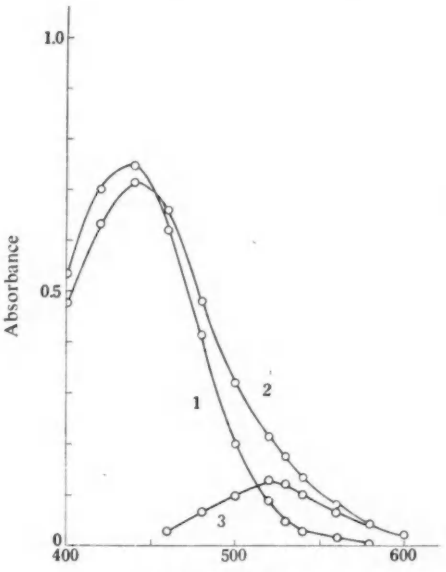

Fig. 1. Absorption spectra;
1. Xylenol Orange (against water),
2. 1.6 p.p.m. Bi (against water),
3. 1.6 p.p.m. Bi (against reagent blank).

Table I. Stability of colored solution

Time after color development, hr.	Absorbance					
	40 μg. Bi HNO_3 soln.*	80 μg. Bi HNO_3 soln.*	40 μg. Bi HNO_3 soln.	80 μg. Bi HNO_3 soln.	40 μg. Bi $HClO_4$ soln.*	40 μg. B. H_2SO_4 soln.*
About 1/4	—	0.244	0.104	0.207	—	—
1	0.128	0.239	0.104	0.208	0.136	0.123
2	0.128	0.235	0.104	0.207	0.132	0.122
3	0.128	—	0.103	0.207	0.134	0.120
16～20(Overnight)	0.128	0.212	0.101	0.206	0.135	0.120

* Ascorbic acid and NaF were not added.

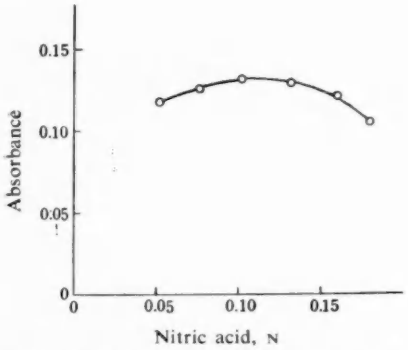

Fig. 2. Effect of nitric acid concentration; 1.6 p.p.m. Bi.

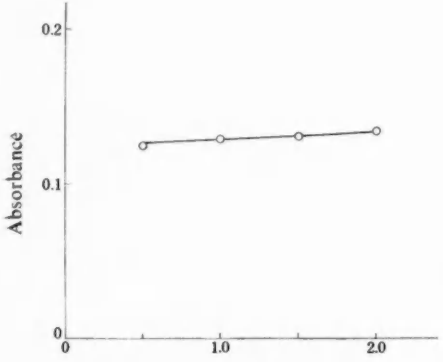

Fig. 3. Effect of Xylenol Orange concentration; 1.6 p.p.m. Bi.

absorbance is obtained by adding more than 0.5 ml. of 0.1% Xylenol Orange solution (final volume = 25 ml.). The absorbances were measured against each reagent blank.

Table I shows the stability of the colored solutions. The absorbances remain constant at room temperature for at least 3 hr.

As shown in Fig. 4, absorbance is proportional to bismuth concentration in the range of 0.4 to at least 3 p.p.m. bismuth (10～80 μg. Bi). At 530 mμ the molar extinction coefficient of bismuth is 1.6×10^4, or 0.014 μg. Bi/cm^2 corresponding to $\log I_0/I = 0.001$. This sensitivity is comparable to that of the iodide method or the thiourea method[5].

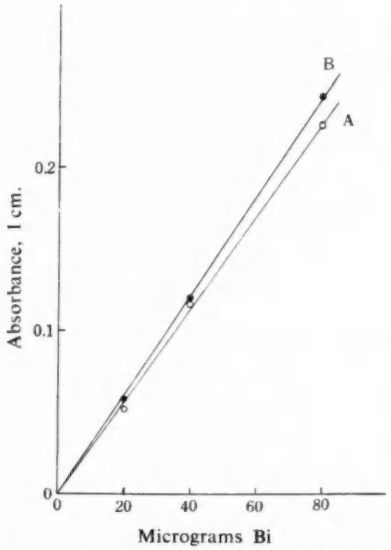

Fig. 4. Absorbance-concentration curve of bismuth;
A. According to the procedure,
B. In the absence of ascorbic acid and NaF.

The effects of many elements on the determination of bismuth were studied under the conditions used in the procedure (Table II). Most of the metals were in the form of nitrate. Microgram amounts of zirconium and thorium can be masked by fluoride ion. The interference of iron(III) can be eliminated by reduction with ascorbic acid. The effect of niobium is

5) E. B. Sandell, "Colorimetric Determination of Traces of Metals", 3rd Ed., Interscience Publishers, Inc., New York (1959), p. 330.

Table II. Determination of bismuth in the presence of foreign substances
(40.0 μg. of Bi taken in each determination)

Addition	Bi found, μg.
10 mg. K	40
0.2 mg. Cu	39
1 mg. Ag[a]	40
88 μg. Au[b]	41
10 mg. Mg	39
10 mg. Ca	39
1 mg. Zn	40
1 mg. Cd	40
2 mg. Hg(II)	41
10 mg. Al	39
0.1 mg. In	41
1 mg. Tl(I)	41
0.1 mg. Ti	39
50 μg. Zr	39
50 μg. Th	42
50 μg. Zr, 50 μg. Th, 1 mg. Fe(III)	37
5 mg. Sn, 5 mg. Sb[c]	36
10 mg. Pb	40
5 mg. P (as KH_2PO_4)	39
0.1 mg. V (as NH_4VO_3)	40
0.1 mg. Nb[d]	38
0.1 mg. Ta	37
1 mg. As(III)	40
1 mg. As(V)	40
0.1 mg. Cr (as $K_2Cr_2O_7$)	38
20 μg. Mo (as NH_4 molybdate)	40
0.1 mg. W (as Na_2WO_4)	39
10 mg. U(VI)	40
0.1 mg. Cl (as NaCl)	40
1 mg. Mn(II)	40
1 mg. Fe(III)	39
2 mg. Co	41
2 mg. Ni	41

a) Solution centrifuged after color development.
b) Ascorbic acid not added.
c) Volatilized with $HClO_4$, HBr and HCl.
d) Fumed with $HClO_4$.

removed by fuming with perchloric acid and treating the residue with 2 ml. of hot 1.4 N nitric acid. Apparently niobium is precipitated by this treatment. Absorbance measurements must be made within an hour after color development. (The absorbance increases after that time.) Tin and antimony can be volatilized by treating with perchloric, hydrobromic and hydrochloric acids. Five milligrams each of these elements were evaporated to fumes at about 180°C with 1 ml. of 60% perchloric acid and 2 ml. each of concentrated hydrochloric acid and hydrobromic acid (sp. gr. 1.48). After cooling 2 ml. of hydrobromic acid was again added and the solution was evaporated to dryness. The residue was treated with 2 ml. of 1.4 N nitric acid previous to color development. Silver is precipitated by ascorbic acid, but this can be removed by centrifugation after color development. Molybdenum interferes rather seriously and more than 50 μg. of this element can not be permitted.

The proposed method will probably be applicable to lead-base and tin-base alloys

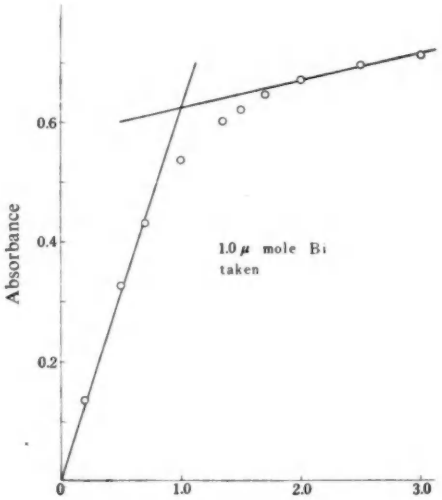

Fig. 5. Mole ratio method.

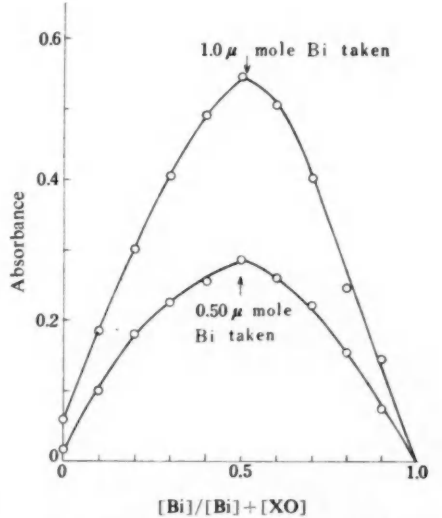

Fig. 6. Method of continuous variation.

after oxychloride precipitation of bismuth[6].

The composition of the bismuth-Xylenol Orange complex was determined by the mole ratio method and by the method of continuous variation (Job's method). The experiments were carried out at room temperatures ranging from 16° to 20°C. From the results obtained (Figs. 5 and 6), a 1:1 complex of bismuth with the reagent is indicated. From the fact that Xylenol Orange is an analogue of EDTA, this composition would be expected. On the basis of the data shown in Fig. 6, the formation constant or stability constant of the complex is calculated to be 1×10^7 by the method described by Majumdar and Chakrabartty[7] and Cheng[8]. This value is greater than that of the iron(III)-Xylenol Orange complex (5×10^5)[4], and is close to that of the zirconium-Xylenol Orange complex (4.0×10^7)[8].

6) B. Bendigo, R. K. Bell and H. A. Bright, *J. Research Natl. Bur. Standards*, **47**, 252 (1951); R. H. Campbell and M. G. Mellon, *Anal. Chem.*, **32**, 54 (1960).
7) A. K. Majumdar and M. M. Chakrabartty, *Anal. Chim. Acta*, **19**, 372 (1958).
8) K. L. Cheng, *Talanta*, **2**, 266 (1959).

Summary

A method is described for the spectrophotometric determination of 10~80 μg. of bismuth with Xylenol Orange. The error is not likely to exceed ±10 per cent. The molar extinction coefficient of bismuth in 0.1 N nitric acid solution is 1.6×10^4 at 530 mμ. Instead of nitric acid perchloric acid or sulfuric acid may also be used. The interference of small amounts of zirconium, thorium, and iron can be eliminated by masking. Lead and thallium do not interfere with the determination of bismuth. A 1:1 complex of bismuth with Xylenol Orange is suggested.

Japan Atomic Energy Research Institute
Tokai, Ibaraki-ken

Studies on Polymerizaton and Depolymerization of ε-Caprolactam Polymer. VIII. The Solution Viscosity of Poly-ε-capramide of Super-high Degree of Polymerization*

By Naoya OGATA

(Received June 6, 1960)

Several equations have been proposed on the relationship between the intrinsic viscosity $[\eta]$ of poly-ε-capramide in sulfuric acid and the polymerization degree $\overline{P}_n$ or the molecular weight $\overline{M}_n$ as follows:

$$\overline{P}_n = 124\,[\eta] - 5^{1)}$$

$$\overline{P}_n = 119\,[\eta]^{2)}$$

$$\overline{P}_n = 170\,[\eta]_{50\%\ H_2SO_4}{}^{3)}$$

$$\log[\eta] = 0.764(\pm0.016)\log\overline{M}_n - 3.20^{4)}$$

These equations were proposed on the polymer with polymerization degrees below 300 and with broad molecular weight distribution, which was polymerized in the presence of water.

Poly-ε-capramide of a super-high degree of polymerization and with the sharp molecular weight distribution can be obtained by the so-called rapid polymerization of ε-caprolactam in the presence of alkali catalyst[5]. It is expected that the behaviour of the solution viscosity of poly-ε-capramide of a super-high degree of polymerization would be quite different from that of poly-ε-capramide polymerized in the presence of water.

Experimental and Results

Polymerization of ε-Caprolactam[6]. — Sodium hydroxide was dissolved in ε-caprolactam at 100°C at the amount of 1/100, 1/500, 1/750 and 1/1000 mol./mol. and then carbon dioxide gas was introduced for 30 min. into the molten ε-caprolactam. ε-Caprolactam containing colloidally dispersed sodium carbonate was heated at 290°C under normal

* VII, *Makromol. Chem.*, **30**, 212 (1959).
1) A. Matthes, ibid., **5**, 165 (1950).
2) H. Staudinger and H. Schnell, ibid., **1**, 43 (1947).
3) K. Hoshino and M. Watanabe, *J. Am. Chem. Soc.*, **73**, 4816 (1957).
4) J. R. Schaefgen and P. J. Flory, ibid., **70**, 2709 (1948).
5) W. Griehl, *Faserforsch. u. Textiltech.*, **7**, 207 (1956).
6) H. Yumoto and N. Ogata, This Bulletin, **31**, 907, 913 (1957).

Table I. The relation among C, η_{rel} and $[\eta]$

Sample No.	Concentration (g./100 cc.)							$[\eta]$
	0.1	0.2	0.5	1.0	1.5	2.0	3.0	
A	1.091	1.185	1.512	2.079	2.752	3.483	5.291	0.91
B	1.151	1.336	1.911	3.340	5.060	6.610	11.48	1·62
C	1.246	1.553	2.634	5.421	8.708	14.34	27.66	2.51
D	1.308	1.689	3.073	7.060	11.45	19.79	39.53	3.09
E	1.383	1.853	3.220	7.260	12.89	23.89	51.29	3.71
F	1.476	1.942	3.789	8.753	15.52	28.18	66.82	4.47
G	1.883	3.008	8.206	19.07	59.05	116.8	357.9	8.32

Table II. The number of carboxyl and amino groups, and $\bar{P}_n$ of the polymer

Sample No.	$-NH_2$		$-COOH$	
	Mol./113 g.	$\bar{P}_n$	Mol./113 g.	$\bar{P}_n$
A	1.300×10^{-2}	77	1.010×10^{-2}	99
B	0.676 〃	148	0.501 〃	199
C	0.415 〃	241	0.189 〃	529
D	0.319 〃	314	0.145 〃	690
E	0.295 〃	339	0.120 〃	833
F	0.289 〃	347	0.098 〃	1025
G	0.155 〃	646	0.053 〃	1910

pressure in a nitrogen atmosphere or at 250°C under the reduced pressure of 250 mmHg in a nitrogen atmosphere. After the polymerization, polymers were quickly cooled and washed with water.

Determination of the Solution Viscosity.—Polymers were dissolved in 98% sulfuric acid at the concentrations of 0.1, 0.2, 0.5, 1.0, 1.5 and 2.0 g./100 cc. and the relative viscosities of the solutions were determined with the Ostwald's viscometer at 25°±0.01°C. The number of carboxyl groups in the polymers was determined by the alkali titration in benzyl alcohol with phenolphthalein as an indicator, and the number of amino groups was determined by potentiometric titration, in phenol-alcohol solvent (1.7/1.0 in volume)[7].

Table I shows relative viscosities η_{rel} of the polymer solutions at various concentrations in 98% sulfuric acid. The number of amino groups in the polymers is about twice as great as that of carboxyl groups, as shown in Table II. Although there have been many discussions on the structure[6,8-12] of the end groups of the alkali-catalyzed poly-ε-capramide, it is assumed that the polymerization degree calculated from the number of amino groups may be correct, since the number of carboxyl groups increases by washing the polymer with water, while that of amino groups does not increase[6,11].

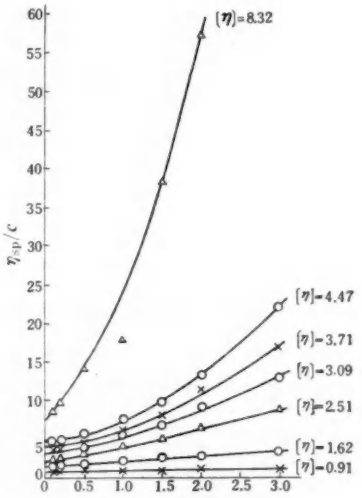

Fig. 1. The relation between η_{sp}/c and c.

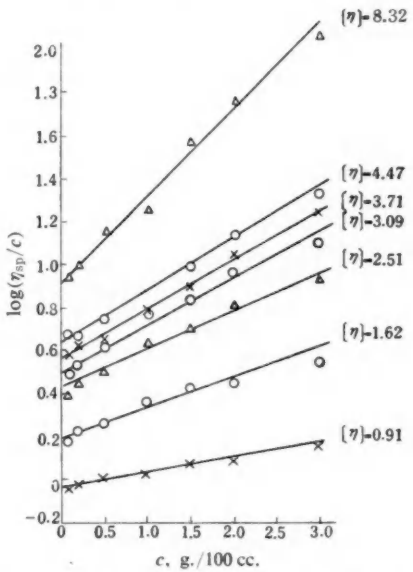

Fig. 2. The relation between log (η_{sp}/c) and c.

7) J. E. Waltz and G. B. Taylor, *Anal. Chem.*, **91**, 418 (1947).
8) D. Heikens, *Makromol. Chem.*, **18**, 62 (1956).
9) W. Griehl and S. Schaaf, ibid., **32**, 170 (1959).
10) J. Králícek and J. Šebenda, *J. Polymer Sci.*, **30**, 493 (1958).
11) S. Schaaf, *Faserforsch. u. Textiltech.*, **10**, 224 (1959).
12) A. Hamann, ibid., **9**, 351 (1958).

The relationships between the polymer concentration c (g./100 cc.) in 98% sulfuric acid and η_{sp}/c (η_{sp} means specific viscosity) shift from a straight line as the polymerization degree increases as shown in Fig. 1. However, as shown in Fig. 2, a linear relation between log (η_{sp}/c) and c is found and can be expressed as follows:

$$\log(\eta_{sp}/c) = K \cdot c + \log[\eta] \quad (1)$$

where K is a constant and $[\eta]$ the intrinsic viscosity of the polymer, which is obtained by extrapolation of linear log (η_{sp}/c) vs. c graphs to infinite dilution. The values of $[\eta]$ of the polymers are shown in Table I.

Plotting K against log$[\eta]$, a straight line is obtained as shown in Fig. 3 and the following equation is obtained.

$$K = 0.33 \log[\eta] + 0.05 \quad (2)$$

From Eqs. 1 and 2, Eq. 3 can be derived.

$$\log(\eta_{sp}/c) = 0.05\,c + (0.33\,c + 1)\log[\eta] \quad (3)$$

Plotting η_r (η_{rel} at $c=1$) against $[\eta]$, a straight line is obtained as shown in Fig. 4, and Eq. 4 is obtained.

$$\eta_r = /2.2[\eta] \quad (4)$$

The relationship between log $\bar{P}_n$ and log $[\eta]$ is in a linear function as shown in Fig. 5, and Eq. 5 is obtained.

$$\bar{P}_{n\,NH_2} = 89[\eta] \quad (5)$$

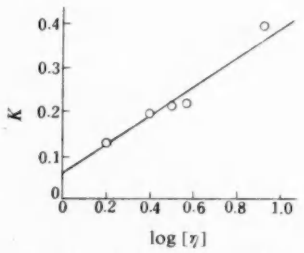

Fig. 3. The relation between K and log $[\eta]$.

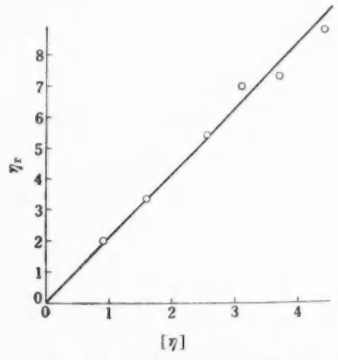

Fig. 4. The relation between η_r and $[\eta]$.

From Eqs. 4 and 5, Eq. 6 can be derived.

$$P_n = 40.5\,\eta_r \quad (6)$$

Fig. 6 shows the relationship between $\bar{P}_n$ and η_r at $c=1$.

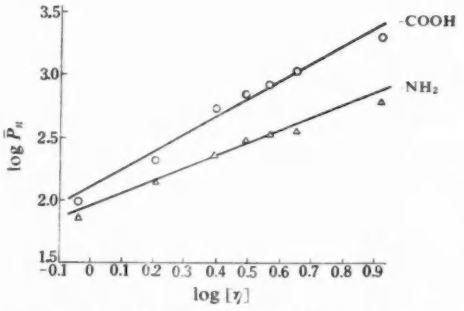

Fig. 5. The relation between log $\bar{P}_n$ and log $[\eta]$.

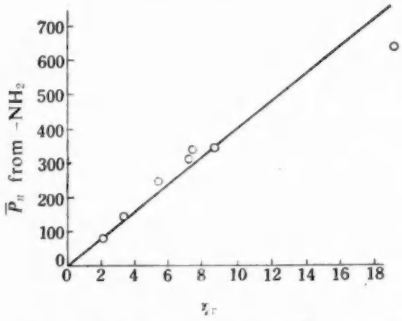

Fig. 6. The relation between $\bar{P}_n$ and η_r.

Change in the Polymerization Degree of the Polymer. — The alkali-catalyzed poly-ε-capramide, which had been washed with water, was preserved in a desiccator with phosphorus pentoxide in a dark place for about 2 years. At that stage, the solution viscosity of the polymers was measured. The polymerization degree of the polymer decreases markedly in comparison with that just after the polymerization and $\bar{P}_n$ becomes about 70, regardless of the initial P_n.

Discussion

Generally, it is recognized that the solution viscosity of high polymers can be expressed in the following equation proposed by Huggins,

$$\eta_{sp}/c = [\eta] + k'[\eta]^2 c \quad (8)$$

where k' is approximately constant for a series of polymers in a give solvent. Matthes[12] has recognized that the solution viscosity of poly-ε-capramide in concentrated sulfuric acid is well expressed in Huggins' equation and the same results have been attained by Rybnikàr[13].

13) F. Rybnikář, ibid., 9, 500 (1958).

TABLE III. CHANGE IN $\bar{P}_n$ OF THE ALKALI-CATALYZED POLY-ε-CAPRAMIDE

$\bar{P}_n$ of the polymer just after the polymerization	$\bar{P}_n$ of the polymer after 2 years
454	71
254	71
241	64
208	72
190	71

Dawydoff[14] has also reported that the relationships between c and η_{sp}/c or $\ln \eta_{sq}/c$ are in linear functions in the range of the concentrations of less than 0.1 g./100 cc.

Plotting η_{sq}/c against c, a straight line is obtained for the alkali-catalyzed poly-ε-capramide of $[\eta] < 2.5$, while the shift from a straight line becomes greater in the polymers of $[\eta] > 2.5$. However, a linear relation between $\log(\eta_{sp}/c)$ and c can be found for the polymers in the wide ranges of the polymerization degrees.

It is expected that the interactions among chain molecules occur strongly, as the polymerization degree of the polymer increases, and a simple equation between η_{sp}/c and c is not found. The relationship between $\bar{P}_n$ and $[\eta]$ is a simple equation as that derived by Matthes[1] for the polymer polymerized in the presence of water, but the value of the proportionality constant for the alkali-catalyzed polymer is smaller than that derived by Matthes. This is expected to be due to the difference in the molecular weight distribution.

The polymerization degree of the alkali-catalyzed polymer decreases markedly even at room temperature, as stated before, in spite of the fact that the polymers were preserved in a dry state in a dark place. As it is expected that no chemical or photochemical reactions occur in such moderate state, it is very interesting to ascertain whether the amide-interchange reactions would occur in poly-ε-capramide even at room temperature in solid phase, especially in that of a super-high degree of polymerization.

14) W. Dawdoff, ibid., **8**, 267 (1957).

Summary

The solution viscosity of poly-ε-capramide of a super-high degree of polymerization in 98% sulfuric acid has been investigated. A linear relation between $\log(\eta_{sp}/c)$ and c (g./100 cc.) is found for the alkali-catalyzed polymers of $[\eta] > 2.5$, as expressed by the following equation.

$$\log(\eta_{sp}/c) = 0.05\,c + (0.33\,c + 1)\log[\eta]$$

The relationship between $\bar{P}_n$ and $[\eta]$ is expressed by the following equation.

$$\bar{P}_n = 89[\eta]$$

The alkali-catalyzed polymer of a super-high degree of polymerization degrades slowly at room temperature in solid phase.

The author wishes to express his gratitude to Dr. K. Hoshino and Dr. H. Kobayashi for their instruction and permission to publish these results. Thanks are also due to Mr. K. Noishiki, Head of the Nagoya Laboratory, and Mr. T. Takayanagi, Chief Research Chemist, for their helpful and discussion. He also thanks Messrs. M. Nakata and T. Ishikawa who collaborated with him in the experiments.

Research Department
Toyo Rayon Co. Ltd.
Minato-ku, Nagoya

Proton Magnetic Resonance of Borazole[1]

By Kazuo Ito, Haruyuki Watanabe and Masaji Kubo

(Received June 8, 1960)

The work described in this paper is part of a physicochemical investigation which has as its object the elucidation of the molecular structures and electronic states of borazole and its derivatives. Previous papers of this series have been concerned with the infrared absorptions of some borazole derivatives[2], the dipole moments of borazole and its derivatives[3] and the diamagnetic anisotropy of a borazole ring[4]. The present paper presents the results of investigation on the proton magnetic resonance of borazole. The problem is of particular interest from the standpoint of both chemical shifts and splittings for the following reasons. In the first place, all the NMR spectra which have ever been recorded on compounds having hydrogen atoms attached to boron are outnumbered by the profusion of those on other types of compounds. Secondly, the nuclei of nitrogen ^{14}N as well as those of boron isotopes, ^{11}B and ^{10}B, have an electric quadrupole moment capable of affecting through its spin-lattice relaxation the relative broadening of multiplet components. The ^{11}B magnetic resonance was also studied in order to facilitate assignments.

Experimental

Sample. — B-Trichloroborazole was prepared by the same method as that described by Brown and Laubengayer[5]. After being sublimed several times under reduced pressure, it was identified by its melting point 83.5~84.5°C, the value reported in the literature being 83.9~84.5°C[5]. The infrared spectra[2] showed absorption bands characteristic of a borazole ring. This compound was reduced to borazole by essentially the same method as that proposed by Schaeffer et al[6]. differing in that $NaBH_4$ was used as a reducing agent in place of $LiBH_4$ and that triethylene glycol dimethyl ether rather than dibutyl ether was employed as a solvent[7]. Triethylene glycol dimethyl ether having a boiling point quite different from that of borazole was more suitable than diethylene glycol dimethyl ether suggested by Schaeffer[8]. Hence, 23.5 g. of sodium borohydride was dissolved in 120 cc. of triethylene glycol dimethyl ether in an atmosphere of dry nitrogen. To this solution, the suspension of 30 g. of B-trichloroborazole in 75 cc. of the same solvent was gradually added at room temperature. Stirring was continued for about 2 hr. After the reaction was over, the product was distilled under reduced pressure and was collected in a trap cooled with dry ice. The yield of crude borazole was about 10 g. Vacuum distillation was repeated several times before use.

Apparatus and Experimental Procedure. — The proton magnetic resonance spectrum was recorded at room temperature by means of a JNM-3 high-resolution NMR spectrometer of Japan Electron Optics Laboratory Company operating at 40 Mc./sec. Cyclohexane was used as an internal standard. Accordingly, corrections for the bulk magnetic susceptibility of the sample were not required. It was further confirmed that dilution with carbon tetrachloride did not affect the spectrum in an appreciable manner. The NMR absorption derivative spectrum of ^{11}B was also recorded with the same spectrometer operated at 12.6 Mc./sec.

Results and Discussion

The proton magnetic resonance spectrum obtained is shown in Fig. 1, in which the absorption intensity is plotted against decreasing magnetic field strength. Chemical shifts defined by

$$\delta = 10^6 (H_s - H_r)/H_r$$

are also protted along the abscissa. Here, H_s denotes the applied magnetic field for the proton signal of the sample and H_r is that of cyclohexane used as a standard. The signal of cyclohexane was identified by the increase in its intensity on further addition of the standard. Two peaks at 1.4_7 and -1.4_9 were ascribed to spinning side bands, because they shifted depending on the spinning rate.

The spectrum is comprised of a triplet centered at -4.0_5 and less intense broad peaks at 2.1_2, -1.3_4 and -8.2_6. The triplet was unequivocally assigned to the proton signal of

1) A part of the results presented here has been reported at the 13th Annual Meeting of the Chemical Society of Japan Tokyo, April 5, 1960. A preliminary report has been published in a short communication: K. Ito, H. Watanabe and M. Kubo, *J. Chem. Phys.*, **32**, 947 (1960).

2) H. Watanabe, M. Narisada, T. Nakagawa and M. Kubo, *Spectrochim. Acta*, **16**, 78 (1960). H. Watanabe, T. Totani, T. Nakagawa and M. Kubo, ibid., **16** (1960).

3) H. Watanabe and M. Kubo, *J. Am. Chem. Soc.*, **82**, 2428 (1960).

4) H. Watanabe, K. Ito and M. Kubo, ibid., **82**, 3294 (1960).

5) C. A. Brown and A. W. Laubengayer, ibid., **77**, 3699 (1955).

6) R. Schaeffer, M. Steindler, L. Hohnstedt, H. S. Smith, Jr., L. B. Eddy and H. I. Schlesinger, ibid., **76**, 3303 (1954).

7) L. Hohnstedt and D. T. Haworth, ibid., **82**, 89 (1960).

8) G. W. Schaeffer, private communication.

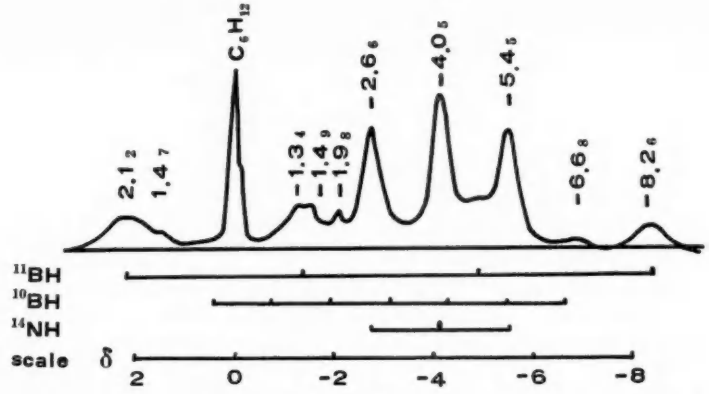

Fig. 1. Proton magnetic resonance spectrum of borazole. The numerical values of shifts are given for major absorption peaks.

^{14}NH with a spin coupling constant $J(^{14}NH) = 56$ cps, because the signal is expected to split into three equally spaced peaks owing to the $2I+1$ orientations of a ^{14}N spin with $I=1$. The spin coupling constant is of the right order of magnitude, since the value for $^{14}NH_3$ is 46 cps[9]. In this triplet pattern, not all of the peaks have the same height, the central line being stronger than the two outer ones, which have the same intensity. Deviation from a simple 1 : 1 : 1 triplet, i.e., the partial collapse of spin multiplets can be ascribed to the presence of ^{14}N nuclei having an electric quadrupole moment, which gives rise to spin-lattice relaxation in fluctuating electric field gradients. A similar pattern has been shown clearly by Ogg and Ray[9], who compared the proton spectra of anhydrous $^{14}NH_3$ and $^{15}NH_3$. An approximate quantitative theory of this collapse mechanism has been developed by Pople[10], who showed that the broadening of the outer components of the proton triplet spectrum should be three halves as great as that of the central component. Strictly speaking, the outer peaks of the triplet draw together as they broaden. Consequently, the separation between adjacent peaks does not correspond exactly to the spin coupling constant. However, the effect is presumed to be very small in the present case, in which the signals are fairly sharp.

Although the number of hydrogen atoms attached to boron in a borazole molecule is exactly the same as that of hydrogen atoms bonded to nitrogen, the proton signal of BH must be weak, because the abundance ratio of boron isotopes is $^{11}B : {}^{10}B = 81.17\% : 18.83\%$ and also because these isotopes have a greater nuclear spin than that of ^{14}N, the abundance of which amounts to as much as 99.635%. Therefore, the proton signal of ^{11}BH must split into four equally spaced peaks in accordance with the spin $I=3/2$ of ^{11}B. The separation, 3.4_6, between the two peaks at 2.1_2 and -1.3_4 is equal to half the difference, 6.9_2, between those at -1.3_4 and -8.2_6, suggesting the presence of another peak at -4.8_6, which, although masked by the ^{14}NH triplet, appears as a hump between two peaks at -4.0_5 and -5.4_5 of the triplet. These four peaks complete the proton quartet of ^{11}BH with $J(^{11}BH) = 138$ cps. This assignment is also consistent with the ^{11}B NMR spectrum of the same sample. Fig. 2 reproduces the NMR absorption derivative spectrum of ^{11}B in a borazole molecule. The curve is symmetric across a point, indicating

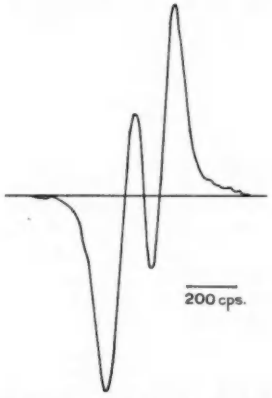

Fig. 2. The NMR absorption derivative spectrum of ^{11}B of borazole.

9) R. A. Ogg, Jr., and J. D. Ray, *J. Chem. Phys.*, **26**, 1515 (1957).
10) J. A. Pople, *Mol. Phys.*, **1**, 168 (1958).

the presence of two lines of equal intensity separated by 140 cps in good agreement with 138 cps evaluated from the aforementioned proton magnetic resonance spectrum. Philips et al.[11] has carried out the ^{11}B magnetic resonance study of boron compounds and reported that $J(^{11}BH)$ was equal to 136 cps for borazole.

The three components of the proton quartet of ^{11}BH have practically the same peak height. Although the intensity of the fourth line, which overlaps with the ^{14}NH proton triplet, is difficult to estimate exactly, it is very likely that the peak height is the same as those of other members of the quartet. The theory of quadrupole relaxation has already been extended to cover the broadening of multiplet components for protons bonded to nuclei with spin greater than unity[10]. It is predicted that, for spin 3/2, all components of the proton 1:1:1:1 quartet should be broadened equally, instead of showing different peak heights as in the ^{14}NH proton triplet. The present results are in agreement with Pople's[10] prediction. A similar quartet pattern having equal spacings and equal peak heights has been shown most clearly for sodium borohydride, $NaBH_4$[12,13]. The partly resolved spectrum of the terminal protons of diborane[13] also appears to be consistent with the prediction.

There are still two weak peaks at -1.9_8 and -6.6_8 remaining unassigned. A possible interpretation is afforded by the proton signal of ^{10}BH. If the peak at -6.6_8 is assumed to be the outermost low-field member of seven peaks predicted for the signal of protons bonded to ^{10}B with its nuclear spin equal to 3, the peak at -1.9_8 can be considered to be the third high-field member of the septet, because the center of the ^{11}BH quartet must coincide with the central line of the ^{10}BH septet. The adequacy of this interpretation is strongly supported by an agreement between the observed spin coupling constant $J(^{10}BH)=48$ cps and the calculated one, 46 cps, based on the observed $J(^{11}BH)=138$ cps and the gyromagnetic ratios γ of boron isotopes.

$$\frac{J(^{10}BH)}{J(^{11}BH)}=\frac{\gamma(^{10}B)}{\gamma(^{11}B)}=\frac{4.575}{13.660}$$

where the numerical denominator and numerator are, respectively, the NMR frequencies of ^{11}B and ^{10}B in Mc. for a 10 kilogauss field. Three peaks between these two observed ones will escape detection owing to overlap with the strong ^{14}NH triplet. Two other peaks expected to appear at about -0.7 and $+0.5$ have not been observed.

The nuclei of ^{10}B have also an electric quadrupole moment. The broadening of multiplet components for protons bonded to nuclei with spin equal to 3 presents an interesting problem from the theoretical point of view. However, it is not feasible to discuss the broadening of the multiplet structure of the septet on the basis of the present investigation.

The proton chemical shifts, -4.0_5 and -3.0_7, of NH and BH in borazole, as referred to cyclohexane, lead to about -0.7 and $+0.3$, respectively, referred to water as a standard[14]. The former differs definitely from the δ values 4.3~4.5 for secondary alkyl amines[15], and is intermediate between about 2.0 for secondary aryl amines[15] and about -2.1 for pyrrole[14]. This is quite reasonable since nitrogen atoms in borazole assume sp^2 hybridization and π-electrons are presumed to migrate to some extent from nitrogen to boron[4,16]. The chemical shift and the spin coupling constant $J(^{11}BH)$ of a BH proton, $+0.3$ and 138 cps, in borazole are closer to those of a terminal proton, $+2.0$ and 125 cps, in diborane, respectively, than to those of a bridge proton, $+6.3$ and 43 cps, in the same molecule[15].

Summary

The proton and ^{11}B magnetic resonances of borazole were recorded at room temperature. The proton magnetic resonance spectrum showed a ^{14}NH triplet, a ^{11}BH quartet and a part of ^{10}BH septet. The broadening of multiplet structure was discussed and the peak heights of the multiplet components were explained in terms of the quadrupole relaxation of nuclei bonded to hydrogen. The chemical shifts and the spin coupling constants were compared with those of related compounds.

The authors wish to thank Dr. T. Seki of Japan Electron Optics Laboratory Company for recording the high-resolution NMR spectra.

Chemistry Department
Faculty of Science
Nagoya University
Chikusa, Nagoya

11) W. D. Philips, H. C. Miller and E. L. Muetterties, *J. Am. Chem. Soc.*, **81**, 4496 (1959).
12) R. A. Ogg, Jr., *J. Chem. Phys.*, **22**, 1933 (1954).
13) J. N. Shoolery, *Discussions Faraday Soc.*, **19**, 215 (1955).
14) J. A. Pople, W. G. Schneider and H. J. Bernstein, "High-resolution Nuclear Magnetic Resonance", McGraw-Hill Book Company, Inc., New York (1959).
15) L. H. Meyer, A. Saika and H. S. Gutowsky, *J. Am. Chem. Soc.*, **75**, 4567 (1953).
16) B. L. Crawford, Jr., and J. T. Edsall, *J. Chem. Phys.*, **7**, 223 (1939). C. C. J. Roothaan and R. S. Mulliken, ibid., **16**, 118 (1948). C. W. Rector, G. W. Schaeffer and J. R. Platt, ibid., **17**, 460 (1949).

A Quantum-mechanical Approach to the Theory of Aromaticity

By Kenichi FUKUI, Akira IMAMURA, Teijiro YONEZAWA and Chikayoshi NAGATA

(Received May 28, 1960)

The term "aromatic" originated from a characteristic odor which was possessed by certain substances isolated from various natural products such as benzoic acid (e.g. from gum benzoin), benzaldehyde (bitter-almond oil), cymene (carraway oil), toluene (tolu balsam) and the like. Hence this terminology essentially involved much ambiguousness since originally it was not based upon any scientific concept of classification. Recently the term "aromaticity" has attracted anew the attention of many organic chemists[1] since the discovery and the synthesis of multifarious non-benzenoid "aromatic" compounds such as tropolone, sydnone, ferrocene and numerous derivatives of these compounds[2].

A quantum-mechanical attack on the problem of aromaticity was for the first time delivered by Hueckel in regard to benzene, who presented the so-called $4n+2$ rule[3]. According to his theory, a conjugated compound has $4n+2$ π electrons on its ring should exhibit an aromatic character. Although long years have passed since his report, only a very few attempts have been made to approach this problem theoretically. Recent conspicuous developments in the synthetic organic chemistry of non-benzenoid compounds, however, forced pressingly a re-examination of the significance of aromaticity. Craig investigated the compounds containing $d\pi$ electrons by simple LCAO MO treatment and defined two types of aromaticity according to the type of $d\pi$ orbital involved[4]. One of them obeys the $4n+2$ rule while the other is of a novel type in which the rule does not hold.

The researchers mentioned above, however, considered only the energy of π electrons and neglected the internuclear repulsion energy. A more dexterous device should accordingly be desired for the elucidation of aromaticity.

The present authors attempted to investigate the aromaticity more minutely from the quantum-chemical point of view. Prior to entering into the main subject it is desirable to define the term "aromaticity". What is meant by aromaticity is of no clear-cut nature and is usually represented by the following characteristics of aromatic compounds.

Aromatic compounds have a plane structure.

Aromatic compounds show a remarkable stability.

Aromatic compounds have a characteristic reactivity.

Aromatic compounds show a peculiarity in such physical properties as ultraviolet absorption spectra[5], molecular refraction[6], magnetic anisotropy[7], and so forth.

Among these properties some have been already solved and explained satisfactorily, while others have yet been left untouched. The distinguished stability of aromatic compounds aroused the present authors' interest above all other things and is mainly discussed in the present paper.

Energetical Consideration

Classical explanation of the stability of aromatic compounds had been based upon the strain theory, referring to the proposition that a six-membered ring is stable since it undergoes no strain force. However, by means of this theory we can not understand the reason why some five-membered rings such as furan are stable while others such as cyclopentadiene

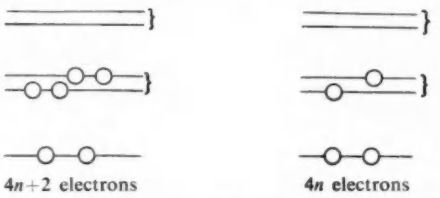

Fig. 1. π-electron configuration of $(4n+2)$- and $(4n)$-membered rings.
The brace } indicates that two levels are degenerate.

1) R. Robinson, *Tetrahedron*, **3**, 323 (1958); H. C. Longuet-Higgins, *Proc. Chem. Soc.*, **1957**, 157.
2) W. Baker and W. D. Ollis, *Quart. Revs. (London)*, **11**, 15 (1957); A. W. Johnson, *J. Chem. Soc.*, **1954**, 1331; T. Nozoe, "Gendai Kagaku", Vol. 10, Iwanami, Tokyo (1957).
3) E. Hueckel, *Z. Physik*, **70**, 204 (1931).
4) D. P. Craig, *J. Chem. Soc.*, **1959**, 997.
5) R. A. Friedel and M. Orchin, "Ultraviolet Spectra of Aromatic Compounds", John Wiley & Sons, Inc., New York (1951); R. Pariser and P. G. Parr, *J. Chem. Phys.*, **21**, 466, 767 (1953).
6) M. Kotake, "Daiyûkikagaku", Vol. 1, Asakura, Tokyo (1958) p. 204..
7) L. Pauling, *J. Chem. Phys.*, **4**, 673 (1936); F. London, *J. de Physique*, **8**, 397 (1937).

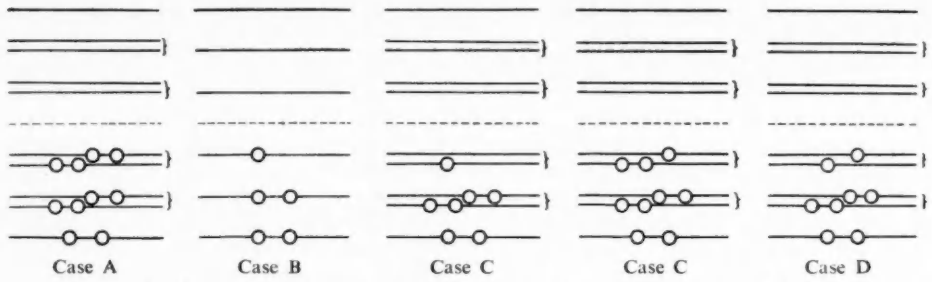

Fig. 2. Electronic configurations which are taken into account in the calculation.
The brace } indicates that two levels are degenerate.

are not. Moreover, recent experiments elucidated that some seven-membered conjugated ring compounds such as tropone and tropolone can exist in a stable form. These facts suggest that, in order to answer the question of aromatic stability, other factors than the strain force, e. g. the magnitude of total π electronic energy, should be taken into consideration. For the purpose of attacking this problem, quantum mechanics must obviously be a powerful weapon. Hueckel's $4n+2$ rule was derived by simple LCAO MO treatment[3]. He showed that the electronic configuration of the compound having $4n+2$ electrons on its ring forms a set of closed shells in MO sense analogous to the atomic structure. In the case of $4n$ electrons the complete closed shell structure is impossible as is seen in Fig. 1.

In Hueckel's $4n+2$ rule, however, the effect of electron-electron repulsion and internuclear repulsion had not been taken into account. Accordingly, this rule is not capable of predicting the number of π electrons which can exist and be stable on a given membered carbon ring. To overcome this difficulty, the π electronic energy is obtained by the formulas utilized by Pople[8]. In the present method the internuclear and electron-electron repulsion energy are considered explicitly and the antisymmetrized product of Hueckel MO were used for the sake of simplicity. Therefore MO is written as

$$\phi_i=\sum_r C_{ir}\phi_r \tag{1}$$

where ϕ_i is the ith MO and ϕ_r represents the AO on the rth carbon atom. Electronic configurations which are taken into account are classified into four cases A, B, C and D and these cases are schematically shown in Fig. 2.

For case A Pople gave the total π electronic energy including nuclear-nuclear repulsion as follows:

$$\varepsilon_\pi=\sum_r P_{rr}\left(U_{rr}+\frac{1}{4}P_{rr}\gamma_{rr}\right)+2\beta\sum_{r<s}^{*}P_{rs}+\sum_{r<s}\left\{(P_{rr}-1)(P_{ss}-1)-\frac{1}{2}(P_{rs})^2\right\}\gamma_{rs} \tag{2}$$

where U_{rr} is a core matrix element, β_{rs} is the resonance integral.

$$\gamma_{rs}=\int\phi_r^*(1)\phi_s^*(2)\frac{e^2}{r_{12}}\phi_r(1)\phi_s(2)\mathrm{d}v_1\mathrm{d}v_2$$

and

$$P_{rs}=2\sum_{i=1}^{n}C_{ir}C_{is} \tag{3}$$

Summation $\sum$ and $\sum^*$ should cover all the atoms and the nearest neighboring atoms, respectively. For the case of regular n-membered ring molecules, U_{rr} and β_{rs} are constant values represented by U and β, respectively. In Eq. 2 the internuclear repulsion energy is included in the following form

$$\varepsilon'=\sum_{r<s}Z_rZ_s\gamma_{rs} \tag{4}$$

and Z_r and Z_s are assumed to be unity. For case B the total π-electronic energy of the non-degenerate system with odd electrons was obtained as follows[5]:

$$\varepsilon_\pi=\sum_r(P_{rr}^0U+P_{rr}^\alpha P_{rr}^\beta\gamma_{rr})+2\beta\sum_{r<s}^{*}P_{rs}^0+\sum_{r<s}\{(P_{rr}^0-1)(P_{ss}^0-1)-[(P_{rs}^\alpha)^2+(P_{rs}^\beta)^2]\}\gamma_{rs} \tag{5}$$

where

$$P_{rs}^\alpha=\sum_{i=1}^{n}C_{ir}C_{is},\quad P_{rs}^\beta=\sum_{i=1}^{n-1}C_{ir}C_{is}$$

and $$P_{rs}^\alpha=P_{rs}^\beta+P_{rs}^\beta \tag{6}$$

For case C the total π electronic energy is obtained by only one electronic configuration for regular n-membered ring system, so that the formula for this case is equal to that of case B. For case D the wave functions are chosen as follows.

8) J. A. Pople, *Trans. Faraday Soc.*, **49**, 1375 (1953); A. Brickstock and J. A. Pople, ibid., **50**, 901 (1954).

TABLE I. THE DELOCALIZATION ENERGY OF FIVE-, SIX- AND SEVEN-MEMBERED RING SYSTEMS

Number of carbon atoms on ring	Number of π electrons	Energy of non-conjugated system, e.V.	Energy of conjugated system, e.V.	Difference e.V.
5	5	5U	5U − 9.80	9.80
	6	6U + 10.53	6U − 0.48	11.01
	7	7U + 26.78	7U + 17.23	9.55
6	4	4U + 4.90	4U − 6.30	11.20
	5	5U	5U − 13.50	13.50
	6	6U	6U − 13.88	13.88
	7	7U + 10.53	7U − 2.97	13.50
	8	8U + 25.96	8U + 14.76	11.20
7	5	5U + 4.38	5U − 10.17	14.55
	6	6U	6U − 17.32	17.32
	7	7U	7U − 14.17	14.17

$$\chi = \frac{1}{\sqrt{2}} \frac{1}{\sqrt{2n!}} \{ |\psi_1 \bar{\psi}_1 \cdots\cdots \psi_n \bar{\psi}_{-n}| - |\psi_1 \bar{\psi}_1 \cdots\cdots \bar{\psi}_n \psi_{-n}| \} \quad (7)$$

where ψ_n and ψ_{-n} are the molecular orbitals for degenerate levels. In this case we get the total π electronic energy by the same method that Pople used as follows:

$$\begin{aligned} \varepsilon_\pi = & \sum_r P_{rr} U + \frac{1}{4} \sum_r \{ (P_{rr})^2 - (C_{nr})^4 - (C_{-nr})^4 \\ & + 6(C_{nr})^2 (C_{-nr})^2 \} \gamma_{rr} + 2\hat{\beta} \sum_{r<s}{}^{*} P_{rs} \\ & + \sum_{r<s} \{ (P_{rr} - 1)(P_{ss} - 1) - \frac{1}{2}(P_{rs})^2 \\ & - \frac{1}{2}(C_{nr} C_{ns})^2 - \frac{1}{2}(C_{-nr} C_{-ns})^2 \\ & + 3(C_{nr} C_{ns})(C_{-nr} C_{-ns}) \} \gamma_{rs} \end{aligned} \quad (8)$$

where

$$P_{rs} = 2 \sum_{j=1}^{n-1} C_{jr} C_{js} + C_{nr} C_{ns} + C_{-nr} C_{-ns} \quad (9)$$

By using these formulas the total π electronic energy including internuclear repulsion energy is obtained.

Before performance of calculation it is necessary to consider what kind of quantity can be the measure for aromaticity. In many cases the resonance energy was adopted as the measure for aromaticity[9]. Recently, Craig tried to specify the aromatic character by its symmetry of molecular structures and spin functions[9]. This method, however, is inapplicable to the molecule which lacks sufficient symmetry. In this paper, we intend to compare the stability of the systems of regular n-membered ring having m π electrons. Since the calculation is restricted to π electronic energy and the effect of σ bond is neglected, the comparison of stability should be confined to the ring system with the same number of members and variable number of π electrons. We, therefore, adopt the energy difference between conjugated regular n-membered ring molecule and non-conjugated system that has electrons on each atom as the measure for aromaticity as is shown in Eq. 10.

$$\Delta E = \varepsilon \left[\text{C}_n \text{ or } \text{C}_n^{+} \text{ or } \text{C}_n^{-} \right] - \varepsilon \left[\text{C}_n \right] \quad (10)$$

This measure is nothing but the delocalization energy of the system. The energy of the neutral or ionic non-conjugated system can be given as follows where electron-electron and internuclear repulsions and electron-nuclear attraction are taken into account.

$$\begin{aligned} \varepsilon_{\text{non-conjugated}} = & \sum_{\mu>\nu} (Z_\mu - 2)^2 \gamma_{\mu\nu} + \sum_{r>s} (Z_r - 1)^2 \gamma_{rs} \\ & + \sum_{r\mu} (Z_\mu - 2)(Z_r - 1) \gamma_{r\mu} + \sum_{\alpha>\beta} Z_\alpha{}^2 \gamma_{\alpha\beta} \\ & + \sum_{\alpha,r} Z_\alpha (Z_r - 1) \gamma_{\alpha r} + \sum_\alpha \gamma_{\alpha\alpha} + nU \end{aligned} \quad (11)$$

where r and s denote the carbon atom which has only one electron on it, α and β two electrons, and μ and ν none, respectively, and n is the number of π electrons. For the sake of simplicity the values of Z_r, Z_α and Z_β are assumed to be unity. Thus the calculated value is the measure of the stability by delocalization of non-conjugated electrons. Therefore the greater the magnitude of delocalization energy is, the more stable the molecule is. Accordingly this measure is expected to be a good index for aromaticity, since the stability of the molecule is the essential character for aromatic compounds. The atomic integral used in calculation is gained by the semiempirical formulas adopted by Pariser and Parr[5]. For brevity, all the C–C bond distances are assumed to be 1.39 Å referring to that of benzene. Thus

9) D. Ginsburg, "Non-benzenoid Aromatic Compounds", Interscience Publishers Inc., New York (1959).

the obtained results of the delocalization energy are listed in Table I.

As is shown in Table I, infive-, six- and seven-membered ring systems the molecule is most stable when it has six π electrons on its ring. In a five-membered ring system this result corresponds to the fact that the five-membered ring molecule with six π electrons such as furan, sydnone exists in stable state. Moreover in the seven-membered ring system the stability of tropone and tropolone corresponds to this result. Accordingly, we can explain and extend Hueckel's $4n+2$ rule on the different physical grounds from Hueckel's and combine the rule with the fact that some five- and seven-membered ring molecules with six π electrons are stable.

In this connection, it may be worth while to add that another approximate method will contribute to the illustration of $4n+2$ rule. This is the method originally presented by Peter[10] in which the resonance energy is approximately obtained by the perturbation method. The wave function of linear polyenes is utilized as a zero order wave function. The intramolecular bonding between the atoms r and s, as is indicated in Fig. 3, is regarded as the perturbation and the stabilization energy due to this bonding is obtained. Result of simple LCAO MO calculation is

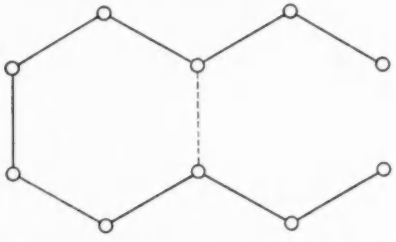

Fig. 3. Scheme for the perturbation method.
Dotted line indicates the new bonding engendered.
Circle and line represent the carbon atom and the C-C bond constructing the linear polyene.

$$\delta\varepsilon = 2P_{rs}\delta\beta_{rs} + \Pi_{rs,rs}(\delta\beta_{rs})^2 + \cdots\cdots \qquad (12)$$

where $\delta\varepsilon$ is the stabilization energy, P_{rs} and $\Pi_{rs,rs}$ are the order of imaginary bond between the atoms r and s and the selfpolarizability of the imaginary bond $r-s$, respectively, each being of the original polyene, and $\delta\beta_{rs}$ denotes the resonance integral of the bond $r-s$.

A glance at Eq. 4 makes it comprehensible that the magnitude of the stabilization energy predominantly depends on the bond order P_{rs}. Peter obtained the resonance energy of various

10) D. Peter, *J. Chem. Soc.*, **1958**, 1023.

TABLE II. THE VALUE OF BOND ORDER OF 4-, 6-, 8-, 10-, 12- AND 14-MEMBERED POLYENES

n	Type of bond formation	Bond order P_{rs}	Number of canonical structure
4		$P_{1,4} = -0.4473$	2
6		$P_{1,6} = 0.3019$	2
		$P_{2,5} = -0.0366$	1
		$P_{1,4} = -0.3874$	2
8		$P_{1,8} = -0.2293$	2
		$P_{2,7} = -0.3333$	2
		$P_{3,6} = 0.0340$	1
	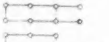	$P_{1,6} = 0.2632$	2
	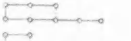	$P_{1,4} = -0.3673$	2
10		$P_{1,10} = 0.1855$	2
	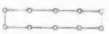	$P_{3,8} = 0.2297$	2
		$P_{2,9} = -0.0170$	1
	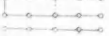	$P_{4,7} = -0.1278$	1
		$P_{1,8} = -0.2028$	2
		$P_{3,6} = -0.2293$	2
		$P_{2,7} = 0.0440$	1
		$P_{1,6} = 0.2469$	2
		$P_{2,5} = -0.1107$	1
		$P_{1,4} = -0.3576$	2
12		$P_{1,12} = -0.1562$	2
		$P_{3,10} = -0.1798$	2
		$P_{5,8} = -0.2938$	2
		$P_{2,11} = 0.0100$	1
		$P_{4,9} = 0.0586$	1
		$P_{1,10} = 0.1660$	2
	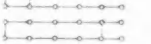	$P_{3,8} = 0.2146$	2
	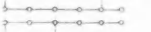	$P_{2,9} = -0.0234$	1
	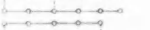	$P_{4,7} = -0.1377$	1
	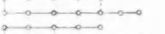	$P_{1,8} = -0.1896$	2
	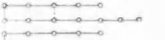	$P_{3,6} = -0.3038$	2
		$P_{2,7} = 0.0485$	2
		$P_{1,6} = 0.2382$	2
	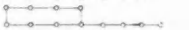	$P_{2,5} = -0.1142$	1
	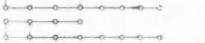	$P_{1,4} = -0.3523$	2
14		$P_{1,14} = 0.1348$	2
		$P_{3,12} = 0.1491$	2
		$P_{5,10} = 0.2000$	2
		$P_{2,13} = -0.0063$	1
	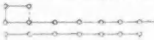	$P_{4,11} = -0.0330$	1
	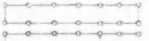	$P_{6,9} = -0.1491$	1

Circle written on the line represents the carbon atom which is a member of linear polyene
Dotted line indicates the new bond to be formed.

compounds by applying this method and the $4n+2$ rule generally, that is, the molecule in the case that the bond formation makes $4n+2$ ring has the largest resonance energy and therefore more stable than that in the case of $4n$ ring.

If we assume that internuclear repulsion energy stated above does not vary so much according to its geometrical structure, so far as the number of the atoms constituting a molecule does not change, the change of total energy of a molecule may approximately be discussed with an aid of Eq. 4. In many cases that the number of carbon atoms constituting the linear polyene is altered, the value of the bond order was calculated between several carbon-carbon atoms in simple LCAO MO treatment.

The result of calculation is collected in Table II for the cases of four, six, eight, ten, twelve and fourteen carbon atoms. Investigation of this table leads to the conclusion that in a polyene molecule the addition of a bond accompanied with the formation of a $4n+2$ ring stabilizes the molecule, while with the formation of a $4n$ ring it becomes unstable. It may be of interest to examine Table II more carefully to find that in the case of the bond formation with a $4n+2$ ring the corresponding value of bond order increases with the number of describable canonical structures which have alternate single and double bonds, while in $4n$ ring formation the relation is reversed. Hence the number of canonical structures can be a measure for the stability of a $4n+2$ ring molecule but no longer so for $4n$ ring molecules.

The way of estimating the stabilization energy mentioned above can be replaced by the calculation of conjugation energy per electron in perturbed molecule with simple LCAO MO treatment. The relation between these two methods is shown in Table III, in which a good parallelism is seen.

TABLE III. THE PARALLELISM BETWEEN BOND ORDER AND CONJUGATION ENERGY

Molecule	Conjugation energy per electron, β	Bond order P_{rs}
	1.100	−0.3874
	1.148	−0.0866
	1.165	0.0000
	1.244	0.0000
	1.333	0.3019

Dotted line indicates the bond formed between atom r and s. β in parenthesis is the resonance integral of carbon-carbon bond for hydrocarbon.

Electron Distribution

According to the $4n+2$ rule, it is seen that π electron distribution should be correlated closely with the stability of aromatic compounds and molecules with the ring containing $4n+2$ π electrons may be more stable than those with $4n$ π electrons. Therefore the aromatic compound should have the ring which has $4n+2$ π electrons on it. With regard to this rule it is non-benzenoid aromatic compounds with substituents such as sydnone, tropone and so on that attract our interest more strongly.

The sum of π electron density on the whole ring was obtained in Fig. 4 in the cases of sydnone, tropone and tropolone. These results suggest that in any cases the aromatic compounds tend to form a ring involving $4n+2$ π electrons. When the sum of π electron density exceeds 6, the 6-membered ring repels electrons to the substituent, and when it is less than 6, the ring attracts electrons to the ring. Further calculation of the electron distribution in some hydrocarbons containing odd-membered ring is done. The result is shown in Table IV, which illustrates that the $(4n+3)$-membered ring repels electrons and $(4n+1)$-membered ring attracts them independently of the ring size. Thus in azulene the seven-membered ring is positively

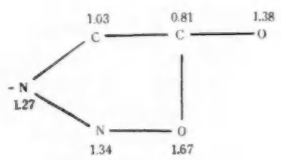

Sydnone 6.12

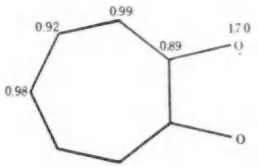

Tropolone 6.58

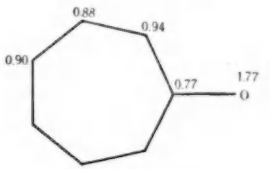

Tropone 6.21

Fig. 4. Total π electron distribution of non-benzenoid aromatic compounds. The value written under the figure is the sum of the π electron density of all member atoms constituting the ring.

TALBE IV. π ELECTRON DISTRIBUTION OF ODD-MEMBERED RING

	Sum of the total π electron density for $(4n+1)$-membered ring	Formal charge of $(4n+1)$-membered ring	Sum of the total π electron density for $(4n+3)$-membered ring	Formal charge of $(4n+3)$-membered ring
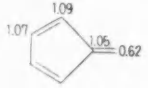	5.37	−0.37	—	—
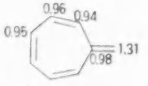	—	—	6.68	+0.32
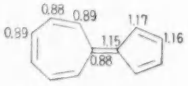	5.81	−0.81	6.19	+0.81
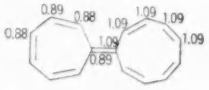	9.81	−0.81	6.19	+0.81
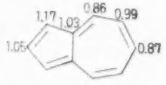	5.45	−0.45	6.63	+0.37

The value written in figures is the total π electron density at each position.

and the five-membered ring negatively charged representing the Fries' rule[11].

The same tendency can also be ascertained by such a perturbation treatmeat as is described above. A $(4n+1)$- or $(4n+3)$-membered ring can be formed as a result of the bond formation between appropriate two atoms in corresponding polyene molecule, as is shown in Fig. 5. This bond formation is considered as

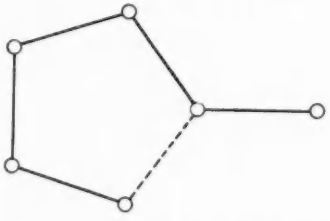

Fig. 5. Adopted model in perturbation method. Circle and line represent the carbon atom and the C-C bond constructing the linear polyene. Dotted line indicates the new bonding engendered.

a perturbation. The wave function for linear polyene is available as a zero order wave function. The total π electron density at the rth carbon atom, q_r, is represented by

$$q_r = 1 + \Pi_{r,st}\hat{\partial}\hat{\beta}_{st} + \cdots\cdots \qquad (13)$$

where $\hat{\partial}\hat{\beta}_{st}$ is the resonance integral of the new bond $s-t$ and $\Pi_{r,st}$ is the atom-bond polarizability of the atom r and the bond $s\cdots\cdots t$ of the original polyene given by

$$\Pi_{r,st} = \frac{\hat{\partial}q_r}{\hat{\partial}\hat{\beta}_{st}} = \sum_{j=1}^{m}\sum_{k=m+1}^{n}\frac{C_{rj}C_{rk}(C_{sj}C_{tk}+C_{tj}C_{sk})}{\varepsilon_j-\varepsilon_k} \qquad (14)$$

TABLE V. THE VALUE OF ATOM-BOND POLARIZABILITY AND THE ENERGY DIFFERENCE BETWEEN THE HIGHEST OCCUPIED ORBITAL OF $(4n+1)$- AND $(4n+3)$-MEMBERED RINGS AND U

$(4n+1)$-membered ring

n	$\Pi_{1,2,4n+2}$ $(1/\hat{\beta})$	$\varepsilon_f - U(\beta)$
1	$\Pi_{1,2,6} = -0.4675$	0.6180
2	$\Pi_{1,2,10} = -0.3148$	0.3474
3	$\Pi_{1,2,14} = -0.2383$	0.2408
4	$\Pi_{1,2,18} = -0.1920$	0.1848
5	$\Pi_{1,2,22} = -0.1242$	0.1474

$(4n+3)$-membered ring

n	$\Pi_{1,2,4n+4}$ $(1/\hat{\beta})$	$\varepsilon_f - U(\beta)$
1	$\Pi_{1,2,8} = 0.2964$	−1.2468
2	$\Pi_{1,2,12} = 0.2709$	−0.8310
3	$\Pi_{1,2,16} = 0.2127$	−0.6180
4	$\Pi_{1,2,20} = 0.1750$	−0.4914
5	$\Pi_{1,2,24} = 0.1146$	−0.4068

$\Pi_{r,st}$ represents atom-bond polarizability.

ε_f is energy level of highest occupied orbitals of $(4n+1)$- and $(4n+3)$-membered ring.

α and β are Coulomb integral of carbon atom and resonance integral of carbon-carbon bond in polyene, respectively.

11) K. Fries, *Ann. Chem.*, **516**, 248 (1935).

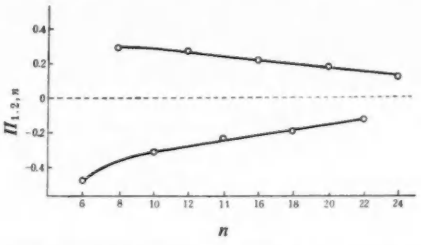

Fig. 6. Atom-bond polarizability and the number of members of linear polyene.

where C_{rj} is the coefficient of the atomic orbital of the rth atom in the jth molecular orbital in the simple LCAO MO treatment, ε_j is the energy of the jth molecular orbital, and subscript 1, 2, 3,……, m and subscript $m+1$, $m+2$ ……, n denote the occupied and unoccupied molecular orbitals, respectively. The calculated result of $\Pi_{r,st}$ is tabulated in Table V and is also plotted against the number of atoms, n, in Fig. 6. In the series of $(4n+3)$-membered rings the value of $\Pi_{r,st}$ is decreased with n and the sum of π electron density of the whole ring tends to approach to the limiting value, $4n+2$. A quite reverse tendency is seen in the series of $(4n+1)$-membered rings. That is, $\Pi_{r,st}$ is increased with n and the sum of π electron density of the whole ring approaches to the value of $4n+2$. Moreover, it is worth noticing that the absolute value of electronic charge transferred from side chain to ring or in the inverse direction decreases with n in regard to both the $(4n+1)$- and $(4n+3)$-membered rings.

These tendencies may qualitatively be understood from an energetical point of view. The energy levels of $(4n+1)$- and $(4n+3)$-membered rings are given schematically in Fig. 7. In the case of five- and nine-membered rings the charge transfer may occur from side chain to ring and the molecule forms a "closed shell" in a MO sense in order to stabilize itself. On the other hand, in the case of seven-membered ring the direction of the charge transfer is converse.

These circumstances can also be elucidated analytically by using the integral formula for atom-bond polarizability of Coulson[12]. Integral formula for atom-bond polarizability is written as

$$\Pi_{r,st}=(-1)^{s+t}\frac{2}{\pi}\int_{-\infty}^{+\infty}\frac{\Delta_{rt}(iy)\Delta_{st}(iy)}{\{\Delta(iy)\}^2}\,dy \tag{15}$$

where Δ is the secular determinant for the corresponding linear polyene and Δ_{rt} denotes the secular determinant with row r and column t struck out. Consider a $(4n+1)$-membered ring with a side chain of one carbon atom formed from a $(4n+2)$-membered polyene by a bridging between the 2nd and the $(4n+2)$th atoms of the polyene. The atom-bond polarizability $\Pi_{1,2.4n+2}$ is given by

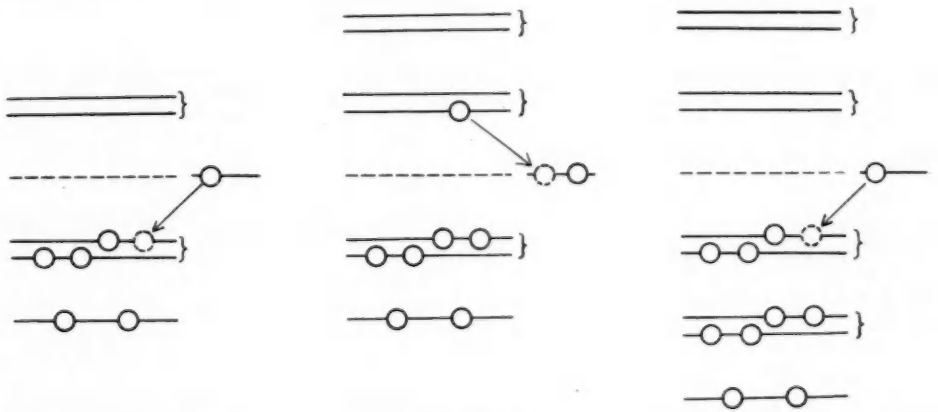

Fig. 7. Energy level of odd-membered ring.
The energy written aside represents that of the side-chain carbon.
The dotted line indicates the π electrons transferred and an arrow shows the direction of the electron transfer.

12) C. A. Coulson and H. C. Longuet-Higgins, *Proc. Roy. Soc.*, **A191**, 39 (1947); **A192**, 16 (1947).

TABLE VI. REACTIVITY INDEXES FOR $(4n+1)$- AND $(4n+3)$-MEMBERED RINGS

Compound	Position	f_r(N)	S_r(N)	q_r
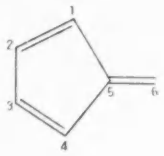	1	0.246	0.906	1.092
	2	0.156	0.784	1.073
	5	0.073	0.598	1.047
	6	1.124	2.701	0.623
Compound	**Position**	f_r(E)	S_r(E)	q_r
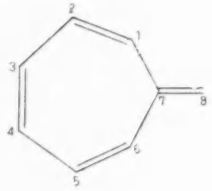	1	0.223	2.049	0.942
	2	0.100	1.071	0.962
	3	0.163	1.502	0.953
	7	0.046	0.756	0.976
	8	0.982	4.744	1.311

f_r, S_r and q_r are frontier electron density, superdelocalizability and total π-electron density at position r, respectively. (N) and (E) denote the reactivity indexes for nucleophilic and electrophilic reaction, respectively.

$$\Pi_{1,2\cdot 4n+2} = (-1)^{2+4n+2}\frac{2}{\pi} \times \int_{-\infty}^{+\infty} \frac{\Delta_{1,2}(iy)\Delta_{1,4n+2}(iy)}{\{\Delta^{(4n+2)}(iy)\}^2}\,dy \tag{16}$$

Following relations are easily proved[12]

$$\Delta_{1,4n+2}(iy) = 1, \quad \Delta_{1,2}(iy) = \Delta^{(4n)}(iy) > 0$$

and $$\Delta^{(4n+2)}(iy) < 0 \tag{17}$$

where $\Delta^{(4n)}$ and $\Delta^{(4n+2)}$ denote the secular determinants for $(4n)$- and $(4n+2)$-membered polyene, respectively. From Eqs. 13 and 16 with the aid of Eq. 17 it follows that

$$\Pi_{1,2\cdot 4n+2} > 0 \quad \text{and} \quad q_1 = 1 + \Pi_{1,2\cdot 4n+2}\delta\beta < 1. \tag{18}$$

Hence the total density at the atom of side chain is less than unity, since $\delta\beta$ is negative. In the case of $(4n+3)$-membered ring originated from a $(4n+4)$-membered polyene the following inequalities are obtained in a similar manner.

$$\Pi_{1,2\cdot 4n} < 0 \quad \text{and} \quad q_1 = 1 + \Pi_{1,2\cdot 4n}\delta\beta > 1 \tag{19}$$

Thus the total density becomes larger than unity.

Moreover, a close relation is observed between the atom-bond polarizability of a polyene and the highest occupied levels of $(4n+1)$- and $(4n+3)$-membered rings formed from the polyene. Table V illustrates this relation with regard to the cases of $(4n+1)$-membered ring formed from $(4n+2)$-membered polyene and $(4n+3)$-membered ring formed from a $(4n+4)$-membered polyene. In the table it is clearly observed that the lower the highest occupied level of $(4n+1)$-membered ring is, ····· and also the higher the highest occupied level of $(4n+3)$-membered ring is, the larger the amount of charge transferred from ring to side chain is. This result also coincides with the fact that the absolute value of the charge transferred decreases with n.

Thus a ring in the molecule has a tendency to approach to a $4n+2$ electron ring by the charge transfer to stabilize the molecule. The position to be attacked by a reagent was predicted for azulene in the paper symposium on aromatic character[13]. The attack of reagent was supposed to occur so as to make the ring possess $4n+2$ electrons by the process of reaction. Similarly, from the consideration stated above, it is predicted that the molecule containing a $(4n+1)$-membered ring and a side chain attached to it such as fulvene may be apt to react with a nucleophilic reagent at the side chain carbon. Inversely, in the case of $(4n+3)$-membered ring, an electrophilic reagent is inclined to attack the side chain carbon. Therefore, $4n+2$ rule can be said to govern the orientation of chemical reaction. Further, this rule also suggests a guiding principle in the syntheses of new aromatic compounds. Namely, we should choose an appropriate substituent attached to the ring that makes the ring possess $4n+2$ electrons. If a molecule

13) D. H. Reid, *Tetrahedron*, 3, 339 (1958).

has excessive electrons on its ring, the substituent to be chosen is electron-attracting, and if it has insufficient electrons, an electron-repelling substituent should be introduced to stabilize it.

This has also been supported by several quantum-mechanical theories of chemical reactivity such as the static method[12] and the frontier electron theory[14]. The reactivity indexes used in these theories have been calculated and tabulated in Table VI, showing that the above-mentioned prediction is correct.

Faculty of Engineering
Kyoto University
Sakyo-ku, Kyoto

14) K. Fukui, T. Yonezawa and C. Nagata, *J. Chem. Phys.*, **26**, 831 (1957); **27**, 1247 (1957).

Intermediate Compounds in the Catalytic Reduction of Aromatic Nitro Compounds with Raney Nickel Catalyst[1]

By Akira SUGIMORI*

(Received June 21, 1960)

There have been some studies on the intermediate compounds in the catalytic reduction of nitro compounds with nickel catalysts. Scholnik, Reasenberg and Smith[2] reported that in the catalytic reduction of sodium *p*-nitrobenzoate with platinized Raney nickel hydrogen uptake stopped when 2 mol. of hydrogen was consumed (3 mol. of hydrogen is required for the complete reduction of a nitro compound to the corresponding primary amine). This would suggest the existence of an intermediate, but they found only the nitro compound and the *p*-aminobenzoate in the reduction product. Shmonina and Sokolski[3] reported that nitrosobenzene was formed as an intermediate in the catalytic reduction of nitrobenzene with Raney nickel.

The present author studied the partial reduction of aromatic nitro compounds with neutral Raney nickel. Contrary to the above reports, phenylhydroxylamine derivatives were identified as intermediates.

Nitrobenzene (0.01 mol.) was reduced in ethanol solution at 25°C under ordinary pressure with Raney nickel prepared by treating 1.00 g. of nickel-aluminum alloy (Ni, 40%) with 5 ml. of 20% aqueous sodium hydroxide at 50°C and by washing 10 times with cold water and twice with 20 ml. of ethanol. Shaking was stopped when 0.02 mol. of hydrogen was consumed, the catalyst was filtered off, and the filtrate was poured into 300 ml. of ice water. Light white crystals of phenylhydroxylamine were obtained and they were recrystallized from petroleum ether. The melting point was 76~78°C. Found: C, 66.20; H, 6.73. Calcd. for C_6H_7ON: C, 66.03; H, 6.47%. This unstable intermediate was easily converted into azoxybenzene on exposure to air according to the following equations:

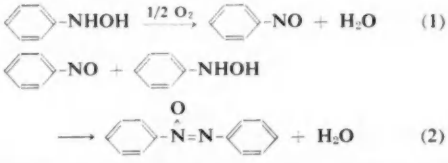

Therefore, the yield of phenylhydroxylamine was calculated from that of azoxybenzene.

In the same way, the partial reduction of *p*-nitroanisole and of ethyl *p*-nitrobenzoate was carried out and the yields of hydroxylamines and amines were determined. The results are shown in Table I. Nitrobenzene and ethyl *p*-nitrobenzoate gave more hydroxylamines than *p*-nitroanisole.

This agrees with the analysis of the curves

TABLE I. THE PRODUCTS OF PARTIAL REDUCTION

Compound reduced	Yield of hydroxylamine, %	Yield of amine, %
Nitrobenzene	77	0
Ethyl *p*-nitrobenzoate	60	0
p-Nitroanisole	22	40

* Present address; Division of Radiation Applications, Japan Atomic Energy Research Institute, Ibaraki-ken.

1) Cf. H. Debus and J. C. Jungers, *Bull. soc. chim. France*, 1959, 785.

2) S. Scholnik, J. R. Reasenberg, E. Lieber and G. Smith, *J. Am. Chem. Soc.*, **63**, 1192 (1941); J. R. Reasenberg, E. Lieber and G. Smith, ibid., **61**, 384 (1939).

3) V. P. Shmonina and D. V. Sokolski, *Zhur. Obshchei Khim. S. S. S. R.*, **26**, 1759 (1956).

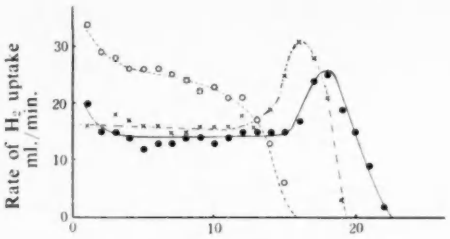

Fig. 1. Rate of Hydrogen uptake.
× Nitrobenzene.
○ *p*-Nitroanisole.
● Ethyl *p*-nitrobenzoate.

of the hydrogen consumption rates in the complete reduction to amines. As is shown in Fig. 1, the reduction rate of *p*-nitroanisole is monotonously decreasing, whereas those of nitrobenzene and ethyl *p*-nitrobenzoate have a remarkable increase towards the end of the reaction. It is likely that this increase in the rate takes place when the hydroxylamines are reduced to the amines. The fact that the hydroxylamines which have greater reduction rates than the parent nitro compounds were isolated as the intermediates in the partial reduction, can be understood from the difference in the affinities of the nitro compounds and hydroxylamines to the nickel catalyst. The nitro compounds with stronger affinities repel the hydroxylamines from the catalyst surface. And it can be said that the affinity difference is greater between nitrobenzene and phenylhydroxylamine and between ethyl *p*-nitrobenzoate (with an electron attracting group) and the corresponding hydroxylamine than between *p*-nitroanisole (with an electron repelling group) and its hydroxylamine. This agrees with the result[4] of the catalytic reduction of nitro compounds with a platinum catalyst.

Therefore, the following sequence of processes is presented:

$$ArNO_2 + Ni \longrightarrow ArNO_2\text{-}Ni \quad (3)$$

$$ArNO_2\text{-}Ni + 2H_2 \longrightarrow ArNHOH\text{-}Ni + H_2O \quad (4)$$

$$ArNHOH\text{-}Ni \begin{cases} \xrightarrow{H_2} ArNH_2 + Ni + H_2O & (5) \\ \xrightarrow{ArNO_2} ArNO_2\text{-}Ni + ArNHOH & (5') \end{cases}$$

$$ArNHOH + Ni \longrightarrow ArNHOH\text{-}Ni \quad (6)$$

$$ArNHOH\text{-}Ni \xrightarrow{H_2} ArNH_2 + Ni + H_2O \quad (7)$$

where Ni means the active center of the nickel catalyst.

The author wishes to express his hearty thanks to Professor Y. Urushibara for his kind guidance and encouragement throughout this work. The author is also very grateful to Dr. M. Kobayashi and Dr. S. Nishimura for their kind discussion.

Department of Chemistry
Faculty of Science
The University of Tokyo
Hongo, Tokyo

4) G. Cusmano, *Ann. chim. applicata*, **12**, 123 (1919), *Chem. Abstr.*, **14**, 1314 (1920).

Intramolecular Interaction between Hydroxyl Group and π-Electrons. X[1]*. Tertiary Alcohols Related to Phenethyl Alcohol and 3-Buten-1-ol**

By Michinori ŌKI and Hiizu IWAMURA

(Received June 16, 1960)

It has been shown in the previous papers[2] that the intramolecular interaction between the hydroxyl group and π-electrons in ω-phenylalkanols and ω-hydroxy-1-alkenes is operative up to phenethyl alcohol and 3-buten-1-ol, respectively. On the other hand, the accumulated data in this laboratory show that there are some alcohols within the above limitation which do not possess the internal interaction, such as 3-cyclohexen-1-ol, and others which have unexpectedly strong O–H stretching absorption (ν_{O-H}) due to the interacting form[3]. The dependence of the occurrence and the

1) Part IX: M. Ōki and H. Iwamura, This Bulletin, **33**, 427 (1960).

* The summary of this work was presented at the 13th Annual Meeting of the Chemical Society of Japan, Tokyo, April, 1960.

2) M. Ōki and H. Iwamura, This Bulletin, **32**, 567, 1135 (1959).

3) M. Ōki, H. Iwamura and T. Onoda, Unpublished work.

strength of the interaction on the conformation and the configuration of the molecule may inversely be taken advantage of for elucidation of some problems in the stereochemistry of complex organic compounds including natural products. From the point of the above purpose it will be of value at this stage of investigations to supply further fundamental knowledge relating the strength of the interaction to the conformation of the molecule.

While many authors[4] have recently observed the doublet character of ν_{O-H} of phenethyl alcohol derivatives and 3-buten-1-ol in the infrared absorption, it has been shown by the present authors[2], that their ν_{O-H} absorptions separate into three (Fig. 1), each being exemplified by the following conformational isomers in Fig. 2, in the case of phenethyl alcohol. The higher two bands are derived from the rotational isomerism about C_α–O bond and observed even in saturated alcohols[5]. The highest absorption at about 3636 cm^{-1} (I) has been assigned to the ν_{O-H} of the hydroxyl group with its hydrogen atom between two hydrogen atoms attached to the α-carbon atom, while the second at about 3627 cm^{-1} (II) to the ν_{O-H} with hydroxyl hydrogen between a hydrogen and a carbon atom. The third band at the lowest region of the spectra (III) is of a different kind and has been assigned to ν_{O-H} of the hydroxyl group having intramolecular interaction with π-electrons of the benzene nucleus. In other words, II and III are the rotational isomers about C_α–C_β bond.

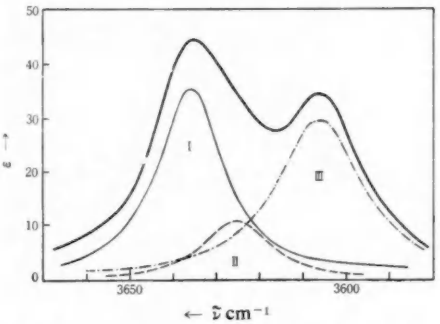

Fig. 1. ν_{O-H} absorption of phenethyl alcohol.

The triplet nature of the infrared absorption mentioned now, however, does not mean the apparent separation of the absorption curve but that the apparent curve can best be represented by an overlap of three symmetric absorption curves of the type of the Lorentz function[6]. Then nine parameters; a_i, b_i and ν_i (i=1, 2 and 3), must be determined in this case and the procedure of the division of the apparent curve is troublesome, whether it is the trial and error method[2] or the least squares method[1]. In the previous paper[1], this difficulty was mentioned and overcome by taking advantage of a tertiary alcohol which shows only doublet ν_{O-H}. The energy of the interaction between an alcoholic hydroxyl group and π-electrons of a benzene nucleus in benzyldimethylcarbinol was thus determined. In the present paper the measurement is extended to the interaction between an alcoholic hydroxyl group and π-electrons of ethylenic double bond in allyldimethylcarbinol. The effect of rotational degrees of freedom on the number of the interacting forms of the molecule and consequently on the apparent ν_{O-H} curve is also discussed.

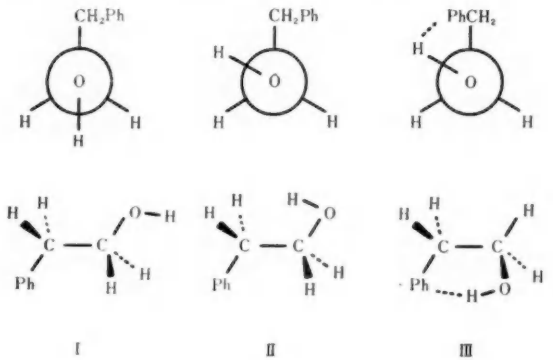

Fig. 2.

4) D. S. Trifan, J. L. Weinmann and L. P. Kuhn, *J. Am. Chem. Soc.*, **79**, 6566 (1957); A. W. Baker and A. T. Shulgin, ibid., **80**, 5358 (1958); I. M. Goldman and R. O. Crisler, *J. Org. Chem.*, **23**, 751 (1958).

5) M. Ōki and H. Iwamura, This Bulletin, **32**, 950 (1959).

6) D. A. Ramsay, *J. Am. Chem. Soc.*, **74**, 72 (1952).

Experimental

Measurement and Calculation.—Measurement of the ν_{O-H} absorption and the calculation of the band properties and the energy of the interaction were carried out as described previously[1,7], for doublet absorption, Eq. 1 being assumed and six parameters determined by means of the least squares method.

$$D(\nu)=\frac{a_i}{(\nu-\nu_i)^2+b_i^2}+\frac{a_f}{(\nu-\nu_f)^2+b_f^2} \quad (1)$$

Materials.—Benzyldimethylcarbinol and allyldimethylcarbinol were prepared by action of acetone on benzyl- and allylmagnesium chlorides, respectively, and their physical constants were as follows: benzyldimethylcarbinol b.p. 70°C/3mmHg, n_D^{25} 1.5158. Found: C, 80.10; H, 9.14. Calcd. for $C_{10}H_{14}O$: C, 79.95; H, 9.39%. (lit.[8], b. p. 59~60°C/1.5 mmHg, n_D^{25} 1.5128): allyldimethylcarbinol b. p. 119°, n_D^{15} 1.4250 (lit.[9], b. p. 118~120°C, n_D^{17} 1.4300).

Dibenzylmethylcarbinol and diallylmethylcarbinol were prepared by action of the corresponding Grignard reagents on ethyl acetate: dibenzylmethylcarbinol b.p. 148°C/3 mmHg, n_D^{23} 1.5686 (lit.[10], b. p. 182°C/15mmHg): diallylmethylcarbinol b. p. 74°C/43 mmHg, n_D^{3} 1.4500 (lit.[11], b. p. 158.4°C). Tribenzylcarbinol and triallylcarbinol were prepared through Grignard reaction between diethyl carbonate and benzyl- and allylmagnesium chlorides, respectively: tribenzylcarbinol m. p. 114~115°C (lit.[12], m. p. 115°C): triallylcarbinol b. p. 82°C/16mmHg, n_D^{23} 1.4682 (lit.[13], b. p. 191~192°C, n_D^{21} 1.468).

Results and Discussion

The apparent ν_{O-H} curves of allyldimethylcarbinol at several temperatures are shown in Fig. 3. Each curve can be regarded as an overlap of two Lorentz function curves as is exemplified by the curve at 24°C in Fig. 4, and six parameters determined by applying Eq. 1 to the apparent curves are summarized in Table I. The characteristic tendencies of the dependence of some band properties on temperature such as decrease of the total intensity, increase of the half band-width and shift of the wave numbers to the higher side, are again observed in this case.

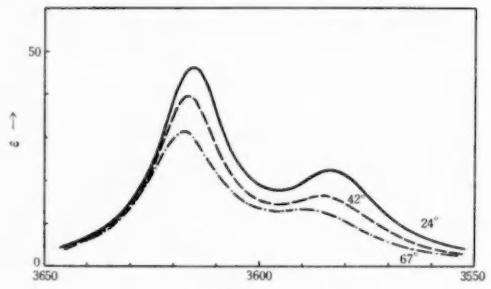

Fig. 3. The apparent ν_{O-H} absorptions of allyldimethylcarbinol at several temperatures; —— 24°C, - - - 42°C, -·-· 67°C.

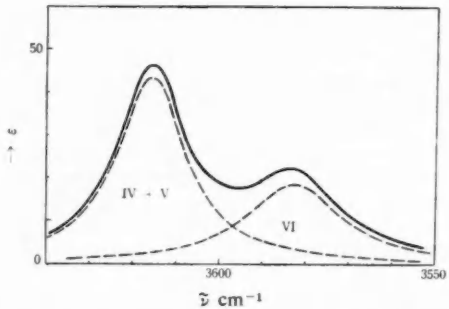

Fig. 4. ν_{O-H} absorption of allyldimethylcarbinol at 24°C.
—— the observed curve
- - - the divided bands

Table I. The effect of temperature on the ν_{O-H} absoption of allyldimethylcarbinol

$1/T\times10^3$ °K^{-1}	ν_{O-H}	ν	a	b	$\ln(A_i/A_f)$
3.37	i	3582.7	21.40	13.18	−0.521
	f	3615.9	26.28	9.61	
3.25	i	3583.7	21.31	13.66	−0.529
	f	3616.2	25.70	9.71	
3.17	i	3583.7	19.50	14.87	−0.593
	f	3616.8	23.11	9.74	
3.02	i	3585.2	16.70	15.21	−0.660
	f	3617.3	21.75	10.24	
2.95	i	3587.4	15.41	15.50	−0.699
	f	3618.0	21.58	10.79	

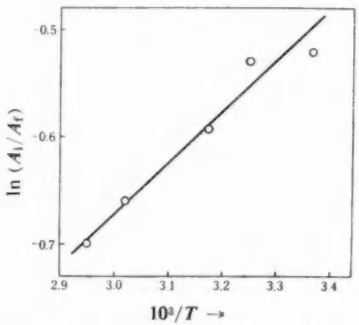

Fig. 5. The temperature dependence of $\ln(A_i/A_f)$.

7) Part VIII: M. Ōki and H. Iwamura, This Bulletin, 33, 717 (1960).
8) R. Heck and S. Winstein, *J. Am. Chem. Soc.*, **79**, 3432 (1957).
9) S. Coffey, *Rec. trav. chim. Pay-Bas*, **41**, 653 (1922).
10) R. Dolique, *Compt. rend.*, **190**, 881 (1930).
11) B. Sorokin, *Ann.*, **185**, 169 (1877).
12) A. A. Morton and J. R. Stevens, *J. Am. Chem. Soc.*, **53**, 4031 (1931).
13) A. Reformatski, *Ber.*, **41**, 4086 (1908).

TABLE II. THE ENERGIES AND THE ENTROPY TERMS OF THE INTERACTION IN ALLYLDIMETHYL- AND BENZYLDIMETHYLCARBINOLS

Carbinol	$-\Delta H$ (kcal./mol.)	$\Delta S/R-\ln a$	$\Delta\nu_{max}$ (cm^{-1})
CH_2=$CHCH_2CMe_2OH$	0.90±0.07	−2.03±.012	33.2
$PhCH_2CMe_2OH$	0.54±0.13	−1.16±0.17	21.4

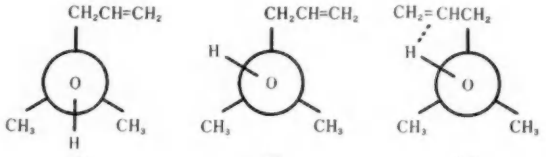

IV V VI

Fig. 6.

Temperature versus $\ln(A_i/A_f)$ relation is shown in Fig. 5. The values obtained therefrom are tabulated in Table II together with those of benzyldimethylcarbinol reported in the preceding paper[1].

The strengths of the interactions are fairly smaller than those ever estimated. That is, Bamford[14] suggested the energy to be 2∼3 kcal./mol. for the interaction between methanol and aromatic nucleus and Schleyer et al.[15] 1.4 kcal./mol. for phenethyl alcohol. However, disappearance of the interacting ν_{O-H} for 3-cyclohexen-1-ol and β-tetralol seems to suggest, that the energy difference between the free and the interacting molecules is less than 1 kcal./mol. While West[16] has recently shown, that olefins are generally stronger proton-acceptors than simple aromatic hydrocarbons in the intermolecular interaction between the hydroxyl group and π-electrons through measurement of the shift of ν_{O-H} from free phenol to phenol in hydrocarbons, it is for the first time that the proposition was realized in the intramolecular interaction through the direct energy measurement.

The doublet nature of the ν_{O-H} of allyldimethylcarbinol as well as benzyldimethylcarbinol shows, that the rotational isomers around C_α–O bond can not be distinguished so far as ν_{O-H} is concerned under the present dispersion of the spectrometer[2]; that is, IV and V in Fig. 6 can not be distinguished and equally give the higher ν_{O-H} at 3616 cm^{-1}. In both forms hydroxyl hydrogen lies between two carbon atoms attached to the α-carbon atom as in *tert*-butyl alcohol[5]. The absorption at 3584 cm^{-1} (VI), on the other hand, can be assigned to the hydroxyl group having internal interaction. In this case, the rotational degree around the C_α–C_β and C_β–C_γ bonds must be fixed favorably for the interaction, i. e., the hydroxyl group and the group carrying π-electrons must be closely situated.

Although it is usual that the energy difference of about one kcal./mol. between two components in an equilibrium mixture makes one at a lower energy level exceedingly predominant, it does not seem to be the case in allyldimethylcarbinol, the ratio A_i/A_f being only 0.59. This could be explained if the absorption intensity per molecule of the interacting ν_{O-H} is much weaker than that of free ν_{O-H} and even small A_i represents a large number of the interacting molecules. However, the assumption is rather contradictory to the knowledge of ordinary hydrogen bonding[17] where the absorption intensity increases on hydrogen bond formation because of increased change of the dipole moment accompanying O–H vibrational motion. The possibility may also be excluded from the fact that, as reported previously[2], the sum of the integrated intensities (A_i+A_f) is almost constant throughout the wide range of substituted phenethyl alcohols. It can preferably be explained by considering the statistical factor contributed from the rotational degree of freedom. Rough computation of the number of the possible conformations for allyldimethylcarbinol was made with the assumption that only the staggered conformations are possible for each bond axis. It may reasonably be assumed that both isomers IV and V have not only the same ν_{O-H} but also almost the same energy in regard to the conformations of the hydroxyl group. As to the C_α–C_β axis, three conformations VII, VIII and the mirror image of the latter in Fig. 7 are assumed to have the same energy as a first approximation. Strictly speaking, however, VII and VIII are different in that the former has

14) C. H. Bamford, *Discuss. Faraday Soc.*, **16**, 229 (1954).
15) P. von Schleyer et al., *Tetrahedron Letters*, No. 14, p. 1 (1959).
16) R. West, *J. Am. Chem. Soc.*, **81**, 1614 (1959).
17) H. Tsubomura, *J. Chem. Phys.*, **24**, 927 (1956).

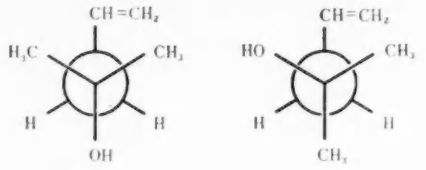

VII VIII

Fig. 7.

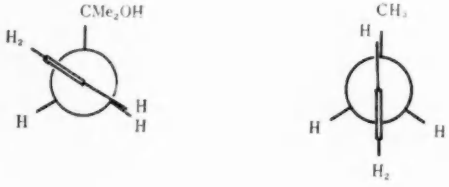

IX X

Fig. 8.

two gauche type interactions in *n*-butane structure, while the latter a gauche interaction in *n*-butane structure and another gauche interaction in *n*-propyl alcohol. Hence the energy difference between VII and VIII becomes $E_g^{bu.}-E_g^{pr.}$, which may be assumed to be zero[18]. Around the C_β–C_γ bond, only the gauche conformations (IX and its mirror image in Fig. 8) may be permitted as in 1-butene, where two gauche forms are more stable than the trans (X) by 1970 cal./mol.[19] Out of eighteen ($3\times3\times2$) conformations thus possible, only two can take part in the internal interaction and are stabilized by the energy of the interaction. Therefore the ratio, $w_i/w_t=1/8$, must be introduced as a weight in the following Eq. 2;

$$n_i/n_t = w_i/w_t \cdot e^{-(E_i-E_t)/(RT)} \qquad (2)$$

where "n" is the number of the molecules. Substitution of the energy of the interaction obtained above gives $n_i/n_t=0.56$ which is in good agreement with A_i/A_t value of 0.59.

The computation was extended to the data of epicholesterol which shows as high A_i/A_t value as 3.14[20]. The molecule has a fairly rigid structure as in Fig. 9 and the freedom of rotation is left only for C_α–O axis. Out of three possible conformations, only one can take part

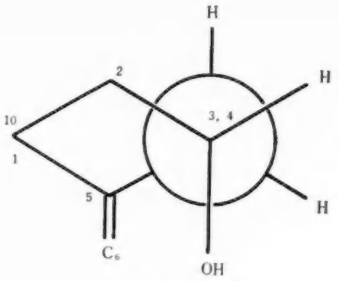

Fig. 9.

in the interaction geometrically, the weight becoming 1/2. As the hydroxyl group is now of the secondary alcohol, it is a stronger proton-donor in hydrogen bonding than those of tertiary alcohols[21], while the ethylenic double bond is regarded to be a stronger proton-acceptor than that of allyldimethylcarbinol, because it possesses three alkyl substituents[14]. The strength of the interaction must therefore be greater than that obtained above and is arbitrarily assumed to be 1.0 kcal./mol[22]. Then n_i/n_t becomes 2.7, which satisfactorily explains why epicholesterol, unlike 3-buten-1-ol, shows larger A_i/A_t value than one.

Benzyldimethylcarbinol may be treated in the same way. The energy difference between two rotational isomers corresponding to VII and VIII would be marked, the latter being more stable, but is neglected for the sake of convenience as no evaluation is possible. As to the C_β–C_γ bond (Fig. 10), every rotational conformation which must be analogous to that of ethylbenzene[23] favors the interaction, and therefore the rotational degree of freedom about this axis is left out of consideration. Thus w_i/w_t becomes 2/7 in all. This value, together with 1/8 in allyldimethylcarbinol, may be regarded to correspond to the entropy terms of the interaction in Table II and well explains the greater absolute value in the latter than in the former, since $\ln 2/7$ is -1.25 and $\ln 1/8$ is -2.08. The energy difference of 0.54 kcal./mol.

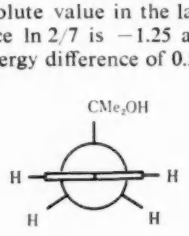

Fig. 10.

18) $E_g^{bu.}$ has been regarded to be 800 cal./mol. (K. S. Pitzer, *J. Chem. Phys.*, **8**, 711 (1940).), while no datum is available for $E_g^{pr.}$, the energy difference between gauche and trans forms in *n*-propyl alcohol.

19) J. G. Aston, S. Isserow and G. J. Szasz, *J. Chem. Phys.*, **12**, 336 (1944); **14**, 67 (1946).

20) M. Ōki and H. Iwamura, This Bulletin, **32**, 307 (1959).

21) L. P. Kuhn, *J. Am. Chem. Soc.*, **76**, 4328 (1954).

22) Assuming that $\Delta\nu_{max}$ is proportional to the energy of the interaction, $-\Delta H=0.9\times34.1/33.2=0.93$ kcal./mol. is obtained, as $\Delta\nu_{max}$ in epicholesterol amounts to 34.1 cm^{-1}.

23) F. G. Brickwedde, M. Moskow and R. B. Scott, *J. Chem. Phys.*, **13**, 547 (1945).

TABLE III. ν_{O-H} OF TERTIARY ALCOHOLS RELATED TO 3-BUTEN-1-OL AND PHENETHYL ALCOHOL

Alcohol	ν_{O-H}	ν_{max} cm^{-1}	$\Delta\nu^a_{1/2}$ cm^{-1}	$A\times10^{-3}$ mol^{-1} l. cm^{-2}	$\Delta\nu_{max}$ cm^{-1}	A_i/A_f	n_i/n_f
CH_2=$CHCH_2CMe_2OH$	i	3582.7	21.4	1.50	33.2	0.59	0.56
	f	3615.9	26.3	2.53			
$(CH_2$=$CHCH_2)_2CMeOH$	i	3580.9	25.2	2.58	33.8	1.38	1.29
	f	3614.7	20.2	1.87			
$(CH_2$=$CHCH_2)_3COH$	i	3577.8	25.4	3.87	33.9	3.37	2.25
	f	3611.7	20.4	1.15			
$PhCH_2CMe_2OH$	i	3593.5	16.1	2.02	21.4	0.75	0.71
	f	3614.9	25.1	2.70			
$(PhCH_2)_2CMeOH$	i	3590.8	26.0	4.35	15.2	3.85	1.97
	f	3606.0	26.0	1.13			
$(PhCH_2)_3COH$	i	3580.3	19.3	6.04	—	—	4.92
	f	—	—	—			

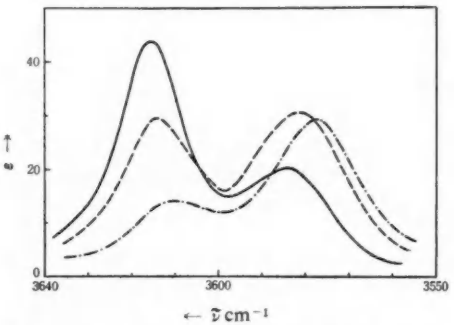

Fig. 11. ν_{O-H} absorptions of allylcarbinols.
—— CH_2=$CHCH_2CMe_2OH$
- - - $(CH_2$=$CHCH_2)_2CMeOH$
-·-· $(CH_2$=$CHCH_2)_3COH$

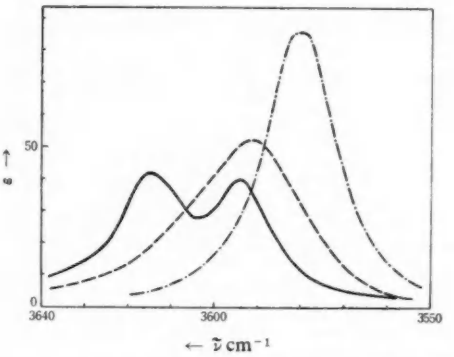

Fig. 12. ν_{O-H} absorptions of benzylcarbinols.
—— $PhCH_2CMe_2OH$ - - - $(PhCH_2)_2CMeOH$
-·-· $(PhCH_2)_3COH$

obtained for benzyldimethylcarbinol was used as the energy of the interaction and n_i/n_f of 0.71 was obtained as shown in Table III.

In order to see these statistical effects on ν_{O-H} absorption curves, the measurements were extended to some tertiary alcohols related to 3-buten-1-ol and phenethyl alcohol. The apparent ν_{O-H} absorptions are shown in Figs. 11 and 12, respectively, and the numericals are summarized in Table III, the last column being the n_i/n_f values computed as above. The energies of the interaction tabulated in Table II were applied to the same type of compounds, and this procedure may be justified from the constant $\Delta\nu_{max}$ values in the series of allylcarbinols.

In both series the fair agreement between the observed A_i/A_f and the computed A_i/A_f in the lowest homologs does not always hold true in the higher homologs, especially in benzylcarbinol series. The discrepancy can almost exclusively be attributed to the incorrect assumption made in the computation of the weight, that is, to the effect of steric hindrance which disfavors such conformations with the free hydroxyl group as shown in Fig. 13.

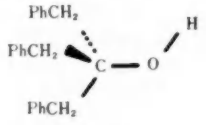

Fig. 13.

It has been shown in this manner, that the ratio of the number of the interacting molecules to the free ones can almost quantitatively be interpreted by considering the statistical or frequency factor of the conformations of the molecules under a given value of the energy of the interaction. In the near future, the computation will be extended to the other organic compounds to explain their ν_{O-H} absorption curves and the conformations of the molecules.

The authors are indebted to Professor Y. Urushibara and Professor T. Shimanouchi for

their encouragement and discussion throughout this work. The authors' thanks are also due to the Ministry of Education for the Grant in Aid for Fundamental Scientific Research.

Department of Chemistry
Faculty of Science
The University of Tokyo
Hongo, Tokyo

*NMR Spectra of Aliphatic Compounds Containing Oxygen Atoms and the Related Compounds**

By Kenkichi NUKADA

(Received April 13, 1960)

Many works concerning the chemical shifts of functional groups in organic molecules[1-4] have been reported, but the systematic study for the chemical shifts of functional groups containing oxygen atoms has not yet been carried out in detail. In this paper, the author presents the NMR spectra of more than thirty aliphatic compounds containing the oxygen atom and the related compounds such as ethers, formals, acetals, ketal, orthoaliphatic acid esters, polyethylene glycol diethers and cyclic compounds. These compounds contain various types of functional groups such as CH_3–O, O–CH_2–O, HC$\langle$O, etc. Comparing spectra with each other, the author obtained a table of chemical shifts of functional groups. It is also found that there exist some correlations between the chemical shifts of the same type of equivalent protons and the type of alkyl groups bonded to the oxygen atom. The origin of the correlation was considered.

Experimental

Measurement of NMR Spectra.—Spectra were obtained by means of a Varian 4300 B spectrometer (40 Mc). The spectra of both pure liquid benzene solution (volume ratio of solute to benzene equals to 4 : 1) for each sample were obtained and the chemical shifts with respect to proton resonance in benzene were calculated. As a field marker, the spectrum of pure propionic acid was used (Fig. 1). The absolute value of shift was calibrated by the displacement between proton resonances in benzene and cyclohexane (223 cps)[3]. Since it is necessary to maintain all the experimental conditions as stable as possible in the accurate chemical shift measurement, a sweep rate of $1p/10^2$ per second was used. When necessary to obtain higher resolved spectra, a smaller sweep rate ($0.4p/10^2$) was used. In the latter case, however, the error of chemical shift was considerably increased. The probable error of the measurement in case of rapid passage was within ±2%. Spectra of pure sample were obtained because sometimes it was necessary to check the solvent effect in benzene solution.

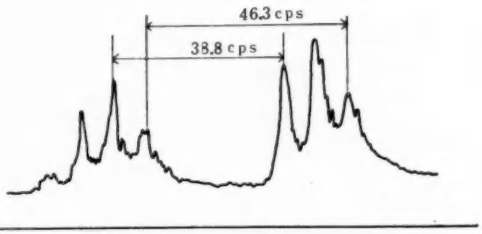

Fig. 1. NMR spectrum of pure propionic acid. This spectrum was used as a field marker, i.e., before and after every chemical shift measurement this spectrum was measured. The absolute values between peaks were calibrated by the displacement between proton resonances in benzene and cyclohexane (223 cps).

Samples.—Formals (dimethyl formal, methyl ethyl formal, diethyl formal and diisopropyl formal) and acetals (dimethyl acetal, methyl ethyl acetal and diethyl acetal) were synthesized in the author's laboratory[5]. All the other compounds are commercial products (Tokyo Kasei and Eastman Kodak Co.).

* This is essentially the extension of the work already reported in this Bulletin as a short communication. (K. Nukada and U. Maeda, This Bulletin, 32, 656 (1959)).

1) L. H. Meyer, A. Saika and H. S. Gutowsky, *J. Am. Chem. Soc.* 75, 4567 (1953).

2) V. D. Tiers, "Characteristic Nuclear Magnetic Resonance Shielding Values (Spectral Position) for Hydrogen in Organic Structures", Organic Section, Exploratory NMR Studies, Project 737602, Minnesota Mining and Manufacturing Co. U. S. A. (1958).

3) N. F. Chamberlain, *Anal. Chem.*, 31, 56 (1959).

4) B. L. Bothner-By, C. Naar-Colin and B. L. Shapiro "NMR Spectra and Structure Correlations", (Vol. II), Harvard University, (1958).

5) K. Nukada, *J. Chem. Soc. Japan, Pure Chem. Sec.* (*Nippon Kagaku Zasshi*), 80, 976 (1959).

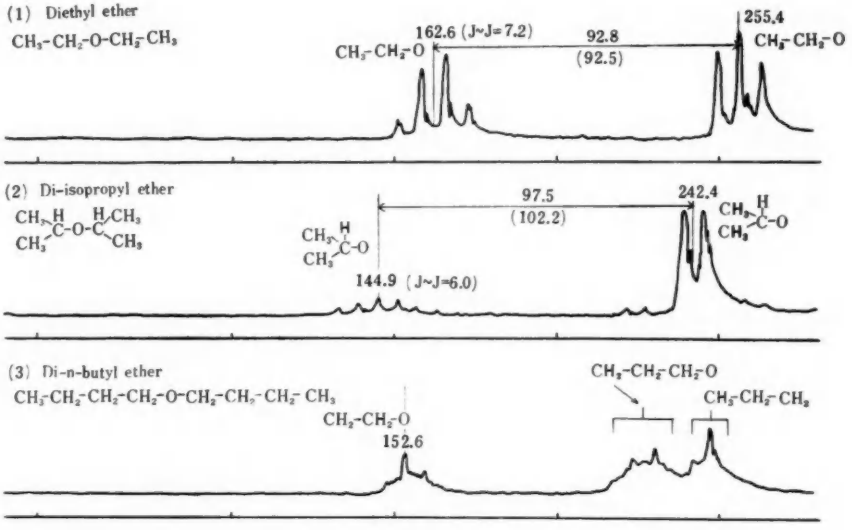
(1) Diethyl ether
CH3-CH2-O-CH2-CH3
162.6 (J~J=7.2)
92.8
(92.5)
255.4
CH3-CH2-O
CH3-CH2-O
(2) Di-isopropyl ether
97.5
(102.2)
242.4
144.9 (J~J=6.0)
(3) Di-n-butyl ether
CH3-CH2-CH2-CH2-O-CH2-CH2-CH2-CH3
CH2-CH2-O
152.6
CH3-CH2-CH2-O
CH3-CH2-CH2

Fig. 2-1.

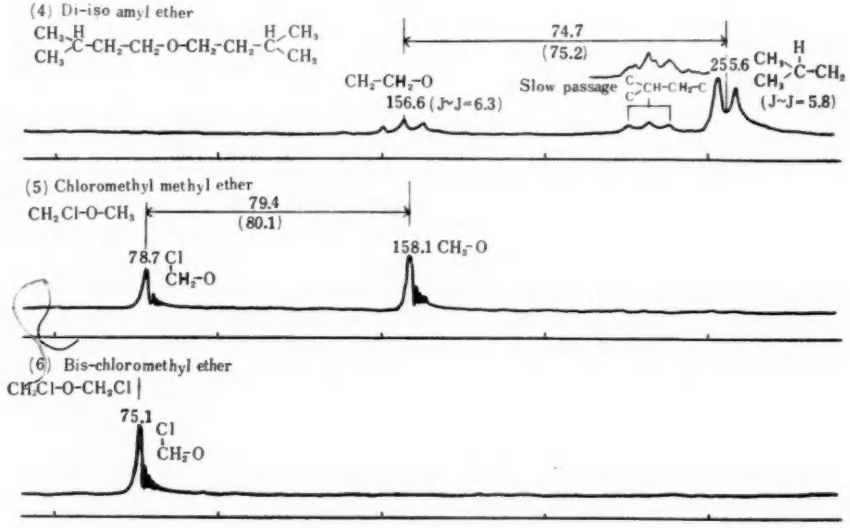
(4) Di-iso amyl ether
74.7
(75.2)
CH2-CH2-O
156.6 (J~J=6.3)
Slow passage
255.6
(J~J=5.8)
(5) Chloromethyl methyl ether
CH2Cl-O-CH3
79.4
(80.1)
78.7
CH2-O
158.1 CH3-O
(6) Bis-chloromethyl ether
CH2Cl-O-CH2Cl
75.1
CH2-O

Fig. 2-2.

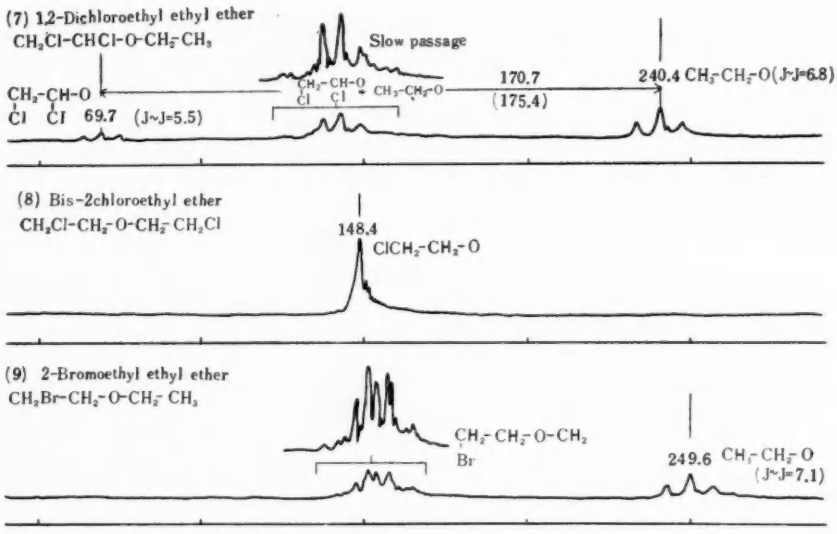
(7) 1,2-Dichloroethyl ethyl ether
CH2Cl-CHCl-O-CH2-CH3
Slow passage
CH2-CH-O
Cl Cl
69.7 (J~J=5.5)
CH3-CH2-O
170.7
(175.4)
240.4 CH3-CH2-O(J~J=6.8)
(8) Bis-2chloroethyl ether
CH2Cl-CH2-O-CH2-CH2Cl
148.4
ClCH2-CH2-O
(9) 2-Bromoethyl ether
CH2Br-CH2-O-CH2-CH3
CH2-CH2-O-CH2
Br
249.6 CH3-CH2-O
(J~J=7.1)

Fig. 2-3.

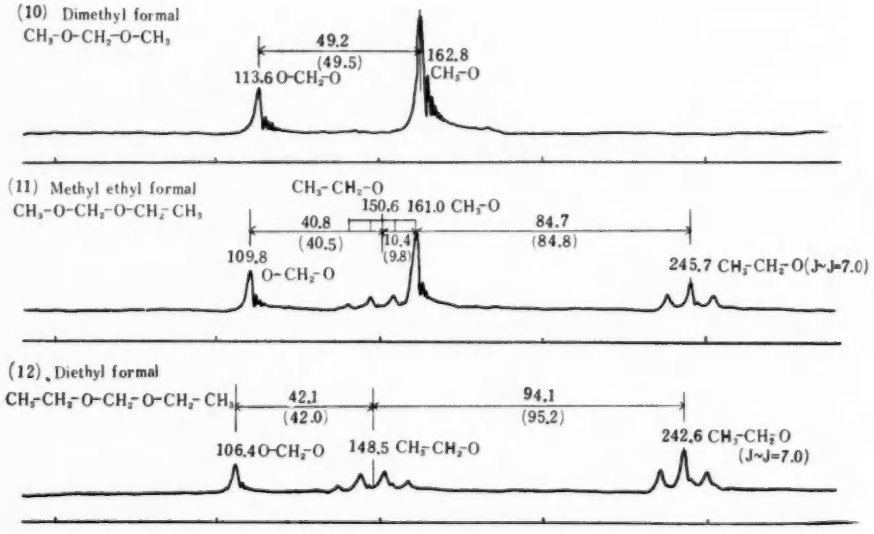
(10) Dimethyl formal
CH3-O-CH2-O-CH3
49.2
(49.5)
113.6 O-CH2-O
162.8
CH3-O
(11) Methyl ethyl formal
CH3-O-CH2-O-CH2-CH3
CH3-CH2-O
150.6 161.0 CH3-O
40.8
(40.5)
10.4
(9.8)
84.7
(84.8)
109.8
O-CH2-O
245.7 CH3-CH2-O(J~J=7.0)
(12) Diethyl formal
CH3-CH2-O-CH2-O-CH2-CH3
42.1
(42.0)
94.1
(95.2)
106.4 O-CH2-O
148.5 CH3-CH2-O
242.6 CH3-CH2-O
(J~J=7.0)

Fig. 2-4.

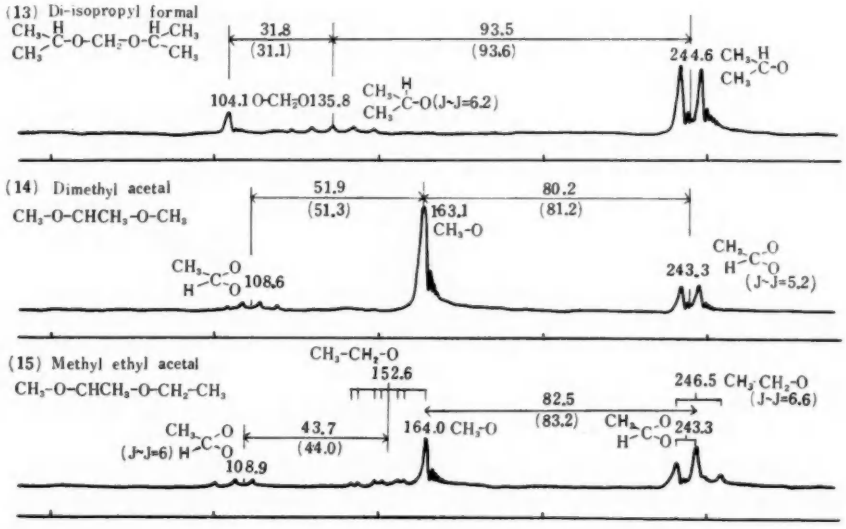
(13) Di-isopropyl formal
31.8
(31.1)
93.5
(93.6)
244.6
104.1
135.8
(J~J=6.2)
(14) Dimethyl acetal
CH3-O-CHCH3-O-CH3
51.9
(51.3)
80.2
(81.2)
163.1
CH3-O
108.6
243.3
(J~J=5.2)
(15) Methyl ethyl acetal
CH3-O-CHCH3-O-CH2-CH3
CH3-CH2-O
152.6
82.5
(83.2)
246.5
(J~J=6.6)
43.7
(44.0)
164.0
243.3
(J~J=6)
108.9

Fig. 2-5.

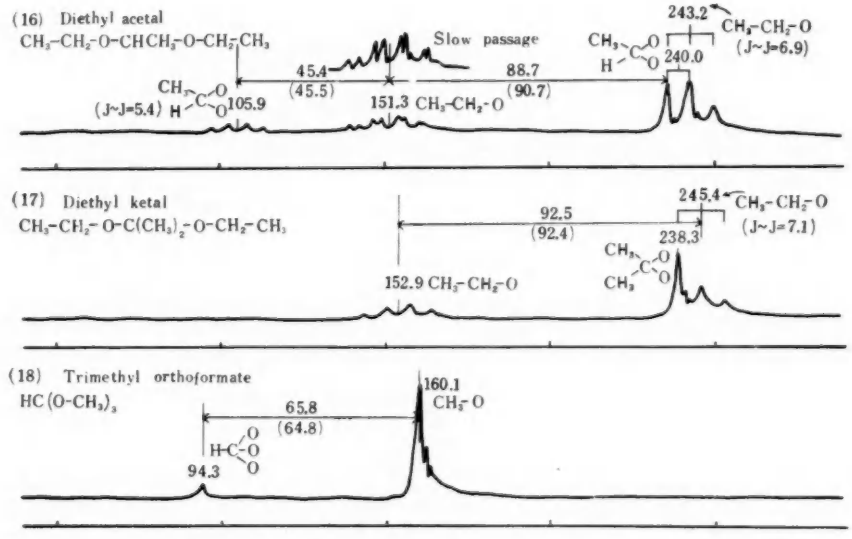
(16) Diethyl acetal
CH3-CH2-O-CHCH3-O-CH2-CH3
Slow passage
243.2
CH3-CH2-O
(J~J=6.9)
45.4
(45.5)
88.7
(90.7)
240.0
(J~J=5.4)
105.9
151.3
CH3-CH2-O
(17) Diethyl ketal
CH3-CH2-O-C(CH3)2-O-CH2-CH3
92.5
(92.4)
245.4
CH3-CH2-O
(J~J=7.1)
238.3
152.9
CH3-CH2-O
(18) Trimethyl orthoformate
HC(O-CH3)3
65.8
(64.8)
160.1
CH3-O
94.3

Fig. 2-6.

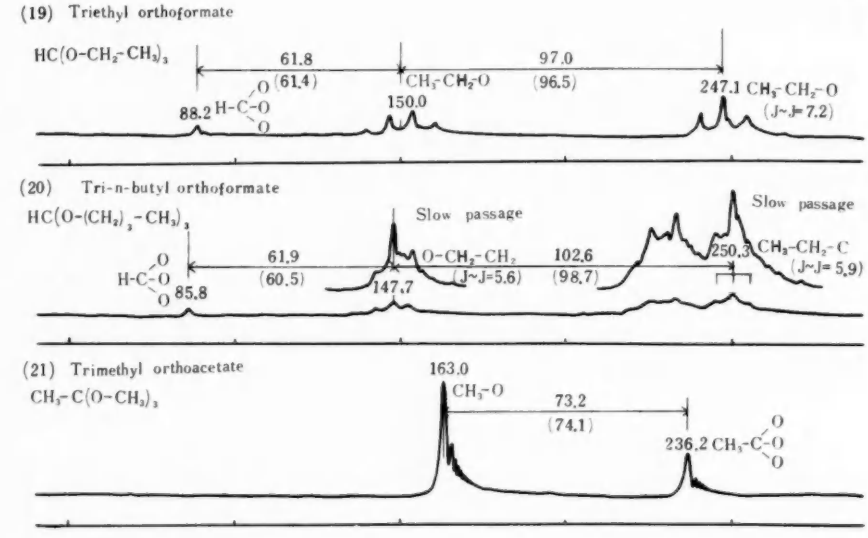
(19) Triethyl orthoformate
HC(O-CH2-CH3)3
61.8
(61.4)
97.0
(96.5)
88.2
150.0
247.1 CH3-CH2-O
(J~J=7.2)
(20) Tri-n-butyl orthoformate
HC(O-(CH2)3-CH3)3
Slow passage
Slow passage
61.9
(60.5)
O-CH2-CH2
(J~J=5.6)
102.6
(98.7)
85.8
147.7
250.3
CH3-CH2-C
(J~J=5.9)
(21) Trimethyl orthoacetate
CH3-C(O-CH3)3
163.0
CH3-O
73.2
(74.1)
236.2 CH3-C-O

Fig. 2-7.

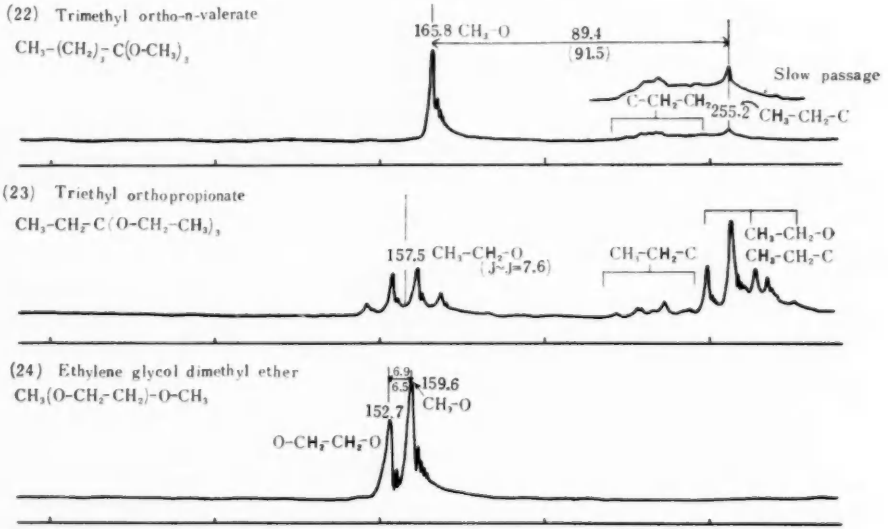
(22) Trimethyl ortho-n-valerate
CH3-(CH2)3-C(O-CH3)3
165.8 CH3-O
89.4
(91.5)
Slow passage
C-CH2-CH2
255.2 CH3-CH2-C
(23) Triethyl orthopropionate
CH3-CH2-C(O-CH2-CH3)3
157.5 CH3-CH2-O
(J~J=7.6)
CH3-CH2-C
CH3-CH2-O
CH3-CH2-C
(24) Ethylene glycol dimethyl ether
CH3(O-CH2-CH2)-O-CH3
6.9
6.5
159.6
CH3-O
152.7
O-CH2-CH2-O

Fig. 2-8.

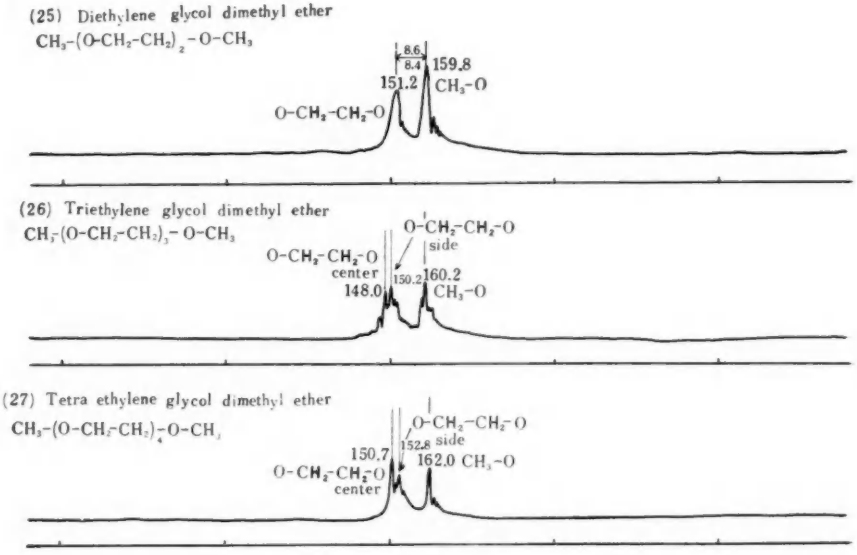

Fig. 2-9.

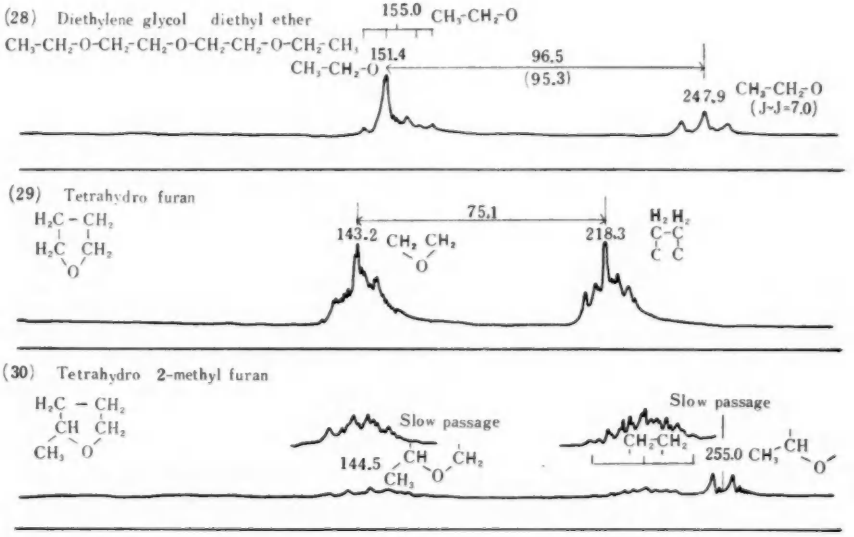

Fig. 2-10.

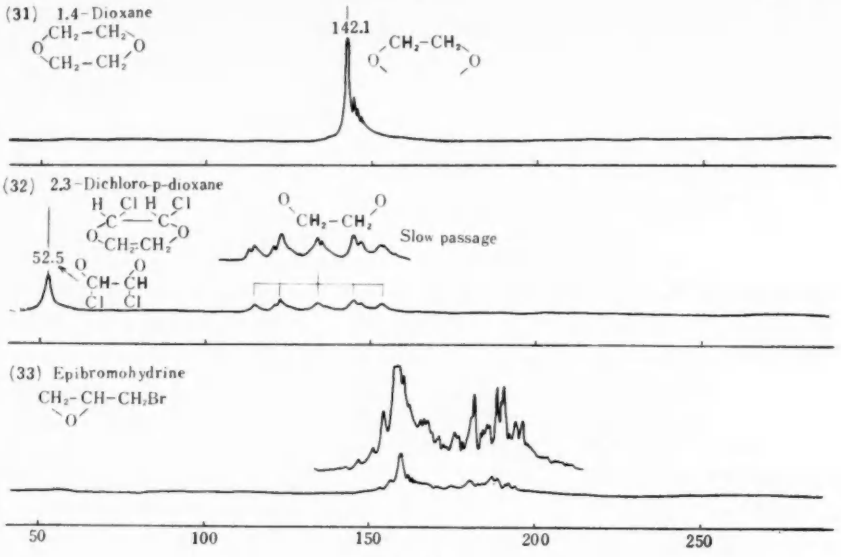

Fig. 2-11.

Fig. 2. NMR spectra of oxygen containing aliphatic compounds. Chemical shift (cps) from benzene protons and assignment are marked on each peak. J-J coupling constant and separation between peaks are also described.

TABLE I. CHEMICAL SHIFT OF FUNCTIONAL GROUP

Name of group	Type of group	Type of sub-group	Chemical shift cps	Number of samples
CH_3-C-C-C-		δ_{CH_3}	253.7±3.4	3
CH_3-CH_2-O-	B	β_{CH_3}	246.4±9.0	10
$(CH_3)_2$>CH-O-	B	β_{CH_3}	243.5±1.1	2
$(CH_3)_2$>C<(O-)(O-)	B	$\beta^2_{CH_3}$	242.2±2.2	3
CH_3-C(O-)(O-)(O-)	B	$\beta^3_{CH_3}$	236.2	1
-CH_2-C-O- (Five members ring)	B	β_{CH_2} (ring)	218.3	1
CH_3-O-	A	α_{CH_3}	161.6±4.2	11
-C-CH_2-O-	A	α_{CH_2}	152.9±9.7	12
-O-CH_2-CH_2-O	A	$\alpha\beta_{CH_2}$	151.0±3.0	5
Cl-CH_2-CH_2-O-		$\alpha'\beta_{CH_2}$, $\alpha\beta'_{CH_2}$	148.4	1
-C-CH_2-O- (Five members ring)	A	α_{CH_2} (ring)	143.9±0.7	2
-O-CH_2-CH_2-O- (Six members ring)	A	$\alpha\beta_{CH_2}$ (ring)	142.1	1
$(CH_3)_2$>CH-O-	A	α_{CH}	140.4±4.6	2
-O-CH_2-O-	A^2	$\alpha^2_{CH_2}$	108.5±5.1	4
CH_3-H>C<(O-)(O-)	A^2	α^2_{CH}	107.8±1.9	3
H-C(O-)(O-)(O-)	A^3	α^3_{CH}	89.4±4.9	3
Cl-CH_2-O-		$\alpha\alpha'_{CH_2}$	76.9±1.8	2
Cl_2>CH-O-		$\alpha\alpha'^2_{CH}$	69.7	1
-O-Cl>CH-CH<O-Cl (Six members ring)		$\alpha\alpha'\beta\beta'_{CH}$	52.5	1

TABLE II. CORRELATION BETWEEN CHEMICAL SHIFT AND THE TYPE OF SUBSTITUENT ALKYL GROUP (I)

Type of molecule	Type of alkyl group	Equivalent proton group	Chemical shift
$HC(OR)(OR)(OR)$	CH_3-	$HC(O)(O)(O)$	94.3
	CH_3-CH_2-		88.2
	$CH_3-(CH_2)_3-$		85.8
$H_2C(OR_1)(OR_2)$	R_1, R_2: CH_3-	$H_2C(O)(O)$	113.6
	R_1: CH_3-, R_2: CH_3-CH_2-		109.8
	R_1, R_2: CH_3-CH_2-		106.4
	R_1, R_2: $CH_3(CH_3)CH-$		104.1
$CH_3H C(OR_1)(OR_2)$	R_1, R_2: CH_3-	$CH_3H C(O)(O)$	108.6
	R_1: CH_3-, R_2: CH_3-CH_2-		108.9
	R_1, R_2: CH_3-CH_2-		105.9
$CH_3H C(OR_1)(OR_2)$	R_1, R_2: CH_3-	$CH_3H C(O)(O)$	243.3
	R_1: CH_3-, R_2: CH_3-CH_2-		343.3
	R_1, R_2: CH_3-CH_2-		240.0

TABLE III. CORRELATION BETWEEN CHEMICAL SHIFT AND THE TYPE OF SUBSTITUENT ALKYL GROUP (II)

Type of molecule	Type of alkyl group	Equivalent proton group	Chemical shift
$RC(O-CH_3)(O-CH_3)(O-CH_3)$	$H-$	$-O-CH_3$	160.1
	CH_3-		163.0
	$CH_3-(CH_2)_3-$		165.8
$RC(O-C_2H_5)(O-C_2H_5)(O-C_2H_5)$	$H-$	$-O-CH_2-CH_3$	150.0
	CH_3-CH_2-		157.5
$HR C(O-CH_3)(O-CH_3)$	$H-$	$-O-CH_3$	162.8
	CH_3-		163.1
$HR C(O-CH_3)(O-C_2H_5)$	$H-$	$-O-CH_3$	161.0
	CH_3-		164.0
$HR C(O-CH_3)(O-C_2H_5)$	H	$-O-CH_2-CH_3$	150.6
	CH_3-		152.6
$R_1R_2 C(O-C_2H_5)(O-C_2H_5)$	R_1, R_2: $H-$	$-O-CH_2-CH_3$	148.5
	R_1: $H-$, R_2: CH_3-		151.3
	R_1, R_2: CH_3-		152.9
$R_1R_2 C(O-C_2H_5)(O-C_2H_5)$	R_1, R_2: $H-$	$-O-CH_2-CH_3$	242.6
	R_1: $H-$, R_2: CH_3-		243.2
	R_1, R_2: CH_3-		245.4
$HR C(O-CH_3)(O-C_2H_5)$	$H-$	$-O-CH_2-CH_3$	245.7
	CH_3-		246.5

The purity of some compounds (formals, dimethyl acetal, methyl ethyl acetal, ethers except 1, 2-dichloroethyl ethyl ether, polyethylene glycol diethers and cyclic compounds except tetrahydrofuran and epibromohydrin) was checked by gaschromatograph. The other compounds were found to decompose in the column of gaschromatograph, and in this case the purity was checked by the infrared spectra*. The detailed description of the purification was reported elswhere[5,6].

Results and Discussion

The spectra obtained may be classified into three types as follows:

a) No peaks overlap with each other, so it is quite easy to assign them from the relative intensity and the appearance of the multiplet structures.

b) Some peaks overlap with each other, but referring to the assignment of class a) it is not so difficult to assign them in most cases.

c) Separation of chemical shift is the same order as J-J splitting. In this paper, the assignment of this class is not given since it is impossible to assign them without exact calculation.

In Fig. 2, the assignment and the value of chemical shifts (in cycle per second) are marked on each peak. The separation between peaks is also shown together with that of pure liquid in parentheses.

* Since the infrared spectra of ketal and orthoaliphatic acid esters have not been reported in the literature, it is impossible to check the purity of these compounds merely by the infrared spectra. Since these compounds were known to decompose gradually to alcohols, esters or to aldehydes in air at room temperature, they were distilled (in vacuo) several times until bands at 3500 cm^{-1} and 1700 cm^{-1} completely disappeared.

6) K. Nukada, *J. Chem. Soc. Japan, Pure Chem. Sec. (Nippon Kagaku Zasshi)*, **81**, 1028 (1960).

The average values of shifts of all functional groups are listed in Table I and these values are consistent with those listed by Chamberlain[3].

Except for halogenated ethers, all functional groups may be divided into four groups, B, A, A^2 and A^3 according to the approximate value of shift. These groups include sub-groups β, β^2 and β^3, $\alpha\beta$ and α, α^2 and α^3, respectively. The notation of "the type of sub-group" is defined as follows*: n equivalent protons bonded to α or β carbon atoms are designated as α_{CH_n} or β_{CH_n}. If carbon atoms are at α and/or β positions with respect to more than two oxygen atoms, several notations are used, i.e., $\alpha^2{}_{CH_n}$ or $\alpha\beta_{CH_n}$, etc. If the carbon atom is at α position with respect to the chlorine atom the notation α' is used. Practically, the chemical shifts of protons bonded to γ or far separated carbon atoms are not influenced by the electronegative atoms interested.

The order of shielding is $B > A > A^2 > A^3$ within the main groups. Further in each group, some correlations are recognized. In groups B and A, the order of shielding is $\beta > \beta^2 > \beta^3$ for CH_3 protons and $\alpha > \alpha\beta$ for CH_2 protons, respectively. In groups A and A^2, the order of shielding is $CH_3 > CH_2 > CH$ for α sub-group and $CH_2 > CH$ for α^2 sub-group, respectively.

The correlation between the chemical shift and electronegativity of the functional group being directly related to "the type of group" and "the type of sub-group" is quite reasonable.

Let us next consider the change in chemical shift within each sub-group in more detail. The chemical shift of equivalent protons in some functional groups changes, though very slightly, in homologue. The methyl proton shift of the methoxyl group in $R\text{-}C\langle^{O\text{-}Me}_{O\text{-}Me}_{O\text{-}Me}$, for example, goes to a higher field as the alkyl-group R becomes larger. In another example, the methylene proton shift in $CH_2\langle^{OR_1}_{OR_2}$, goes to a lower field as the alkyl groups R_1 and R_2 become larger. In Tables II and III, the correlations between the chemical shift and the type of attached alkyl group are shown in the former and the latter cases, respectively. Although the change of chemical shift is very slight and some correction of the solvent effect should be considered, surprisingly regular correlations are obtained.

If it is assumed that after a possible correction due to the solvent effect the order of the magnitude of the chemical shift does not change, the result obtained here will give some information concerning the molecular structure and electron density distribution in the molecule.

The possible explanation for the slight change of chemical shift is as follows:

1) **Steric Effect.**—By the steric repulsion between alxyl groups, the X-C-H bond angle changes slightly, following the slight change in hybridization of the carbon atom in C-H bond.

2) **Inductive Effect.** — As R goes from H through CH_3 to higher alkyl groups in R'-O-R, the electron affinity of oxygen atom for R' is lowered causing protons in R' to be more shielded*.

3) **Steric and Inductive Effect.**—As R goes from H to higher alkyl groups in R'-O-R, by the steric hindrance the C-O-C bond angle in R'-O-R increases slightly causing a slight change of hybridization of the oxygen atom and further the increase of electron affinity of the oxygen atom.

4) **Direct Effect.** — As R goes from H to higher alkyl groups, the bond angle in molecules change slightly, causing the slight change of magnetic anisotropy of atoms and then shielding for the protons interested.

At present, it is impossible to decide immediately which cause is predominant, since it is quite difficult to estimate the amounts of the influences of these effects on chemical shift quantitatively. The author could say, however, that at least two causes must be considered since opposite senses are obtained in the correlations shown in Tables II and III.

More detailed discussion concerning this problem will be reported in the near future.

The author wishes to express his sincere thanks to Drs. Y. Mashiko and A. Kuboyama of this Institute and Dr. S. Hattori of Kanazawa University for their valuable discussions, and to Dr. H. Honda and Mr. K. Nagata of the Resources Research Institute and Mr. A Suzuki of this Institute, for their help in the laboratory work.

Government Chemical Industrial Research Institute of Tokyo
Shibuya-ku, Tokyo

* It is essentially the same as the notation given by Chamberlain. See Ref. 3.

* Dewar described this as I effect of alkyl group in his text book. M. J. S. Dewar, "The Electronic Theory of Organic Chemistry", Oxford Univ. Press, London (1949), p. 52.

SHORT COMMUNICATIONS

Proton Magnetic Resonance in Cocoon

By Shizuo FUJIWARA* and Makoto NAKAJIMA**

(Received May 16, 1960)

As the application of the nuclear magnetic resonance, we made a preliminary measurement of the proton resonance in cocoon in order to obtain information about the general features of the thermal motions of molecules. The line shape, the width, and the second moments of the absorption curves were investigated in usual way[1].

Apparatus and Sample

Most part of the apparatus of NMR measurements is same as described by Gutowsky et al.[2], and has been published elsewhere[2]. The magnetic field applied was about 4000 gauss. The intensity of the rf-field, H_1, was about 0.1 gauss. The samples were slightly saturated by this strength of H_1, but we could not reduce H_1 to the lower level. Measurements were made at room temperature as well as at lower temperatures which were obtained by using the Gutowsky's type[2] Dewar vessel. The temperature of the sample was measured by a copper-constantan thermocouple placed 5 mm. apart from the sample.

Several species of cocoon produced by the Tokyo University of Agriculture and Technology were used as the samples which were hereditally different from each other. Measurements of the temperature dependence of the NMR spectrum were made for the species, Shuka×Ginrei. Samples of four species including two yellow, one white, and one red were measured at the room temperature. They have the genes as shown in Table II, and each of them was divided into two parts of the outer and the inner layers.

Temperature Dependence of the Line Shape

Fig. 1 shows the results of the measurements for Shuka×Ginrei at different temperatures,

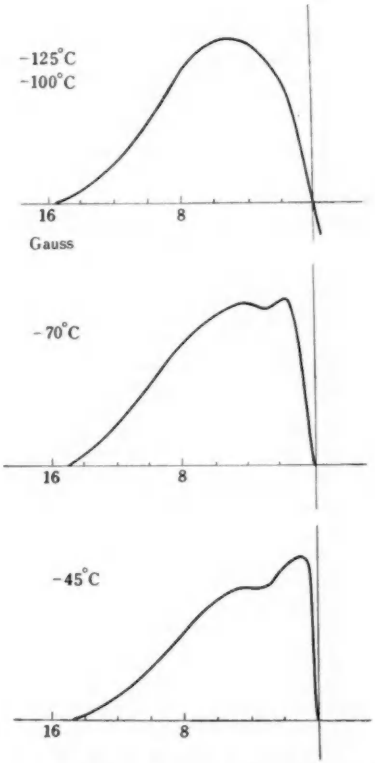

Fig. 1. Proton magnetic resonance in cocoon (species: Shuka×Ginrei). One half of the derivative of the absorption curve is presented as the function of temperature.

where a half of the derivative of each absorption curve is presented. It is noted in the figure that the observed spectrum shows a compound structure, and, moreover, that the relative intensity of the central peak with respect to that of the outer shoulder is much reduced at the lower temperatures, and not detectable at −100°C. The line widths of both the central- and the outer-peaks are not much changed by the temperature.

Besides the principal aminoacids of the silk fibroin, glycine (44%), alanine (26%), and tyrosine (13%), the native cocoon contains sericin. Hence, apart from the amido hydrogens, silk fibroin will contain approximately

* Present address: Department of Chemistry, Faculty of Science, The University of Tokyo, Hongo, Tokyo.
** Tokyo University of Agriculture and Technology, Koganei, Tokyo.

1) General aspect of the proton magnetic resonance in solid will be obtained in Chapter 6 of "Nuclear Magnetic Resonace" by E. R. Andrew, Cambridge University Press, Glasgow (1955), p. 151.

2) H. S. Gutowsky, L. H. Meyer and R. E. McClure, *Rev. Sci. Inst.*, **24**, 644 (1953).

3) S. Fujiwara and S. Hayashi, *Rep. of University of Electro-Communications*, No. 8, 96 (1956).

36% of the protons in methylene groups, but also about 27% in methyl groups, and 36% in CH, OH, or aromatic positions.

Although one may interpret that the existence of a compound structure (as in the cases of polyethylene and polytetrafluoroethylene[4,5]) does not necessarily imply that there are two separate regions differing in their degree of motion as proved for natural rubber[6], polymethylmethacrylate[7] and so on, however, we assume that the structure of the observed spectra is due to the net contribution of the protons in different phases, very motional and rigid, since the relative intensity of the central peak is so strongly temperature dependent, and its width is almost independent.

Table I gives the characteristic figures of the spectrum.

As the component I is observable even at −70°C, it can not be attributed to the sorbed water which might be existent in the sample. The line width of II is invariant with temperature over a range of about 130°C, and if our assumption on the structure of the line

TABLE I. NMR LINE WIDTH OF COCOON (SHUKA×GINREI)

Component	Line width (in gauss)			
	<−100°C	−70°C	−45°C	21°C
I(narrow)	(−)	(0.8)	0.8	0.8
II(broad)	8.0	8.0	8.0	8.0

The value for I at −70°C was difficult to determine exactly, since its intensity was low.

TABLE II. CHEMICAL COMPOSITION AND THE NMR DATA FOR SEVERAL SPECIES OF COCOON AT 21°C

Sample		Layer	Color	Sericine			Fibroin		$\langle \Delta H^2 \rangle$ gauss^2	$(\Delta H)_{max}$. sl. for component II in gauss	Weight % of component I.
				Sericine %	Amido-N %	Carbon %	Amido-N %	Carbon %			
Osmt × Ci	C	outer	yellow	36.2	0.63	47	0.36	47	9.0	6.4	10.0
		inner	white	17.2	0.45	48	0.35	48	10.8	7.0	12.5
	Ci	outer	white	32.8	0.65	47	0.33	48	9.5	7.0	11.0
		inner	yellow	16.5	0.46	48	0.34	47	9.8	7.5	15.7
	+Ci	outer	white	30.2	0.68	47	0.34	48	9.7	7.0	16.0
		inner	white	15.4	0.48	49	0.36	47			
Pk	Pk+c	outer	red	30.0	0.64	47	0.35	48	9.7	7.9	12.0
		inner	white	17.7	0.51	48	0.33	48	11.6	8.3	14.5

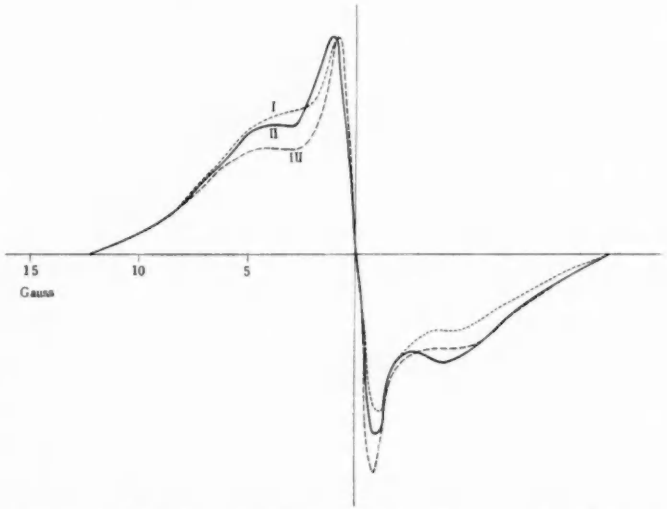

Fig. 2. Derivatives of the NMR absorption spectra for different species of samples at 20°C.
I Shuka×Ginrei, II Osmt, III Pk

4) C. W. Wilson and G. E. Pake, *J. Poly. Sci.*, **10**, 503 (1953).
5) C. W. Wilson and G. E. Pake, *J. Chem. Phys.*, **27**, 115 (1957).
6) H. S. Gutowsky and L. H. Meyer, ibid., **21**, 2122 (1953).
7) J. G. Powles, *Proc. Phys. Soc.*, **69B**, 281 (1956).

shape is correct, this will suggest that the protons in this component are effectively rigid.

The second moments at -100 and -125°C, where no central peak was observale, were 26.8 and 26.1 gauss^2, respectively, and those at -75°, -45° and $+21$°C were 26.1, 24.3 and around 10 gauss^2, respectively, which could be explained by the variation of the relative intensities of I and II.

Line Shapes for Different Species of Cocoon

Measurements were made for the samples different in species. The results of the measurements were shown in Table II, where the results of the chemical analyses were also shown. Though there is not much difference either in the chemical composition or in the features of the NMR data, among the samples of different species, we notice that the behavior of saturation is different: Fig. 2 shows the normalized derivative curves for the samples, where no saturation effect is observed in the record of Pk, since the each half of the spectrum is completely symmetric with respect to the center of the base line, whereas, in Shuka×Ginrei, the intensity of the right-hand side half is strongly reduced.

Authors thank to Mr. Michio Horinouchi for his assistance in making measurements.

The University of Electro-Communication
Chofu, Tokyo

Separation of Uranium from Fission Products Using Cellulose

By Noboru Oi

(Received August 16, 1960)

It has been previously known[1] that cellulose has the property of adsorbing metals such as rare earths from impure uranyl nitrate in ether-nitric acid mixture. We could separate uranium from fission products by dissolving uranyl nitrate in organic solvent and percolating the solution through a column of cellulose pulp. Almost all parts of fission products (99% or more) were retained on the cellulose, while uranyl nitrate passed unadsorbed.

Experimental procedure was as follows. A glass tube, 18 mm. in diameter and 10 cm. long, was packed with 1 g. of activated cellulose (100～200 mesh). Uranyl nitrate (1 g.) which includes fission products (about 10^6～10^8 cpm) was dissolved in 5 ml. of the solvent and was transferred to the top of the column. After washing out uranium with further 25 ml. of the solvent, 30 ml. of 0.2 M nitric acid was passed to elute fission products. The activity of the combined organic solvent, nitric acid and the remained cellulose were analyzed by a γ-scintillation spectrometer.

Organic solvents suitable for this procedure were oxygen-containing compounds which dissolve uranyl nitrate but have small water-insolubility, perhaps less than 2%. Tri-*n*-butylphosphate was found to elute fission products.

The organic solvent was preferably used without nitric acid. Presence of nitric acid enhanced the elution of fission products, especially ruthenium. For example, from 1-month-cooled irradiated uranium, 1% of fission products were eluted by ethyl ether, while 4.5 and 6.6% were eluted by ethyl ether containing 3 and 5% nitric acid, respectively. In this case the ratio of eluted ruthenium was 1 : 18 : 27.

As regards the influence of water in this procedure, it was shown that fission products were eluted more by decreasing the water content of the system. For example, in the case of uranyl dihydrate, fission products were eluted about twice as much as that of uranyl trihydrate. This fact seems to indicate that this separation method resembles to ordinary liquid-liquid extraction. The cellulose seems to act as the water layer.

Behavior of various nuclides in this separation were as follows. Nuclides which were found to contaminate the organic solvent were mainly iodine, ruthenium and cesium. From these, ruthenium is most troublesome. It was eluted 1% by ethyl ether, 4% by *n*-butyl acetateand 20% by methyl isobutyl ketone. Elution of cesium ceases by lowering the initial uranium concentration. Result of the batch method showed that distribution ratio of cesium-137 between *n*-butyl acetate and the cellulose were 2.1 (1.0 M), 9.5 (0.5 M), 450 (0.1 M), and 6300 (0.0 M) in each uranium concentration written in the parentheses. Zirconium and niobium were eluted only to a small extent. Rare earths remained on cellulose.

Example of treatment of 1 g. of 100 days-cooled irradiated uranium are shown in the table. These results may also be improved by lengthening the column or lowering the initial uranium concentration in the solvent.

It seems that this method is also interesting for handling large amounts of irradiated uranium. In this method mass transfer of

1) F. H. Burstall and R. A. Wells, *Analyst*, **76**, 396 (1951).

uranium between two different phases is not performed, so that the contamination of fission products is rather small. Moreover uranium can be easily recovered and fission products are condensed on the small amounts of cellulose.

TABLE

	The amounts of γ-activity eluted, %
Ethyl ether	0.42
n-Butyl acetate	0.68
Isoamyl acetate	0.89
Isopropyl acetate	1.1
Methyl isobutyl ketone	3.1
Total activity	about 10^7 γ cpm

The author wishes to express sincere thanks to Mr. Kakuzo Tada of Matsuda Research Laboratory of Tokyo Shibaura Electric Co., Ltd. for kind suggestion and encouragement.

Matsuda Research Laboratory
Tokyo Shibaura Electric Co., Ltd.
Kawasaki

The Crystal Structure of Pyridine N-Oxide Hydrochloride and Hydrobromide

By Yoshiyuki NAMBA, Tsutomu ODA, Hideo ITO and Tokunosuke WATANABE

(Received August 22, 1960)

Pyridine *N*-oxide has recently been a target of investigations by electronic and infrared absorption spectra[1] and by molecular orbital calculations[2], to elucidate its molecular symmetry, bond orders and electronic states, etc. In order to amplify informations about the molecular structure of this compound, the present authors have attempted an X-ray study of its hydrochloride and hydrobromide.

Hydrochloride and hydrobromide of pyridine *N*-oxide were prepared by adding hydrogen chloride or bromide gas to an alcoholic solution of pyridine *N*-oxide. Crystals of these salts were obtained by slow evapolation of alcoholic solutions. They are of a form of a short rod-like prism. The melting points were determined to be 181°C for the hydrochloride and 168°C for the hydrobromide.

No cleavage was observed with both crystals. As these crystals are hygroscopic, we employed a crystal enclosed in a thin-walled capillary made of borosilicate glass for X-ray analyses.

Oscillation and Weissenberg photographs taken with copper K_α radiation ($\lambda=1.54$ Å) indicate that the two crystals are isomorphous and belong to the orthorhombic system. The unit cell dimensions are: $a=11.06\pm0.02$ Å, $b=7.70\pm0.02$ Å, $c=7.25\pm0.02$ Å for the hydrochloride and $a=11.40\pm0.02$ Å, $b=7.87\pm0.02$ Å, $c=7.42\pm0.02$ Å for the hydrobromide. From the density values as determined by the flotation method, each unit cell is found to contain four chemical units. The systematic absences recognized were the $(h\,0\,0)$ reflections with h odd, $(0\,k\,0)$ with k odd and $(0\,0\,l)$ with l odd. Hence the space group was uniquely determined to be D_2^4–$P2_12_12_1$. The intensities of $(h\,k\,0)$ and $(h\,0\,l)$ reflections were estimated visually by comparison with calibrated intensity scales, and they were corrected for Lorentz and polarization factors. Approximate temperature and scale factors were obtained by Wilson's method.

From the Patterson projections, $P(uv)$ and $P(uw)$, approximate positions for the halogen atoms were obtained. They are, $x=11/60$, $y=11/60$ and $z=0$. As it was clear that the hydrochloride was more suitable for obtaining atomic positions of light atoms, further analyses were made mainly with the hydrochloride.

A two-dimensional Fourier projection, $\rho(xz)$, was prepared for the hydrochloride using the structure factors whose signs were determined by the chlorine atoms. There appeared in this projection in addition to a predominant peak whose parameter values were those expected for the chlorine atom, a ring-like structure suggesting the location of the skeleton of pyridine *N*-oxide. We calculated the structure factors as a function of the rotation angle of the C···N—O axis of pyridine *N*-oxide within its plane and found that the C···N—O axis is almost parallel with the *c*-axis. In these calculations, we assumed for pyridine *N*-oxide a planar configuration having the symmetry C_2-2 with bond lengths, 1.4, 1.4 and 1.3 Å for the C—C, C—N and N—O bonds, respectively. The atomic scattering factors for the carbon, nitrogen and oxygen atoms were those taken from McWeeny's values. In determining the y-coordinates, there remained two possibilites for the orientation of the pyridine *N*-oxide plane referred to the $(0\,1\,0)$ plane. Structure factor calculations for $(h\,k\,0)$ reflections were carried out as a functions of the y-coordinate of the center of the pyridine ring, for the two orientations of its plane ($+30°$, $-30°$), and found a structure which explained fairly well lower order reflections.

1) M. Ito and N. Hata, This Bulletin, **28**, 260 353 (1955).
2) H. H. Jaffe, *J. Am. Chem. Soc.*, **76**, 3527 (1954); **77**, 4441, 4445, 4448, 4451 (1955); T. Kubota, *J. Chem. Soc. Japan, Pure Chem. Sec.* (*Nippon Kagaku Zasshi*), **80**, 578 (1959).

Successive refinements were made. However, as the overlap of light atoms did not permit to give individual atomic coordinate accurately. Therefore an effort was made to improve the y-coordinate of each atom, using the least square method. The $\rho(xz)$ and $\rho(xy)$ are illustrated in Figs. 1 and 2. The atomic arrangement projected along the c and b axes are illustrated in Fig. 3.

The configuration of pyridine *N*-oxide is found to be almost planar. Each chlorine atom is surrounded by six pyridine *N*-oxide groups as neighbors. Namely, if we take a chlorine atom marked (A) in Fig. 3, the neighboring pyridine *N*-oxide groups are those designated by (1), (2), ···, (6). If we assume the pyridine *N*-oxide group behaves as a positive ion and the chlorine atom as an anion, as the results of proton transfer, the structure could be described as an ionic structure. However, the chlorine atom has one oxygen atom at a close distance 2.9 Å ((A)·····0 atom of pyridine *N*-oxide (2)) which suggests a strong interaction between these two atoms, presumably by a hydrogen bond, O—H···Cl. This point of view is supported by the investigation made by the infrared absorption spectra[3]. If this hydrogen bond is strong enough, pyridine *N*-oxide would form a dipolar molecule with hydrogen chloride, leading to a packing of dipolar molecules. The actual state may be just between two extremes.

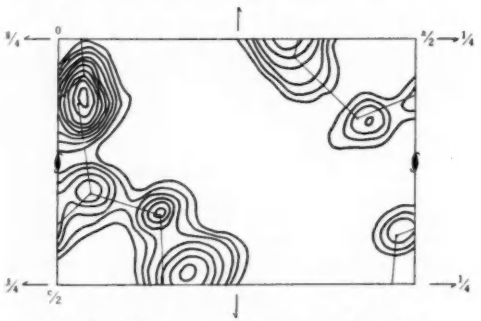

Fig. 1. Electron density map projected on *ac* plane. The intervals of contours for chlorine are twice as much as those for the other atoms.

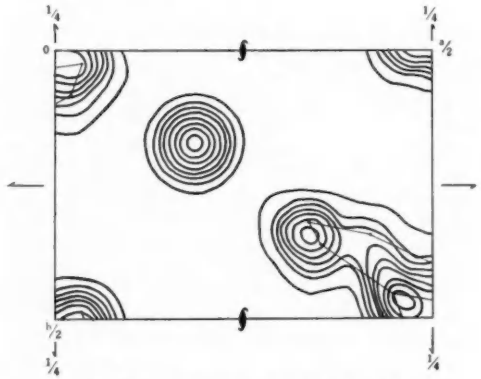

Fig. 2. Electron density map projected on *ab* plane. The intervals of contours for chlorine are twice as much as those for the other atoms.

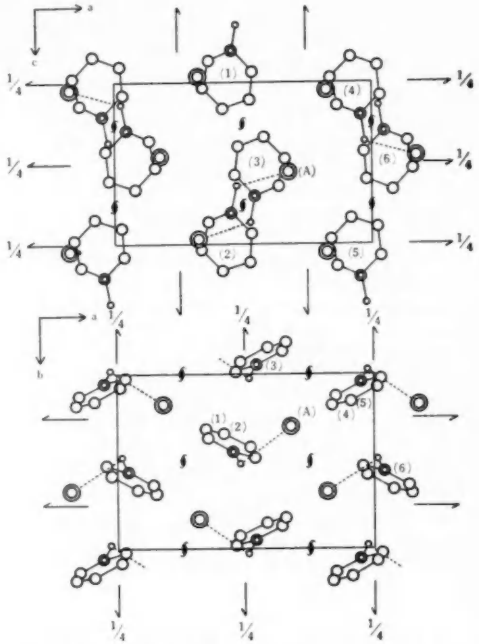

Fig. 3. Projections of the structure, on (010) and (001), showing shorter O···Cl contact with dotted line.
- Oxygen
- Nitrogen
- Carbon
- Chlorine anion

We shall postpone discussing the precise configuration of the pyridine *N*-oxide molecule concerning to the electronic state of π electrons involved in pyridine ring and those of oxygen atom, in conjugation with each other, untill three-dimensional analyses are made.

Laboratory of Physical Chemistry
Osaka University of Liberal Arts and Education, Minamikawahoricho
Tennoji, Osaka (Y. N. and T. O.)

Department of Physics, Osaka University, Nakanoshima, Osaka
(T. W.)

3) Y. Matsui and T. Kubota, Presented at the 12th Annual Meeting of the Chemical Society of Japan, Kyoto, April, 1959.

The Crystallization of "Allophane" under Hydrothermal Conditions

By Mitsue KOIZUMI*, Ryôiti KIRIYAMA** and Wataru MURAYAMA**

(Received September 10, 1960)

Allophane, a hydrous silica-alumina mineral, is classified into mineral allophane, soil allophane and "precipitation allophane"[1] from their ways of occurrence. They are almost X-ray amorphous and show the similar thermal behavior characterized by mullite formation at 900~1000°C under atmospheric condition.

In hydrothermal synthesis experiments, crystallization of some amorphous materials, gels or glasses, occurs at fairly low temperatures. In such a condition, phase assemblages more stable than the reactants may easily be formed. An attempt has been made to observe structural differences of allophane and consequently to establish a picture of structural classification of X-ray amorphous minerals by applying the crystallization method under hydrothermal conditions.

The general procedure was to allow samples of allophane to react with water over the range 200~500°C at 1000 atm. H_2O and then to quench into water. The type of pressure vessel used was of the "test-tube" bomb[2]. Running was made for two weeks at maximum. The products were then examined with an X-ray diffractometer.

Soil allophane from Kanuma[3] and Imaichi[4], mineral allophane from Bihoro[5] and precipitation allophane from Asama[6] and Fukazawa[7] were used for the experiment[8]. Synthetic silica-alumina gels prepared by the homogeneous precipitation method over the chemical composition range of $2SiO_2 \cdot Al_2O_3$-$SiO_2 \cdot 5Al_2O_3$ were kindly supplied for this investigation by

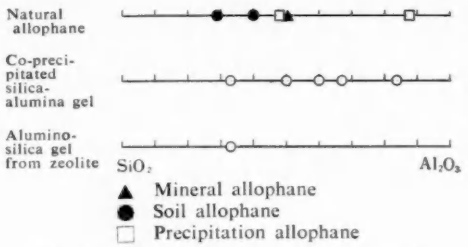

Fig. 1. The chemical composition of the starting materials.

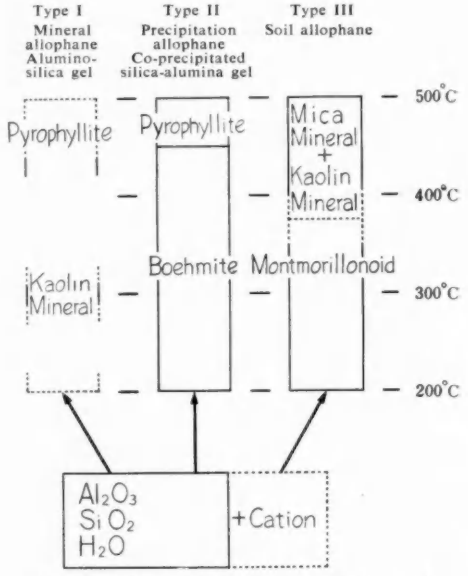

Fig. 2. Diagrammatic representation of phase assemblages obtained from the various starting materials.

Dr. J. Ossaka. The thermal properties of these gels has been studied by Ossaka and found to be identical with those of the natural allophanes[7]. The aluminosilica gel was also prepared from synthetic zeolite, Type A[9], by destructing the framework with hydrochloric acid and then washing sodium ion off with water. The mole ratios of SiO_2/Al_2O_3 of these starting materials are illustrated in Fig. 1.

The experimental results are summarized diagrammatically in Fig. 2. Owing to the poor crystallinity of the products, the prcise phase determination was somewhat difficult for several specimens. As indicated in Fig. 2, the crystallization process of the starting materials in this investigation are classified into the following types.

* Present address, Institute of Geological Sciences, College of General Education, Osaka University, Toyonaka, Osaka.
** Present address, The Institute for Scientific and Industrial Research, Osaka University, Sakai, Osaka.

1) This amorphous mineral found from mineral spring was classified by J. Ossaka into a variety of the species of allophane.
2) R. Roy and E. F. Osborn, *Econ. Geol.*, **47**, 717 (1952).
3) T. Sudo and J. Ossaka, *Japanese J. Geol. Geogr.*, **22**, 215 (1952).
4) R. Morimoto, J. Ossaka and T. Fukuda, *Bull. Earthq. Res. Inst.*, **35**, 359 (1957).
5) H. Minato, *Advances in Clay Sci.*, **2**, 350 (1960).
6) J. Ossaka, ibid., **2**, 339 (1960).
7) J. Ossaka, read before the Annual Meeting of the Mineralogical Society of Japan, Tokyo, June, 1959.
8) The authors are indebted to Dr. J. Ossaka and Dr. H. Minato of the University of Tokyo who kindly supplied the specimens for the experiment.
9) D. W. Breck, W. G. Eversole, R. M. Milton, T. B. Reed and T. L. Thomas, *J. Am. Chem. Soc.*, **78**, 5963 (1956).

Type I: From the materials of this type, a kaolin mineral was formed at 300°C, and then pyrophyllite was obtained at 430°C. The mineral allophane and the aluminosilica gel appeared to crystallize in this manner.

Type II: The two samples of precipitation allophane and all the co-precipitated silica-alumina gels with various compositions were classified into this type. It should be noted that, from these samples, only a boehmite phase appeared in the temperature range between 200 and 450°C and above 450°C pyrophyllite was formed.

Type III: The three samples of soil allophane yielded a montmorillonoid phase in the region from 200 to 350°C. The (0 0 1) spacing was 15 Å and expanded to 18 Å when treated with glycol. Above 400°C, a mica and a kaolin mineral were obtained together.

Important factors controlling what phases crystallize from the amorphous minerals may be considered to involve (i) SiO_2/Al_2O_3 ratio, (ii) impurity cations and (iii) the gel structure. It is probably possible to remove SiO_2/Al_2O_3 ratio out of the major factors on the following basis. Each of the three specimens with the almost same ratio of 2:1, including aluminosilica gel, soil allophane and one of co-precipitated silica-alumina gels, gave a product of its own phase. Such was the case also with mineral allophane, precipitation allophane and co-precipitated gel of the same SiO_2/Al_2O_3 ratio of 1:1. The products of type III were obtained only from soil allophane. It is considered that their formation may be effected by the presence of a considerable amount of cation impurities which have been contained in every soil allophane. On the contrary, all the starting materials of the types I and II are chemically free from any cations. It is thus reasonable to assume that gel structure plays a role in deciding the product from the starting materials of the similar chemical composition.

From the preparation method previously mentioned, it is suggested that the co-precipitated gels are homogeneous mixtures of the two species of gel particles, silica and alumina, finely dispersed in each other. This concept is supported by the experimental result that the materials of the type II do not yield an aluminosilicate phase but an alumina mineral, boehmite, in the lower temperature range. Thus the precipitation allophane is possibly considered to be structurally identical with the co-precipitated gel.

Mineral allophane showed the same crystallization behavior with an aluminosilica gel prepared from the zeolite. It is obvious, therefore, the mineral allophane is probably an aluminosilicate with four-coordinated aluminum.

As it is well known, our present knowledge is insufficient to discuss the gel structure precisely. From the above results, however, we may now recommend that study on crystallization under hydrothermal conditions will be applicable to deduce a structure of X-ray amorphous mineral. In this way natural allophane of this investigation can be classified into three groups.

The detailed description of this work will be given elsewhere in near future.

Faculty of Science
Osaka University
Nakanoshima, Osaka

---

*Hot-atom Chemistry of Radiocobalt in Nitroammine Cobalt Complex Salts**

By Nobufusa SAITO, Takeshi TOMINAGA and Hirotoshi SANO

(Received September 10, 1960)

The present authors had previously reported[1,2] that radiobromine recoil atoms arising from thermal neutron capture in outer anions of various cobaltammine bromides could substitute in the cobalt coordination sphere to form ^{80m}Br- or ^{82}Br-labeled complex cations. In this investigation they found that outer anions of nitroammine cobalt(III) nitrates and nitrites could replace ligand NH_3 groups in the radiocobalt coordination sphere when cobalt atom was activated by slow neutron bombardment.

Seven kinds of crystalline complex salts listed in Table I were irradiated in an experimental hole in JRR-1 reactor for one to six hours at pile temperature. Thermal neutron flux was approximately 3×10^{11} n/cm^2 sec. After standing for one day at room temperature, the irradiated salts were dissolved in water and ^{60}Co-labeled species were separated by procedures involving paper electrophoresis[3], paper chromatography[4],

* Presented at the 13th Annual Meeting of the Chemical Society of Japan, Tokyo, April, 1960.

1) N. Saito, H. Sano and T. Tominaga, This Bulletin, 33, 20 (1960).
2) N. Saito, T. Tominaga, and H. Sano, ibid., 33, 120 (1960).
3) M. Maki, *Japan Analyst*, 4, 217 (1955).
4) Y. Yamamoto, A. Nakahara and R. Tsuchida, *J. Chem. Soc. Japan, Pure Chem. Sec.* (*Nippon Kagaku Zasshi*), 75, 114 (1954).

TABLE I. PERCENTAGE DISTRIBUTION OF ^{60}Co-LABELED SPECIES AFTER THE DISSOLUTION OF IRRADIATED NITROAMMINE COMPLEXES

Target	^{60}Co-labeled species, %*						
	CoA_6^{3+}	$CoA_5NO_{2,3}^{2+,+}$	$CoA_4(NO_{2,3})_2^+$	$CoA_3(NO_{2,3})_3$	$CoA_2(NO_{2,3})_4^-$	Co^{2+}	R**
$[Co(NH_3)_6](NO_2)_3$	0.9	17	38	13.5	9	19	19
$[Co(NH_3)_6](NO_3)_3$	4.5	11.5	26	<1.7	<0.8	58	3
$[Co(NH_3)_5NO_2](NO_2)_2$	≤0.6	39	18	3.9	1.4	38	0.5
$[Co(NH_3)_5NO_2](NO_3)_2$	≤0.7	34	23	4.0	1.1	37	0.7
cis-$[Co(NH_3)_4(NO_2)_2](NO_3)$	~0	<1.4	{cis: 47, trans: 4}	4.2	0.9	43	0.08
trans-$[Co(NH_3)_4(NO_2)_2](NO_3)$	~0	0.5	{cis: 4.6, trans: 45}	3.1	0.4	46	0.07
$[Co(NH_3)_3(NO_2)_3]$	~0	~0	0.5	55	~0	44	0

* "A" denotes an NH_3 group in most cases. However, it is possible that small amounts of species with one or two of A's being H_2O may also be present in some cases.

** $R = \dfrac{\text{Percentage of labeled species containing one more anionic ligand than the target complex}}{\text{Percentage of labeled species containing the same number of anionic ligands as the target complex}}$

ion exchange, or precipitation. The results are summarized in Table I.

As shown in Table I, substitution of ligand NH_3 groups by outer anions (NO_2^- or NO_3^-) was observed** in most complex salts whenever the substitution product was considerably stable in aqueous solutions. On the contrary, labeled complexes containing less anions in ligands than the target complex were not found in practice after dissolution of almost all the irradiated salts. The factor, R, in Table I is the ratio of percentage of labeled species containing one more anionic ligand than the target complex to percentage of labeled species containing the same number of anionic ligands as the target complex. It is interesting that this ratio increases with the increase in electric charge on the target complex ion, or with the increase in number of neighboring outer anions. The results may be generally explained by assuming the electrostatic interaction between the outer anions and the complex ions fragmented more or less during recoil reactions.

It is worth mentioning that cis-trans isomerization of dinitrotetrammine complexes occurs during recoil processes. Cis isomer was found with an enrichment factor of 23±5 in the irradiated *trans*-$[Co(NH_3)_4(NO_2)_2](NO_3)$, while trans isomer with an enrichment factor of 80±10 in the irradiated cis salt.

Department of Chemistry
Faculty of Science
The University of Tokyo
Hongo, Tokyo

** This shwos a similarity to the well-known thermal transformation reactions of nitroammine cobalt(III) nitrites.

The Electron Spin Resonance Absorption of Molecular Addition Compounds

By Hiroo INOKUCHI, Kunihiko IKEDA* and Hideo AKAMATU

(Received September 12, 1960)

Recently, a number of molecular complexes formed between electron donors and acceptors have been investigated by the method of electron spin resonance (ESR) and also by the measurement of electrical conductivity[1-3]. On the molecular complexes formed between phenylene diamines and halogenated quinones, Bijl, Kainer and Rose-Innes[3] and also Matsunaga and McDowell[4] reported the existence of unpaired electrons in those complexes. However, it has been found that the observed intensity of ESR absorption fluctuate from specimen to specimen.

In this report, we present the electron spin resonance absorption of the molecular complexes, formed between dimethyl-aniline (I, DMA; liquid) and halogenated benzoquinones (II, *x*-anils) and of those between also tetramethyl-*p*-phenylene diamine (III, TMPD) and *x*-anils as a function of time.

* Present Address: Aeronautical Research Institute, University of Tokyo, Komaba, Meguro-ku, Tokyo.

1) D. D. Eley and H. Inokuchi, Proc. Third Carbon Conf., 91 (1959).
2) D. D. Eley, H. Inokuchi and M. Willis, *Discussions Faraday Soc.*, **28**, 54 (1959).
3) D. Bijl, H. Kainer and A. C. Rose-Innes, *J. Chem. Phys.*, **30**, 765 (1959).
4) Y. Matsunaga and C. A. McDowell, *Nature*, **185**, 916 (1960).

TABLE I. THE PARAMAGNETIC PROPERTIES OF MOLECULAR COMPLEXES FORMED BETWEEN PHENYLENE DIAMINE AND HALOGENATED QUINONES

Donor	DMA			TMPD		
Acceptor	chloranil	bromanil	iodoanil	chloranil	bromanil	iodoanil
Color	blue violet	black violet	black violet	black	brownish black	brownish black
g-value	2.0003±0.0004	2.0071±0.0005	2.0000±0.0004	2.0036±0.0004	2.0043±0.0004	2.0037±0.0004
Line width (gauss)	20	4 (*) 32 (†)	22	7	13 (*) 40 (†)	22
Spin population (**)	~0.01%	5%	17%	5%	7%	10%

* Observed with freshly prepared specimen.

† Observed with specimen left for 40 days in air.

** Maximum value.

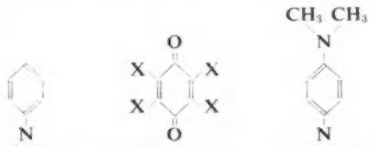

(I) (II) (III)

These complexes were made as follows: 50 mg. of purified *x*-anil were dissolved in 5 cc. of DMA, and one-fifth of its volume of ethanol was added into the solution to precipitate the deep colored molecular complex. After filtration, crystals of the complex were sealed up immediately into glass tubings (diameter 2 mm.) under an atmosphere of argon or oxygen. In the case of TMPD-*x*-anil complexes, the solutions of TMPD and of *x*-anil in benzene were mixed with each other to produce the precipitate of the complex. The precipitate was filtered and washed with a small amount of benzene and of ether successively. These complexes were also kept in glass tubings to prevent a decomposition of TMPD by humidity.

The electron spin resonance absorption spectra of these complexes were observed in association with *x*-band microwave spectrometer, Hitachi MPS-1. The spin concentrations in these complexes were measured in comparison with a standard piece of α,α'-diphenyl-β-picrylhydrazyl or 'violanthrone'*. The *g*-values of these complexes possessed near 2.0 and was estimated from the value of ultramarine which is 2.028.

As illustrated in Table I, it was found that DMA-*x*-anil complexes, for which Bijl et al.[3] observed no ESR signals possess definite ESR absorption around $g=2.0$. This fluctuation of intensity of ESR absorption may depend upon preparation techniques of these complexes. The study of *g*-values of DMA-chloranil and also of DMA-iodoanil, which are fairly smaller than the value of free electron itself ($g=2.0023$), is a noteworthy problem.

In the case of TMPD-*x*-anil molecular complexes (Table I), the spin concentrations changed strongly with great regard to the time after preparation as shown in Fig. 1 for TMPD-bromanil. However, the atmospheric gases surrounding the complexes were not so sensitive to the spin concentration of the complexes excepting TMPD-chloranil.

The ESR absorption curve of TMPD-bromanil complex also changed violently with time in its shape. At first, two ESR absorption peaks, their *g*-values were 2.0030 and 2.0043 respectively, were observed for freshly prepared specimen (curve A of Fig. 2). After a couple of days, a new absorption peak appeared (curve B). However, during a next few days, two of them disappeared and only one ESR absorption peak having $g=2.0043\pm0.0004$ remained (curve C). Through a long period observation, the line width of the

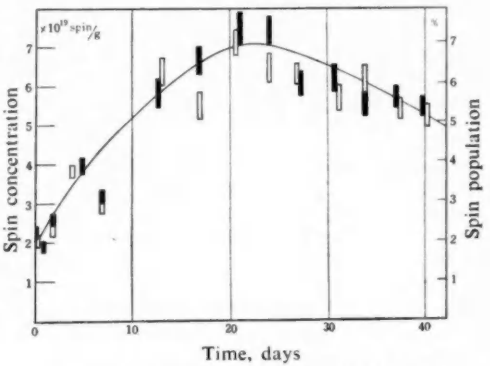

Fig. 1. The time dependence of spin population of tetramethyl-*p*-phenylene diamine-bromanil complex.
■ in air, □ in argon

* Crude violanthrone comprises a small amount of free radicals. This compound can be applied as a substandard piece for the estimation of spin concentration because the free radical is stabilized in the matrix, violanthrone.

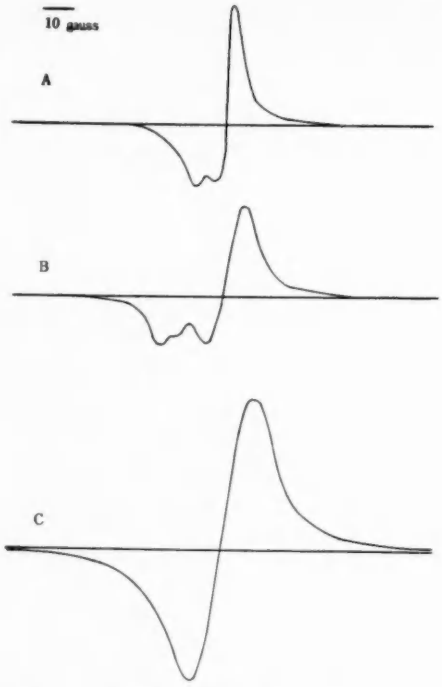

Fig. 2. The derivative curves of electron spin resonance absorption of tetramethyl-*p*-phenylene diamine-bromanil complex in air: (A) for fresh specimen, (B) and (C) for specimen which is exposed in air for 2 days and also for 4 days respectively.

absorption curve was spread from 12~13 gauss to 50 gauss (120 days after preparation).

It seems likely that these changes of spin concentrations and also line widths with time are introduced from the progress of complex formation and/or decomposition of these addition compounds.

Department of Chemistry
Faculty of Science
The University of Tokyo
Hongo, Tokyo

Detection of End-groups in Polyacrylonitrile by Differential Infrared Spectroscopy

By Ikuo MATSUBARA

(Received September 19, 1960)

The differential infrared spectroscopy, which is useful for the identification or quantitative estimation of minor constituents in organic substances[1], has been applied to the detection of the end-groups in polyacrylonitrile. As O'Connor et al.[2] have described, the infrared measurements of polymers can be successfully performed with the potassium bromide disk technique, particularly when the samples are obtained in the form of a fine powder or fibers. In the present study the differential analyses of polymers have been carried out with success in combination with the potassium bromide disk technique.

Fig. 1 shows the infrared spectra obtained from the potassium bromide disks of some different polyacrylonitrile samples. The disks were prepared from the mixtures of 400 mg. of potassium bromide and 4 mg. of the sample material, both screened through 250-mesh stainless-steel cloth, by applying a pressure of 8 tons for 10 min. in the evacuated die mount. The infrared spectra were obtained using a Perkin-Elmer model 21 spectrophotometer (with NaCl optics). Samples A and B are polyacrylonitriles of different degrees of polymerization ($\bar{M}_n$=49500 and 11000, respectively)*, both being polymerized by using ammonium persulfate-sodium bisulfite redox system as initiator. Sample C is one polymerized using azo-bis-isobutyronitrile as initiator ($\bar{M}_n$=7000). By inspection of the spectra of samples A and B it has been found that the intensities of the weak shoulder band at 1041 cm^{-1} and the one around 1200 cm^{-1} increase remarkably with the lowering of the degree of polymerization. On the contrary, as is evident from the spectrum of sample C, no such absorption bands of variable intensities are observable at the corresponding frequencies in the case of polyacrylonitrile polymerized using azo-bis-isobutyronitrile as initiator, while the situation is the same for the sample obtained by γ-ray initiated polymerization. Therefore, it seems that these bands are characteristic of the polymer obtained

1) See for example, D. Z. Robinson, *Anal. Chem.*, **24**, 619 (1952); H. Powell, *J. Appl. Chem.*, **6**, 488 (1956).
2) R. T. O'Connor, E. F. DuPré and E. R. McCall, *Anal. Chem.*, **29**, 998 (1957).
* Measured according to the method of P. F. Onyon, *J. Polymer Sci.*, **22**, 13 (1956).

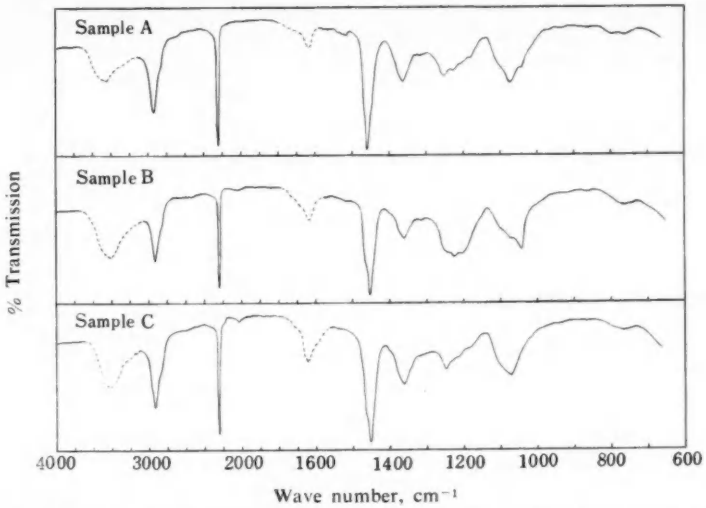

Fig. 1. Infrared spectra of some polyacrylonitriles. Sample A and B were polymerized using ammonium persulfate-sodium bisulfite redox system as initiator ($\overline{M}_n$=49500 and 11000, respectively). Sample C was polymerized using azo-bis-isobutyronitrile as initiator ($\overline{M}_n$=7000). (Dashed lines indicate the absorptions due to water adsorbed by potassium bromide).

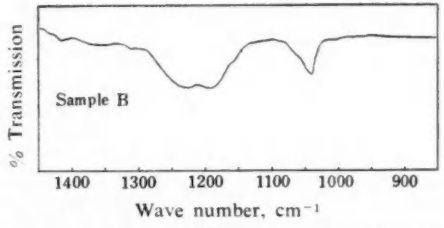

Fig. 2. Differential spectrum of polyacrylonitrile sample B (initiator=ammonium persulfate-sodium bisulfite redox system) against sample C (initiator=azo-bis-isobutyronitrile).

using persulfate-bisulfite redox system as initiator. In order to make clear the nature of these bands, the differential method has been applied, in which the disk containing sample B is put in the sample beam of the spectrometer and the absorption bands due to polyacrylonitrile proper are cancelled out by placing the disk containing sample C in the reference beam. The differential spectrum is shown in Fig. 2, in which two independent bands have been separated; one at 1041 cm^{-1} and a doublet with peaks at 1227 and 1190 cm^{-1}. It has been predicted from the analyses by tracer methods[3] that, when the persulfate-bisulfite redox system is usedto initiate polymerization, both sulfate and sulfonate end-groups may be introduced into

3) Y. Tsuda, *J. Appl. Polymer Sci.*, in press.

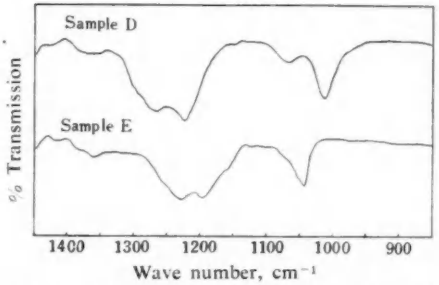

Fig. 3. Differential spectra of polyacrylonitrile sample D (initiator=ammonium persulfate, $\overline{M}_n$=9600) and sample E (initiator=Fe^{3+}-sodium bisulfite redox system, $\overline{M}_n$=30300) against sample C (initiator=azo-bis-isobutyronitrile).

the polymer, and these groups are expected to show characteristic absorptions in the 1200~1000 cm^{-1} region[4]. Therefore, the above two bands are suspected to be due either to the sulfate or sulfonate end-groups. To clarify this point further, two other polyacrylonitrile samples have been examined by the differential method. Sample D was polymerized using ammonium persulfate as initiator ($\overline{M}_n$=9600), and it is expected that the sulfate end-groups

4) L. J. Bellamy, "The Infra-red Spectra of Complex Molecules", 2nd Ed., Methuen & Co., Ltd., London (1958), Chapt. 22.

alone may be incorporated in this polymer. Sample E was polymerized using Fe^{3+}-sodium bisulfite redox system as initiator ($\overline{M}_n$ = 30300), so that the polymer may contain only the sulfonate end-groups. Fig. 3 shows the results of the differential measurements, in which the absorptions due to polyacrylonitrile have been cancelled out by placing sample C in the reference beam. In complete agreement with expectation, the spectrum of sample D corresponds well to those of aliphatic sulfates ($R-O-SO_3^-$), and we may ascribe the doublet with peaks at 1264 and 1224 cm^{-1} to the S–O degenerate stretching vibration, the band at 1065 cm^{-1} to the S–O symmetric stretching vibration of the sulfate ion, while the band at 1011 cm^{-1} may be ascribed to the C–O stretching vibration. In the same way, the spectrum of sample E agrees well with those of aliphatic sulfonates ($R-SO_3^-$)[5], and the doublet with peaks at 1225 and 1195 cm^{-1} may be assigned to the S–O degenerate stretching vibration and the band at 1041 cm^{-1} to the S–O symmetric stretching vibration of the sulfonate ion. Liang and Krimm[6] have reported that there exists a weak shoulder band at 1044 cm^{-1} in the spectrum of polyacrylonitrile and assigned this to a combination or overtone of some skeletal deformation vibrations of this molecule. Although they have not made mention of the initiator by which their polyacrylonitrile sample has been polymerized, it seems quite probable from the above results that this band corresponds to the vibration of the sulfonate end-groups. It is to be wondered why the spectrum of sample B, in which both sulfate and sulfonate end-groups are expected to exist, almost completely agrees with that of sample E and the absorptions due to sulfate end-groups are hardly observable. According to Tsuda's results[3], however, in the polymerization initiated by persulfate-bisulfite redox system the ratio of the concentrations of the sulfate and the sulfonate end-groups produced varies depending on the initial concentrations of the salts and of the acrylonitrile monomer, so that the relative intensities of the absorption bands due to these groups may vary from sample to sample. Therefore, it seems not improbable that the sulfonate end-groups are predominant in the case of sample B.

Quantitative estimations of the end-groups by the differential method were also carried out using the polymers of known end-group contents, and the limit of detectability of both sulfate and sulfonate end-groups by this method is estimated to be about 0.002 millimol./g. polymer.

The author wishes to thank Dr. H. Kobayashi and Dr. K. Kato of Toyo Rayon Co., Ltd. who permitted the publication of this work. He also wishes to thank Mr. H. Kataoka and Mr. K. Shirasaki for their help in experiments.

Central Research Laboratories
Toyo Rayon Co., Ltd.
Otsu, Shiga

5) K. Fujimori, This Bulletin, 32, 850 (1959).
6) C. Y. Liang and S. Krimm, *J. Polymer Sci.*, 31, 513 (1958).

Proton Magnetic Resonance Studies on the Thermally Dehydrated Products of Alumina Trihydrate

By Tatsuo SAITO*

(Received September 21, 1960)

In our previous communication[1], the thermal decomposition of alumina trihydrate was studied from the change of line shapes of proton magnetic resonance absorption in the thermally dehydrated products. In the present communication, the phase transformations accompanied with the thermal dehydration process of alumina trihydrate have been studied from the variation of second moments of the resonance lines in dehydrated products.

The starting material, bayerite, and the detecting apparatus here employed were the same as those used in the previous experiments[1]. The specimens used for the NMR measurements were prepared from this bayerite by the thermal dehydration at 100~800°C which was carried out for 3 hr. in the air. Each specimen was sealed into an evacuated glass tube which was pumped out to a high vacuum at 110°C for 6 hr.

The variation of the second moments calculated from the experimental derivative curves are shown in Fig. 1 as the function of the temperature. Below 220°C, the second moment was 13~14 $gauss^2$ showing no significant change with the temperature. However, in the range from 220 to 400°C the second moment

* Present address, Government Chemical Industrial Research Institute, Tokyo, Honchō 1-Chome, Shibuya-ku, Tokyo.

1) T. Hagiwara and T. Saito, This Bulletin, 33, 1463 (1960).

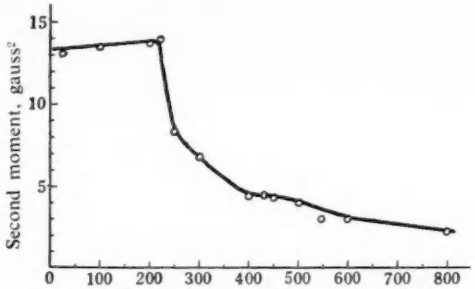

Fig. 1. Variation of the second moments with the temperature in dehydrated products of the starting material.

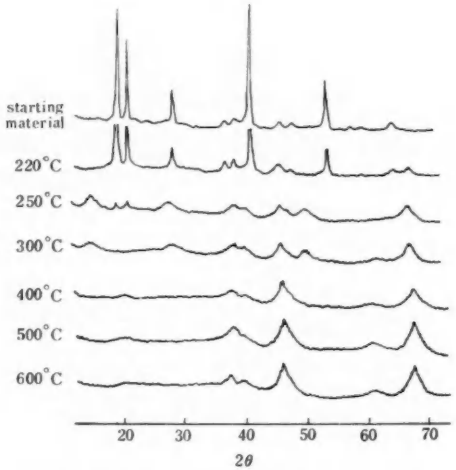

Fig. 2. X-ray diffraction diagrams of the samples dehydrated at various temperatures.

decreases gradually with the rise of temperature, and then at about 400°C the second moment becomes roughly stationary value of 4∼5 gauss². Above 550°C the second moment gradually decreases again.

The above variation of second moments is interpreted as follows:

1) The sudden decrease of second moment at about 220°C seems to show the phase transition from the starting material to the hydrous alumina which has a low value of second moment.

2) The gradual decrease of second moments with the rise of temperature in the range from about 250 to 400°C could be regarded as a result due to the change of mixing ratio of the aluminum hydroxide-hydrous alumina phase.

3) The roughly stationary values of 4∼5 gauss² at about 400∼500°C seem to show the phase of hydrous alumina.

The X-ray diffraction study of the compounds was also done. The diffraction diagrams of several specimens which were obtained from this study are shown in Fig. 2. From these diagrams, it is ascertained that the specimens below 220°C having the value of 13∼14 gauss² are crystallographically the same as the starting material, bayerite, and that each specimen at 250° and 300°C shows the diagram of mixed phase of böhmite and γ-alumina, but that the specimens at about 400∼500°C having the value of 4∼5 gauss²—which are explained to be hydrous alumina—are γ-alumina[2].

It is interesting to note that the transition temperatures of 220 and 400°C are obtained from the variation curve of second moment showing in Fig. 1, while each transition temperature coincides with that of phase transformations obtained from X-ray diffraction studies, respectively.

The author wishes to express his hearty thanks to Professor Tokutaro Hagiwara for his kind direction and also wishes to express his sincere thanks to Professor Tunahiko Shidei and Dr. Syukuro Yano in Kyoto University for their continual guidance and encouragement throughout this study.

Department of Chemistry
Faculty of Science
Hiroshima University
Hiroshima

2) A. S. T. M., X-ray powder data file.

The Oxygen Effect on Electronic Properties of α, α'-Diphenyl-β-picrylhydrazyl

By Hiroo Inokuchi and Minoru Kinoshita

(Received September 21, 1960)

There is one unpaired electron in each molecule of α, α'-diphenyl-β-picrylhydrazyl. In the study of unpaired spin by means of the method of electron spin resonance (ESR), thereby, this free radical ($g=2.0036\pm0.0003$) is widely used as a standard for estimation of the spin population and also the g-value of the applied specimen. However, it has been already known that the ESR absorption spectrum of free radical changes strongly under the influence

TABLE I. THE ELECTRON SPIN RESONANCE ABSORPTION DATA OF D.P.P.H.

Sample	D.P.P.H.-Single			D.P.P.H.-Free			D.P.P.H.-Ether		
	ΔH_{msl}[1]	ΔH[2]	I[3]	ΔH_{msl}	ΔH	I	ΔH_{msl}	ΔH	I
Evacuated at 80°C(10^{-6} mmHg) for 18 hr.	1.7	3.0	1.0	1.5	2.4	1.0	1.6	2.6	1.0
Exposed to air for 2 hr.	1.7	3.0	1.0	2.25	4.2	0.9	1.75	2.9	1.0
Exposed to air for 2~3 days.	1.9	3.2	1.0	2.5	4.7	0.9	1.75	2.9	1.0

1) ΔH_{msl}: Distance between inflection points on absorption curve in gauss.
2) ΔH: Line width at half power of absorption curve in gauss.
2) I: Integrated intensity (products of ΔH and height of the absoption curve) in arbitrary unit.

of gaseous oxygen[1-3]. Further, the existence of stable addition compound between α, α'-diphenyl-β-picrylhydrazyl and a organic solvent*, such as benzene, cyclohexane or ether, has been reported frequently[4]. In this brief report, we are presenting the effects of oxygen on the spin population and also on the electronic conduction of α, α'-diphenyl-β-picrylhydrazyl itself.

The observation of ESR absorption spectra was carried out at room temperature with association of Hitachi MPS-1 type x-band spectrometer. This prime free radical was made from α, α'-diphenyl-β-picrylhydrazine by oxidation with PbO_2 in ether. The dependence of the line width and of the intensity of ESR absorption spectra on the three different samples have been observed. One of them, recrystallized from carbon disulfide solution, was a solvent free powdered sample (D.P.P.H.-Free). The second sample was a large single crystal (1.3 mg.) grown from carbon disulfide solution (D.P.P.H.-Single) and the third sample was deposited from ether solution (D.P.P.H.-Ether).

We found that the spin populations in these samples, keeping in vacuo, were coincident with each other as shown in Table I. When these materials were exposed to air, the line width of ESR spectrum of D.P.P.H.-Free was spread remarkably. However, no change of the integrated intensity of ESR absorptions was found practically in spite of broadening of their line widths. These results indicate that the interaction between α, α'-diphenyl-β-picrylhydrazyl and applied solvent or gaseous oxygen is physical instead of chemical one.

1) J. J. Lothe and G. Eia, *Acta. Chem. Scand.*, **12**, 1535 (1958).
2) J. E. Bennett and E. J. H. Morgan, *Nature*, **182**, 199 (1958).
3) A. E. Arbuzov, F. G. Volitova, N. S. Grif'yanov and B. M. Kozyrev, *Doklady Akad. Nauk, S. S. S. R.*, **126**, 774 (1959).
* No addition compound between D. P. P. H. and carbon disulfide is found.
4) J. A. Lyons and W. F. Watson, *J. Polymer Sci.*, **16**, 141 (1955).

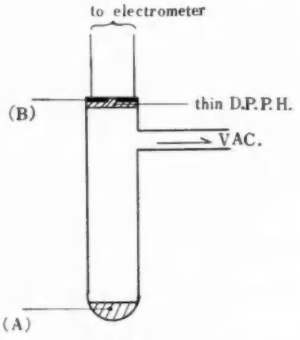

Fig. 1.

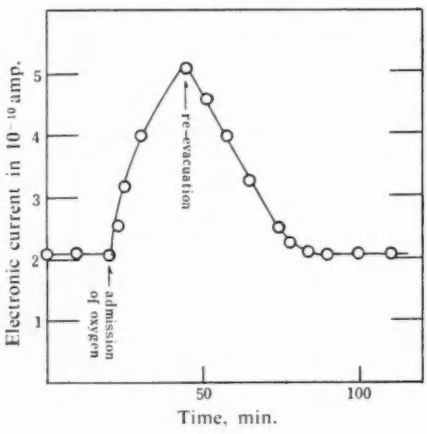

Fig. 2.

We also observed the oxygen effect on the electric conduction of thin D.P.P.H. film. The D.P.P.H. crystal to be evaporated was placed on the bottom (A) of glass vessel as shown in Fig. 1. By heating the vessel, the free radical was evaporated in vacuo to form a continuous thin film inside the top of vessel (B) between the two graphite (colloidal) electrodes. The resistance of this thin film

was observed with association of a vibration-reed electrometer. The admission of oxygen into the vessel caused a marked increase of conduction of the film. However, this effect was reversible as on pumping out the oxygen, then, the resistance of the cell returned to its original value. One of these behaviors is illustrated in Fig. 2. These behaviour also suggests that the interaction between D.P.P.H. and oxygen is almostly phyical. The detail of this work may be submitted in elsewhere.

One of the present authors has already found that the absence of the hydrogen deuterium reaction at the surface of the D.P.P.H. crystals shows that the unpaired electrons in the molecules react with adsorbed hydrogens physically[5].

From these observations, the integrated intensity of ESR absorption of D.P.P.H. is independent on the conditions of preparation and also on the exposing time in the air. Therefore, we can conclude that various sorts of the D.P.P.H. crystals are applied as a standard to estimate the spin population of paramagnetic materials.

The authors express their hearty thanks to Professor H. Akamatu for his direction of this study.

Department of Chemistry
Faculty of Science
The University of Tokyo
Hongo, Tokyo

5) D. D. Eley and H. Inokuchi, *Z. Elektrochem.*, **63**, 29 (1959).

The Distribution of Recoil Tritium in Benzoic Acid

By Jiro Okamoto

(Received September 13, 1960)

Recently, so-called "Recoil labeling" by tritium has been developed in various organic compounds[1,2]. It is a interesting problem to study replacement of hydrogen at various positions of an aromatic ring by recoil tritium. However this has not been reported by far. Therefore, the author investigated the distribution of recoil tritium produced by $^6Li(n,\alpha)^3H$ reaction in benzoic acid and found the interesting facts as follows. The mixture of benzoic acid and lithium carbonate as tritium source was sealed in a quartz ampoule, in the presence of air. The irradiation was carried out in No. 15 hole of JRR-I for 15 hr. at 2×10^{11} n/cm^2 sec. The irradiated material was dissolved in 150 ml. of pure benzene, then 10 g. of pure benzoic acid was added into the solution as carrier. This solution was refluxed for one hour and was immediately filtered to separate insoluble material from the solution, and then benzene solution was evaporated in vacuo and the crystal was dissolved in hot water to remove the labile tritium of the carboxyl group. A liquid scintillation detector (Tracerlab Model CE-1) was used to assay tritium. High voltage of the instrument was chosen at 1700 V. and temperature was kept at -10°C.

An outline of the procedures are shown in Fig. 1. The specific activities of the various

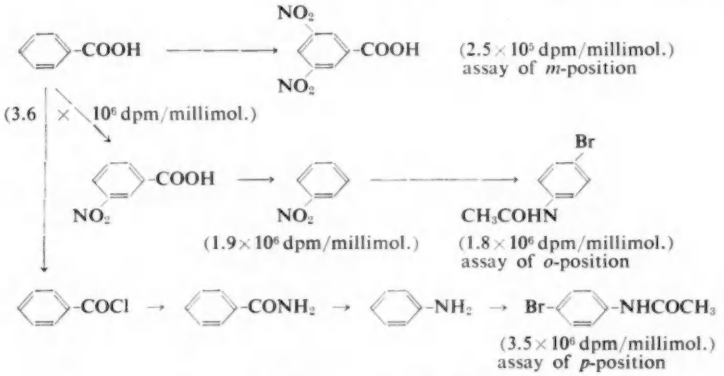

Fig. 1. Derivative and specific activities.

1) F. S. Rowland, A/CONF. 15/P/798.

2) F. S. Rowland and R. Wolfgang, *Nucleonics*, **14**, (8) 58 (1956).

compounds which were derived from the irradiated benzoic acid are also shown in Fig. 1. From these results, the percentage of ortho-, meta- and para-positions were determined. In Fig. 2, the values are shown. As is seen in Fig. 2, the replacement of hydrogen at meta-position by recoil tritium is dominant. Therefore, from the replacement process of recoil tritium in the solid phase in this experiment, it is inferred that tritium reacts after being thermalized. Ivanoff[3] stated that in the

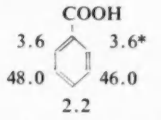

Fig. 2. Distribution of tritium in benzoic acid.

liquid phase, recoil bromine reacts with an aromatic ring after being thermalized. This resulte may support the present author's opinion on the mechanism of replacement reaction of recoil tritium in the solid phase. The furthermore details are to be published later.

Radioisotope Production Laboratory
Japan Atomic Energy Research Institute
Tokai, Ibaraki-ken

3) M. Ivanoff, *Bull. soc. chim. France*, **1953**, 266 (1953).

*Monascoflavin**

By Mamoru Ohashi, Shosuke Yamamura, Akira Terahara and Koji Nakanishi

(Received October 6, 1960)

Structure Ia[1] was forwarded as a working hypothesis for monascoflavin[2-4], $C_{21}H_{26}O_5$, $[\alpha]_{700}^{16}+418$ (c: 0.0062 in ethanol), plain positive RD curve, one active hydrogen, three C-CH_3, no OH and OCH_3. However, the NMR spectra[5], especially the AB type quartet around 140 cps (vs. chloroform, at 56.4 Mc) arising from two protons in monascoflavin and dihydromonascoflavin could not be satisfactorily accounted for by the structure. Further studies on new derivatives, corrections of the molecular formula of hydrogenated products, a re-interpretation of the NMR spectra, and considerations of the biogenetic relations with monascorubrin[6] have led to structure I (or Ib). The mentioned quartet is now comfortably assigned to the methylene protons Ha and Hb. Some pertinent compounds are listed in Table I. The dihydro (II), tetrahydro (III) and hexahydro (IV) derivatives are those in which the double bonds (1), (2) and (3) in I have successively been hydrogenated. The 116 cps peak in I and

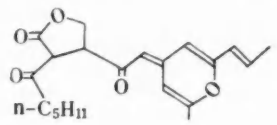

Ia

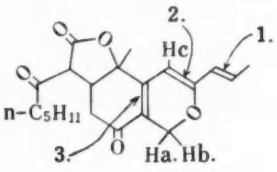

I

II is absent in III and IV, and the peak can be assigned to Hc. Presence of the n-$C_5H_{11}CO$ side-chain was shown by the production of capronic acid upon ozonolysis, oxidation with potassium permanganate, or fusion with potassium hydroxide, and production of amylamine upon Beckmann rearrangement of the oxime and hydrolysis. The lactone ring is cleaved and amides are formed, though sluggishly, when monascoflavin and hydrogenated products are treated with various amines, i.e., tetrahydromonascoflavin hexyl amide (V, R=C_6H_{13}). The amides, unlike the starting materials, no more showed the appearance or intensification of a ca. 288 mμ peak upon addition of base, and thus an enolizable β-keto-γ-lactone moiety is present in monascoflavin. Compound V (R=H) did not consume lead tetraacetate and this suggested it was not

* Reported at the 1st IUPAC Symposium on Natural Products, Australia, August, 1960.

1) Presented at the 3rd Symposium on the Organic Chemistry of Natural Products, Tokyo, 1959.

2) A. Nishikawa, *J. Arg. Chim. Soc. Japan* (*Nippon Nogeikagaku Kaishi*), **5**, 1007 (1932).

3) H. Salomon and P. Karrer, *Helv. Chim. Acta*, **15**, 18 (1931); P. Karrer and A. Geiger, ibid., **25**, 289 (1941).

4) A. D. G. Powell, A. Robertson and W. B. Whalley, *Chem. Soc. Spec. Publ.* No. 5, 27 (1956).

5) M. Ohashi, A. Terahara, K. Nakanishi, I. Yamaguchi and N. Hayakawa, This Bulletin, **33**, 1312 (1960).

6) K. Nakanishi, M. Ohashi, S. Kumasaki and S. Yamamura, *J. Am. Chem. Soc.*, **81**, 6339 (1959).

TABLE I. IR AND UV ABSORPTIONS

Compound	M.p., °C	Solvent	IR -COO-	IR -CO-	IR $\Delta^{\alpha\beta}$CO	UV λ_{max}^{MeOH} mμ(log ε)
Mf1.[a] (I) $C_{21}H_{26}O_5$	143~145	$CHCl_3$	1786	1720	1673	225(4.21), 288(3.41), 385(4.21)
2H-Mf1. (II) $C_{21}H_{28}O_5$	122	〃	1791	1723	1672	220(3.77), 237(3.61), 364(3.91)
4H-Mf1. (III)[b] $C_{21}H_{30}O_5$	136~137	〃	1790	1725	1703	244(4.03)[c]
6H-Mf1. (IV)[b] $C_{21}H_{32}O_5$	211~212	〃	1778	1742[d] 1723		
4H-Mf1.-C_6-amide[e] (V) $C_{27}H_{41}O_5N$	177~178	〃		1702	1665	241[c]
nor-4H-Mf1. (VI) $C_{20}H_{30}O_3$	41~ 44	CCl_4		1712	1668	242[c]
4Br-Mf1. (VII) $C_{21}H_{24}O_5Br_4$	162~164	$CHCl_3$	1786	1711	1690	225(3.93), 365(3.95)

a) Abbreviation for monascoflavin.
b) Tetra- and hexahydromonascoflavin were formulated as the hexa- and octahydro derivatives, respectively, in reference 5.
c) The difference with the calculated λ_{max} of 249 mμ is presumably caused by a transannular effect of the oxygenic *p* electrons on the $\alpha\beta$-unsaturated system. A similar effect has been reported for nitrogen: A. Marchant and A. R. Pinder, *J. Chem. Soc.*, **1956**, 327.
d) This unusually high $\nu_{C=O}$ value for a six-membered ring ketone is due to ring strain imposed by the γ-lactone. A similar effect is observed when the 1703 cm^{-1} band in III is compared with the 1668 cm^{-1} band in VI.
e) Amide I and II bands at 1665 and 1520 cm^{-1}, respectively.

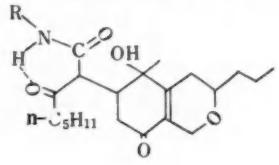

V

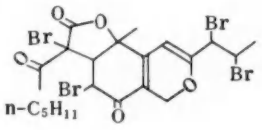

VII

an α-ketol. Ozonolysis of I and II gave acetaldehyde and butyric acid, respectively, while base hydrolysis of I and II gave crotonic acid and butyric acid, respectively. These results show that a propenyl side-chain is attached to the α-position of the pyran ring and that it should be conjugated with the α, β-unsaturated carbonyl group (to permit the occurrence of a vinylogous β-diketone cleavage). The conspicuous methyl peak at 330 cps in I remains constant and uncoupled in II-IV[5], and the position is lower than ordinary methyl peaks by ca. 30 cps. This, coupled with the production of methylglyoxal from the ozonolysis of I places a methyl group on a tertiary carbon atom bearing a oxygenic function (the lactone ring). Tetrabromomonascoflavin (VII) has no active hydrogen. Furthermore, the +17 cm^{-1} shift of the 1673 cm^{-1} band of I suggests that the α-position of the α, β-unsaturated carbonyl group must be substituted by an equatorial bromine. Boiling III in 20% alkali under nitrogen yielded VI. The facts mentioned are best explained by structure I.

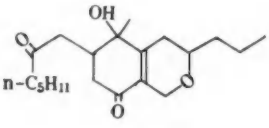

VI

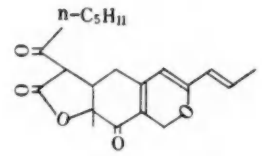

Ib

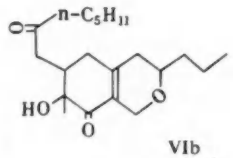

VIb

The alternative structure Ib is also conceivable

but it is difficult to account for the 1690 cm^{-1} band in tetrabromo-monascoflavin and the non-consumption of lead tetraacetate by V(R=H). However, Ib is the conclusion reached by English chemists[7] who base their conclusion on analogies with other azaphilones, e. g., monascorubrin[8], the structure of which also differs from that of the present authors[6,9], and the fact that nortetrahydromonascoflavin (VIb instead of VI) consumed periodic acid with the production of a methyl ketone. These inconsistencies will be settled in the near future.

We are grateful to Professor E. Nishikawa, formerly of Nagoya University, for an abundant supply of starting material and suggestions.

Department of Chemistry
Faculty of Science
Tokyo University of Education
Bunkyo-ku, Tokyo
(M. O., A. T. and K. N.)

Chemical Institute
Nagoya University
Chikusa-ku, Nagoyo
(S. Y.)

7) The authors are most grateful to Dr. W. B. Whalley, University of Liverpool, for informing us of their results prior to publication and for discussion at the IUPAC Symposium.

8) B. C. Fielding, F. J. Haws, J. S. E. Holker, A. D. G. Powell, A. Robertson, D. N. Stanway and W. B. Whalley, *Tetrahedron Letters*, No. 5, 24 (1960).

9) M. Ohashi, A. Terahara and K. Nakanishi, This Bulletin, 33, 1311 (1960).

Intramolecular Interaction between Hydroxyl Group and π-Electrons. XI[1]*. High Resolution Proton Magnetic Resonance Spectra of Tertiary Alcohols Having π-Electrons*

By Michinori Ōki and Hiizu Iwamura

(Received October 8, 1960)

It has been shown through infrared studies[1] that the intramolecular interaction between hydroxyl groups and π-electrons shifts the O–H stretching vibration (ν_{O-H}) to lower frequencies in comparison with an ordinary hydrogn bonding. In connection with recent high resolution nuclear magnetic resonance spectroscopy which has successfully been applied to the study of hydrogen bonding[2], variation of the proton resonance of some alcohols with concentration changes in carbon tetrachloride was studied in order to detect any effect of the aforementioned interaction to the NMR spectra, which must give rise to a different magnetic shielding of hydroxylic proton of the interacting form from that of the free one.

A Varian model V-4300 high resolution NMR spectrometer was operated at 56.4 Mc/sec. Samples include *tert*-amyl alcohol, allyldimethylcarbinol, benzyldimethylcarbinol and tribenzylcarbinol. Preparations and purities of the samples are specified in the preceding paper[1]. Measurements were carried out at 20°C, the samples being dissolved in a given amount of carbon tetrachloride and sealed in glass tubes with the outer diameter of 5 mm. The magnetic field was swept twice in both decreasing and increasing directions and the average of the records of both directions of the sweep taken. The calibration of the sweep rate was made by recording the spectrum of toluene and by reading the separation of the two peaks as 4.90 ppm[3]. The chemical shift (δ) was referred to water as an external standard and corrected for bulk diamagnetic susceptibilities of *tert*-amyl alcohol, allyldimethylcarbinol and benzyldimethylcarbinol, $-\chi_v \times 10^6$ being 0.644, 0.585 and 0.696[4], respectively.

While the absorption lines assigned to hydrogen attached to carbon atom shifted less than 0.5 ppm from thet pure liquid to the sample at infinite dilution, that of hydroxyl proton showed a marked concentration dependence as shown in Figs. 1 and 2. On dilution, the chemical shifts gradually moved to higher magnetic field and at about 0.02 mol. fraction a reversal of the curvature was observed with three carbinols. This phenomenon is understood to be characteristic of a system consisting of monomer, dimer and high polymer[2a]. Tribenzylcarbinol showed, unlike these, no association pattern within the measured concentration range. The curves were extrapolated to infinite dilution and the chemical shifts of pure monomers obtained. Under these conditions, *tert*-amyl alcohol is quite free from association and tribenzylcarbinol possesses only

1) Part X: M. Ōki and H. Iwamura, This Bulletin, 33, 1600 (1600); see also the foregoing papers.

2) a) E. D. Becker and U. Liddel, *J. Mol. Spectroscopy*, 2, 1 (1958), and others cited in the literature. b) The NMR study of the interaction pertaining to the π-electron system was presented by N. Nakagawa at the Symposium on Structural Chemistry, the Chemical Society of Japan, Tokyo, September, 1959, phenylacetylene being the example.

3) N. F. Chamberlain, *Anal. Chem.*, 31, 56 (1959).

4) Measurements were kindly made by Mr. Minoru Kinoshita, to whom the authors, thanks are due.

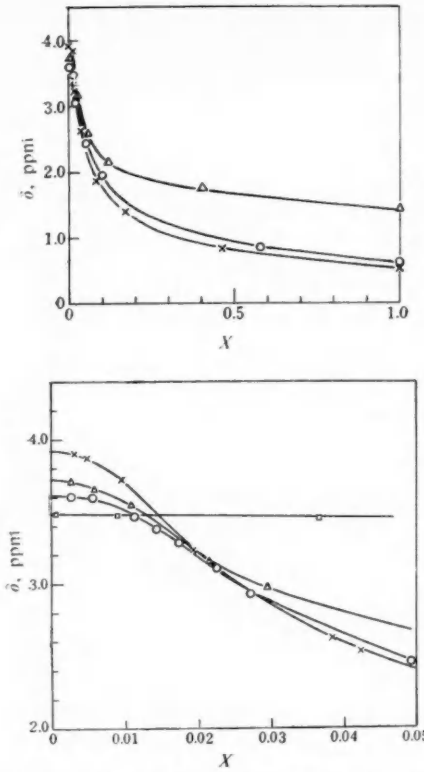

Figs. 1 and 2. Chemical shifts of the OH proton resonance, δ in ppm, vs. mole fraction of alcohols, X.

I. *tert*-Amyl alcohol -×-×-
II. Allyldimethylcarbinol -○-○-
III. Benzyldimethylcarbinol -△-△-
IV. Tribenzylcarbinol -□-□-

the hydroxyl group which is intramolecularly interacting with π-electrons of the benzene nucleus, while allyldimethylcarbinol and benzyldimethylcarbinol are in equilibrium mixtures of free and interacting hydroxyl groups. The composition of the equilibrium estimated from the integrated intensities of infrared absorption is added to the last column in Table I.

TABLE I. CHEMICAL SHIFTS AND THE COMPOSITION AT INFINITE DILUTION IN CARBON TETRACHLORIDE

	$\delta_{X=0}$ ppm	$\Delta\delta$ ppm	Mole fraction of the interacting form
tert-Amyl alcohol	3.92	0	0
Allyldimethylcarbinol	3.61	0.31	0.37
Benzyldimethylcarbinol	3.72	0.20	0.43
Tribenzylcarbinol	3.49	0.43	1

In contrast with the infrared spectra which show separate ν_{O-H} bands, the NMR spectra of hydroxyl proton are absolutely single. This must be attributed to the short lifetime and rapid exchange of free and interacting forms of these carbinols. The single proton resonance is therefore observed at the field corresponding to the average shielding of the two forms. When δ value of *tert*-amyl alcohol is taken as the chemical shift of purely free tertiary alcohols and that of tribenzylcarbinol as that interacting form, the composition of the equilibrium of benzyldimethylcarbinol may be computed from its δ value. The $\Delta\delta$ (0.20) of benzyldimethylcarbinol is divided by 0.43 and the quotient (0.47 mole fraction) is found to be in good agreement with the infrared datum (0.43). Unfortunately, the true chemical shift of hydroxyl proton taking part in the interaction with π-electrons of ethylenic linkage can not be determined because of lack of the sample which possesses only the interacting form. Assuming that the observed $\delta_{X=0}$ value of allyldimethylcarbinol is a weighted mean between free and interacting forms, the δ value of the interacting form can be estimated with use of composition datum (0.37 mole fraction) obtained from the infrared spectra. Thus $\Delta\delta$ is 0.31/0.37 or 0.838 ppm, δ being 3.08 ppm. Therefore, it may be said that, with the intramolecular interaction of the hydroxyl group with π-electrons of ethylenic linkage, the magnetic shielding of tertiary hydroxyl proton becomes less and δ value shifts to the lower magnetic field by less than one ppm. The chemical shift of the hydroxyl proton having interaction with π-electrons of the benzene nucleus is 0.41 ppm higher than this value. The ring current diamagnetic effect must be operative in the latter case. More precise evaluation is in progress in the hope of obtaining the knowledge about the geometry of the interacting form.

Department of Chemistry
Faculty of Science
The University of Tokyo
Hongo, Tokyo

*Association Shifts of NMR Spectra of Phenylacetylene**

By Naoya NAKAGAWA** and
Shizuo FUJIWARA***

(Received October 15, 1960)

Solvent effects have recently attracted the attention of several workers in the investigations of the chemical shift phenomena of proton magnetic resonance in the –OH, –COOH, –NH, and $-SO_3H$ groups of organic compounds. The results of NMR measurements were interpreted in terms of proton exchange and of hydrogen-bond formation[1]. Some of the most interesting results of these investigations are that obtained by Huggins, Pimentel and Shoolery[2], and by Korinek, Reeves and Schneider[3,4] for chloroform, which revealed us the fact that the association of the chloroform molecules can be studied by the proton resonance shifts of chloroform.

Since this technique is quite useful for the investigations of intermolecular interactions in liquid state, we made measurements of the solvent effects on the proton resonance shifts of phenylacetylene. The apparatus used for NMR measurements was constructed at the University of Electro-Communications and was operated at 27 Mc. In each of these samples, molecules are assumed to be associated with each other (self-association) or with solvent molecules; hence, the results of these measurements can be compared to those of chloroform.

Fig. 1 shows the results of NMR measurements of the solvent effects for the ethinyl proton of phenylacetylene. The resonance position of the ethinyl proton is shifted to lower field by the addition of solvents such as Et_3N, Et_2NH, Et_2O, EtOH, and Me_2CO. This can be explained as being due to hydrogen bonding with nitrogen or with oxygen atoms of the solvent molecules. The high-field shift observed in the system with benzene

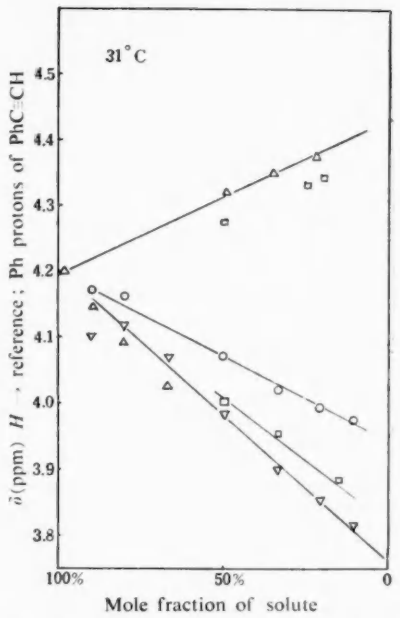

Fig. 1. Chemical shifts of C≡CH of PhC≡CH.
Solvent, △ C_6H_{12}, □ CCl_4
○ Et_3N, □ Me_2CO, ▽ Et_2NH,
△ EtOH

is explained, as in the case of chloroform, by hydrogen bonding with the π-electrons of benzene. On the other hand, the high-field shifts observed in the system with carbon tetrachloride and with cyclohexane may be explained by assuming that the self-association of phenyl acetylene molecules is broken by the solvent molecules. This may be regarded as evidence for the proposition that the phenylacetylene molecules are associated with each other through interaction of the triple-bond π-electrons. This conclusion seems to be consistent with the finding of West in the infrared spectra of triple-bond compounds[5].

The authors thank to Mr. Hiroshi Shimizu of the University of Tokyo for valuable discussions.

Department of General Education
Nagoya University
Nagoya (N. N.)

Department of Chemistry
Faculty of Science
University of Electro-Communications
Chofu, Tokyo (S. F.)

* Presented at the Symposium of Structural Chemistry, the Chemical Society of Japan, Tokyo, September, 1959.
** Present address: University of Electro-Communications, Chofu, Tokyo.
*** Present address: Department of Chemistry, Faculty of Science, The University of Tokyo, Tokyo.

1) J. A. Pople, W. G. Schneide and H. J. Bernstein, "High-resolution Nuclear Magnetic Resonance", McGraw-Hill, New York (1959), p. 401.
2) C. M. Huggins, G. C. Pimentel, and J. N. Shoolery, *J. Chem. Phys.*, **23**, 1244 (1955).
3) G. J. Korinek and W. G. Schneider, *Can. J. Chem.*, **35**, 1157 (1957).
4) L. W. Reeves and W. G. Schneider, ibid., 251 (1957).
5) R. West lectured at the Symposium of Electronic States of Molecules, the Chemical Society of Japan, September, 1959, Tokyo.